Application of microprocessor based model reference adaptive control to servosystems

Figueredo, Kenny Robert Agnelo

Award date:
1987

Awarding institution:
University of Bath

APPLICATION OF MICROPROCESSOR BASED MODEL REFERENCE ADAPTIVE CONTROL TO SERVOSYSTEMS

Submitted by

KENNY ROBERT AGNELO FIGUEREDO

for the degree of Ph.D.

of the University of Bath

1987

COPYRIGHT

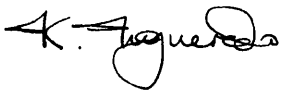

ProQuest LLC
789 East Eisenhower Parkway
P.O. Box 1346
Ann Arbor, MI 48106-1346

SUMMARY

A methodical procedure is outlined for the design of an adaptive controller. The elements that make up the control system are specified within a sampled data context. The need for this representation is due to the use of a micro-processor based system to realise the control scheme.

A model reference approach is used to specify the components and their relative configuration in the adaptive controller. The parameter adaptive part of this system is designed on the basis of a structured application of hyperstability theory.

Initially, the basic adaptive control algorithm is developed within the framework of an idealised system representation. A range of modifications are therefore devised to reflect its eventual application to real systems. This is considered to be an important stage in the design process because it enhances the robustness characteristics of the overall control scheme.

A brief discussion is included on implementing the adaptive algorithm. The pragmatic issue of having to accommodate a fractional delay that arises when evaluating the process control signal is covered comprehensively. In addition, guidelines to the initialisation of various free controller parameters are provided.

Finally, the performance characteristics of the adaptive algorithm are examined with reference to its application to two real devices. The first of these is a d.c. servomotor and the second an electro-hydraulic servomechanism; both are configured as position control systems. Evaluation of control system performance employed a variety of operating conditions and command input waveforms. Perturbations were deliberately induced in the dynamics of the controlled process to investigate the performance of the parameter adaptive system. During these tests, parameter adaptation was observed to be highly effective in maintaining a consistent level of model following behaviour.

ACKNOWLEDGEMENTS

I would like to the thank my parents as well as numerous friends and colleagues for their encouragement and assistance during the course of this research project.

Special thanks go to my supervisor, Dr. K.A. Edge, for his invaluable advice and guidance.

I also wish to acknowledge the help that I obtained through many useful discussions with Dr. N.D. Vaughan and my predecessor in adaptive control at Bath, Dr. I.M. Whiting.

I am also grateful to Mr. A. Rayment of the Fluid Power Centre and to Mr. D. Ashman and his technician colleagues for their assistance during the experimental stages of this project.

Finally, I would like to extend my gratitude to the University Of Bath for providing the finance and facilities which made this project possible.

CONTENTS

Title Page No.

Title Page No.

NOTATION

$A(z^{-1})$	denominator of controlled process transfer function
a_i	i^{th} coefficient of the $A(z^{-1})$ polynomial
$A'(z^{-1})$	denominator of reference model open loop transfer function
a'_i	i^{th} coefficient of the $A'(z^{-1})$ polynomial
$A_m(z^{-1})$	denominator of reference model closed loop transfer function
$a_{m,i}$	i^{th} coefficient of the $A_m(z^{-1})$ polynomial
$B(z^{-1})$	numerator of controlled process and reference model transfer function
b_0	controlled process forward path gain
b_m	reference model forward path gain
$C(z^{-1})$	error filter transfer function
c_i	i^{th} coefficient of the $C(z^{-1})$ polynomial
$\underline{\mathbf{d}}$	fixed compensator parameter vector
$\underline{\hat{\mathbf{d}}}$	adjustable compensator parameter vector
e^o	'a priori' reference model-process output error
e	'a posteriori' reference model-process output error
$F(z^{-1})$	process loop forward path compensator transfer function
f_i	i^{th} coefficient of the $F(z^{-1})$ polynomial

$G(z^{-1})$	process loop feedback path compensator transfer function
g_i	i^{th} coefficient of the $G(z^{-1})$ polynomial
h	variable dead-band filter output
K	continuous-time process forward path gain
$q(\epsilon h, \nu)$	variable dead-band function
$\tilde{r}$	order of reference model and process time delay term
s	Laplace transform operator
T	sampling period
u^p	partial evaluation of controlled process drive signal
u'	controlled process drive signal (from D/A converter)
u	control signal to D/A converter
w	input command signal
x	reference model output
y	controlled process output
z	z-transform operator

SUBSCRIPTS

m	reference model

GREEK SYMBOLS

Γ	adaptive gain matrix
γ_1	adaptive gain
ϵ_0	constant input signal to variable dead-band filter
ϵ	variable dead-band filter gain
ν^o	'a priori' filtered output error
ν	'a posteriori' filtered output error
ζ	continuous-time process damping coefficient
σ_0	variable dead-band filter pole location
τ	continuous-time process time constant
τd	controlled process time delay
$\underline{\Phi}$	observation vector
$\underline{\tilde{\Phi}}$	filtered observation vector
ω_n	continuous-time process natural frequency
ω_w	pseudo frequency

ABBREVIATIONS

A/D	Analogue to Digital (converter)
B.C.P.L.	Basic Combined Programming Language

D/A	Digital to Analogue (converter)
M.R.A.C.	Model Reference Adaptive Control
P.R.B.S.	Pseudo Random Binary Signal
P.Z.	Pole-Zero
S.P.R.	Strictly Positive Real
S.T.C.	Self-Tuning Control
V.D.U.	Visual Display Unit
Z.O.H.	Zero Order Hold

CHAPTER 1

INTRODUCTION

1.1 COMPUTER ASSISTED CONTROL ENGINEERING

The field of control engineering has achieved considerable prominence in recent years. Several reasons can be put forward to explain this phenomenon. One explanation derives from the need to upgrade the performance of existing systems; improvements are being sought through the use of versatile, software based controllers, as opposed to major reconfigurations of existing hardware systems. Similarly, technological advances and the design of complex new mechanisms also pose considerable challenges to practitioners in the field of control engineering. Developments such as these are unlikely to abate in coming years. Moreover, an increased awareness and greater utilisation of control engineering techniques seem assured in future years. This observation gains added importance in view of the fact that 5-year-olds will soon be able to experiment with computerised control systems [1].

Computers have long been used in the field of control engineering as a tool for system analysis and controller evaluation. Recently however, there has been a significant increase in the attention being paid to the synthesis and implementation of computer based control systems. This development is attributed to two main factors; namely, a greater awareness of novel controller design techniques [2] and, an increased availability of relatively low cost micro-processor systems.

Much of the early work with digital control systems followed classical approaches to control system synthesis. In general, digital control systems were analysed and designed using the same techniques and knowledge base accumulated from working with pure analogue systems. Only then were the resulting controllers reconfigured into a form suitable for computer system implementation. Typically, this design procedure would consist of carrying out some form of identification on the process to be controlled; as examples, common procedures include frequency response analysis using either sinusoidal or Pseudo-Random Binary Sequence (P.R.B.S.) test signals. Subsequently, compensator design would be

carried out on the basis of data culled from the identified transfer function. Control system implementation then followed, once the compensator scheme had been translated into a discrete form acceptable for computer realisation. As with most schemes, there was also the expectation of having to carry out some final 'on-line' fine tuning of the compensator.

Gradually, as the attributes of computer based control systems achieved wider acknowledgement, control system synthesis began to be carried out using sampled data theory. This necessitated some modification to the way that the control system was represented. In essence however, the same basic design strategy as before was pursued. That is; process identification, compensator design and finally control system implementation. Since control system synthesis was carried out within a discrete context however, components of the control system were consistently represented with discrete transfer functions. The most tangible benefit of this switch in design procedure was the avoidance of numerous transformations from continuous-time to discrete transfer functions and vice-versa. It also implied a more accurate representation of the control system.

A greater familiarity with discrete control system synthesis also lead to a proliferation of novel controller techniques. Some of these, such as dead-beat control, had no counterpart in the analogue sense. Moreover, supplementary features were being added to very simple control schemes as a means of incorporating desirable, non-linear forms of control action. The ease with which such complex control algorithms could be implemented meant that attention was soon being devoted to integrating more sophisticated features into the basic control scheme. The justification for more advanced forms of control are self-evident. The evolution of complex devices and the emergence of novel areas of engineering applications mean that new problems are constantly being encountered in control engineering. Hence, as pointed out in [3], earlier methods of control system synthesis need to be reviewed in the light of more stringent performance specifications. Another issue that should also be considered is that classical control design procedures are essentially based on identified process transfer functions which are assumed to be linear and largely time invariant. Understandably, such simplifications are frequently very useful and even necessary to facilitate control system analysis and synthesis. Nevertheless, potential difficulties can arise all too easily, at a later stage, because the entire analytical process relies on the integrity of

an identified process transfer function; in many cases, this is liable to vary according to the control system operating condition and the particular test method used in the identification procedure.

1.2 ADAPTIVE CONTROL

The theoretical branch of adaptive control has developed in parallel and at much the same rate as computer controlled systems in engineering. Activity in the field of adaptive systems can be associated with two main aspirations [4]. In the first of these, adaptive systems theory offers one possibility for developing the concept a control loop tuning algorithm. With this approach, an adaptive mechanism could be set up to carry out an identification procedure, on some system of interest, automatically. Information gained in this manner could then be used to design a fixed compensator scheme, in accordance with some pre-defined performance specification. Such a facility would prove useful in situations where variations in the controlled process dynamics are not expected to be significant or, where the benefits of a full adaptive control scheme are not considered to be indispensable. A notable benefit of such a scheme would be the standardisation of a controller design methodology as a result of automating the control system synthesis procedure. It would also be of considerable assistance to plant operators as a learning tool and in initialising control system compensators. This would be a direct consequence of its capability to provide information on the identified transfer function of the process under examination.

The second of the two motivating factors behind adaptive systems involves a more complex realisation of the scheme described above. Now, instead of using the adaptive algorithm as a once-off tuning mechanism, it could be modified to operate continuously. The concept of a fully adaptive control system seems highly desirable in cases where fixed control schemes are liable to falter, as in controlling processes susceptible to time dependent variations in their dynamics. An extreme example of this type of problem concerns the control of multiple degree of freedom, load carrying manipulators [5].

Conceptually, the two forms of adaptive system discussed above call for a control system comprising the following elements. The basic control loop obviously includes a controlled process. In addition however, it must also include some form of compensation. The goal of the adaptive system is to obtain a pre-specified level of behaviour from the control loop. This is made possible by designing the compensator in a manner which causes the complete controlled process loop to behave in accordance with some desired performance specification. The adaptive part of this control scheme calls for a mechanism that is responsible for adjusting the compensation network. This becomes necessary whenever the dynamics of the controlled process change by a significant amount, as this implies a corresponding divergence from the desired level of control system performance.

In the light of these statements, the marriage of micro-processor systems and adaptive control techniques seems a logical progression of their parallel developments. Micro-processor systems offer considerable scope for the implementation of complex control schemes with relative ease and flexibility. Current systems boast significant information storage capacities and constantly improving speeds of operation. Transportability is gradually becoming less of a problem both in terms of software realisation and the physical size of computers. These aspects are complemented by studies into adaptive control theory, which have ably demonstrated their potential [6-9]. It has also been shown that adaptive algorithms can be computationally intensive but are of a form which can be readily accommodated by micro-processor systems [10,11].

The material covered in this thesis considers the design and application of an adaptive control strategy. Motivation for the study is attributed to a desire to evaluate the potential of linking adaptive control theory and the increasing availability of relatively low cost, powerful micro-processor systems.

Until recently, considerable attention has been devoted to the purely theoretical aspects of adaptive control. When applications have been reported, they have generally been on systems with very slow response times. Failing this, experimental investigations with various adaptive algorithms have frequently been undertaken and validated within the context of simulations. Relatively little information is to be found on the problems associated with implementing adaptive controllers on real processes. This is especially true of the added complexity that

arises from having to take their inherent non-linearities into account. These are bound to place certain constraints on the levels of performance that can realistically be attained.

If the ideas of adaptive control systems are to achieve wider acceptance amongst the industrial community, greater effort has to be expended on research into practical applications. The development of adaptive systems and the presentation of experimental results should ideally be of a form that empathises with the working methods of practising engineers. The highly mathematical bias of a great deal of current adaptive systems theory significantly restrains wider use of this branch of control engineering. One of the aims of this study is to translate a portion of the considerable amount of theoretical material that is available into a readily usable form. The path that is followed involves the development of a systematic adaptive controller design methodology. The design procedure is subsequently applied to two real position control servo-systems. A number of tests are carried out to evaluate the effectiveness of these applications.

One of the primary objectives of this thesis is the development of a general controller design procedure. There exists a number of different approaches to the problem of adaptive control. The choice of method that will be pursued is made below, once the various options have been explored.

1.3 ADAPTIVE CONTROL TECHNIQUES

Although not universally acknowledged, the main approaches to adaptive control can be separated into three areas [4,12]; gain scheduling, self tuning control (S.T.C) and model reference adaptive control (M.R.A.C). Discussion still continues on the correctness of including gain scheduling as an adaptive control technique. It is hoped that the reasons for these differences of opinion will become clearer, upon closer examination of each of the three approaches.

1.3.1 GAIN SCHEDULING

Successful implementation of a gain scheduling form of adaptive control requires a considerable amount of prior knowledge about the controlled process. The reason for this concerns the way in which the adaptive control scheme is formulated. Basically, the controlled process needs to be rigorously examined over the entire range of operating conditions likely to be encountered in practice. Significant variations in process behaviour, over the operating range, can then be identified from the test results. From such information, localised operating regions are delineated, where the process behaviour is considered to remain acceptably constant. Analysing each of the operating regions in turn, a controller design procedure is instigated. This process is repeated for each of the localised operating regions that span the process operating range. The object of this exercise is to achieve a consistent and acceptable level of performance by specifying a suitable form of compensation for each distinct region. In this way, consistent control system performance can eventually be assured by switching between compensators, according to the appropriate process operating condition [12].

The term gain schedule derives from the setting up of a schedule or table. This relates the gains of a compensator, with a fixed structure, to one or more monitored, auxiliary variables which characterise the process operating point.

The greatest advantage of the gain scheduling technique arises from the relative simplicity of its implementation. However, it also possesses a number of drawbacks. One of these is that a potentially large number of auxiliary signals may need to be monitored if the process operating condition is to be deduced correctly. This could have serious implications in terms of cost and the possible need for specialised forms of transducers. An additional source of problems is that it might not always be possible to monitor important system parameters. An example cited here is the wear associated with different system components; these could easily give rise to significant changes in system performance. Another drawback of the gain scheduling technique relates to its problem specific nature. As a consequence, a detailed system evaluation procedure would be necessary for different applications.

In terms of assuring correct control action at all times, difficulties could arise as a result of the open loop nature of the gain scheduling technique. This means that it would be possible for an incorrect schedule to be selected, and remain undetected, as long as the monitored auxiliary variables remained unaffected. The open loop nature of this scheme goes some way towards explaining its occasional exclusion from the adaptive control system set. This precise lack of feedback action was probably a contributory factor in motivating research into closed loop forms of adaptive control.

1.3.2 SELF TUNING CONTROL

Figure 1:1 shows an example of a self tuning controller in its simplest form. The controlled system comprises a tunable compensator and a process to be controlled. The adaptive part of the control scheme can be broken down into two stages [13,14]. The first of these involves an identification procedure. The identification block of figure 1:1 contains a model of the controlled process. In the context of a sampled data system, this model would be expressed as an algebraic transfer function, using, for example, z-Transform notation. Initially, the numerical values of its coefficients are unknown. The model acts as the basis for the process identification routine. Since the model exists within the computer system, it is a relatively straightforward matter to assign numerical values to the coefficients and to adjust them.

Within the identification block of figure 1:1, a recursive least squares type of algorithm is applied to the process input-output information to identify its transfer function [15,16]. This is achieved by gradually adjusting the numerical values of the software implemented process model coefficients. Input signals to the controlled process are simultaneously fed to the adjustable model. Using exactly the same driving signals for the two systems, the response of the adjustable model is evaluated and compared with that of the actual process. The difference between the two responses is used as a measure for updating the coefficients in the process model. Successful identification is obviously accomplished once the process model mimicks the behaviour of the actual process itself.

The identified process transfer function is used, in the second stage of the adaptive scheme, to design a suitable compensator. This step is carried out on the basis of some pre-defined performance criterion. A number of different compensator design schemes are possible. Notable examples include such forms of control action as minimum variance, dead-beat [17] and LQG (Linear Quadratic Gaussian) control [18].

Just as there exists several alternative forms of control action, so the same applies for the recursive estimator used to generate the coefficients of the process model [19]. In fundamental terms, common patterns can be discerned in these algorithms. Variations do however arise, in terms of the measures used to reduce the computational burden of the estimator algorithm, for example [20,21]. The same is true of the different schemes put forward to improve the robustness properties of the estimator algorithm [13,21-23]. This last issue can pose quite a serious problem. Any breakdown in the identification stage of the adaptive scheme is liable to have disastrous consequences on control system performance. This type of situation is likely to arise when data fed to the identification algorithm is of an insufficiently rich quality. The most obvious example of such an eventuality is the case of a steady input to the controlled process. The lack of dynamic information makes it impossible to carry out a meaningful comparison between the response of the process and its identified transfer function.

1.3.3 MODEL REFERENCE ADAPTIVE CONTROL

A schematic representation of a model reference adaptive controller is shown in figure 1:2. As its name implies, the desired performance characteristics are specified in terms of a reference model transfer function. In common with gain scheduling and self tuning control, the controlled system includes a controlled process and a tunable compensator [12,24].

The reference model in figure 1:2 is operated in parallel with the controlled system. This configuration means that the response of the reference model to the command signal, w, can be readily compared against that of the controlled process loop. The model reference control objective is one of making the process loop behave in an identical fashion to the reference model system. Satisfaction of this

condition implies that the difference between the output from the reference model and process is zero; this difference signal is more commonly referred to as the output error signal [24].

In attempting to meet the model following requirement, the output error signal is fed to a suitably designed adaptation algorithm. Its task is to adjust the tunable compensator in a manner which reduces the output error to zero. Once this has been achieved, the control objective is satisfied and adaptation stops. Should, at some later stage, the process dynamics alter, then the error term becomes non-zero. As before, suitable corrective action ensues through the adaptation algorithm being reactivated.

Unlike the self tuning controller described in the previous section, the control objective of this scheme is fixed. This is a direct consequence of the lack of a process transfer function identification routine.

Early work on M.R.A.C. was based on an intuitive derivation of adaptive laws [4,25]. The abject failure of some of the resulting adaptive controllers led to a temporary lull in interest in this area of control systems. Towards the early 1970s, attention was once again focused on this subject. Part of the motivation for this change was the development of other branches of control theory and the ever increasing availability of versatile micro-electronic products [4]. The renewed vigour of researchers led to greater attention being devoted to the development of formal techniques for designing adaptive controllers. One consequence of this outcome was the emergence of a mathematical treatment of the subject, centered on stability considerations. Early adaptive system analysis was carried out in conjunction with Lyapunov's stability theory [26-28]. Later, attention was also turned to hyperstability theory, based on work carried out by Popov [29]. The application of such techniques to designing adaptive control systems has shown that a wide class of adaptive laws can be derived [24]. This is clearly advantageous in terms of offering the control engineer a greater degree of choice. Before this ideal can be realised however, the current body of adaptive control theory needs to be cast in a more favourable mould, such that it offers greater attractions to practising control engineers.

1.4 SELECTION OF ADAPTIVE TECHNIQUE

The work reported in this thesis aims initially to develop a systematic adaptive controller design procedure. Ideally, this should be a general procedure which calls for a minimum amount of prior knowledge about the controlled process. These requirements immediately rule out the gain scheduling option as it is arguably applications dependent. Moreover, it has already been demonstrated that the open loop form of this approach places a question of doubt over the true nature of its adaptive properties. By contrast, the alternatives of S.T.C. and M.R.A.C. appear to offer a clear opportunity to develop a general design procedure that is also flexible.

Considering the two main-stream approaches to adaptive control, much of the work being carried out currently, centers on adaptive systems based around S.T.C. [11,13,30,31]. This has contributed to the building up a considerable body of information on a range of adaptive algorithms and factors associated with their implementation. By comparison, less information is available on the realisation and performance of digital M.R.A.C. schemes.

A simplistic examination of the self tuning concept indicates a two step adaptive control procedure. Conversely, the model reference approach involves a single step scheme. Clearly, these factors confer certain benefits and disadvantages on the two approaches. Without doubt, the self tuning avenue offers the practising engineer a greater choice in terms of the extent of adaptive system complexity that can be included in the control system synthesis [13]. At the lowest level of involvement the identification procedure can be used, quite simply, for that purpose alone [19]. This increases its applicability to other areas of engineering such as condition monitoring. Here, for example, changes in the identified transfer function could be used as advance warning of machine wear or imminent failure. Further applications can also be envisaged, this time within the context of automatic controller design. This would comprise a single pass identification procedure, carried out with the intention of characterising a given process. Once an identified transfer function has been obtained this information could be applied to designing compensation schemes from the wide choice that is available [32]. This would clearly be useful where the designer is interested in realising a fixed compensator scheme. An extension of this procedure could be applied to setting up a

comprehensive gain schedule. In this case, a self tuning scheme could be tailored to identify the transfer function of a given process and use this data to specify the coefficients of a given form of compensation network. This procedure would be applied, almost mechanically, to set up a comprehensive gain schedule for later use. Finally, it is possible to design and employ fully adaptive control systems, dedicated to a given process. The depth and breadth of choice can be considered a disadvantage, in complicating matters by offering too many options to those unfamiliar with adaptive systems. In contrast to S.T.C., the M.R.A.C. approach does not offer a similar degree of flexibility or as wide a range of options in terms of applications; its sole rationale is to provide consistent control system performance. The very simplicity of this objective should be considered a positive attribute.

The computationally intensive nature of adaptation algorithms commonly associated with S.T.C. is a recognised problem [13]. A considerable amount of literature has been published on this aspect in recent years. More recently, practical applications of adaptive control schemes have been forced to confront and overcome this phenomenon. Some of the modifications to control system implementation that have been proposed are both practical and ingenious [13,20]. Such factors offer yet more reasons for studying whether the computationally intensive nature of such schemes can be circumvented by an M.R.A.C. approach. A cursory examination of some of the most commonly employed parameter estimation algorithms in M.R.A.C. goes some way towards supporting this viewpoint [33,34].

Since the S.T.C. concept effectively relies on a two stage, series adaptation procedure, the possibility of control system failure is increased; the second stage of compensator design can not be carried out successfully if the identification routine malfunctions. The situation cited earlier, for example, concerns the case where there is no dynamic input to the controlled process in figure 1:1. Under such circumstances, there is clearly insufficient information for identification to proceed usefully [20]. An alternative scenario concerns the identification of a high order system when it is being driven with a sinusoidal signal [13]. Clearly, it would be possible for a large number of systems, each possessing different dynamic characteristics, to respond to this particular input in a singular fashion. Identification is guaranteed to fail because the excitation signal is what is commonly termed, not 'sufficiently rich' [35,36]. Difficulties in this sphere of the adaptive system risk jeopardising the quality of behaviour of the overall control system. It

is more difficult to make this criticism of the M.R.A.C. of figure 1:2 since it does not depend on identifying the controlled process transfer function. The latter remark contributed significantly to the choice of a model reference option in preference to a self tuning approach. Two supporting factors in this decision are a general awakening of interest in this technique and a need for greater information on its performance capabilities.

A common complaint about adaptive control in general concerns the unhealthy bias towards validating control schemes by computer simulation. This criticism is equally as valid when applied to the paucity of information on applications and performance data [31,37]. Calls are periodically made for greater efforts to be directed towards the implementation of adaptive controllers on real processes [38]. The material presented here is an attempt to redress such imbalances. Moreover, by adopting the M.R.A.C. approach, it offers an opportunity to examine a less thoroughly researched area of adaptive systems.

1.5 ORDER OF PRESENTATION

In an attempt to maintain a logical order of presentation, the contents of this thesis are arranged into three main parts.

The first of the three parts comprises chapters 2 through to 5. These deal with the theoretical aspects of adaptive control. Initially, a rudimentary explanation of the definitions and concepts of adaptive control schemes are presented. The basic ideas introduced in chapter 2 are subsequently expanded upon when considering the detailed design of an adaptive control system. The procedure that is followed begins by defining the essential components of a fixed compensator control system. This task is divided between chapters 3 and 4. A suitable parameter adaptive algorithm (P.A.A.) is then developed, on the basis of the previously defined generalised control system. The full adaptive control scheme results from marrying the parameter adaptive algorithm to the basic control scheme.

The second part of the presentation spans chapters 6 and 7. These deal with various aspects of implementing the adaptive controller. The basic adaptive control scheme is developed within the framework of an idealised system representation. Therefore, as a precautionary measure, suitable supervisory functions are appended to the control scheme. This reflects the physical limitations that arise from controlling real systems. The modifications that are made are discussed in chapter 6. Various aspects relating to the adaptive controller software realisation are dealt with in chapter 7. A section dealing with the initialisation of various free design parameters in the adaptive control algorithm is also included.

The third part of this thesis considers the application of the adaptive controller design method to two real systems. These are dealt with on an individual basis in chapters 8 and 9. Chapter 8 deals with an angular position control system, based around a d.c. servomotor. A similar scheme is presented in chapter 9 although it deals with a much larger scale system involving an electro-hydraulic linear position control servomechanism. Comprehensive accounts are provided on the actual design and implementation procedures for each system. Test results covering a variety of operating conditions are finally presented and discussed.

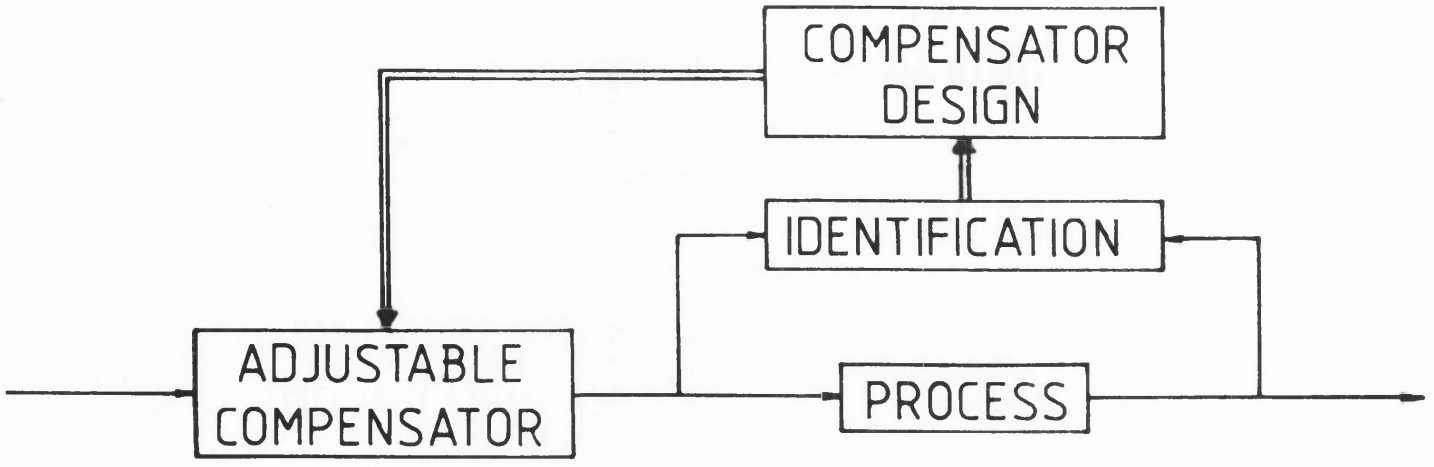

FIGURE 1:1 Schematic Representation Of A Self Tuning Controller

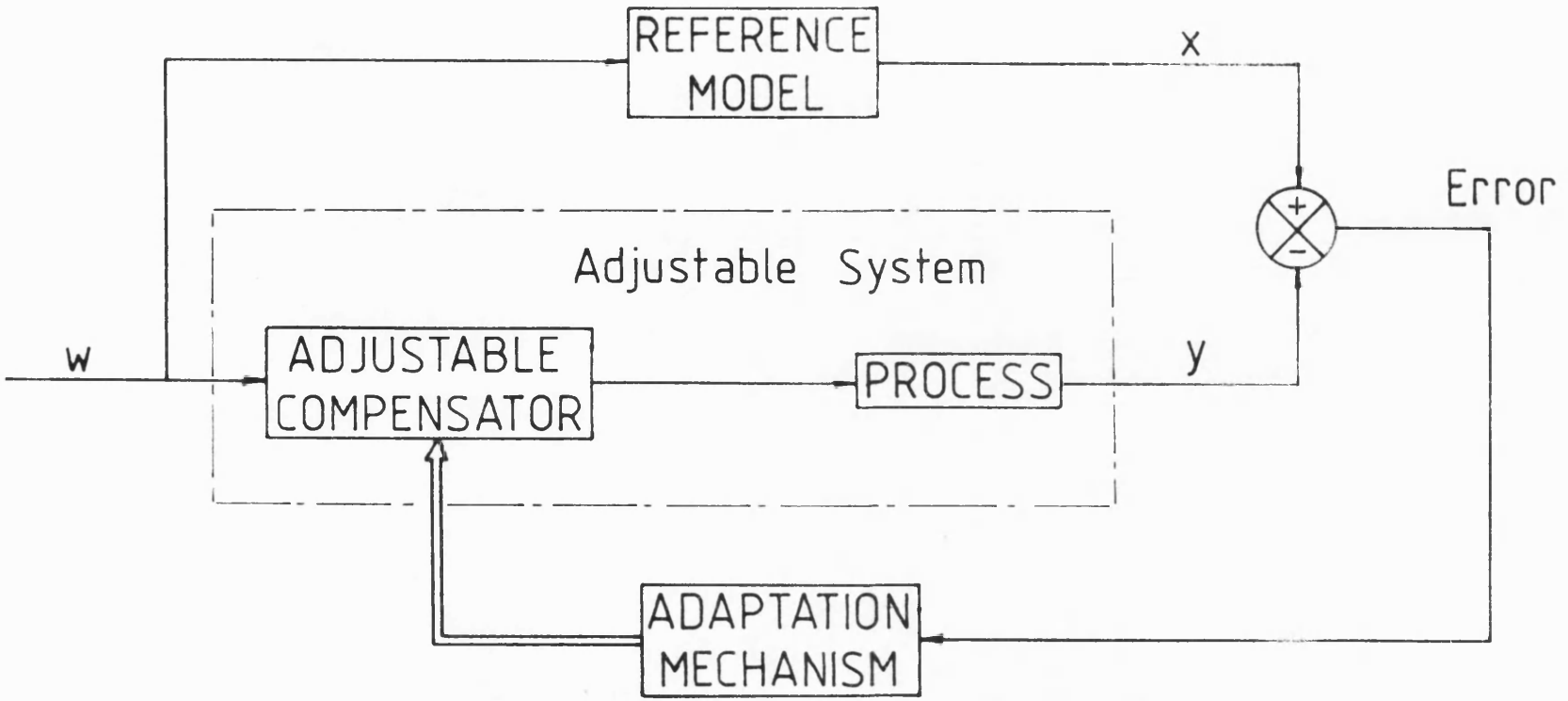

FIGURE 1:2 Schematic Representation Of A Parallel Model Reference Adaptive Controller

CHAPTER 2

THE MODEL REFERENCE ADAPTIVE CONTROL CONCEPT

2.1 INTRODUCTION

The M.R.A.C. scheme that is presented in this thesis represents one particular interpretation of the existing body of adaptive control theory. Consequently, before it is described more fully, a comprehensive introduction to some preliminary aspects of adaptive control will be undertaken.

The title 'Adaptive Control' is all embracing and open to differing interpretations; this fact can be appreciated simply by comparing the three main forms of adaptive control presented in the introductory chapter of this thesis. As with any other specialised field therefore, a certain amount of technical jargon has been conceived to try and differentiate between various sub-topics in adaptive control. The most commonly encountered, and therefore useful, terms will be introduced in the subsequent sections of this chapter. They relate entirely to self tuning and model reference forms of adaptive control. As will become evident, a certain degree of duality between terms of definition from the two fields can be perceived.

2.2 DIRECT AND INDIRECT ADAPTIVE CONTROL

Although they appear outwardly different, self tuning and model reference adaptive control schemes display a number of close similarities [4,24]. These become most apparent in terms of the M.R.A.C. adaptation and the S.T.C. identification algorithms. Ultimately, their tasks involve generating a set of parameters, be they of an identified transfer function or a compensator network. For this reason, they are frequently referred to as parameter adaptive algorithms (P.A.A.).

Structurally, the model reference and self tuning parameter adaptive algorithms bear a strong degree of resemblance. Distinctions do nevertheless arise. Amongst others, some of these concern the realisation of the adaptive control scheme and the way in which the parameter adaptive algorithms are employed [13,39]. One of the most frequently cited characteristics concerns the way in which the tunable compensator is adjusted. For example, the self tuning controller of figure 1:1 employs an indirect form of adaptive control. This is because the compensator is adjusted on the basis of an identified transfer function. Conversely, the model reference scheme of figure 1:2 is termed a direct adaptive controller because the compensator coefficients are generated directly, by a recursive algorithm within the adaptive mechanism.

2.3 EXPLICIT AND IMPLICIT IDENTIFICATION

Another method for highlighting subtle differences between the M.R.A.C. and S.T.C. schemes concerns the way in which the controlled process is represented within the adaptive scheme. In the S.T.C. of figure 1:1, a recursive algorithm is used to generate the coefficients of an explicit model of the controlled process; this procedure constitutes the process identification stage. For this reason, it is known as an explicit self tuning controller. Conversely, the adaptive scheme in figure 1:2 is known as an implicit model reference adaptive controller. This is due to the fact that the compensator coefficients are generated directly, without recourse to an intermediate identification stage. It should be noted, however, that in specifying the structure of the compensator, some prior assumptions have to be made in modelling the controlled process. In retrospect, this implies the existence of a process model.

Obvious parallels can be drawn between the definitions of direct and indirect adaptive control and, explicit and implicit identification. Direct adaptive control and implicit identification both refer to a particular type of situation. By analogy, a similar link can be drawn between indirect adaptive control and explicit identification [4].

From these definitions, the dual nature of self tuning and model reference adaptive systems becomes more apparent [29]. In a model reference adaptive control scheme, the reference model is kept fixed. An adjustable system, containing a tunable compensator and a process, is altered to make it behave like the reference system. In a self tuning framework, the controlled process is emulated by means of an explicit model which acts as the adjustable system in this case. Similarities such as these between M.R.A.C. and S.T.C. are useful from a conceptual viewpoint. For example, better insight into the behaviour of an adaptive scheme can be facilitated by examining it in terms of such definitions. Conversely, it can be argued that the dual nature of these two schemes can result in unnecessary confusion, most notably in terms of the quantity of terminology that is available. In this thesis, the convention adopted is to associate S.T.C. with an indirect form, and M.R.A.C. with a direct form of adaptive control. Due to the unfortunate ambiguity with which certain definitions can be interpreted, this particular convention should be applied with caution in dealing with existing literature on adaptive control.

2.4 CONTROL SYSTEM CONFIGURATION

One other important way in which adaptive systems are described is in terms of the control system configuration [24]. These will be described in the context of M.R.A.C. systems, though they can be applied equally as well to self tuning controllers.

The most common control system configuration is the parallel M.R.A.C. as shown in figure 1:2. Conceptually, it is a relatively simple scheme to appreciate. This feature is probably a notable contributor to the relatively widespread acknowledgement of parallel schemes over the two other approaches described below. For its implementation, the reference model is selected on the basis of some desired performance criteria. The role of the adaptation mechanism is to assure this level of performance in the controlled system. The latter comprises a controlled process and an adjustable compensator network which combine to form an adjustable system. The ultimate goal of the adaptive controller is to have the two parallel paths behaving identically; this is especially important when changes occur in the dynamics of the controlled process.

A series M.R.A.C. can be placed at the opposite end of the adaptive control system spectrum. A generalised example is shown in figure 2:1. Although included here for completeness, this technique is rarely used due to the following drawback. As with the parallel scheme, the desired performance characteristics are specified in terms of a set reference model. When this reference model is incorporated into a series scheme however, an inverted version has to be used. This ensures that the adjustable system and series reference system transfer functions cancel when the control objective is satisfied. Consequently, the parallel paths, in figure 2:1, become identical and the error signal is nullified. Clearly, this set-up imposes a considerable restriction on the control schemes that can be attempted because of the pre-requisite for a stably invertible reference model.

The third alternative, a series-parallel scheme, draws on elements from the previous two approaches. A typical example is shown in figure 2:2. Basically, the reference model is separated in a way which permits one part of it to be operated in series, and the other in parallel with the adjustable system. For example, a transfer function, expressed as a quotient, can be separated in terms of its numerator and denominator parts. This allows one to be used as a series term and the other as a parallel one [24].

The series-parallel technique is used primarily in the context of explicit identification schemes. Problems concerning the physical impossibility of separating a real process into two constituent transfer functions are thereby simply overcome through dealing with an algebraically realised model. This software implemented model resides within the micro-processor system and is used as the transfer function around which an identification routine is built.

The use of a series-parallel configuration has been proposed within the context of a direct M.R.A.C. scheme. The suggestion for its use has been as a performance enhancing feature [8,41]. This can be justified by considering a state space realisation of parallel and series-parallel model reference schemes as shown in figures 2:3a and 2:3b. The reference model and controlled process loops share the following standard form of transfer function,

$$\dot{\underline{x}} = A\,\underline{x} + B\,\underline{u} \tag{2.1}$$

$$y = C\,\underline{x} \tag{2.2}$$

For clarity of presentation, the adjustable compensator in the controlled process loop has not been shown explicitly in figures 2:3a and 2:3b. The state space configuration of the controlled process loop actually represents the combination of an adjustable compensator and a controlled process.

The usefulness of the series-parallel mode of operation is demonstrated with reference to the following examples. Firstly, consider a case where the controlled process is subjected to an externally generated disturbance. It is likely that this phenomenon will affect the controlled process output. This would result in an adverse affect on the adaptation mechanism; the disturbance component in the process output signal would be interpreted as a parametric error between the reference model and controlled process loop. The second example highlighting the usefulness of the series-parallel technique was described in [41]. It was argued that perfect model following would not always be possible because of physical limitations in the controlled process itself. A degraded level of approximate model following, with the response of the controlled process limit cycling or 'hunting' about that of the reference model, was considered to be a more likely outcome. Clearly, while the limit cycles persist, parameter adaptation would continue to take place. In both of the cases discussed above, undesirable parameter adaptation occurs as a result of phenomena that have not been accounted for in designing the adaptive scheme. The series-parallel mode of operation offers one means of accounting for such effects. It can be argued that 'disturbances', in a general sense, acting on the controlled process have an effect on the output and other states of the controlled process. By operating the reference model in a series-parallel manner its state vector is made identical to that of the controlled process. If this procedure is carried out periodically, as indicated in [41], then the degree of parameter adaptation attributable to 'disturbances' can be reduced advantageously. This is a consequence of using potential disturbance signals in the controlled process loop to affect the reference model behaviour and hence the model-process error signal.

The three definitions of control system configuration described above relate predominantly to direct model reference adaptive control systems. Similar adaptive techniques used therein can also be applied to the recursive identification of the dynamic parameters of a given process. The estimation model of the process to be identified can be organised in three different ways [24]. Distinct relationships can be drawn between these three configurations and their direct model reference adaptive system counterparts. The following display summarises these links.

Adaptive Control	**Adaptive Identification**
Parallel Configuration	Output Error Method
Series Configuration	Input Error Method
Series-Parallel Configuration	Equation Error Method

In general, only one set of terminology is employed in literature on adaptive systems; this depends on whether the subject matter concerns identification or control.

2.5 THE MODEL REFERENCE CONTROL CONCEPT

A generalised, discrete parallel model reference control scheme is shown in figure 2:4. In this instance, the adjustable part of the process control loop comprises three compensators. These are given by the discrete polynomials $F(z^{-1})$, $G(z^{-1})$ and $T(z^{-1})$. The control objective of this scheme is perfect model following. For this to be achieved, the input-output relationships of the reference model and controlled process loop need to be made identical. In practical terms, this is the only condition which results in a zero output error, e(k), for some dynamic input, w(k).

In order to gain an appreciation of the role of the three compensator networks in figure 2:4, consider a controlled plant, as shown in figure 2:4, and represented with a continuous-time transfer function, G(s), of the form,

$$G(s) = \frac{\hat{b}_0+\hat{b}_1 s \ldots+\hat{b}_m s^m}{1+\hat{a}_1 s \ldots+\hat{a}_n s^n} \qquad m < n \tag{2.3}$$

$$= \frac{N(s)}{D(s)} \tag{2.4}$$

The control signal driving the process is computer generated and applied via a D/A converter. Assuming that the D/A converter acts as a zero order hold [42], an exact, discrete-time transfer function of the process can be derived. A transfer function of the following form, relating the response between the sampled input and sampled output, is obtained by using the hold equivalence transform technique [42].

$$\frac{y(z^{-1})}{u(z^{-1})} = \frac{(b_0 z^{-1}+b_1 z^{-2}\ldots+b_n z^{-n})}{1+a_1 z^{-1}\ldots+a_n z^{-n}} \tag{2.5}$$

$$= \frac{b_0 B'(z^{-1})}{A(z^{-1})} \tag{2.6}$$

where z can be considered as a shift (delay) operator. The negative indices in equation (2.5) indicate the delay factor associated with each signal element; this is expressed in terms of whole sampling periods. The behaviour of the continuous-time transfer function, equation (2.3), and the discrete one of equation (2.5) is identical, for some given input, only at the sampling instants. The examination of inter-sample behaviour calls for more complex levels of analysis.

The roots of the $A(z^{-1})$ polynomial of equation (2.6) bear a simple relationship to the poles of the continuous-time system. The same cannot be said of the $B'(z^{-1})$ polynomial in the numerator. Its roots are related to the finite zeros of the continuous-time system as well as being some function of the denominator roots and the sampling period [43].

Before considering the model reference control problem, it is necessary to complete the specification of the individual blocks in figure 2:4 and define a reference model. In carrying out this task, considerable importance needs to be attached to the following proposition. The development of an adaptive control scheme stands a greater degree of success if the controlled process is required to behave like a reference model with a similar structure to its own. To this end, the reference model open loop transfer function is specified on the basis of equation (2.5). In essence, the reference model transfer function should duplicate the orders of the numerator and denominator polynomials in the model of the process open loop transfer function. The same requirement applies to any time delay present in the original continuous-time transfer function. The controlled process is operated within a closed loop control system environment. The same is done for the reference model. Hence, a closed loop reference model transfer function is derived from an open loop transfer function, of the structure given in equation (2.6). The open loop transfer function is configured within a unity feedback closed loop system. This ensures that the reference model has unity steady state gain. For the purpose of the current discussion, the following expression is used to represent such a transfer function.

$$\frac{x(z^{-1})}{w(z^{-1})} = \frac{b_m B(z^{-1})}{A_m(z^{-1})} \tag{2.7}$$

The requirements for perfect model following can now be determined by equating the reference model and process closed loop transfer functions. With reference to figure 2:4, this condition can be seen to be satisfied by the following equation.

$$\frac{b_m B(z^{-1})}{A_m(z^{-1})} = \frac{b_0 B'(z^{-1}) T(z^{-1})}{A(z^{-1})F(z^{-1}) + b_0 z^{-1} B'(z^{-1}) G(z^{-1})} \tag{2.8}$$

By suitable design of the compensator networks $T(z^{-1})$, $F(z^{-1})$ and $G(z^{-1})$ in figure 2:4 the process zeros must be cancelled and replaced with the same zeros that occur in the reference model. A gain term in the $T(z^{-1})$ polynomial must also act to scale the parameter b_0 such that the combined gain of the two is equal to the reference model forward path gain, b_m. Simultaneously, the characteristic equation of the process loop has to be made equal to that of the reference model; it is possible to interpret the role of the $F(z^{-1})$ and $G(z^{-1})$ polynomials as affecting the two separate parts of the process loop characteristic equation, such that the whole may be made identical to $A_m(z^{-1})$, the reference model characteristic equation. When these conditions are satisfied, the parallel paths are identical; this implies that the control objective is being met.

The form of control action described above is known as pole-zero placement. The danger with this strategy is that any attempt at cancellation of process zeros outside the unit disc in the z-plane will result in an unstable system [42]. Such a situation will arise if the continuous-time system, preceded by a D/A converter, has non-minimum phase zeros. A similar outcome is also possible if the continuous-time system transfer function is of relative degree greater than one [43]. However, difficulties arising from this quarter are not easily predictable, since they vary with individual situations. This is a consequence of the $B'(z^{-1})$ process polynomial being a function of several variables. For example, it was shown in [43] that the choice of sampling period affects the zero locations in a discrete transfer function. One observation made was that a given continuous-time transfer function is more likely to have zeros outside the unit z-plane disc if it is sampled with a very short time interval.

The possibility of having to deal with discrete transfer functions having zeros outside the unit z-plane disc appears to place significant constraints on the applicability of discrete M.R.A.C. This problem has recently begun to prompt research into ways of overcoming it. In [44], the approach presented involved modelling the controlled process with an incremental difference operator, δ, instead of the more usual shift operator, z. The following simple relationship was specified between the two operators.

$$\delta = \frac{z-1}{T} \tag{2.9}$$

where, T is the sampling period. This technique was developed in an attempt to address the following paradox. Numerous results are available on the model reference control of continuous-time systems with relative degree greater than one. However, since such systems can give rise to non-stably invertible discrete systems, at fast sampling rates, discrete model reference control appears to be ruled out. Part of the motivation for using the alternative δ-operator was due to the fact that, at fast sampling rates, there exists a close connection between the exact continuous and exact δ-operator discrete models. By using this alternative representation, the authors proposed an adaptive scheme which avoided a pole-zero placement form of control scheme. In order to be fully effective however, this technique calls for fast sampling rates.

The approach presented in this thesis is to use an approximate model of the process, based on the shift operator, z, in a manner which overcomes the need for any zero cancellation. Although an approximation, the resultant model must nevertheless be such that the dominant features of the process are captured, albeit with some slight modelling error. The means developed to achieve this objective are addressed in chapter 3.

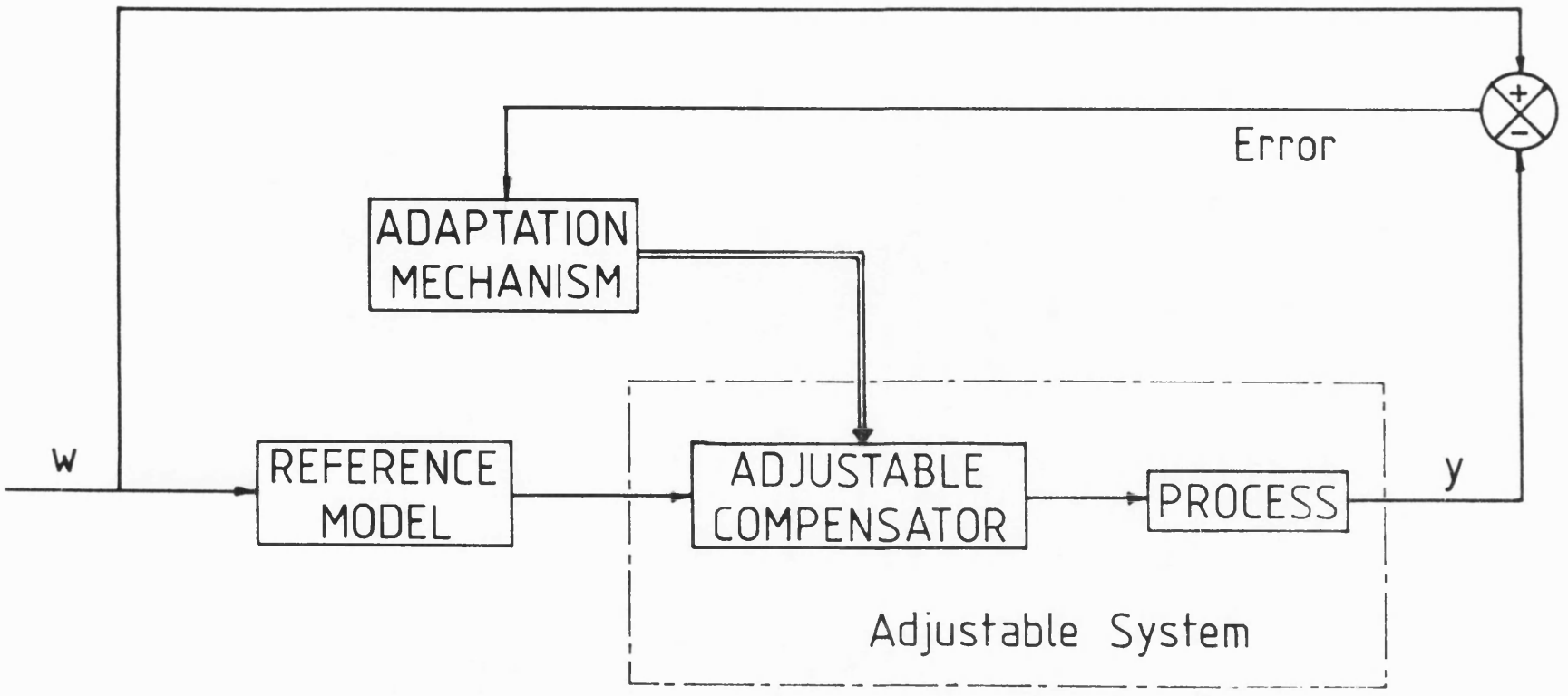

FIGURE 2:1 Schematic Representation Of A Series Model Reference Adaptive Controller

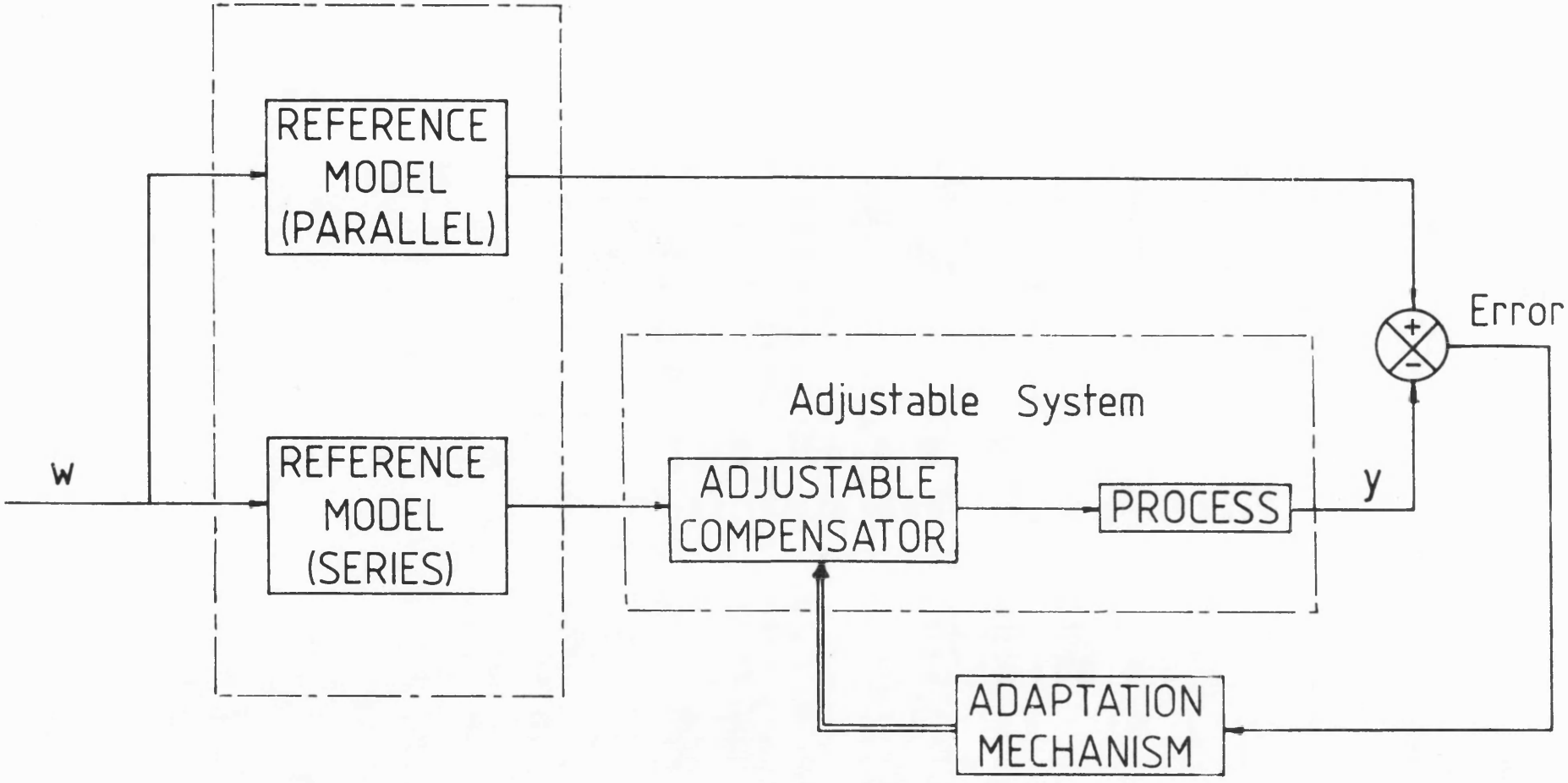

FIGURE 2:2 Schematic Representation Of A Series-Parallel Model Reference Adaptive Controller

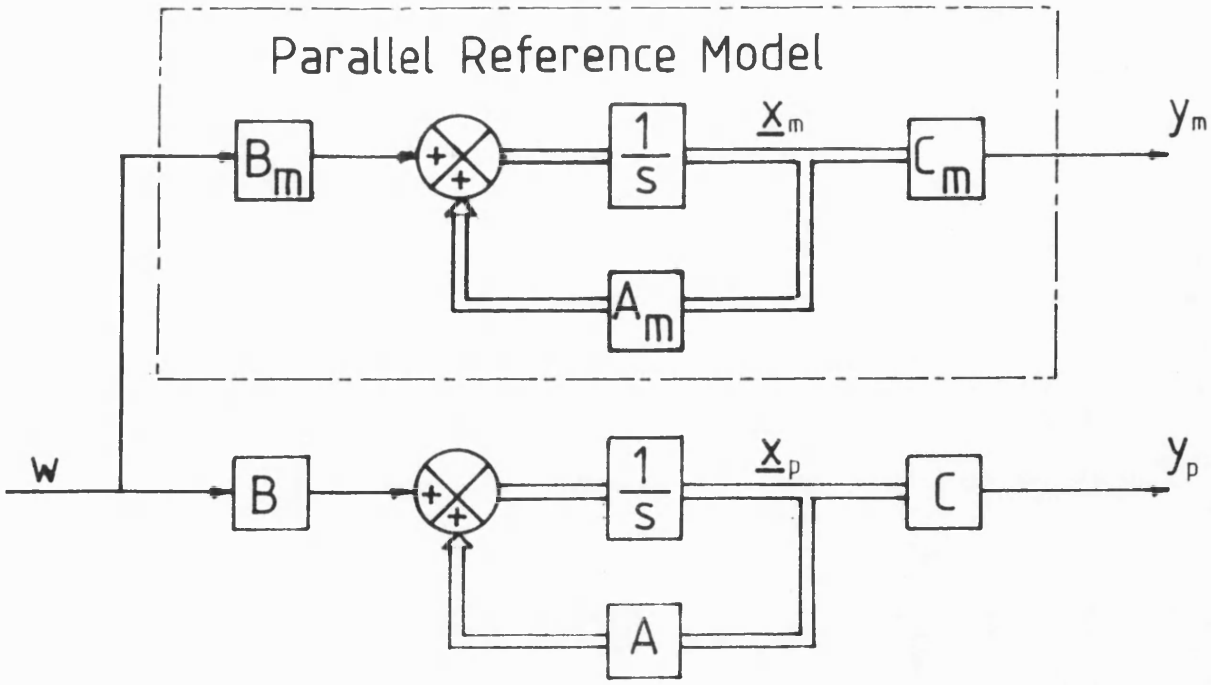

FIGURE 2:3a State-Space Configured Parallel Model Reference Adaptive Control Scheme

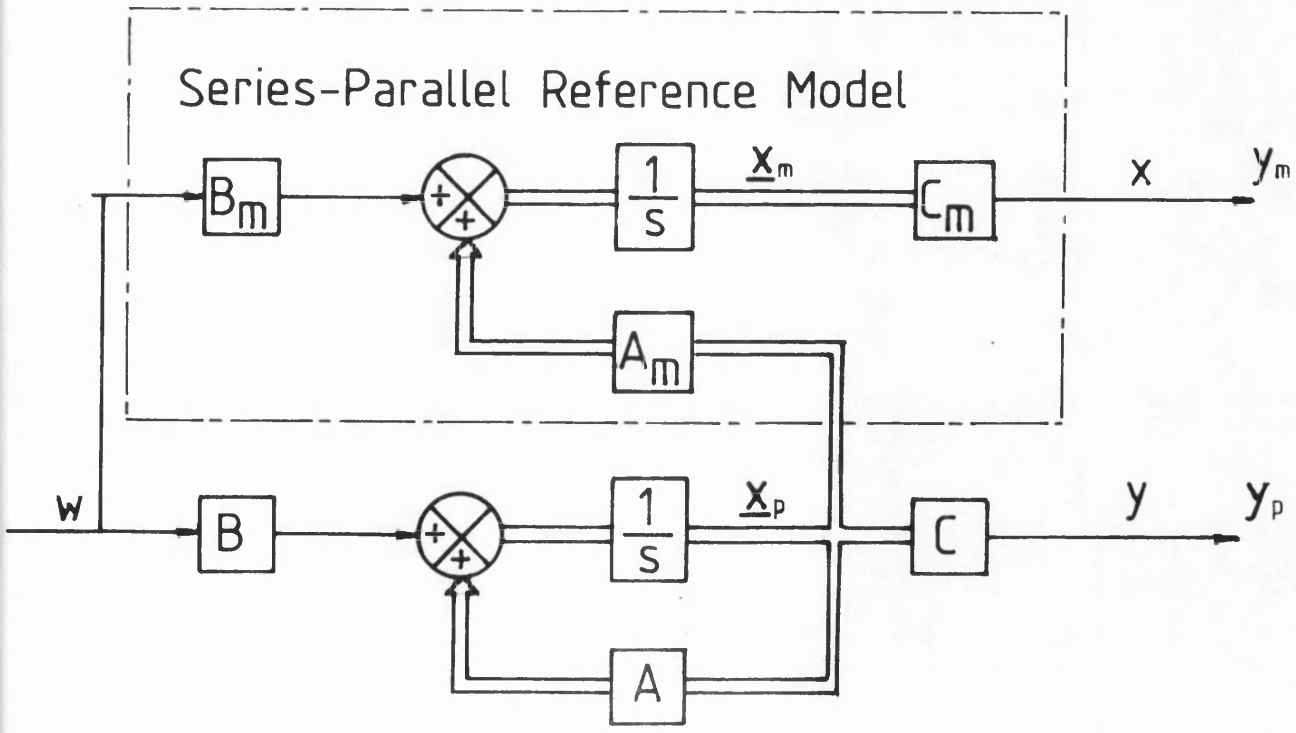

FIGURE 2:3b State-Space Configured Series-Parallel Model Reference Adaptive Control Scheme

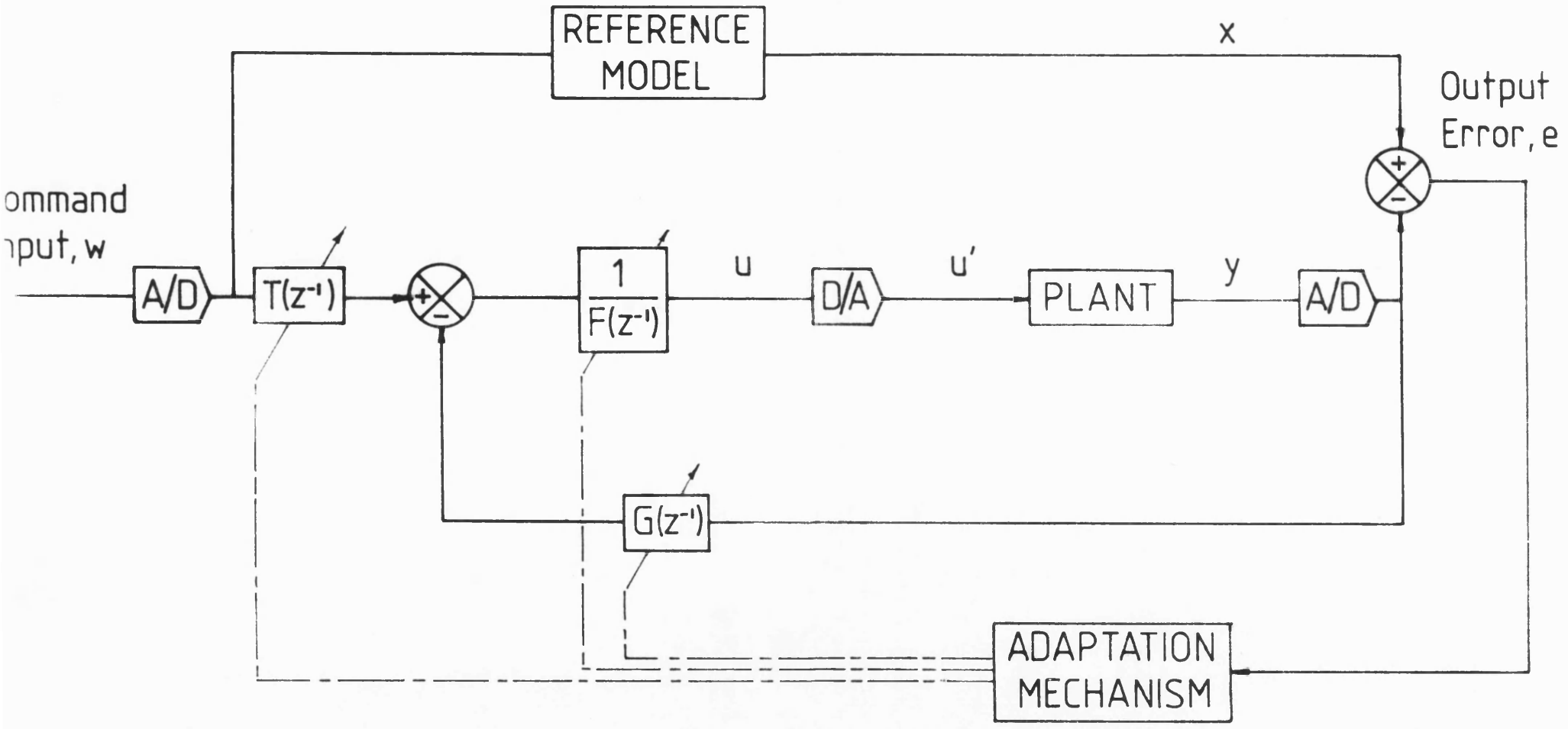

FIGURE 2:4 Generalised Discrete Parallel Model Reference Adaptive Control Scheme

CHAPTER 3

DISCRETE MODELLING PROCEDURE

3.1 INTRODUCTION

In the previous chapter it was shown how the exact method for modelling the controlled process could give rise to stability problems in a model reference control scheme. The twin areas of difficulty are continuous-time systems with non-minimum phase zeros and those which are of relative degree greater than one. Problems with the former do not arise in the material presented in this thesis. This is because the two applications considered involve processes which have been modelled with transfer functions free of finite, continuous-time zeros. In an attempt to overcome problems associated with the latter of the two difficulties, an approximate discrete process model is to be used. This discrete model is to be derived from its continuous-time counterpart by the pole-zero mapping procedure. The advantages of using this method will become evident, following a demonstration of its application.

3.2 THE POLE-ZERO MAPPING PROCEDURE

The pole-zero mapping procedure is applied through the use of the following set of heuristic rules. For a sampling period T, a discrete transfer function, $G_{P.Z.}(z)$, which approximates a given continuous-time one, G(s), is obtained from the following rules:

1) All poles of G(s) are mapped on the basis of the relationship, $z = e^{sT}$. If G(s) has a pole at $s = -p$, then $G_{P.Z.}(z)$ has a pole at $z = e^{-pT}$. Complex conjugate poles must be mapped together. Hence, a pair at $s = -a \pm jb$ will be mapped to $z = e^{-aT} e^{\pm jbT}$.

2) All finite zeros are mapped by the same relationship, $z = e^{sT}$, as before. Therefore, if G(s) has a zero at $s = -b$, then $G_{P.Z.}(z)$ has a zero at $z = e^{-bT}$. Complex conjugate zeros must be mapped together, in the same way as complex conjugate poles.

3) All infinite zeros of G(s) are mapped to the point $z=-1$ in $G_{P.Z.}(z)$.

4) Should it be necessary to model a unit delay in the digital filter transfer function then one infinite zero of G(s) is mapped as an infinite zero in the z-plane. This rule is included to accommodate phenomena such as a computational delay. Where G(s) does not contain a pure time delay then $G_{P.Z.}(z)$ is left with the number of zeros being one less than the number of poles in the continuous-time transfer function.

5) The gain of the discrete transfer function is selected to match the gain of G(s) at some critical frequency condition, depending upon the application. As examples, this could be the steady state gain of the continuous-time system (s=0) or, the central frequency in a passband filter network.

The reasoning behind rule 3) is that it caters for those cases where the continuous-time transfer function is zero at the highest continuous frequency. This permits the discrete transfer function to be assigned an analogous property, according to the following rationale. The concepts involved are diagrammatically represented in figure 3:1 which shows a unit disc in the z-plane. The locus of the circumference of the unit z-plane disc, travelling anti-clockwise from $z=1$ to $z=-1$, represents the range of real frequencies from $\omega=0$ to the Nyquist frequency, $\omega=f_N$. The Nyquist frequency corresponds to one half of the sampling frequency. Signals beyond this frequency, which correspond to continuing around the perimeter of the unit disc, are simply aliased, or repeated, versions of those in the range $0\leqslant\omega\leqslant f_N$. The point $z=-1$ thus represents the highest frequency possible in a discrete transfer function. The effect of placing a zero at $z=-1$ is to make the discrete transfer function have zero amplitude response at the Nyquist frequency. This helps to achieve an analogy with the continuous-time transfer function since it too has zero amplitude response at its highest frequency.

The use of rule 4) confers a characteristic structural property on the discrete equivalent of a delay-free continuous-time system. This feature can be verified by reference to standard tables relating s- and z-Transform transfer functions. An examination of [45], for example, makes it is clear that the numerator in the discrete transfer functions is consistently of a lower order than the denominator by a difference of one.

The use of the rules listed above is demonstrated in subsequent sections of this chapter.

3.3 PROCESS MODELLING

A discrete approximation to the continuous-time controlled process can now be derived in conjunction with the set of rules presented above. The first step is to select a nominal continuous-time transfer function, G(s), to represent the process. This can be carried out either by analysing the physical characteristics of the process or by carrying out a series of tests on it. As an example, consider that this stage has already been covered. From the information gathered, the designer selects a representative continuous-time transfer function, G(s). This is characterised as a type 1, n^{th} order servo-system, with a time delay of τd seconds, given by,

$$G(s) = \frac{\hat{b}_0 e^{-\tau d\, s}}{s(s-\hat{a}_1)...(s-\hat{a}_{n-1})} \tag{3.1}$$

The full implications of the modelling problem are summarised in figure 3:2. The accepted procedure in sampled data control system design is to use an effective model of the controlled process. This is obtained by combining the controlled process with the D/A converter preceding it. An effective transfer function is then derived for the cascaded elements. Referring to figure 3:2, the transfer function of greatest interest is that which relates the sampled input and output signals, u(z) and y(z), respectively.

The discrete transfer function corresponding to the transfer function of equation (3.1) and based on a sampling period of T seconds, is of the following form,

$$G_{P.Z.}(z) = \frac{b_0 z^{-\tilde{r}}(1+z)^n}{(z-1)(z-e^{\hat{a}_1 T})\cdots(z-e^{\hat{a}_{n-1} T})} \tag{3.2}$$

where,

$$(\tilde{r}-1)T<\tau d<\tilde{r}T \tag{3.3}$$

The continuous-time integrator is mapped to the point z=1 in the discrete plane. The poles of equation (3.1) are mapped according to the first rule of the pole-zero mapping procedure. Since the continuous-time transfer function has n infinite zeros, these are mapped as n discrete zeros at z=-1. To emphasise the input-output relationship of the controlled plant, equation (3.2) is expressed in terms of the relevant set of signals according to figure 3:2. Hence,

$$\frac{y(z)}{u'(z)} = \frac{b_0 z^{-\tilde{r}}(1+z)^n}{z^n + a_1 z^{n-1} \cdots + a_{n-1} z} \tag{3.4}$$

where, $u'(z)$ is the output from the D/A converter, driving the process in figure 3:2.

For the control scheme developed in this thesis, the D/A converter preceding the servo-valve acts as a zero order hold. Its presence prior to the controlled plant is acknowledged in terms of the delay element that it introduces [42]. Using rule 4) of the pole-zero mapping procedure, one infinite s-plane zero is mapped to $z=\infty$ in the discrete transfer function. This means that only (n-1) infinite continuous-time zeros should be mapped as discrete zeros at z=-1. Consequently, the transfer function that is used to model the controlled process becomes,

$$G(z) = \frac{y(z)}{u(z)} = \frac{b_0 z^{-\tilde{r}}(1+z)^{n-1}}{z^n + a_1 z^{n-1} \cdots + a_{n-1} z} \tag{3.5}$$

Adopting the delay operator convention throughout, this transfer function can be rewritten as,

$$\frac{y(z^{-1})}{u(z^{-1})} = \frac{b_0 z^{-\tilde{r}-1}(1+z^{-1})^{n-1}}{1+a_1 z^{-1} \cdots + a_{n-1} z^{-n}} \tag{3.6}$$

$$= \frac{b_0 z^{-r} B(z^{-1})}{A(z^{-1})} \tag{3.7}$$

where,

$$r = 1+\tilde{r} \tag{3.8}$$

and $u(z^{-1})$ is the computer generated control signal fed to the D/A converter in figure 3:2.

An important point to note is that the $B(z^{-1})$ polynomial can be expressed in a form which makes it one order lower than the number of infinite zeros in the continuous-time transfer function. This is a direct consequence of using rule 4) of the pole-zero mapping procedure to account for the D/A in series with the controlled plant.

3.4 FREQUENCY RESPONSE COMPARISON OF TRANSFORM METHODS

In section 3.3, application of the pole-zero mapping procedure was demonstrated with reference to a generalised continuous time transfer function. This section begins by presenting its use with a numerical example. The same example continuous-time transfer function is then used to derive a second discrete transfer function. This time however, the hold equivalence transform technique is used as the mapping procedure between the continuous and the discrete domains. A graphical comparison is made between the two, in terms of their frequency response characteristics.

The continuous time transfer that will be examined is given below.

$$G(s) = \frac{K\omega_n^2}{s(s^2+2\zeta\omega_n s+\omega_n^2)} \tag{3.9}$$

This expression represents a third order, type 1 servo-system. It does not incorporate a pure time delay.

The particular set of parametric values used for this study result in the second order denominator polynomial of equation (3.9) being characterised by a natural frequency of 10 Hz. and a damping coefficient of 0.4. In addition, a gain of 15 was selected for K. In the light of this choice of values, equation (3.9) can be

numerically expressed as,

$$G(s) = \frac{59217.6}{s(s^2+50.26s+3947.8)} \tag{3.10}$$

A sampling frequency of 10 ms. was chosen to examine the continuous-time system in the discrete sense. This choice of sampling frequency results in a Nyquist frequency of 50 Hz. The dominant dynamics of the continuous-time transfer function correspond to the 10 Hz. natural frequency. This should be accurately represented in the discrete transfer functions; the sampling frequency is ten times greater than the dominant continuous-time system dynamics. In addition, this choice falls comfortably within the bounds suggested in order to avoid problems with aliasing [42].

The continuous-time system under examination is cascaded with a D/A converter. In the process of deriving a discrete representation of this combination, attention is initially turned to the transfer function, G(s). Application of the pole-zero mapping rules to this expression results in the following discrete relationship.

$$G'_{P.Z.}(z) = \frac{b_0(1+z)^3}{(z-1)(z^2-1.3z+0.605)} \tag{3.11}$$

Three infinite continuous-time zeros are mapped as discrete zeros at z=-1 according to rule 3) from section 3.2. However, when an effective transfer function for the controlled process is developed it is necessary to consider the D/A converter cascaded with the continuous-time system. This entails mapping one infinite s-plane zero as an infinite z-plane zero. It reduces the relationship of equation (3.11) to the following,

$$G_{P.Z.}(z) = \frac{b_0(1+z)^2}{(z-1)(z^2-1.3z+0.605)} \tag{3.12}$$

The last stage of the pole-zero mapping procedure entails specifying a transfer function gain, b_0. According to rule 5), this is carried out by matching the amplitude response of the continuous-time and discrete transfer functions at some critical frequency. Since it includes an integrator, the continuous-time transfer function has an infinite gain at zero frequency. Therefore, the critical frequency was arbitrarily selected as that corresponding to an amplitude response of 0 dB. This

frequency was evaluated as 2.489 Hz. In order to duplicate this condition in the discrete transfer function of equation (3.12), it is first necessary to develop an expression for its amplitude response characteristics. This is done by making use of the mapping function, $z=e^{sT}$, and then substituting $j\omega$ for s. The resulting expression is simplified and evaluated with ω set to 15.64 rad/s (2.489 Hz.). To make the simplified expression equal to unity (0 dB.) required a value of 0.0114 for b_0. Hence, the discrete representation of the complete controlled process is given by the following transfer function.

$$G_{P.Z.}(z) = \frac{0.0114(1+z)^2}{(z-1)(z^2-1.3z+0.605)} \tag{3.13}$$

An exact representation of the continuous-time system of equation (3.9) preceded by a D/A converter acting as a zero order hold element can be derived by using the hold equivalence transform method. This procedure can be applied in a number of different ways, the simplest of which involves using standard, tabulated sets of transfer function relationships [45]. Accordingly, the discrete transfer function that is derived for the basic system of equation (3.10) is as follows,

$$G_{Z.O.H.}(z) = \frac{0.009z^2+0.0298z+0.00695}{(z-1)(z^3-1.3z+0.605)} \tag{3.14}$$

As before, a sampling period of 10 ms. was used in the derivation of this transfer function. A comparison with its discrete relation of equation (3.13) highlights a number of interesting features. From a structural aspect, the numerator and denominator polynomials in the two expressions are of identical orders, respectively. Moreover, both transfer functions share identical denominator coefficients and hence pole positions. The same is not true of the numerators. In the pole-zero mapped version there are two roots at z=-1. Conversely, the hold equivalence transfer function has its zeros at z=-3.059 and z=-0.252.

A frequency response comparison of the three transfer functions of equations (3.10), (3.13) and (3.14) is shown in figure 3:3. The amplitude response characteristics of the continuous-time and the hold equivalence models are virtually identical. There is a difference between the two beyond the Nyquist frequency; this is a consequence of the aliasing phenomenon that is inherent in discrete transfer functions. There is a close degree of similarity between the amplitude response characteristics of these two systems and those of the pole-zero mapped one. Slight

differences that do arise occur over a small band of frequencies in the region of the Nyquist frequency. The higher levels of attenuation in the pole-zero mapped model are a result of its zeros at z=-1. Looking to the phase response diagrams, it is encouraging to note the close level of agreement between the two versions of discrete models.

Although these results consider just one example, they do provide some indication of the modelling errors likely to be occasioned by the pole-zero mapping technique. However, such errors are not considered to be of tremendous significance. For example, the sampled data control systems designed in this thesis are not expected to operate with driving signals which have a significant spectral content in the frequency region where the modelling error is greatest. This is not considered to be an onerous limitation on the way that the system can be operated. This will become apparent in subsequent chapters which deal with applications of such models in designing adaptive systems. It is also possible that modelling errors, attributable to non-linear characteristics in the controlled process, for example, could be of much greater significance.

3.5 REFERENCE MODEL

In defining a suitable reference model, it is necessary to duplicate the structure of the process transfer function. This is done to avoid forcing the process to behave like a reference system which has a structure that is significantly different from its own.

Another important factor in defining the reference model concerns the zeros in its transfer function. These should be chosen to be the same as those occurring in the controlled process discrete transfer function. The objective of this action is to develop a simplified control law, as will be explained in chapter 4. It now becomes possible to avoid the stability problem, outlined earlier, that could result from employing a pole-zero placement form of control law.

By this stage, appropriate values will have been selected for the time delay and the dimensions of the numerator and denominator polynomials in the controlled process transfer function of equation (3.7). The structure of an open loop reference model transfer function can easily be defined on the basis of these values.

An additional stage has to be covered before the reference model is of an appropriate form for the adaptive control scheme. Both the reference model and the controlled process transfer functions contain a free integrator. Under the usual form of control system configuration, the controlled process will be operated as a closed loop (feedback) system. Hence, in specifying the reference system that the controlled process has to follow, it is necessary to specify a closed loop reference model transfer function. This is done by using the previously specified open loop reference model. It is considered to be operated as a unity feedback closed loop system as shown in figure 3:4. This ensures that the closed loop reference system has unity steady state gain. From figure 3:4, the closed loop reference model transfer function can be seen to be derived as follows.

$$\frac{x(z^{-1})}{w(z^{-1})} = \frac{1}{\dfrac{A'_m(z^{-1})}{b_m z^{-r} B(z^{-1})} + 1}$$

$$= \frac{b_m z^{-r} B(z^{-1})}{A'_m(z^{-1}) + b_m z^{-r} B(z^{-1})} \qquad (3.15)$$

$$= \frac{b_m z^{-r} B(z^{-1})}{A_m(z^{-1})} \qquad (3.16)$$

where,

$$\text{Order}(A'(z^{-1})) = \text{Order}(A(z^{-1})) \qquad (3.17)$$

The time delay, z^{-r}, and the polynomial $B(z^{-1})$ are identical to those in the controlled process transfer function of equation (3.7).

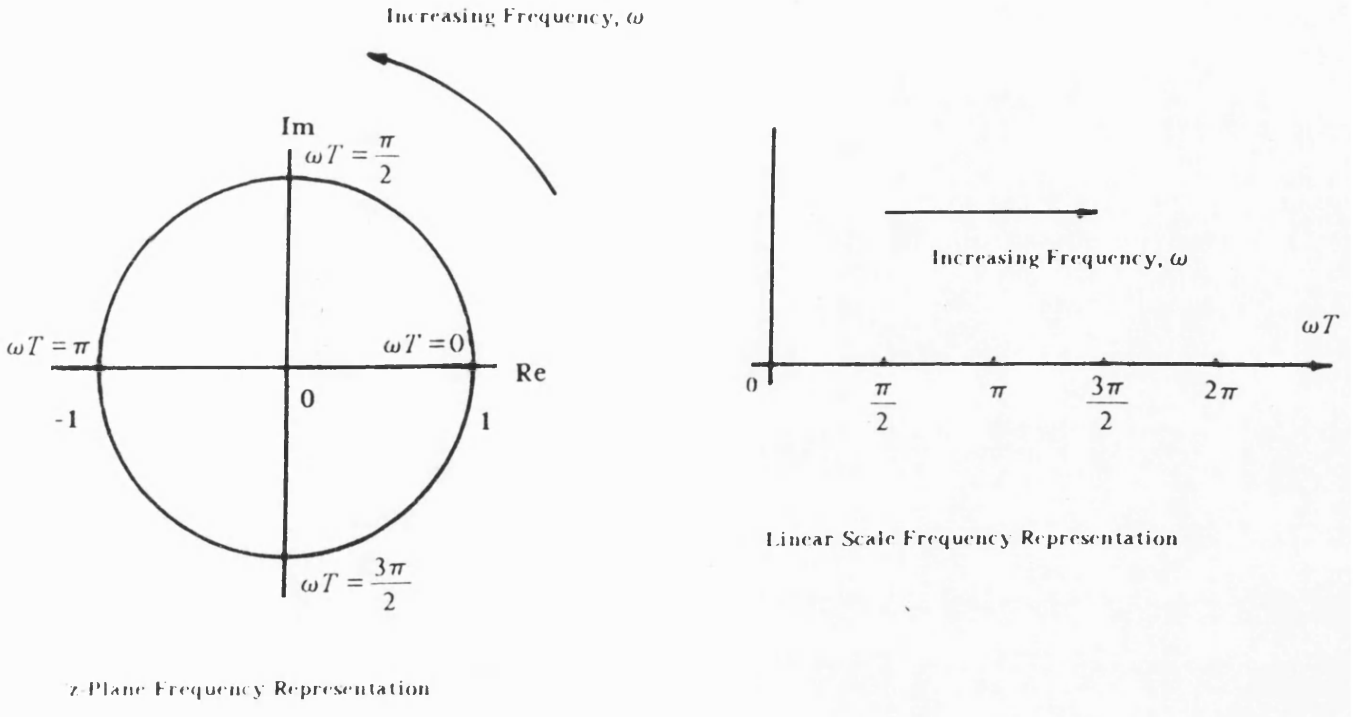

FIGURE 3:1 Frequency Representation In The z-Plane

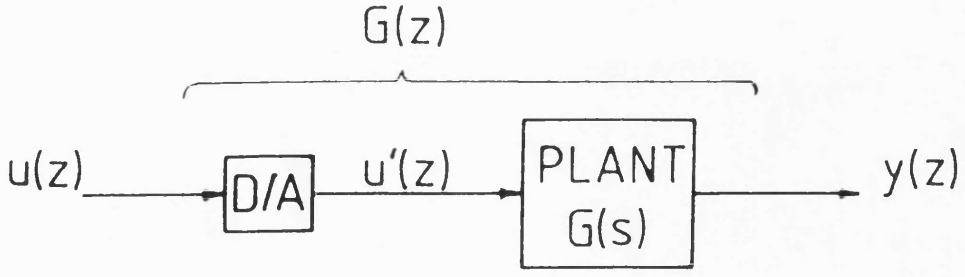

FIGURE 3:2 Schematic Representation Of Effective Controlled Process

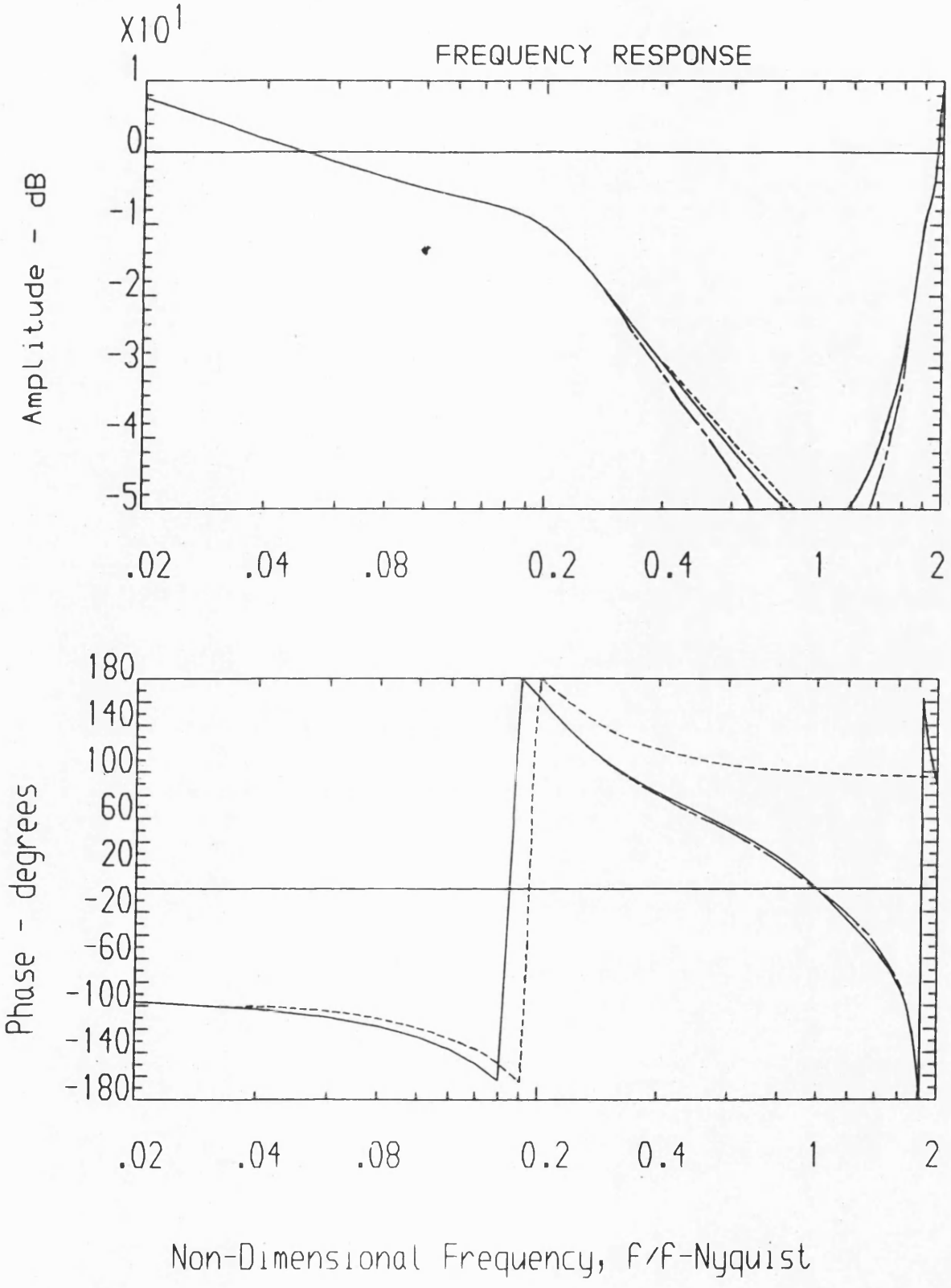

FIGURE 3:3 Frequency Response Comparison Of An Example Transfer Function

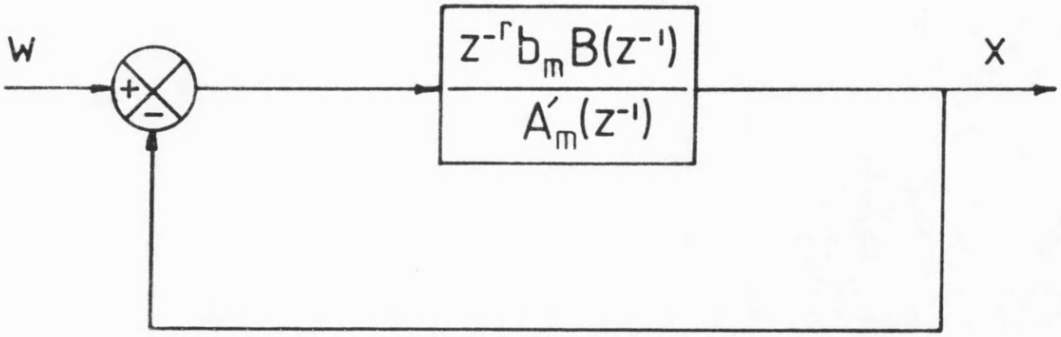

FIGURE 3:4 Feedback Representation Of Reference Model System

CHAPTER 4

COMPENSATOR FILTER SPECIFICATION

4.1 CONTROL SCHEME SIMPLIFICATION

A generalised parallel model reference control scheme is shown in figure 4:1. The model reference control concept requires the parallel paths to be made identical. From figure 4:1, it is clear that this condition can be expressed as the equality of the transfer functions of the respective paths, hence,

$$\frac{b_m z^{-r} B(z^{-1})}{A_m(z^{-1})} = \frac{b_0 z^{-r} B'(z^{-1}) T(z^{-1})}{A(z^{-1}) F(z^{-1}) + b_0 z^{-r} B'(z^{-1}) G(z^{-1})} \tag{4.1}$$

In chapter 3, the pole-zero mapping technique was used as the means for deriving a discrete approximation of the continuous-time controlled process. An important consequence of using this transform method concerns the process numerator dynamics. For continuous-time systems without any finite zeros, the corresponding discrete transfer function has a numerator polynomial, $B'(z^{-1})$, which is of a special form; this polynomial, when it exists, is such that all its roots lie at $z = -1$. On this basis, one of the conditions used in specifying the reference model transfer function is that it too should share an identical numerator polynomial. Therefore, with reference to equation (4.1), it is possible to write,

$$B(z^{-1}) = B'(z^{-1}) \tag{4.2}$$

An examination of equation (4.1) reveals that, by making use of this equality, the model reference control objective can be drastically simplified. This becomes possible when the $T(z^{-1})$ compensator is discarded, by effectively setting it to unity. Since this compensator is a designer tunable variable, this is a perfectly valid step. As a consequence of the alteration, the simplified control objective becomes,

$$\frac{1}{b_m}A_m(z^{-1}) = \frac{1}{b_0}A(z^{-1})F(z^{-1})+z^{-r}B(z^{-1})G(z^{-1}) \tag{4.3}$$

where the following generalised forms for $F(z^{-1})$ and $G(z^{-1})$ apply.

$$F(z^{-1}) = f_0+f_1z^{-1}+....+f_iz^{-i}+\cdots \tag{4.4}$$

$$G(z^{-1}) = g_0 \quad +g_1z^{-1}+....+g_iz^{-i}+\cdots \tag{4.5}$$

By comparison with the earlier pole-zero placement control law of equation (4.1), the condition specified in equation (4.3) corresponds to a pole-placement one. The control scheme, in this case, is only attempting to adjust the characteristic equation of the controlled process loop. No attempt is made to affect the numerator dynamics of the controlled process.

In the context of a non-adaptive model reference control scheme, it is only the coefficients of the $F(z^{-1})$ and $G(z^{-1})$ compensators that remain unknown. The process discrete transfer function can be enumerated once its continuous-time transfer function has been identified. This can be achieved by means of either, an analysis of the system or, through tests followed by data reduction on the process to be controlled. The reference model parameters are specified according to some desired performance criterion. To complete the trinity that makes up the control scheme, it is necessary to specify filters, $F(z^{-1})$ and $G(z^{-1})$, of sufficiently high orders to allow the pole-placement control objective to be met. Compensator coefficient initialisation is a direct outcome of solving a set of simultaneous equations based on the pole-placement control law of equation (4.3). Before this can be achieved however, it is necessary to specify the orders of the compensator networks. This question is dealt with in the next section of this chapter.

4.2 COMPENSATOR ORDER SPECIFICATION

This step in the control system design procedure involves determining minimal realisations for the compensator polynomials $F(z^{-1})$ and $G(z^{-1})$. These have to be sufficient to allow complete control over the right hand side of equation (4.3). This part of the design only becomes possible once the reference model and process transfer function polynomial orders are known.

From an examination of equation (4.3), it is possible to develop the following conditions. For clarity of presentation, simplified notation of the form $A \equiv A(z^{-1})$, will be used henceforth.

1) Both parts of the r.h.s. of equation 4.3 must be of the same order. Hence,

$$\text{Order(A)} + \text{Order(F)} = \text{r} + \text{Order(B)} + \text{Order(G)} >= \text{Order}(A_m) \qquad (4.6)$$

2) The compensator polynomials in equation (4.3) are expressed in terms of a number of 'f' and 'g' coefficients as indicated by equations (4.4) and (4.5). Upon equating like powers of z, in equation (4.3), there must be as many equations as there are unknown 'f' and 'g' coefficients. According to equation (4.4) for example, an n^{th} order $F(z^{-1})$ compensator has (n+1) unknown coefficients. This statement is equally as valid when applied to the $G(z^{-1})$ compensator. It is thus possible to write,

$$\text{Order(F)} + \text{Order(G)} + 2 = \text{Order(A)} + \text{Order (F)} + 1 \qquad (4.7)$$

The right hand side of equation (4.7) could equally well be replaced by the expression, r+Order(B)+Order(G)+1.

The two equations, (4.6) and (4.7), can be solved for explicit conditions on the $F(z^{-1})$ and $G(z^{-1})$ compensators. The results obtained from this exercise are given below.

$$\text{Order(F)} = \text{Order(B)} - 1 + \text{r} \qquad (4.8)$$

$$\text{Order}(G) = \text{Order}(A) - 1 \tag{4.9}$$

Having evaluated conditions for minimal realisations of the compensator polynomials, the derivation of the adaptive algorithm that generates the compensator coefficients can now be considered.

It is worth noting that in a non-adaptive context, a numerically expressed process transfer function would be obtained by applying some form of identification routine to the controlled process. In an indirect adaptive control scheme, the coefficients of the transfer function would be supplied by a parameter adaptive algorithm. Having defined a desired level of system performance, the reference model transfer function would also be available in a numerical format. Thus, a set of simultaneous equations based on equation (4.3) would have to be solved in order to ennumerate the 'f' and 'g' the compensator coefficients. By contrast, in a direct adaptive scheme, it is the parameter adaptive algorithm that generates the compensator coefficients without recourse to an explicit identification of the process transfer function. The design of such a mechanism is discussed in the next chapter.

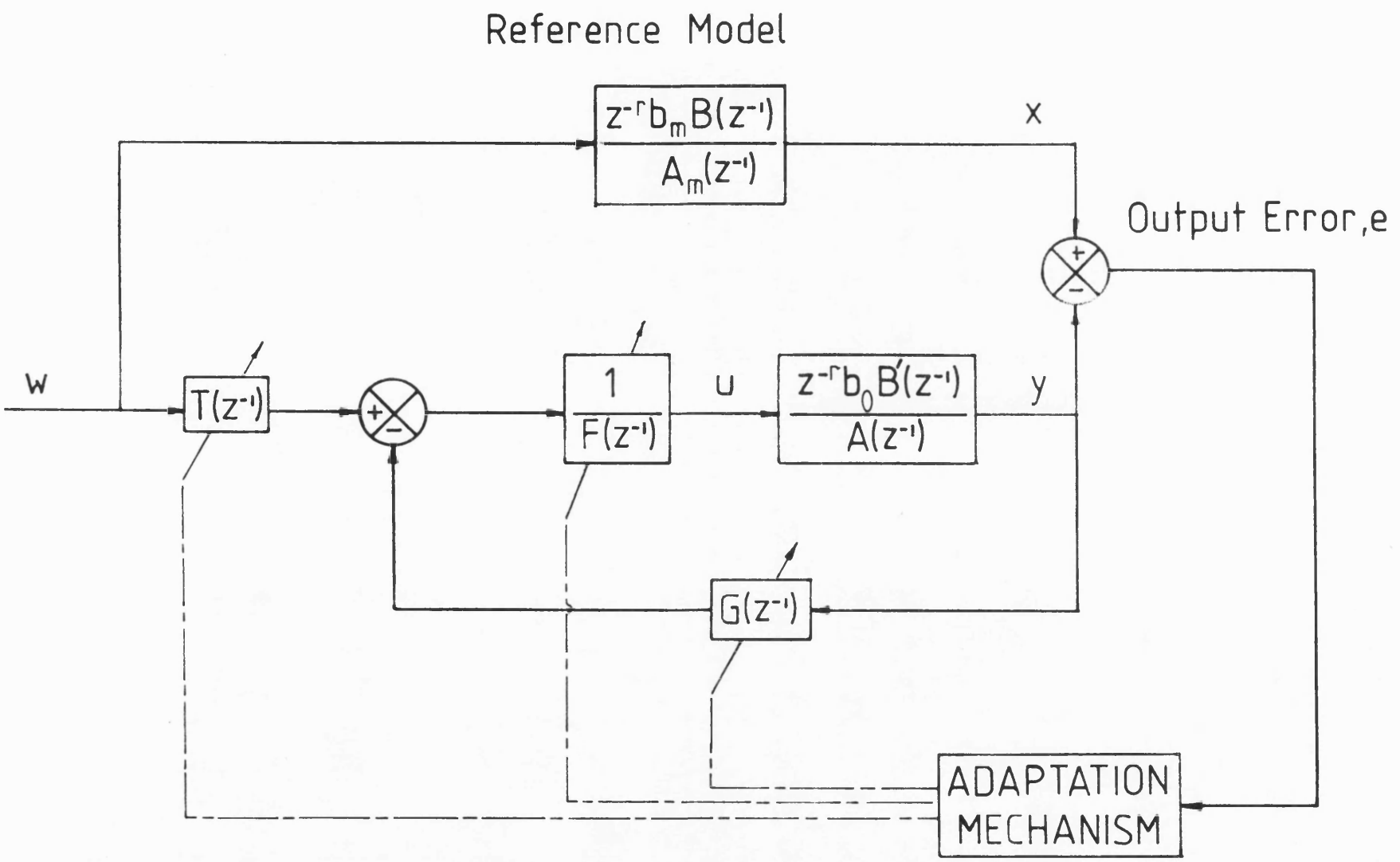

FIGURE 4:1 Block Diagram Representation Of A General Parallel Model Reference Adaptive Control Scheme

CHAPTER 5

THE PARAMETER ADAPTIVE ALGORITHM

5.1 INTRODUCTION

There are a number of different possibilities for designing the adaptive part of the control system [24,25]. Apart from the early intuitive suggestions, other possibilities include the following: sensitivity analysis, Lyapunov stability and hyperstability based procedures. In spite of the range of options that can be pursued, the end results all display a remarkably high degree of similarity. Bearing this in mind, it is arguable that the choice of design method is very much a question of individual taste. In this thesis, the hyperstability based approach has been adopted. The reason for its choice over the other methods is that it allows a well structured approach to the design problem, which makes it relatively straightforward to apply. Another factor that was taken into account concerns the wide class of adaptive laws that can be generated via hyperstability analysis [24]. This is a desirable feature since it allows a choice of adaptation algorithms. The development of similar adaptive laws is possible with the other methods although the procedure is unlikely to be as straightforward to use.

5.2 ADAPTIVE CONTROLLER DESIGN METHODOLOGY

The basic control scheme is specified in terms of the transfer functions of a reference model, a controlled process and a set of compensator networks. Using this information, a parameter adaptive algorithm is to be designed. The basis for this procedure centers on elements of hyperstability theory and is applied according to the four steps outlined below [24].

Step 1: Transform the model reference control system into the form of an equivalent feedback system composed of two blocks, one in the forward path and the other in the feedback path. The forward path block must be linear and time invariant, and the block in the feedback path must be non-linear and time varying.

Step 2: Find solutions for that part of the adaptive scheme, which appears in the forward path of the equivalent feedback system, such that it becomes a hyperstable block. This implies global (asymptotic) stability for the whole system. Appendix 1 provides a graphical interpretation of this stability terminology.

Step 3: Find solutions for the remaining part of the adaptation law, which appears in the feedback block of the equivalent feedback system, such that a particular stability condition is satisfied. The stability condition, expressed as the input-output relationship of a given system, is otherwise known as the Popov integral inequality.

Step 4: Convert the results of the previous two steps into a form that is appropriate to the original control system description. The application of hyperstability concepts in steps 2 and 3 is carried out on the basis of an idealised representation of the control scheme. As a consequence, the results obtained relate to the idealised system representation. This step in the design procedure converts the basic results into a form that applies to the real control system environment.

The design methodology summarised above will now be put into perspective with a detailed presentation of its application to a generalised control problem.

5.3 STEP 1: FEEDBACK REPRESENTATION OF THE MODEL REFERENCE CONTROL SYSTEM

The first step in deriving the adaptation laws that make up the parameter adaptive algorithm (P.A.A.) consists of reconfiguring the control system as an error system; the error in this context is the difference between the output from the reference model and the process. In so doing, the adaptive system can be studied in terms of the parameter to be controlled - the reference model/process output error. To be of any use, the error system that is derived must result in a particular form of feedback system, as outlined in the first step of the design procedure.

As a preliminary step in presenting the design procedure, the defining equations of the various elements in the control loop are repeated below. Moreover, a number of new parameters, which are relevant to the adaptive scheme, are introduced. With reference to figure 5:1, the equations that define the control system are as follows:

Controlled Process Open Loop Transfer Function

$$\frac{y(z^{-1})}{u(z^{-1})} = \frac{b_0 z^{-r}(1+z^{-1})^m}{1+a_1 z^{-1}+....+a_n z^{-n}}$$

$$= \frac{b_0 z^{-r} B(z^{-1})}{A(z^{-1})} \tag{5.1}$$

Reference Model Closed Loop Transfer Function

$$\frac{x(z^{-1})}{w(z^{-1})} = \frac{b_m z^{-r} B(z^{-1})}{A'(z^{-1})+z^{-r} b_m B(z^{-1})} \tag{5.2}$$

$$= \frac{b_m z^{-r} B(z^{-1})}{A_m(z^{-1})} \tag{5.3}$$

where,

$$\text{Order}[A'(z^{-1})] = \text{Order}[A(z^{-1})] \tag{5.4}$$

Pole-Placement Control Law

$$\frac{1}{b_m} A_m(z^{-1}) = \frac{1}{b_0} A(z^{-1}) F(z^{-1}) + z^{-r} B(z^{-1}) G(^{-1}) \tag{5.5}$$

where,

$$F(z^{-1}) = f_0 + f_1 z^{-1} + \ldots + f_i z^{-i} + \ldots \tag{5.6}$$

and,

$$G(z^{-1}) = g_0 + g_1 z^{-1} + \cdots + g_i z^{-i} + \cdots \tag{5.7}$$

In chapter 4, the following conditions were shown to define appropriate orders for the $F(z^{-1})$ and $G(z^{-1})$ compensator filters.

$$\text{Order}[F(z^{-1})] = \text{Order}[B(z^{-1})] - 1 + r \tag{5.8}$$

$$\text{Order}[G(z^{-1})] = \text{Order}[A(z^{-1})] - 1 \tag{5.9}$$

Reference Model - Process Output Error

The model-process 'a priori' output error is defined as,

$$e^{o}(k) = x(k) - y^{o}(k) \tag{5.10}$$

Similarly, an 'a posteriori' output error is defined as,

$$e(k) = x(k) - y(k) \tag{5.11}$$

These definitions are used to highlight subtle differences between the analysis and realisation of the adaptive control scheme.

5.3.1 ERROR SYSTEM DERIVATION

Combining equations (5.1), (5.3) and (5.5), an error equation to describe the control system can be developed in the following manner. Wherever convenient, the notation $A \equiv A(z^{-1})$ will be used henceforth. Subtracting equation (5.1) from equation (5.3) yields,

$$A_m x(k) - Ay(k) = b_m z^{-r} Bw(k) - b_0 z^{-r} Bu(k)$$

$$A_m e(k) = b_m z^{-r} Bw(k) - b_0 z^{-r} Bu(k) - A_m y(k) + Ay(k) \tag{5.12}$$

But, from equation (5.1), $Ay(k) - b_0 z^{-r} Bu(k) = 0$. Therefore,

$$A_m e(k) = b_m z^{-r} Bw(k) - A_m y(k) \tag{5.13}$$

A_m is now taken into account, in the right hand side of equation (5.13), by using the expression for the pole-placement control law. Upon making the appropriate substitution based on equation (5.5), equation (5.13) above becomes,

$$A_m e(k) = b_m z^{-r} Bw(k) - \frac{b_m}{b_0} AFy(k) - b_m z^{-r} BGy(k)$$

$$= b_m z^{-r} Bw(k) - b_m z^{-r} BFu(k) - b_m z^{-r} BGy(k) \tag{5.14}$$

The 'f' and 'g' coefficients of the $F(z^{-1})$ and $G(z^{-1})$ compensator networks in equation (5.14) are grouped together in a column vector, $\underline{\mathbf{d}}$. The signals that are premultiplied by these compensator coefficients are similarly grouped together in an observation vector, $\underline{\Phi}(k)$. Equation (5.14) can now be simplified to,

$$A_m e(k) = z^{-r} b_m B(w(k) - \underline{\mathbf{d}}^T \underline{\Phi}(k)) \tag{5.15}$$

with,

$$\underline{\mathbf{d}}^T = [\, f_0 f_1 \cdots f_f \cdots g_0 g_1 \cdots g_g \cdots \,] \tag{5.16}$$

$$\underline{\Phi}^T(k) = [\, u(k)\, u(k-1) \cdots u(k-f) \cdots$$

$$y(k)\, y(k-1) \cdots y(k-g) \cdots \,] \tag{5.17}$$

The elements of the parameter vector, $\underline{\mathbf{d}}$, are the set of compensator coefficients which would satisfy the requirement of perfect model following; in future, this case will be referred to as the 'tuned' condition. Clearly, under 'tuned' circumstances, the error signal would be equal to zero; this would imply that the desired objective of perfect reference model following was being met. Under usual operating conditions however, the control loop functions with an adaptively generated set of compensator coefficients. Ultimately, the parameter adaptation algorithm aims to drive these coefficients to their respective 'tuned' values. Nevertheless, cases are bound to arise where the predicted set of coefficients does not match the 'tuned' set required for perfect model following. The following examples are representative of this type of situation: adaptive control start-up conditions with a set of initial estimates for the compensator coefficients; and, changes in the dynamics of the controlled process which call for the compensator networks to be retuned. Since the compensator coefficients that are actually employed in the control scheme are time varying, they are grouped together in what is termed an 'adjustable' parameter vector, $\underline{\hat{\mathbf{d}}}(k)$. By analogy with the definition of the 'tuned' parameter vector, $\underline{\mathbf{d}}$, the adjustable vector is given as follows,

$$\underline{\hat{\mathbf{d}}}^T(k) = [\, \hat{f}_0(k)\, \hat{f}_1(k) \cdots \hat{f}_f(k) \cdots$$

$$\hat{g}_0(k)\, \hat{g}_1(k) \cdots \hat{g}_g(k) \cdots \,] \tag{5.18}$$

The next step in the design procedure is to introduce the 'adjustable' parameter vector into the error system description of the control scheme. This is carried out by first considering the manner in which the process control signal is evaluated. An examination of the basic control loop, shown in figure 5:1, reveals that the control signal , u, is formed as follows. Sampled versions of the process output, y, are filtered by the feedback compensator, $G(z^{-1})$; the resulting signal is

subtracted from the input command signal, w, prior to being filtered by the forward path compensator, $1/F(z^{-1})$ to produce the desired result, u. In equation form, the control signal, at some given instant in time, k, can be expressed as,

$$u(k) = \frac{1}{\hat{f}_0(k-1)}[w(k) - \hat{f}_1(k-1)u(k-1) \ldots - \hat{f}_f(k-1)u(k-f) \cdots$$

$$- \hat{g}_0(k-1)y(k) - \hat{g}_1(k-1)y(k-1) \ldots - \hat{g}_g(k-1)y(k-g) \ldots] \qquad (5.19)$$

The reason for using the $(k-1)^{th}$ set of parameters in equation (5.19) results from the way in which the process control signal is evaluated. To remain faithful to the set of equations that describe the control scheme, there should ideally be little or no delay in carrying out the three sampling actions whereby the input command and process output signals are read into the computer system and the process control signal is output. This would imply that the three events occur simultaneously. Now, the control signal at the k^{th} sampling instant, for example, depends upon the command input, w(k), the process output, y(k), and, ideally, the set of compensator coefficients corresponding to the k^{th} sampling interval. The sequential nature of computer system operation means that, in evaluating u(k) according to this mode of operation, some degree of computational delay is inevitable [46]. This delay is attributable to two causes which are; evaluation of the compensator coefficients corresponding to the k^{th} sampling interval and, evaluation of the control signal from these coefficients. The time taken by the former is considerably greater than that due to the latter. Consequently, in an attempt to remove the effect of the delay factor due to compensator parameter generation, the control signal is calculated on the basis of the most recent set of compensator parameters, at every sampling interval. These coefficients correspond to those generated during the course of the previous interval, hence the use of the $(k-1)^{th}$ set of parameters in equation (5.19).

Returning to the substance of the original problem, equation (5.19) can be rearranged to yield,

$$w(k) = \hat{f}_0(k-1)u(k)+\hat{f}_1(k-1)u(k-1)...+\hat{f}_f(k-1)u(k-f)...$$

$$\hat{g}_0(k-1)y(k)+\hat{g}_1(k-1)y(k-1)...+\hat{g}_g(k-1)y(k-g)\cdots$$

This expression can be simplified with the aid of equations (5.17) and (5.18), the definitions for the filtered observation vector and the adjustable parameter vector respectively.

$$w(k) = \underline{\hat{d}}^T(k-1)\underline{\Phi}(k) \tag{5.20}$$

Substitution for w(k) in the right hand side of the error system of equation (5.15) converts it to the following form,

$$b_m z^{-r} B(w(k)-\underline{d}^T \underline{\Phi}(k)) = b_m z^{-r} B[\underline{\hat{d}}^T(k-1)-\underline{d}^T]\underline{\Phi}(k) \tag{5.21}$$

Hence, the error system equation becomes,

$$A_m e(k) = b_m z^{-r} B[\underline{\hat{d}}^T(k-1)-\underline{d}^T]\underline{\Phi}(k) \tag{5.22}$$

In order to facilitate the analysis involved in deriving suitable adaptation laws, the control system is initially modelled as if the control signal for the k^{th} sampling period was evaluated with coefficients generated during the same interval; it is also assumed that all sampling actions occur simultaneously. According to these assumptions, it would appear that adaptation laws are being derived within the framework of an idealised environment. However, suitable action is taken, during the fourth step of the design procedure, to correct for the idealisation introduced at this stage. In the light of these statements, the definitions of 'a priori' and 'a posteriori' output error signals can now be appreciated. The 'a priori' output error signal results, when the $(k-1)^{th}$ set of compensator coefficients is used to evaluate the process control signal for the k^{th} sampling period. When, instead, the k^{th} set of compensator coefficients is used, the output error signal becomes 'a

posteriori'.

The error system equation must now be re-specified, in a more precise fashion, in terms of the 'a priori' and 'a posteriori' output error signals. The two relevant versions of equation (5.22) thus become, in the order 'a priori', 'a posteriori',

$$A_m e^o(k) = b_m z^{-r} B[\,\underline{\hat{d}}^T(k-1) - \underline{d}^T\,]\underline{\Phi}(k) \tag{5.23}$$

and,

$$\begin{aligned} A_m e(k) &= b_m z^{-r} B[\,\underline{\hat{d}}^T(k) - \underline{d}^T\,]\underline{\Phi}(k) \\ &= -b_m z^{-r} B[\,\underline{d}^T - \underline{\hat{d}}^T(k)\,]\underline{\Phi}(k) \end{aligned} \tag{5.24}$$

The reconfigured adaptive scheme of equation (5.24) can now be redrawn as a particular type of feedback system as shown in figure 5:2. This feedback network is characterised by having a linear, time-invariant forward path block and a non-linear, time-varying feedback block. The $A_m(z^{-1})$ polynomial in the forward path depends on user defined criteria for a linear reference model. Time-invariance is a consequence of desiring a consistent level of performance from the control system. The feedback block is clearly non-linear and time variant since it is expressed in terms of time varying compensator coefficients and signals. Moreover, this block implicitly contains a non-linear parameter adaptive algorithm.

5.4 APPLICATION OF HYPERSTABILITY THEORY

The application of hyperstability theory to the type of feedback system developed above involves a two stage procedure which treats the two blocks individually. The following two sub-sections describe the operations that are carried out.

5.4.1 STEP 2: FORWARD PATH STABILITY ANALYSIS

With regard to the forward path block, the stability requirement is that it be made strictly positive real, (S.P.R.) . One interpretation of this condition is that phase response of this block must lie inside the -90° to $+90^{\circ}$ range, over all frequencies. The forward path transfer function is fixed since it is specified on the basis of some desired performance criterion. Therefore, an additional filter, $C(z^{-1})$, is introduced into the forward path. Now, the S.P.R. condition can be applied to the combined transfer function, $C(z^{-1})/A_m(z^{-1})$.

The following procedure, a graphical approach, is one way in which the coefficients of the error filter can be specified [24]; the basis for its use rests on the phase response properties of a strictly positive real transfer function. The transfer function, $C(z^{-1})/A_m(z^{-1})$ is first mapped to a pseudo-frequency domain, ω_w , with the following bi-linear transform,

$$z = \frac{(1+j\omega_w)}{(1-j\omega_w)} \tag{5.25}$$

To make the resulting ω_w transfer function S.P.R., its real part has to be positive for all frequencies; this condition corresponds to the $+90^{\circ}$ to -90° region on a Nyquist diagram. The S.P.R. requirement leads to a set of constraints on the values that the error filter coefficients can be assigned. A graphical interpration of these constraints is used to determine the allowable set of filter coefficient values. This aspect of the adaptive controller design scheme is covered in greater depth, during subsequent chapters which deal with the implementation of the adaptive control algorithm. A general discussion is presented in section 7.5.3 of chapter 7. Specific examples are subsequently covered in chapters 8 and 9, which describe the application of M.R.A.C. theory to two real systems.

5.4.2 STEP 3: FEEDBACK PATH STABILITY ANALYSIS

The introduction of the $C(z^{-1})$ filter in the adaptive scheme means that the new output from the forward path of the error system, $\nu(k)$, is a filtered version of the output error, e(k).

$$\nu(k) = C(z^{-1})e(k) \tag{5.26}$$

It is useful to note, at this stage, that the notion of 'a priori' and 'a posteriori' output error signals applies identically to the filtered error signal, $\nu(k)$.

As a result of modifying the forward path of the error system, the filtered output error, $\nu(k)$, now becomes the signal entering the feedback block. The stability criterion for the feedback block, expressed in terms of its input-output relationship, is given by,

$$\sum_{k=0}^{k=k_1} \nu(k)\, b_m\, (\underline{d}^T - \underline{\hat{d}}^T(k))\underline{\tilde{\Phi}}(k-r) \geq -\lambda_0^2 \quad \text{for all } k > k_1 \tag{5.27}$$

where, λ_0^2 is some arbitrary positive constant, and $\underline{\tilde{\Phi}}(k-r)$ is a filtered observation vector derived in the following manner,

$$\underline{\tilde{\Phi}}(k-r) = z^{-r} B\, \underline{\Phi}(k) \tag{5.28}$$

The prime objective of this part of the design procedure is the formulation of a parameter adaptive algorithm which will generate the coefficients of the adjustable parameter vector. In order to assure the stability of the adaptive control scheme, the adaptation algorithm has to be conceived in a manner which satisfies the stability condition of inequality (5.27). A full examination of this problem is provided in part A of appendix 2. One of the points to emerge from the analysis concerns the existence of a number of different ways for realising the adaptation algorithm. For the purpose of this study, the following method of updating the adjustable parameter vector was chosen.

$$\underline{\hat{d}}(k) = \underline{\hat{d}}(k-1) - \Gamma \underline{\tilde{\Phi}}(k-r)\nu(k) \tag{5.29}$$

Γ is a square, diagonal matrix of fixed adaptive gains which affect the alertness of the P.A.A. to changes in the process dynamics. Equation (5.29) corresponds to an integral form of adaptation and is used because of its memory-like properties. This means that the compensator parameters remain fixed when the filtered error signal reduces to zero. Other alternatives exist, as indicated above and in appendix 2. The two most important categories correspond to proportional and relay types of adaptation algorithms. Since all of these adaptation laws are valid from the hyperstability design viewpoint, increased flexibility can be gained by using different combinations of more than one law [47,48]. Research has also indicated that these algorithms do not necessarily share similar behavioural characteristics [49]. Depending on the application being considered, judicious choice of the adaptation law used can prove to be beneficial.

5.5 STEP 4: ORIGINAL CONTROL SYSTEM CONFIGURATION

In section 5.2 of this chapter, it was mentioned that hyperstability analysis of the adaptive scheme would be carried out within the context of an artificial environment. This was characterised by the use of an 'a posteriori' system configuration. The parameter updating algorithm of equation (5.29) is expressed in terms of an artificial signal, namely the 'a posteriori' filtered error signal. However, the true implementation of the control system, as described earlier, would result in the generation of an 'a priori' filtered error signal.

The transition from the 'a posteriori' environment to the original 'a priori' control system setting is achieved in the manner described in part B of appendix 2. The net effect of the analysis that is presented is to alter the parameter updating algorithm, from the form given in equation (5.29) above, to the following,

$$\underline{\hat{d}}(k) = \underline{\hat{d}}(k-1) - \frac{\Gamma \underline{\tilde{\Phi}}(k-r)\nu^{o}(k)}{1+\underline{\tilde{\Phi}}^{T}(k-r)\Gamma \underline{\tilde{\Phi}}(k-r)} \tag{5.30}$$

5.6 DISCUSSION

The design procedure outlined above was developed in a way which would allow subsequent application to be carried out in a systematic manner. The presentation was geared more towards familiarising the reader with the use of hyperstability theory in the context of adaptive systems. The following discussion examines certain aspects of the parameter adaptive algorithm within the global context of the adaptive control system.

5.6.1 THE $B(z^{-1})$ POLYNOMIAL

One of the conditions imposed in developing the adaptive control scheme concerns the type of processes to be controlled. These are constrained to those capable of being modelled with continuous-time transfer functions free of finite zeros. This property, in conjunction with the pole-zero mapping procedure outlined in chapter 3, results in discrete, process transfer functions having one or more zeros at $z = -1$; this will arise in cases where the transfer function is of a relative degree greater than 1.

In the presentation above, the discrete process numerator dynamics are grouped under the $B(z^{-1})$ polynomial. This polynomial is specifically selected to be identical in the reference model and process transfer functions.

The polynomial, $B(z^{-1})$, is a simplified representation of the true controlled process numerator dynamics; these could be obtained by using the hold-equivalence transform method to derive the process discrete transfer function. Clearly, differences between the two forms of discrete transfer function are more likely to increase with the order of the continuous-time system. As the process model becomes less representative, so the assumptions made in formulating the pole placement control law and the P.A.A. begin to break down. A degradation in the performance and, ultimately, failure of the adaptive control scheme in such circumstances is highly probable.

The parameter updating algorithm of equation (5.30) makes use of a filtered observation vector, $\underline{\tilde{\Phi}}(k-r)$. This vector is obtained, in part, by pre-filtering the observation vector, $\underline{\Phi}(k)$, with $B(z^{-1})$ according to equation (5.28). For the processes considered in this study, the $B(z^{-1})$ filter can be expressed as a polynomial with one or more roots at the point z=-1. This gives rise to a low-pass filtering effect, with increasing levels of attenuation in proportion to the number of roots at z=-1. In one sense, the filtering operation on the observation vector is likely to be beneficial. This is because it will tend to reduce the effect of higher order, unmodelled process dynamics; this type of situation will invariably arise as a consequence of representing processes with reduced order models. In [50,51], low pass filtering of signals in the observation vector was intentionally introduced as a means of improving the robustness properties of an adaptive control algorithm.

In contrast to the benefit described above, problems could develop if the $B(z^{-1})$ polynomial is of a very high order. In such situations, severe filtering, due to a high order low-pass filter, can be expected to affect adversely the quality, or 'richness', of information being fed to the updating algorithm. The foreseeable outcome is that signals in the region of the Nyquist frequency will be severely attenuated. Whereas the filtering action was previously directed at eliminating high frequency parasitics, now it will start to affect lower frequency signals associated with the correctly modelled part of the adaptive system. Intuitively, this lowering in the quality of signals entering the adaptation algorithm implies a parameter adaptive system with a reduced 'bandwidth'. This suggests a move towards sluggish performance characteristics. As a consequence, it is arguable that this type of algorithm would be better suited to controlling processes which are not subject to rapid changes in the dynamics of the controlled process.

5.6.2 THE G(z^{-1}) POLYNOMIAL

The $G(z^{-1})$ polynomial represents the compensator network in the controlled process feedback path. When correctly designed, the $G(z^{-1})$ filter coefficient values should satisfy the previously cited expression for the pole-placement control law. In addition, the $G(z^{-1})$ filter must simultaneously satisfy a steady state gain condition. The coefficients of this filter are generated adaptively. As such it is possible to envisage certain situations during which adaptive control action is degraded. This type of phenomenon and the full relevance of the adaptively

generated feedback compensator are explained below.

An examination of figure 5:1 indicates that the controlled process, closed loop transfer function can be written as,

$$\frac{y(z^{-1})}{w(z^{-1})} = \frac{b_0 z^{-r} B(z^{-1})}{A(z^{-1}) F_(z^{-1}) + b_0 z^{-r} B(z^{-1}) G_(z^{-1})} \tag{5.31}$$

The applications considered in this thesis are based on processes which include a free integral term in their open loop transfer functions. It follows therefore, that the corresponding discrete, open loop transfer functions will have a pole located at z=1; this results from a continuous-time pole at s=0 being mapped to the z=(1,0j) point in the discrete plane. The presence of this pole means that there is a $(1-z^{-1})$ factor present in the $A(z^{-1})$ polynomial of equation (5.31).

The steady state gain of the transfer function given in equation (5.31) is obtained by making use of the final value theorem. The rule for its application to an example transfer function, $Q(z^{-1})$ is summarised below.

If $(1-z^{-1})Q(z^{-1})$ does not have any poles on or outside the unit z-plane disc, then,

$$\lim_{k \to \infty} q(k) = \lim_{z \to 1} (1-z^{-1}) Q(z^{-1}) \tag{5.32}$$

Application of the final value theorem to the problem considered here consists of examining the controlled process steady state response to a unit step input. The final value theorem is subsequently applied to the z-Transform expression of the process output, y; this is expressed as a product of the input command signal and the control system closed loop transfer function. A unit step input, w, has a z-Transform given by,

$$w(z^{-1}) = \frac{1}{1-z^{-1}} \tag{5.33}$$

Consequently, the steady state response of the controlled process to an input of this

form is,

$$\lim_{k\to\infty} y(k) = \lim_{z\to 1}(1-z^{-1})w(z^{-1})\frac{b_0 z^{-r} B(z^{-1})}{A(z^{-1})F(z^{-1})+b_0 z^{-r} B(z^{-1})G(z^{-1})}$$

Cancellation of the z-Transform of the input command signal with the $(1-z^{-1})$ term leads to,

$$\lim_{k\to\infty} y(k) = \lim_{z\to 1}\frac{b_0 z^{-r} B(z^{-1})}{A(z^{-1})F(z^{-1})+b_0 z^{-r} B(z^{-1})G(z^{-1})}$$

Recalling that the $A(z^{-1})$ polynomial includes a root at z=1, the previous expression can be reduced to the following.

$$\lim_{k\to\infty} y(k) = \frac{b_0 1^{-r} B(1)}{0+b_0 1^{-r} B(1)G(1)}$$

$$= \frac{1}{G(1)} \qquad (5.34)$$

Clearly, the controlled process closed loop steady state gain depends upon the feedback compensator steady state gain. Consequently, the following condition has to be satisfied if the process loop is to have unity steady gain.

$$G(1) = g_0+g_1\ldots+g_g \cdots = 1 \qquad (5.35)$$

Since the 'g' coefficients are generated adaptively, it is possible that the condition specified by equation (5.35) might occasionally be violated. The most obvious case where this is likely to occur relates to the question of finite numerical accuracy of digitally implemented algorithms. Other less well known situations also give rise to such difficulties. Their influences will be be highlighted in later chapters of this thesis, where their effects can be more readily visualised. Since the model following objective requires the condition expressed in equation (5.35) to hold, variations are likely to be small. Nevertheless, a possible deterioration in steady state model following cannot be discounted totally.

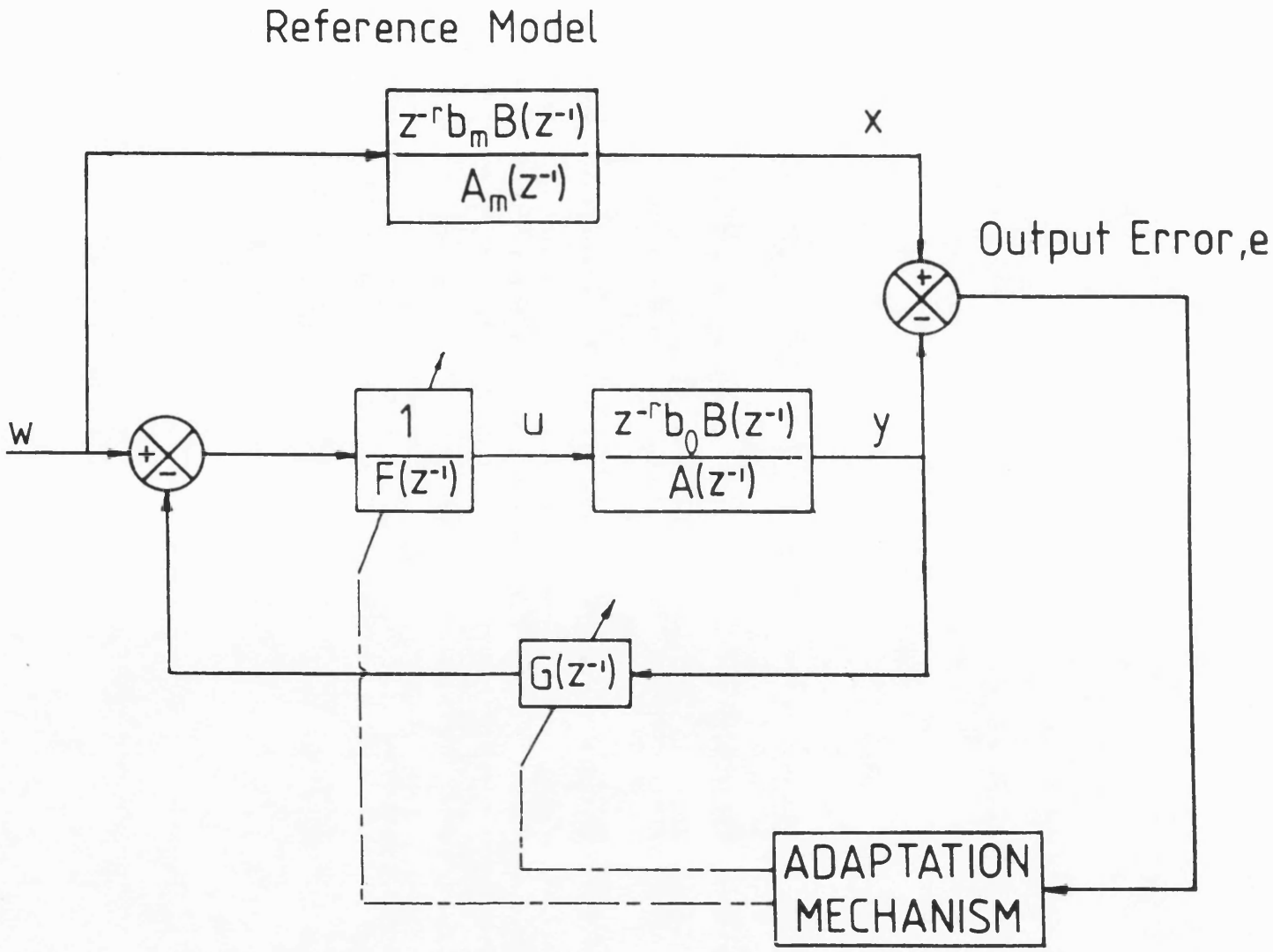

FIGURE 5:1 Block Diagram Representation Of A Parallel Model Reference Adaptive Control Scheme

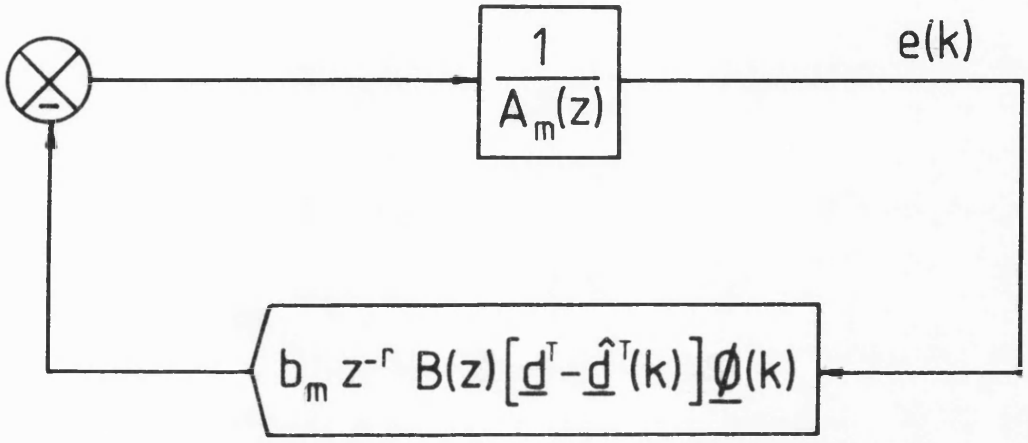

FIGURE 5:2 Feedback Representation Of Error Equation

CHAPTER 6

ROBUST ADAPTIVE CONTROL

6.1 INTRODUCTION

During the course of the preceding chapters, a number of simplifications were made in designing the model reference adaptive control scheme. These include the use of a linearised, reduced order model and the derivation of a discrete representation of the continuous-time system via the pole-zero mapping technique. The modelling simplifications that were made, allied to the physical limitations and non-linear nature of real systems could lead to inadequate reference model following behaviour. An additional factor is that such phenomena could give rise to erroneous adaptation. In turn, this could lead to an unstable closed loop system. One other area of concern is that at some point the effects of physical constraints, such as saturation, will tend to limit the maximum level of performance that can be attained by a given device.

A number of supervisory features have been added to the adaptive control algorithm to try and cater for the types of eventuality described above. The procedure of augmenting the basic adaptive system with protective features is commonly referred to as 'jacketing' [21]. The adaptive controller is effectively being enhanced with an outer control loop of safety mechanisms [52]. The procedure of 'jacketing' is one that is universally applied to all control schemes, irrespective of whether they are adaptive or not. They generally involve intuitively developed solutions to particular problems. Unfortunately, this means that they rarely receive the degree of attention that they merit. The extremely flexible nature of micro-processor based controllers makes for a very simple implementation of such protective features. Individual descriptions for the supervisory functions added to the adaptive control algorithm are dealt with in the subsequent sections.

6.2 AN ENHANCEMENT TO THE PARAMETER ADAPTIVE ALGORITHM

It is reasonable to speculate that unless neglected dynamics in the controlled process are of a sufficiently 'weak' nature, they are liable to compromise the robustness of the eventual adaptive control scheme. In recent years, the attention of a small body of researchers has been directed towards studying the robustness properties of some of the more commonly encountered forms of adaptation algorithm. Their work has indicated that serious problems can arise under a variety of different operating conditions. The most notable of these is the case of unmodelled (or neglected) process dynamics [53]. A considerable amount of vigorous discussion subsequently ensued over their findings. This is witnessed by the welter of claims and counterclaims that followed the initial studies questioning the degree of robustness of adaptive systems [54-58]. This period in the development of adaptive control theory can be viewed as a boon to practising control engineers in generating a less mathematical and more practical analysis of adaptive systems [59-61]. Gradually however, these developments were superseded by more theoretically oriented studies into the robustness issue.

Recently, a number of researchers have proposed different solutions for enhancing the robustness of adaptive control schemes [44,62-64]. The techniques presented involve modifications to the parameter adaptive process, under certain operating regimes. The following two approaches stand out as representative examples of these developments. The first one considered uses some measure of the reference model-process output error to control the adaptation algorithm [62]; parameter adaptation is either suspended or allowed to proceed if the magnitude of the error signal falls within a certain tolerance band. Robustness of the parameter adaptive algorithm is enhanced by making this dead-zone variable. Amongst other parameters, the width of this region is affected by the controlled process input-output information. This can be considered to provide some indication of the quality of adaptive system behaviour.

The second approach to robustness enhancement makes use of a signal normalising factor in the parameter adaptive algorithm [63]. Like the previous approach, this factor is also a time varying parameter, affected, in part, by the controlled process input-output information. It too is constrained to be positive and non-zero. Individual terms in the process observation vector are divided by this factor in order to obtain a normalised observation vector. This then becomes the

process input-output information vector that is used in the parameter updating algorithm. The underlying concept of this solution is to offer a means of reducing the influence of the observation vector in the parameter updating algorithm. This results from the use of increasingly larger values of normalising gain.

The protection strategy selected for the adaptive system designed here uses a variant of the error tolerance scheme, as presented in [44] and [62]. This solution is preferred because of its clear cut ability to switch off the adaptation process completely; this is not possible with the alternative scheme, due to the use of a finite normalising factor.

The chosen protection mechanism works by using a variable dead-band to define an acceptable tolerance on reference model following performance. This is expressed in terms of the filtered error signal. If this signal falls within the dead-band limits, adaptation is suspended.

In cases where small modelling errors are expected, [34,44], perfect model following may prove impossible. This is because of the lack of a set of values in the adjustable parameter vector which satisfies the pole-placement control law. At worst, the persistence of a model-process error could result in parameter adaptation leading to an unstable closed loop system. Part of the motivation for using a dead-band characteristic is to accommodate the idea of 'sufficiently close' model following. This overcomes the need for perfect model following by permitting a certain tolerance level. Clearly, while this level of response is being met, the P.A.A. is freed from the task of adjusting the compensator coefficient settings.

Modification of the adaptive scheme to attain the objective outlined above is achieved in the following manner. The parameter updating algorithm of equation (5.30) is altered by replacing the filtered error signal, ν^o , with the output from the variable dead-band characteristic, $q(\epsilon h(k),\nu^o(k))$. From [44], the equations governing the basic variable dead-band function are,

$$q(\epsilon h(k),\nu^o(k)) = \begin{cases} \nu^o(k)-\epsilon h(k) & \text{if } \nu^o(k) > \epsilon h(k) \\ 0 & \text{if } |\nu^o(k)| \leqslant \epsilon h(k) \\ \nu^o(k)+\epsilon h(k) & \text{if } \nu^o(k) < -\epsilon h(k) \end{cases} \tag{6.1}$$

where the time varying dead-band, $h(k)$, is generated according to,

$$h(k) = \sigma h(k-1) + (|y(k-1)| + |u(k-1)| + \epsilon_0) \tag{6.2}$$

with,

$$h(0) = \frac{\epsilon_0}{(1-\sigma)} \tag{6.3}$$

and,

$$0 < \sigma < 1 \tag{6.4}$$

$$\epsilon_0 > 0 \tag{6.5}$$

A diagrammatic representation of the characteristic given by equation (6.1) is shown in figure 6:1.

Equation (6.2) is a first order type of filter, with a pole located at $z = \sigma$. The choice of σ is a compromise between the degree of robustness and the alertness of the P.A.A. The use of a value of σ close to 0 will result in a P.A.A. weighted more in favour of robustness. This conclusion can be drawn by considering that a low valued σ results in the first order type of dead-band filter with a small time constant. Hence, the output from this filter will be highly responsive to inputs in the form of controlled process related data. Its likely effect would be to desensetise the P.A.A. by reducing the magnitude of the error signal used in the updating expression.

The minimum dead-band size can be set by selecting an appropriate value for ϵ_0. The choice of this value will clearly specify a lower bound on the acceptable level of model following performance.

The width of the variable dead-band is a function of the controlled process input-output information and the value of ϵ_0. It is important to examine the input-output related aspect since this plays an important part in influencing the permitted tolerance on model following. This is especially relevant where the control scheme is implemented within the context of a uni-polar coordinate measurement framework. Consider, for example, the situation depicted in figure 6:2. Here, the controlled process is excited with a step input command signal, w, figure 6:2a. The contribution of the process input-output information, figures 6:2b and 6:2c, to the behaviour of the variable dead-band characteristic is shown in the final diagram, figure 6:2d. The time response shown corresponds to the expected output, h(k), generated by the variable dead-band filter. This indicates a gradual relaxation of the permitted tolerance on model following performance. It is attributable to the use of the process output signal to generate the variable dead-band characteristic. This is an undesirable consequence of using the variable dead-band characteristic specified in equations (6.1-5) since a lax tolerance on model following performance is generated for an inappropriate reason.

The problem of a gradually relaxing tolerance on model following behaviour could be overcome in a number of different ways. One approach would consist of high-pass pre-filtering of the process output signal prior to its use in the variable dead-band filter. The drawback with this method is that it results in an additional complication to the adaptive scheme because of the introduction of an extra signal processing mechanism. This would result in an increase in the workload when designing an adaptive control scheme. It would also increase the computational burden on the micro-processor system. With the aim of simplifying matters, an alternative procedure is pursued here. The new approach consists of altering the variable dead-band filter to the following form,

$$h(k) = \sigma h(k) + (\mid u(k-1) \mid + \epsilon_0) \qquad (6.6)$$

This solution clearly overcomes the problem associated with using the process output signal in the variable dead-band filter characteristic.

An additional feature of the variable dead-band characteristic relates to particular problems associated with the types of controlled processes dealt with in this thesis. The two applications that are considered in subsequent chapters are capable of being modelled to a reasonable accurate degree with continuous-time transfer functions. However, prudency governs that some degree of caution should be adopted when discrete models are developed to represent these processes. The use of the pole-zero mapping procedure to derive equivalent discrete models raises doubts on the fidelity of the discrete model in the high frequency region in the neighbourhood of the Nyquist frequency. The respective Nyquist frequencies for the control applications discussed later are sufficiently low as to suggest that the controlled processes have non-zero amplitude responses in this region. Use of the pole-zero mapping procedure to derive discrete models of controlled processes means that they are specified as having zero amplitude response at this frequency. The reference model, for a particular control scheme, is specified on the basis of a discrete model of the controlled process. The error in modelling the controlled process in the region of the Nyquist frequency will be transmitted to the reference model because of the way in which the latter is specified. It is argued that a model-process error will be generated during control system operation as a consequence of this phenomenon. This effect would be heightened in situations where the command input signal contains a significant high frequency content. The ensuing parameter adaptation would not be totally correct because a part of the error signal could be traced back to a structural modelling factor. The effect of the $| u(k-1) |$ term in the variable dead-band filter can be viewed as a means of alleviating this condition. This idea is explained below, with reference to a hypothetical situation.

Consider the case of a step input command signal to the adaptive system. Expected forms for the reference model and process outputs are shown in figure 6:3. The high frequency amplitude response limitations in the reference model impair its initial rise. The controlled process, having better high frequency amplitude response characteristics, is able to react more rapidly. The model-process error that is engendered is acceptable as long as the level of model following behaviour is satisfactory for the major part of the response. However, the P.A.A. is still excited, for a short period, by this error. It was considered desirable to isolate the P.A.A. from this phenomenon. The influence of the $| u(k-1) |$ term, in conjunction with the ϵ_0 parameter in the variable dead-band filter, goes some way towards achieving this goal. This is explained with reference to figure 6:2. Following a step input command to the control scheme, figure 6:2a, the process control signal is expected to

become suddenly large, as shown in figure 6:2b. A similar increase will occur in the size of the variable dead-band as indicated in figure 6:2d. The timing of this effect is likely to coincide with the occurrence of a model-process error that is partly attributable to the causes described above. However, the influence of this error signal on the P.A.A. will be reduced as a consequence of the increase in the tolerance limits on model following performance.

One consequence of using a dead-band characteristic is that the coefficients of the parameter vector might not converge to their true values. A possible outcome is that they will assume values falling somewhere in the proximity of their converged values, as long as the 'sufficiently close' model following criterion is met [62]. This factor is not considered to be a problem since the control objective is one of 'sufficiently close' model following and not parameter convergence.

6.3 CONTROL SIGNAL SATURATION

The problem of saturation is one that that stands a strong likelihood of being encountered. This is due to the unavoidable presence of finite performance components within the control system. The simplest example of this concerns the finite ranges of the micro-computer A/D and D/A converters. An equally important case is the possibility of saturating the controlled process by means of large amplitude control signals. It is necessary to consider situations where such phenomena are likely to occur. They have serious implications in terms of the performance of the parameter adaptive algorithm and, by implication, the control scheme. The P.A.A. is designed on the assumption of a linear controlled process. However, system behaviour during saturation is clearly non-linear. This constitutes a violation of the assumptions under which the adaptive control scheme was formulated. Consequently, it is justifiably desirable to take suitable precautions and suspend the adaptation process on such occasions. The detailed realisation of this strategy is discussed below.

The type of problem considered here is where the onset of saturation can be related to the magnitude of the control signal. In many applications, this is likely to be the most readily identifiable condition as well as being the one most frequently encountered. The problem becomes system specific, and more complex, if saturation occurs within the process in a manner which can not be related to a

measurable variable.

In the event of control signal saturation the first action that should be taken is to stop parameter adaptation [24]. This is because further adaptation, to speed up the process response say, will have no effect on the model-process output error. The controlled process is effectively behaving as if it has zero gain. Consequently, the P.A.A. attempts to correct for this by increasing the forward path gain of the controlled process loop. Adaptation here is ineffective since it is trying to overcome a model-process structural difference, as opposed to a purely parametric difference. If left unchecked, it could lead to serious difficulties, not least, when linear behaviour resumes; the strong possibility of an extremely large forward path gain cannot be dismissed lightly.

By carrying out a set of tests or studying the components that comprise the controlled process, it should be possible to evaluate the maximum usable control signal. The onset of saturation can then be detected by comparing the evaluated control signal against the limit value during each sampling period. Should this condition be detected then it is proposed that the parameter vector be frozen. This course of action preserves the most recent set of compensator coefficients which resulted in a control signal falling within the allowable, linear operating range. In addition to fixing the adjustable parameter vector, the reference model should also be 'locked' onto the process. The aim of this measure is twofold. Firstly, it ensures that both reference model and controlled process continue with identical initial conditions once the process control signal de-saturates; the benefits gained from this procedure will become apparent during the latter stages of this presentation. Secondly, the output error is maintained at zero. This makes it certain that the adaptation process is automatically overridden.

The technique used to 'lock' the reference model onto the process is to operate it in a series-parallel configuration; a conceptual interpretation of this procedure was provided in chapter 2. In order to provide a tangible insight into its action, the technique is explained in fuller detail below.

During normal operating conditions, the reference model response is derived in the following manner. Consider, as an example, the reference model transfer function given by,

$$\frac{x(z^{-1})}{w(z^{-1})} = \frac{z^{-r}(b_{m,0} + b_{m,1}z^{-1}+...+b_{m,m}z^{-m})}{(1+a_{m,1}z^{-1}+.....+a_{m,n}z^{-n})} = \frac{z^{-r}b_m B(z^{-1})}{A_m(z^{-1})} \tag{6.7}$$

The reference model output can be expressed in polynomial form as,

$$x(z^{-1}) = z^{-r}b_m B(z^{-1})w(z^{-1}) - \tilde{A}_m(z^{-1})x(z^{-1}) \tag{6.8}$$

where,

$$\tilde{A}_m(z^{-1}) = A_m(z^{-1}) - 1 \tag{6.9}$$

A schematic representation of the procedure used to evaluate the reference model response is shown in figure 6:4.

By separating the reference model of figure 6:4 into two parts, it can be operated in a series-parallel configuration, as shown in figure 6:5. The modified expression for evaluating the reference model output thus becomes,

$$x(z^{-1}) = z^{-r}b_m B(z^{-1})w(z^{-1}) - \tilde{A}_m(z^{-1})y(z^{-1}) \tag{6.10}$$

In effect, this simply requires the reference model state vector be updated with elements from that of the controlled process.

The safety procedure outlined above appears to be unnecessarily complicated. However, when it is viewed within the context of the following situation, there can be little argument as to its value to the adaptive control system. Consider the response of a system to a step input. Control signal saturation is assumed to occur over part of its transient response. Without the 'locking' procedure, a typical response pattern for the controlled process and reference model might be as shown

in figure 6:6. By the time that the process control signal comes out of saturation, the reference model response has nearly attained the set-point. Hence, considering only the non-saturation related portion of the controlled process response, the adaptive control system perceives a reference model with an exceptionally 'fast' speed of response. This is shown in figure 6.6a, as an enlarged version of the encircled region in figure 6.6. The type of reference model behaviour depicted in figure 6.6a clearly implies an unrealistic level of performance expectation from the controlled process. In addition, it also perturbs the P.A.A. undesirably. The series-parallel mode of operation results in this type of situation being avoided, as shown in figure 6:7. Here, the reference model initially responds as expected. The series-parallel mode of operation is invoked when the controlled process signal is detected as being saturated. In contrast to figure 6:6 however, the reference model response, upon the resumption of linear behaviour, is of a more acceptable nature. This results from the reference model and process state vectors sharing the same initial conditions.

6.4 THE $F(z^{-1})$ COMPENSATOR ROOT LOCATIONS

The task of the P.A.A. is to generate the coefficients of the $F(z^{-1})$ and $G(z^{-1})$ compensators with the aim of nullifying the model-process output error. The $G(z^{-1})$ compensator is a non-recursive digital filter; the root positions of this filter polynomial are not restricted from the stability point of view. Conversely, the $F(z^{-1})$ compensator is a recursive digital filter which introduces a number of poles into the process loop. Stability in this case will only be preserved as long as the pole locations lie inside the unit z-plane disc [42].

While the $F(z^{-1})$ polynomial coefficients are changing, its root positions are unlikely to be stationary. Consequently, an unstable closed loop system is possible if one or more of its roots migrate outside the unit disc. To prevent this problem from occurring, the following check procedure was incorporated into the adaptive control algorithm. To begin with, a stability test is carried out on the $F(z^{-1})$ polynomial every time its coefficients are updated. Should the most recent set of coefficients result in roots falling outside some pre-defined stability region then they are to be discarded. Instead, the previous set of coefficients should be retained since they correspond to a stable compensator network. This technique of constraining a subset of the adaptive parameter vector is discussed in [65].

The safety procedure outlined above acts as a check on parameter updating; this is only allowed to proceed under rigidly determined conditions. The use of this concept in the context of parameter adaptive systems is typically realised with a particular form of algorithm as discussed in [62,65] for example. Essentially, this involves the specification of individual maximum and minimum limits for each of the coefficients in the adjustable parameter vector. During operation, parameter updating is only permitted as long as the value of a given coefficient falls within its permitted tolerance range. This technique calls for a considerable degree of prior knowledge about the control system as a whole in order to facilitate the specification of limit values for the individual coefficients. The reason for not pursuing this procedure is that it is more involved, and hence computationally intensive, by comparison with the original procedure.

The simplest safety check to preserve the stability of the filter block containing the $F(z^{-1})$ polynomial requires verification that its roots lie inside the unit disc. Analytical solutions can be used to determine the root positions of polynomials including cubics and quartics [66]. A significant disadvantage of these techniques is the need for a considerable number of arithmetic operations. For higher order polynomials, recursive solutions are called for. Both of these outcomes are undesirable for a number of reasons, the most notable of which concerns their computational requirements. The number of iterations required to determine all of the root locations in the latter case, for example, is likely to vary from one sampling interval to the next. This could have serious implications for systems with fast sampling rates as it might not always be possible to iterate to convergence within the time available. In addition, the precise locations of the roots of the polynomial are irrelevant as long as they are known to lie inside some prescribed stable region. These difficulties can be overcome by using an alternative test method which avoids an explicit solution for the $F(z^{-1})$ polynomial roots. The procedure adopted here is based on Jury's method for testing the stability of polynomials [67]. This is carried out on the basis of their coefficient values only. It is similar to the Routh-Hurwitz test for continuous-time systems. Application of the test is illustrated with the following example. Consider a general, quartic polynomial, F(z), given by,

$$F(z) = a_4z^4+a_3z^3+a_2z^2+a_1z+a_0 \quad with \quad a_4>0 \tag{6.11}$$

Using the coefficients of this polynomial, form the array shown below, noting that each of the even-numbered rows is simply the preceding row in reverse order.

z^0	z^1	z^2	z^3	z^4
a_0	a_1	a_2	a_3	a_4
a_4	a_3	a_2	a_1	a_0
b_0	b_1	b_2	b_3	
b_3	b_2	b_1	b_0	
c_0	c_1	c_2		
c_2	c_1	c_0		

where,

$$b_0 = \begin{vmatrix} a_0 & a_4 \\ a_4 & a_0 \end{vmatrix} \quad , \quad b_1 = \begin{vmatrix} a_0 & a_3 \\ a_4 & a_1 \end{vmatrix} \quad , \quad b_2 = \begin{vmatrix} a_0 & a_2 \\ a_4 & a_2 \end{vmatrix} \quad , \quad b_3 = \begin{vmatrix} a_0 & a_1 \\ a_4 & a_3 \end{vmatrix}$$

and,

$$c_0 = \begin{vmatrix} b_0 & b_3 \\ b_3 & b_0 \end{vmatrix} \quad , \quad c_1 = \begin{vmatrix} b_0 & b_2 \\ b_3 & b_1 \end{vmatrix} \quad , \quad c_2 = \begin{vmatrix} b_0 & b_1 \\ b_3 & b_2 \end{vmatrix}$$

The necessary and sufficient conditions for the F(z) polynomial of equation (6.11) to have no roots on or outside the unit disc are as follows:

$$F(1) > 0 \tag{6.12}$$

$$(-1)^n F(-1) > 0 \tag{6.13}$$

$$|a_0| < a_4 \tag{6.14}$$

$$|b_0| > |b_3| \tag{6.15}$$

$$|c_0| > |c_2| \tag{6.16}$$

It should be noted that the last entry in the Jury array is of a quadratic form. In addition, for an n^{th} order system, there are a total of n+1 constraints. Thus, for the quartic polynomial considered above, this results in a total of five constraints.

Use of the check procedure discussed above will help to uphold the stability of the $F(z^{-1})$ compensator network in the control scheme. By allowing the filter polynomial roots to lie anywhere inside the unit disc however, it is possible to envisage certain situations which could give rise to highly oscillatory, process control signals. Such an eventuality will arise if one or more of the $F(z^{-1})$ compensator roots lies in the approximate shaded region of the unit disc as shown in figure 6:8 [42]. For example, a pair of complex poles in this area would correspond to a very underdamped system with a high natural frequency. This becomes apparent upon closer examination of the characteristic damping and natural frequency loci superimposed on the unit disc in figure 6:8; these provide an indication of the effects of different pole locations within the z-plane unit disc. In many control schemes it is a commonplace procedure to ignore the effects of high frequency dynamics when modelling the controlled process. This course of action is dictated by the fact that it is unrealistic to attempt to model every phenomenon in a

given system since this would lead to overly complex models. The modelling simplification is acceptable as long as the neglected phenomena do not provide a significant contribution to the way in which the controlled process behaves. Clearly, the potential use of high frequency control signals runs a significant risk of exciting neglected high frequency dynamics [68]. These are likely to exert a parasitic influence on the parameter adaptive system. In order to assure a control signal of improved quality, it is proposed that the roots of the $F(z^{-1})$ polynomial be constrained to a reduced region instead of the full unit disc. The region selected is a disc of radius 0.8 and centred on (0,0.2j) as shown in figure 6:9. This choice eliminates the possibility of a highly oscillatory control signal. At the same time it assures the stability of the $F(z^{-1})$ polynomial. The Jury test procedure can still be used to test for this condition. However, before it can be applied, the original $F(z^{-1})$ polynomial must first be altered to reflect the use of a new constrained region. The modification consists of transforming the original polynomial with the following function.

$$F'(z) = F(z)_{z = (0.8z + 0.2)} \tag{6.17}$$

The mapping function of equation (6.17) causes the off-centre, reduced radius disc of figure 6:9 to be transformed into unit disc centred on the point (0,0j). Following this transformation, $F'(z)$ now becomes the polynomial that is passed to the stability test routine.

6.5 THE f_0 COEFFICIENT

The control signal used to drive the process is generated from an equation of the following form:

$$u(k) = \frac{w(k) - \hat{f}_1 u(k-1) \ldots - \hat{f}_i u(k-i) \ldots - \hat{g}_0 y(k) \ldots - \hat{g}_j y(k-j) - \ldots}{\hat{f}_0} \tag{6.18}$$

It is clear that the value of $\hat{f}_0$ should never become zero if the control signal is to remain finite. A check should be carried out on this coefficient to prevent this situation from arising. Adopting a similar line of reasoning to that presented in the

previous section, the $\hat{f}_0$ coefficient is not updated if a zero or negative valued term is generated by the P.A.A.

By making use of the check procedure outlined in section 6.4, it is possible to dispense with an explicit check on the $\hat{f}_0$ coefficient. This can be deduced by examining the conditions that have to be satisfied to verify the stability of a given polynomial. In the example cited above, one of these involves the test, $|a_0| < a_4$, where a_4 corresponds to the forward path gain, $\hat{f}_0$. Clearly, if $\hat{f}_0$ is negative or zero then this test will fail. Hence, the $F(z^{-1})$ compensator coefficients will not be updated and the calculation procedure of equation (6.18) can be carried out safely.

6.6 DISTURBANCE REJECTION AND INTEGRAL ACTION CONTROL

Disturbances acting on the controlled process will have a detrimental effect on control system performance if they are allowed to pass unchecked [69]. The case for a corresponding, detrimental effect on the parameter adaptive algorithm can also be made. This argument can be appreciated by analysing the consequences for the updating procedure. While still maintaining full generality, this analysis can be greatly simplified by examining the case of a single adjustable compensator parameter. Consider, as an example, the case of a feedback gain, $\hat{g}_0$. An examination of the P.A.A. developed earlier in chapter 5 indicates that the particular updating expression for the $\hat{g}_0$ coefficient can be written as,

$$\hat{g}_0(k) = \hat{g}_0(k-1) - \frac{\gamma y^o(k-r)\nu^o}{1+\tilde{\Phi}^T(k-r)\gamma\tilde{\Phi}(k-r)} \qquad (6.19)$$

However, the 'a priori' filtered error signal can be broken down as follows,

$$\nu^o(k) = C(z^{-1})e^o(k)$$

$$= C(z^{-1})[\,x(k) - y^o(k)\,]$$

It is thus possible to expand the parameter updating expression of equation (6.19) to the following form.

$$\hat{g}_0(k) = \hat{g}_0(k-1) - \frac{\gamma y^o(k-r)C(z^{-1})[x(k)-y^o(k)]}{1+\tilde{\Phi}^T(k-r)\gamma\tilde{\Phi}(k-r)}$$

$$= \hat{g}_0(k-1) - \frac{\gamma C(z^{-1})[y^o(k-r)x(k)]}{1+\tilde{\Phi}^T(k-r)\gamma\tilde{\Phi}(k-r)} + \frac{\gamma C(z^{-1})[y^o(k-r)y^o(k)]}{1+\tilde{\Phi}^T(k-r)\gamma\tilde{\Phi}(k-r)} \quad (6.20)$$

Clearly, the disturbance related signal can assume a variety of different forms. However, the simplest case of a steady disturbance suffices to develop the current argument; other cases have been considered elsewhere [70]. By invoking the principle of superposition, both $y^o(k-r)$ and $y^o(k)$ will share a common component, y_D, attributable to the steady disturbance. Therefore,

$$y^o(k) = y_t^o(k)+y_D(k) \quad (6.21)$$

$$y^o(k-r) = y_t^o(k-r)+y_D(k-r) \quad (6.22)$$

with,

$$y_D(k-r) = y_D(k) \quad (6.23)$$

The subscript, t, denotes the non-disturbance related process output signal. Problems with the P.A.A. are unavoidable, in the situation described above, as $y_D(k)$ and $y_D(k-r)$ are correlated. This outcome implies that the term, $C(z^{-1})[y^o(k)y^o(k-r)]$, contains a positive component, $y_D(k)y_D(k-r) = y_D^2(k)$, according to equation (6.23). Since the adaptation algorithm is of an integral form, the effect of this constant input can be expected to cause the magnitude of the adaptive coefficient $\hat{g}_0$ to become progressively larger. A similar scenario can be developed for the remaining adaptive coefficients. The adaptive behaviour of the adjustable parameter vector, under these circumstances, is not the consequence of a parametric mismatch between the reference model and controlled process loop [60]. As such, it is undeniably detrimental to the correct operation of the complete adaptive control system.

Where the disturbance effects can be suitably well parametrised, this information can be taken into account and the P.A.A. modified appropriately. For example, it would be a relatively straightforward matter to deal with a fixed offset transducer error. Various situations have been examined by researchers in adaptive control and a number of solutions have been suggested [70,71]. In [71] for example, the adaptive law was modified by introducing a dead-zone, in a similar manner to that described in section 6.2 of this chapter. The width of this dead zone was kept fixed and was selected on the basis of prior knowledge about the upper bound of the disturbance signal. This approach to the problem has been referred to by a number of authors. However, although techniques such as these go some way towards enhancing the performance of the P.A.A. they are unlikely to have addressed fully the question of control system performance and set-point tracking. The latter aspect is more relevant to the systems examined in this thesis and led to the developments detailed below, which are targeted at the disturbance rejection properties of the control system.

Viewed simply as a control engineering problem, the level of performance specification outlined above calls for the introduction of an integral action compensator in the process control loop. Typically, this could be carried out in the manner shown in figure 6:10. The relative simplicity of this solution to the control problem does however create difficulties by increasing the complexity of the adaptive scheme. This arises because the controlled process and integral term are linked together. This combination acts as the model for the new controlled process. The addition of the integral compensator makes it of a higher order than the process model employed previously. This new model is subsequently used to determine suitable orders for the reference model and compensator transfer functions, according to the pattern established earlier. Clearly, the new adaptive scheme to emerge from these changes will necessarily be more complicated. This will be one consequence of requiring higher order compensator networks, and hence, a greater number of adaptively generated parameters.

An alternative means of implementing an integral action controller is possible. This method, as shown in figure 6:11, makes use of the model-process output error signal [24,72]. This approach has the advantage of not increasing the complexity of the compensator networks and reference model transfer function. It is straightforward to implement [24,72] and, more importantly, does not result in a significant addition to the computational workload.

In situations where integral action is employed, it is generally advisable to incorporate some form check mechanism to prevent integrator wind-up. A control scheme containing an explicit integrator within the process control loop will already be subjected to such a check. The control signal saturation monitoring procedure, described in section 6.2, is responsible for this. A similar form of check mechanism would be necessary for the alternative realisation of an integral action controller.

6.7 DISCUSSION

The modifications to the basic adaptive scheme that are described above act as a series of safety mechanisms. In effect, they represent a supervisory form of control loop. The aim of their inclusion is to cater for eventualities that are considered to be detrimental to the adaptive scheme; they are not expected to play a major role in shaping the model following ability of the control scheme under usual operating conditions. Rather, the intention is that they should help to maintain an acceptable quality of control system performance when the adaptive system is 'disturbed'. Moreover, this should of benefit in allowing a smooth transition when favourable operating conditions resume. Consider, as an example, the case of an adaptive scheme without an integral action controller and where the controlled process is subjected to a steady disturbance. The disturbance signal will appear as a steady component in the process output and control signals. This will result in an increase in the minimum size of the variable dead-band characteristic and help to attenuate the degree of parameter adaptation; this is desirable because parameter adaptation is not being caused by a model-process parametric error. When the disturbance effect is removed, parameter adaptation continues with the objective of returning to the original situation. However, it can be argued that the use of a variable dead-band characteristic was advantageous in limiting the degree of incorrect parameter adaptation.

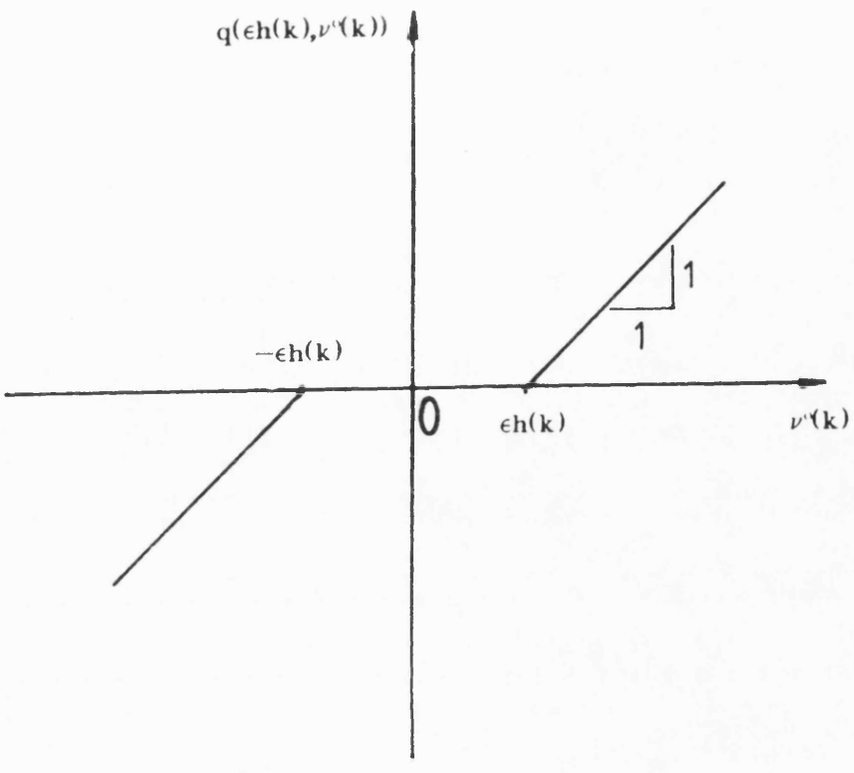

FIGURE 6:1 Variable Dead-Band Filter Characteristic

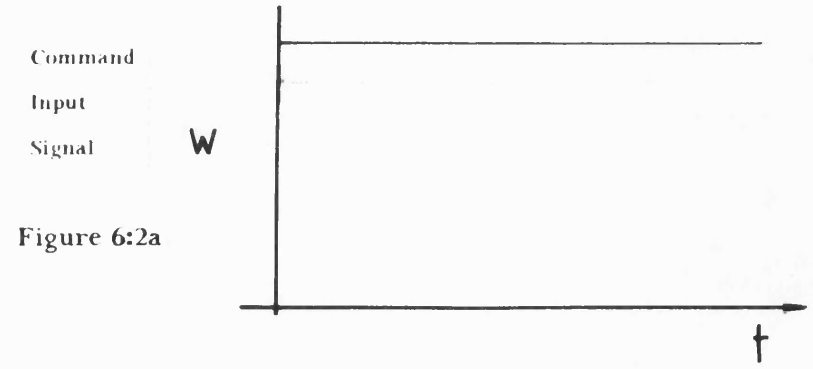

Figure 6:2a

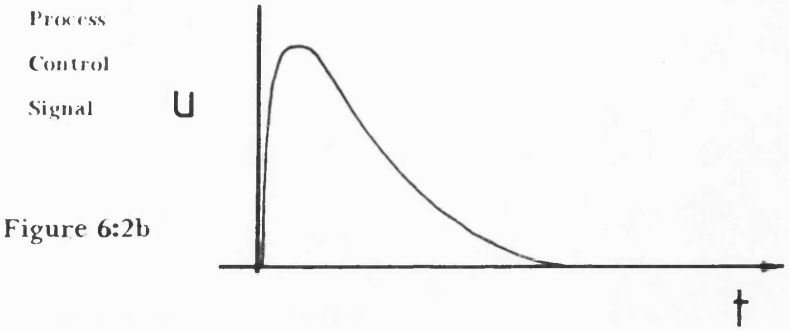

Figure 6:2b

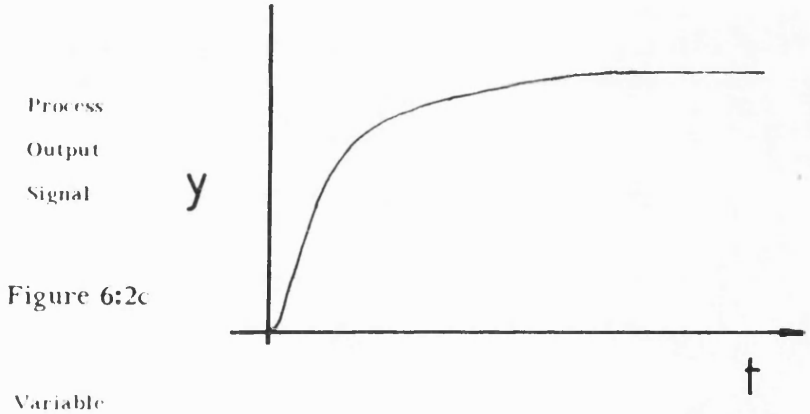

Figure 6:2c

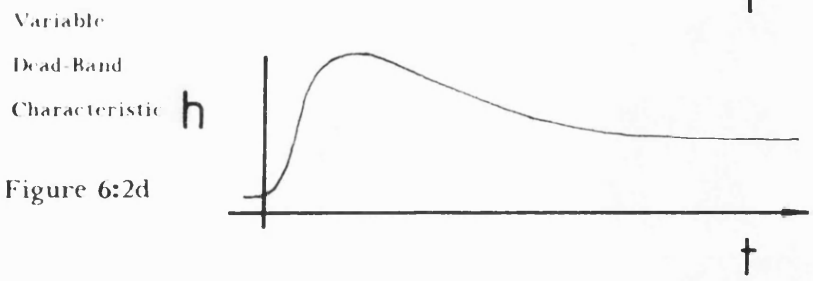

Figure 6:2d

FIGURE 6:2 Relationship Between The Variable Dead-Band Filter Characteristic And Process Input/Output Information

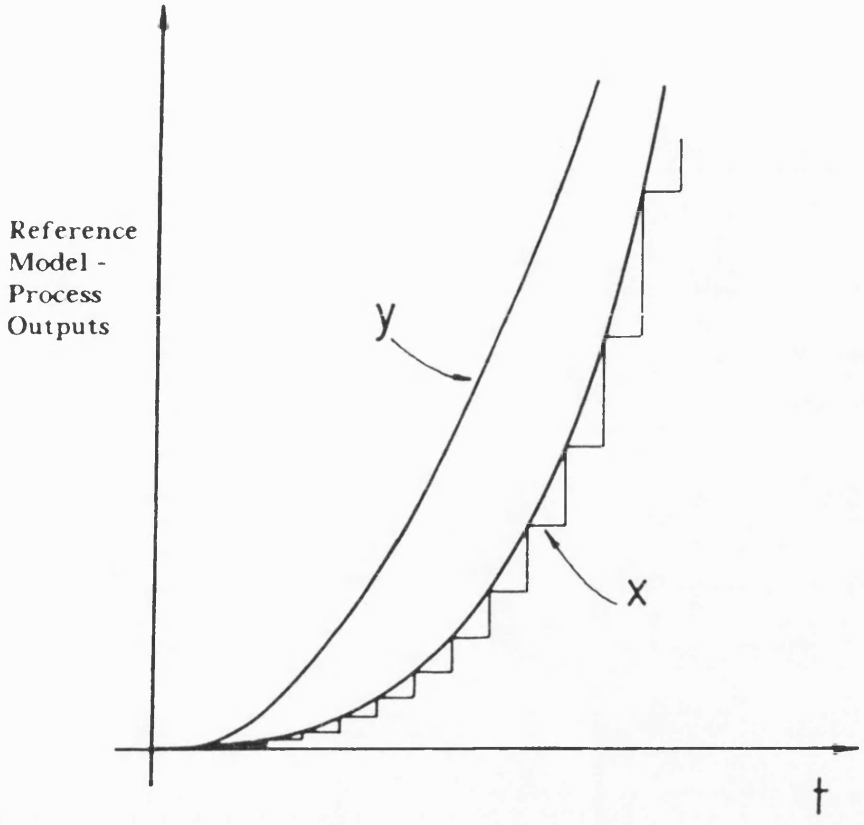

FIGURE 6:3 Example Initial Responses Of Reference Model And Controlled Process To A Step Input

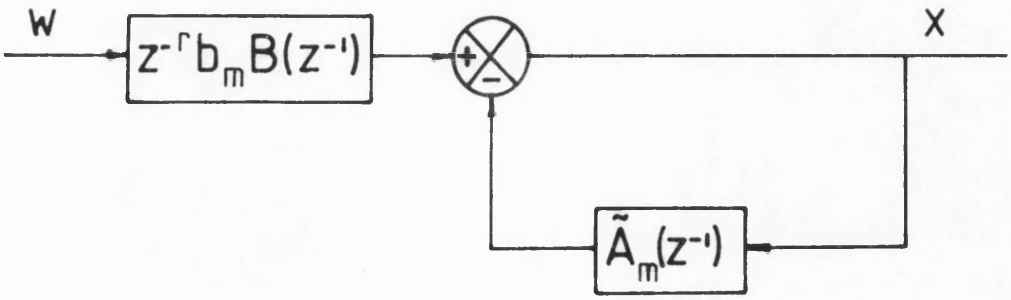

FIGURE 6:4 Block Diagram Representation Of Reference Model Transfer Function

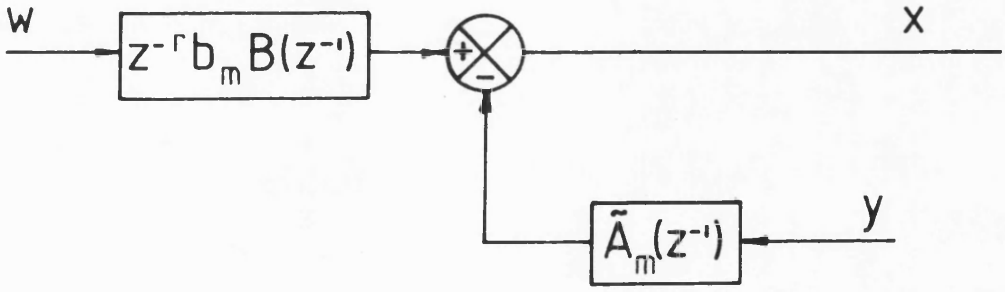

FIGURE 6:5 Series-Parallel Configuration For Reference Model Transfer Function

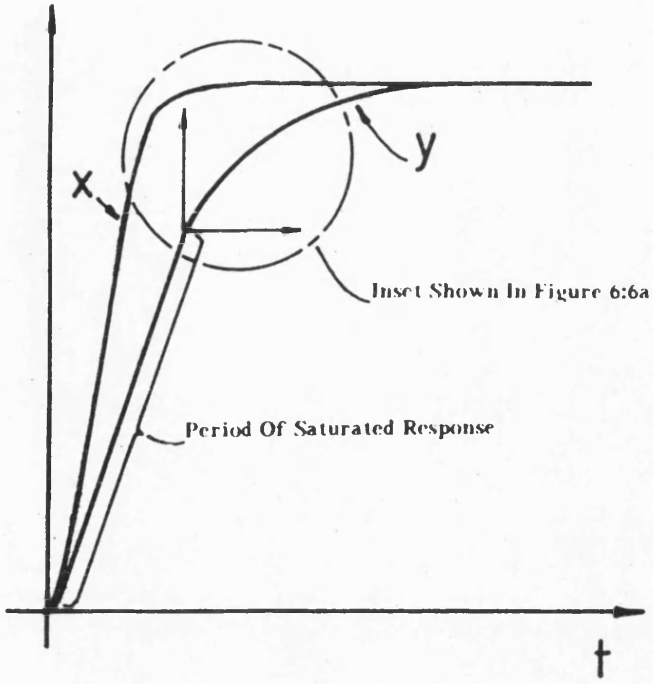

FIGURE 6:6 Slew-Rate Limited Process Step Response Caused By A Saturated Control Signal

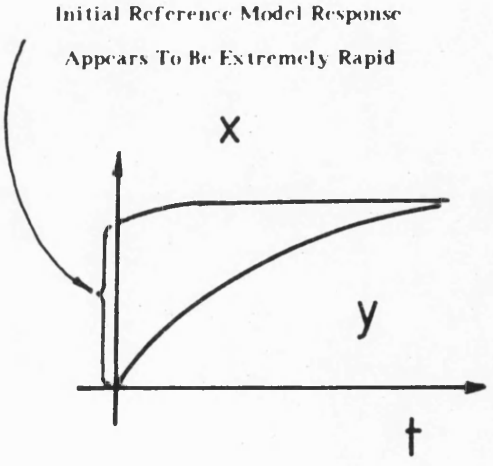

FIGURE 6:6a Reference Model And Process Responses Corresponding To A Non-Saturated Process Control Signal

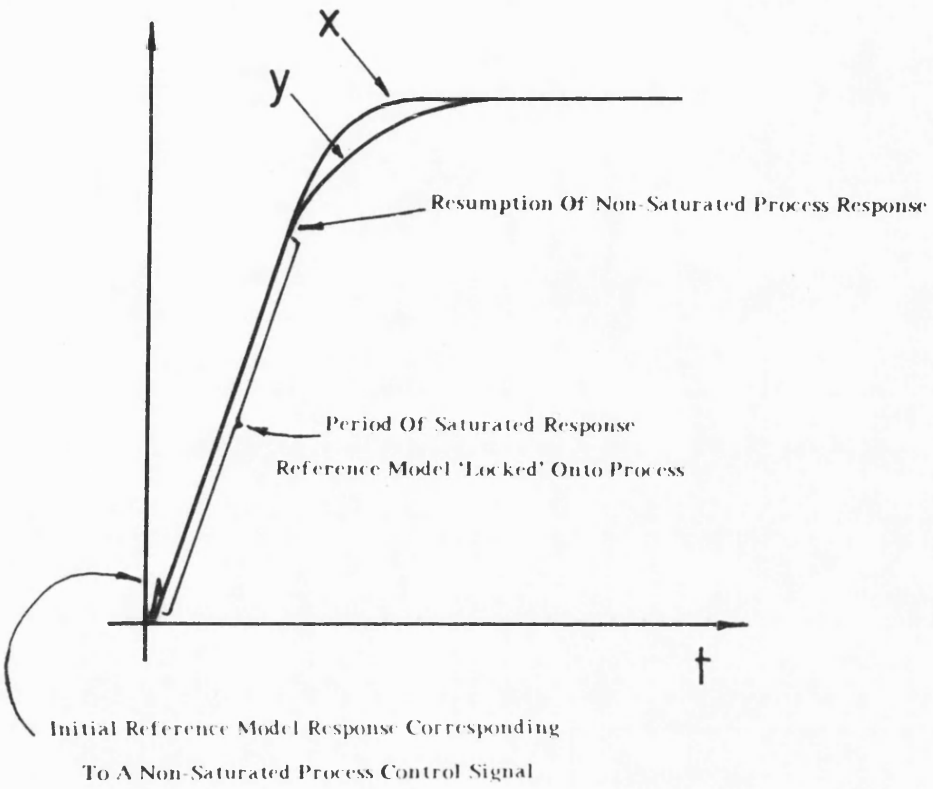

FIGURE 6:7 Reference Model And Process Responses Corresponding To The Use Of A Series-Parallel Mode Of Operation

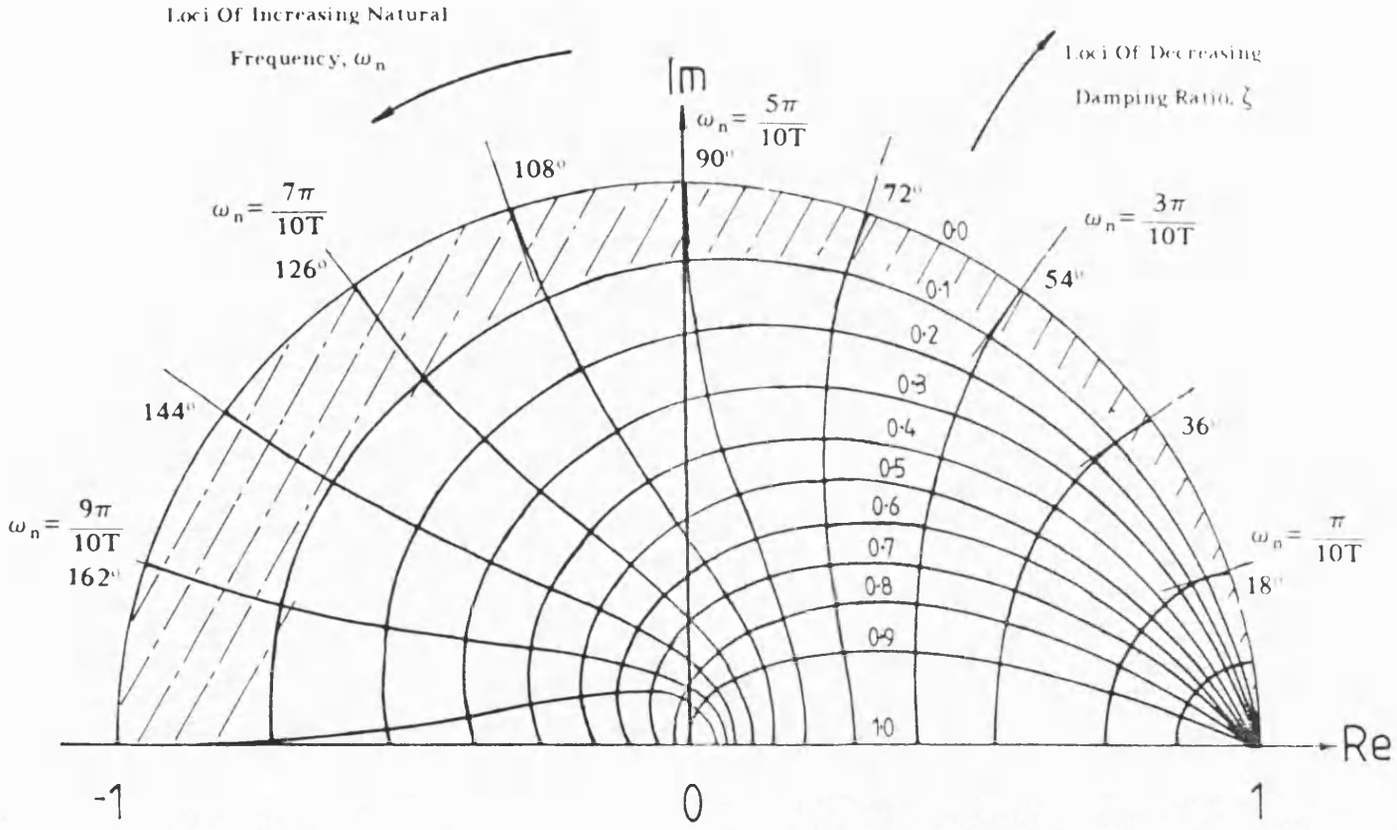

FIGURE 6:8 z-Plane Diagram Showing Loci Of Constant Damping And Natural Frequency

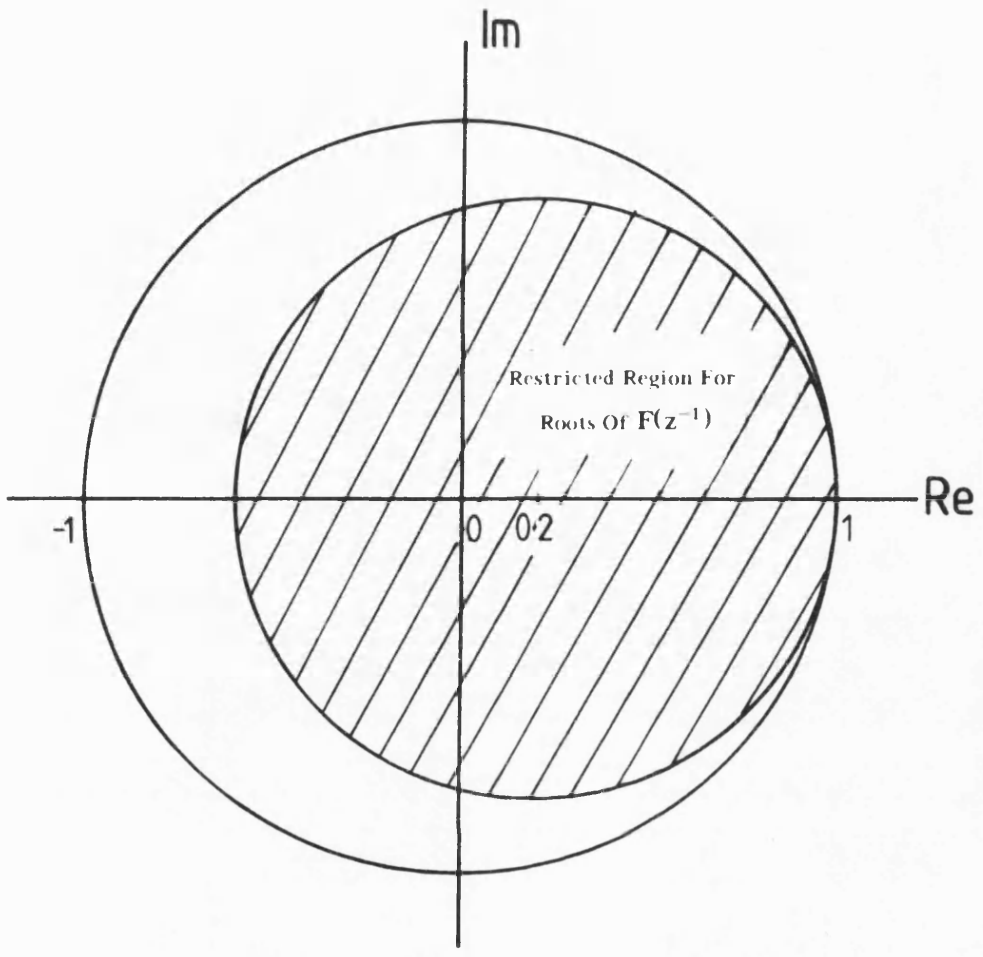

FIGURE 6:9 Restricted Region For Roots Of The $F(z^{-1})$ Compensator Polynomial

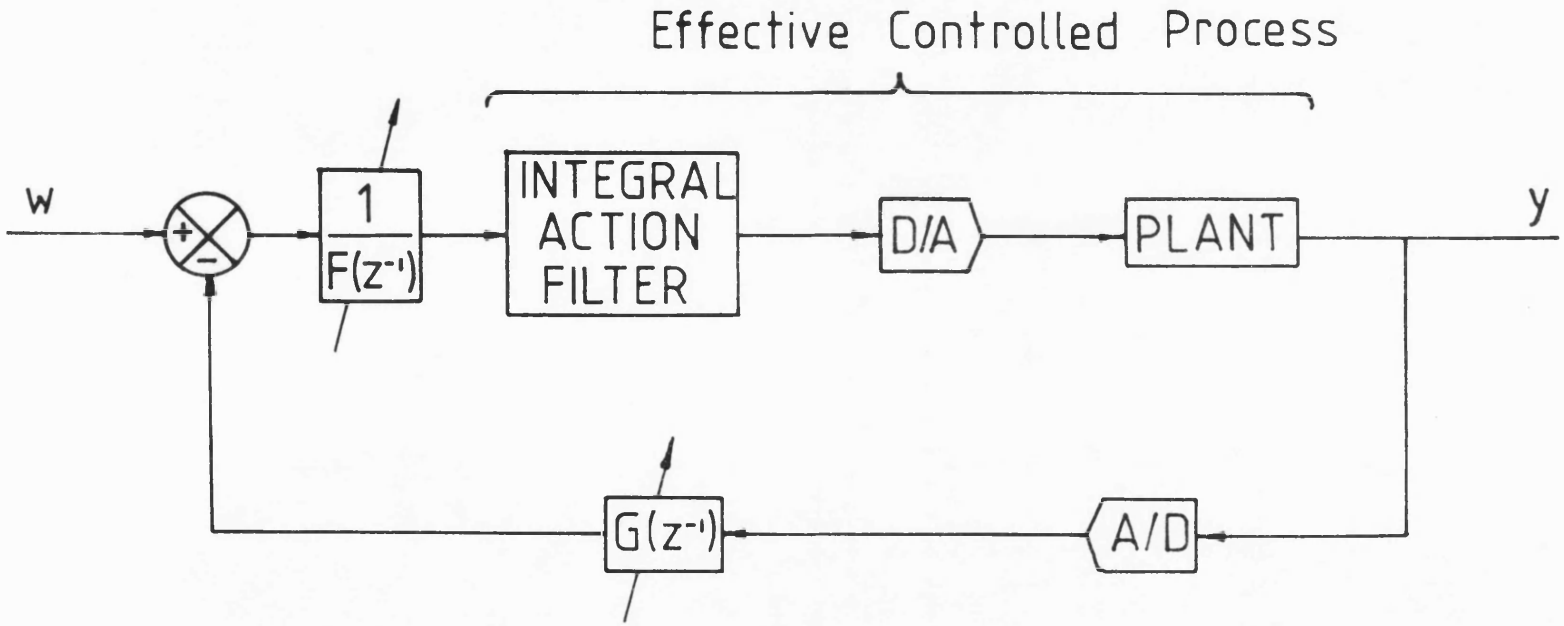

FIGURE 6:10 Block Diagram Representation Of A Conventional Integral Action Control Scheme

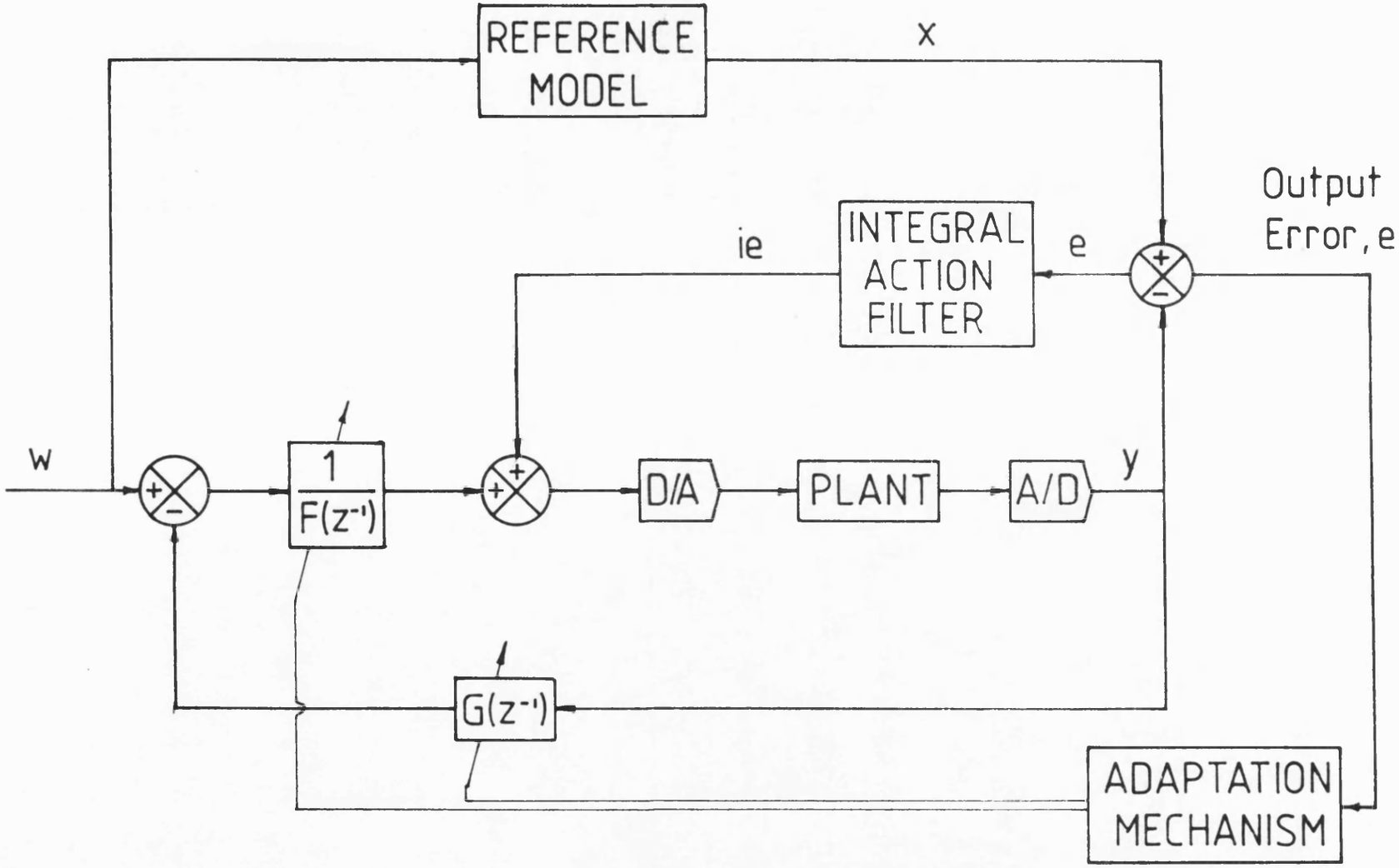

FIGURE 6:11 Block Diagram Representation Of A Model Reference Based Integral Action Control Scheme

CHAPTER 7

ADAPTIVE CONTROL SYSTEM REALISATION

7.1 INTRODUCTION

Implementation of the adaptive control scheme developed in the preceding chapters can be considered from two viewpoints; hardware and software. These aspects of the control scheme form the core material discussed in this chapter.

Initially, the micro-processor system that was used for the experimental work is described. It is followed by an examination into one particular implication of realising the adaptive control scheme within a real time computing environment. Important factors emerging from this discussion are put into perspective by means of a flow-diagram representation of the adaptive control algorithm. The final part of this chapter is devoted to those parts of the adaptive system which have to be initialised by the designer.

7.2 MICRO-PROCESSOR SYSTEM

A 'DARKSTAR' computer system was used as the basis for implementing model reference adaptive control algorithms. The DARKSTAR was designed and built in the School of Electrical Engineering at the University of Bath; figure 7:1 is a photograph of the system. The machine itself is based on a Motorola 68000 CPU, a 16-bit device, driven at a clock frequency of 8MHz.

The DARKSTAR was designed as a development tool for use in a wide variety of applications. These include operating as a multi-user system and as an on-line data acquisition and storage device. The multi-user operating environment is supported by the TRIPOS operating system [73]. A multi-tasking option is also available within this framework.

In the context of an on-line data acquisition device, the computer system possesses 500Kbytes of on-board memory. This capacity is further augmented with twin disc drives, each capable of storing 800Kbytes. In addition to the usual range

of interfaces as shown in figure 7:2, the computer is also provided with a data acquisition card. This contains eight A/D converters and four D/A converters; all converters are 12-bit devices. Their sensitivities and ranges can be set up according to user defined requirements, within reason. For the experimental work reported here, all converters were initialised with a single sensitivity setting of 5mV. per bit. In addition, a bi-polar measurement convention was used.

7.2.1 ANTI-ALIASING

The use of anti-aliasing filters in computer controlled systems is widely advocated [42,46]. They are needed in order to avoid high-frequency signals being sampled and subsequently appearing to be low-frequency components. A common procedure for overcoming this problem is to pre-filter analogue signals prior to their being sampled; the filtering action should be geared to removing the frequency content above the Nyquist frequency used by the sampling mechanism. Unfortunately, this solution poses an important problem for sampled data adaptive control schemes. This arises because the frequency response characteristics of the controlled process appear to be altered as a result of the anti-aliasing filter characteristics. It would be possible to redesign the adaptive control scheme by using a new model of the effective controlled process, incorporating the dynamics of the anti-aliasing filter. However, this is undesirable since it would involve a higher order controlled process model which would result in undesirably complex control schemes.

The anti-aliasing filters on the DARKSTAR analogue-to-digital converters were set up with a bandwidth of 150 Hz. This value was far too high to be effective for the control schemes reported in this study. This was not considered to be a problem for the following reasons. The first sampled signal, the command input, was always controlled carefully; there was no likelihood of using signals of a high enough dominant frequency to cause aliasing difficulties. The second sampled signal was the controlled process output. The types of processes considered in this study were all based on servo-systems. This means that the controlled process transfer functions include a free integral term. This results in significant attenuation of high frequency signals above the Nyquist frequency and was considered to be an adequate safeguard in preventing aliasing problems with this signal.

7.3 SOFTWARE IMPLEMENTATION - ARITHMETIC OPERATIONS

Since the control algorithms involve a significant amount of computation, this calls for rapidly executable code, amongst other things. This is most readily attainable through coding in a low level language, such as assembler or machine code. This option was nevertheless rejected. Controller design and implementation was, and still is, at an early stage of development. It was therefore considered that the increased workload of programming in assembler or machine code was not justifiable. Consequently, controller implementation was carried out in the high level language, BCPL (Basic Combined Programming Language) [74]. A comparison of algorithms coded in BCPL and assembler highlights significant differences in their respective speeds of execution [75]. On this basis, there is considerable justification for eventually using the latter, especially where fast sampling frequencies are required.

Within the control algorithm software, the majority of arithmetic operations were carried out with 32-bit real arithmetic instructions. In an attempt to improve the speed of execution of the control algorithm, a small amount of work was carried out with integer arithmetic. This was only done in cases where the potential for numerical overflow problems was considered to be negligible. Integer addition and subtraction was carried out in usual fashion using 32-bit parameters. However, for added assurance, integer multiplication and division was undertaken with a locally implemented function called muldiv. Muldiv employs three parameters and is invoked with the command, muldiv(a,b,c); the three parameters represent 32-bit integer values. When muldiv is executed, the ensuing sequence of operations causes the parameters a and b to be multiplied. Rather than being truncated to a 32-bit value, the result is stored as a 64-bit integer. This value is subsequently divided by c to provide a 32-bit integer result. A considerable reduction in the computational effort is possible if a large number of real arithmetic operations can be safely replaced with integer operations of this type.

7.4 THE COMPUTATIONAL DELAY FACTOR

The system equations that completely specify the adaptive scheme imply that all sampling actions occur concurrently. This is clearly not the case, as the micro-processor system carries tasks out in a sequential manner. The most serious

violation of the concurrency assumption occurs in generating the process control signal, u, [46]. Considering a general case, the situation that arises is schematically demonstrated in figure 7:3. The process output, y, must first be sampled before the control signal, u, can be evaluated from the command signal and the $F(z^{-1})$ and $G(z^{-1})$ compensators. A certain amount of delay is therefore inevitable.

A reduction in the computational delay can be made by separating the control signal evaluation procedure into two parts. The first of these would involve evaluating that component of the control signal which is dependent on available information; this includes the adjustable compensator coefficients and previously delayed process input-output information. The second part would consist of sampling the command input and process output signals. Their contribution to the control signal could then be added to the result of the first part. Consider, as an example, a control scheme with $F(z^{-1})$ and $G(z^{-1})$ compensators, both of order two, thus,

$$F(z^{-1}) = \hat{f}_0+\hat{f}_1z^{-1}+\hat{f}_2z^{-2} \tag{7.1}$$

$$G(z^{-1}) = \hat{g}_0+\hat{g}_1z^{-1}+\hat{g}_2z^{-2} \tag{7.2}$$

Ordinarily, as indicated in chapter 5, the process control signal is evaluated according to the following expression.

$$u(k) = \frac{w(k)-\hat{f}_1u(k-1)-\hat{f}_2u(k-2)-\hat{g}_0y(k)-\hat{g}_1y(k-1)-\hat{g}_2y(k-2)}{\hat{f}_0} \tag{7.3}$$

Within the context of the control scheme modification being discussed here, this calculation can be separated as shown below.

$$u(k) = \frac{w(k)-\hat{g}_0y(k)+u^p(k)}{\hat{f}_0} \tag{7.4}$$

where,

$$u^p(k) = -\hat{f}_1u(k-1)-\hat{f}_2u(k-2)-\hat{g}_1y(k-1)-\hat{g}_2y(k-2) \tag{7.5}$$

It is clear that the u^p contribution to the process control signal can be evaluated

during the sampling interval prior to its use. This procedure is graphically represented in figure 7:4. It is clearly a more efficient procedure than the original proposal.

In spite of the modification proposed above a certain amount of delay is obviously unavoidable. This is because the command input and process output signals have to be sampled and then processed. In attempting to account for this delay two options are considered in this thesis.

The first option relates to lengthy control algorithms. Such an eventuality will arise when controlling high order processes. The reason for this is that the process order effectively determines the number of compensator coefficients to be generated. Obviously, this affects the computational workload, and hence the length of the sampling period, for a given computer system. Where the sampling period is long, the fractional delay required to generate the control signal is likely to be proportionately small. No modifications are proposed for the control scheme if this delay is less than 20% of the sampling period. Flow-diagram 7.1 provides an indication of the control algorithm format associated with such a scheme.

In contrast to the previous situation, control schemes designed around low order processes will necessarily have relatively short sampling periods. Consequently, the fractional delay element will be of a higher percentage value than before. The importance of this unmodelled phenomenon is considered to be sufficiently significant as to warrant modification of the control scheme. A possible solution would involve arbitrarily lengthening the sampling period in order to make the fractional delay less than 20% of the sampling period. One negative aspect of this solution is that the micro-processor system is periodically idle; it might not always be possible to include other tasks which can be accommodated perfectly, or at all, into the free computing time thus created. More importantly, an increase in the sampling period corresponds to a reduction in the Nyquist frequency. By implication, this will result in a reduction in the available bandwidth within which to implement the control scheme.

The difficulty with the existing control scheme arises from a need to minimise the time taken to generate and send out the process control signal. In order to overcome this problem, the solution employed here involves purposely extending this fractional delay to a full sampling period. By sending the control signal out at

the end of every sampling period, all sampling actions can be carried out within a very short span of time; in relation to the length of the sampling interval, sampling actions can effectively be said to occur instantaneously. This modification is represented in the control scheme by adding a 1/z term to the controlled process in order to derive an effective controlled process transfer function. This situation is depicted in figure 7:5. Figure 7:5a shows the original situation where the computational delay is not accounted for. In figure 7:5b, the control signal is delayed by one sampling period, according to the modification proposed above. Figure 7:5c represents the same situation as figure 7:5b although it employs an alternative interpretation. In it, the control signal corresponding to the sampling period u(k) appears to have been evaluated and sent out without any computational delay. However, when this control signal arrives at the input to the system, $\hat{G}(z)$, the situation becomes identical to that shown in figure 7:5b. By modelling the controlled process as if it included a 1/z term it is possible to make it appear as if the control signal is evaluated and output without any computational delay; in reality, the unit delay is implicit and represents the time taken for one pass of the adaptive system computation process.

The following alteration, aimed at enhancing the control scheme by taking advantage of the modification proposed above, is also proposed. In the modified adaptive control scheme the control signal, for a given sampling interval, is evaluated from the set of compensator coefficients generated during the previous sampling interval. Having evaluated the control signal, the remainder of the interval is devoted to updating the set of compensator coefficients, in readiness for the following time step. At the end of the sampling period, the control signal is sent to the process and the control algorithm repeated for the next sampling interval. Clearly, since the control signal is delayed to the end of the sampling interval in the modified adaptive scheme, there is no longer any need to evaluate it at the earliest possible moment. Consequently, the alteration proposed here involves reversing the order of operations in the control scheme; this results in the compensator coefficients being updated at the start of the sampling interval. Subsequently, they are used to evaluate the control signal. In this way, the most recently generated information is used to evaluate the process control signal. As a means of comparison with the original control algorithm configuration, and shown in flow-diagram 7.1, the new scheme is shown in flow-diagram 7.2.

It should be noted that in altering the make-up of the control system, the

procedure followed in appendix 2 to derive the adaptation algorithm needs to be reassessed. When a similar stability analysis is applied to the new control system configuration, the adaptation laws are of the following form as can be appreciated by referring to appendix 2, part b.

$$\underline{\hat{d}}(k) = \underline{\hat{d}}(k-1) - \Gamma\underline{\tilde{\Phi}}(k-r)\nu(k) \tag{7.6}$$

It is evident that the main differences between this expression and the usual form of updating algorithm involve the following: the addition of a denominator to the incremental part of the updating algorithm and, the use of an 'a priori' filtered error signal. In spite of these differences, the initial form of updating algorithm, repated below, will still be used.

$$\underline{\hat{d}}(k) = \underline{\hat{d}}(k-1) - \frac{\Gamma\underline{\tilde{\Phi}}(k-r)\nu^{o}(k)}{1 + \underline{\tilde{\Phi}}^{T}(k-r)\Gamma\underline{\tilde{\Phi}}(k-r)} \tag{7.7}$$

The justification for this decision concerns the action of the denominator in equation (7.7). It is possible to interpret its action as that of an adaptive gain, comprising a fixed component and a time varying one. The positive influences that they exert are considered to be an enhancement to the adaptive scheme, as explained below. Consider, for demonstration purposes, the case of an adaptive scheme with only a single adjustable parameter, $\hat{d}$. Now, the adaptive gain matrix, Γ, reduces to a single term, γ. It is therefore possible to rewrite the denominator of equation (7.7) as,

$$1+\gamma\tilde{\phi}^{T}(k-r)\tilde{\phi}(k-r) = 1+\gamma\tilde{\phi}^{2}(k-r) \tag{7.8}$$

The relevance of the filtered observation signal can now begin to be appreciated. In some of the adaptive control literature, the observation vector dependent term has been accorded the status of a signal scaling factor in the adaptive algorithm. In effect, it acts to desensetise the P.A.A. to variations in the magnitude of signals fed to the adaptive system [60]. To appreciate fully the importance of this concept, consider the following single adjustable coefficient version of the parameter updating algorithm.

$$\underline{\hat{d}}(k) = \underline{\hat{d}}(k-1) - \gamma\tilde{\phi}(k-r)\nu^{o}(k) \tag{7.9}$$

This expression has effectively been obtained by eliminating the denominator in equation (7.7). From equation (7.9), the incremental part of the updating expression is a function of the fixed adaptive gain, γ, a signal, $\tilde{\phi}(k-r)$ and the filtered output error, $\nu^o(k)$. The choice of γ, governed by the designer, offers some degree of control over this incremental term. The sensitivity of the latter will be influenced quite considerably by variations in the magnitude of the signal $\tilde{\phi}(k-r)$. This effect will be less significant in terms of the filtered error signal, $\nu^o(k)$, since it is likely to be evaluated as the difference of two signals with similar orders of magnitude. In [61,68,76], analytical studies went some way towards examining the importance of variations in the magnitude of $\tilde{\phi}(k-r)$. The behaviour of the P.A.A. was shown to depend on the magnitude of signals in the filtered observation vector; the relative stability of the updating algorithm gradually worsened as these signals increased. This is clearly an undesirable characteristic of the adaptive system in spite of being perfectly valid within the context of the hyperstability design analysis. In [60], parameter adaptive algorithms of the form given by equation (7.9), were examined with a view to overcoming this problem. The solution that was proposed involved the introduction of a $\underline{\tilde{\Phi}}^T(k-r)\underline{\tilde{\Phi}}(k-r)$ term in the denominator of the incremental component. To prevent numerical difficulties, when terms in the observation vector are zero, it is necessary to append a fixed value to this signal scaling term. The simplest solution is to alter the denominator to the following,

$$1+\underline{\tilde{\Phi}}^T(k-r)\underline{\tilde{\Phi}}(k-r) \tag{7.10}$$

This leads to an expression that is very similar to the denominator of the incremental component in equation (7.7), hence the retention of this form of parameter adaptive algorithm. To maintain strict correctness, the P.A.A. is given by the following equation (7.11), in which an 'a priori' filtered error signal is used.

$$\underline{\hat{d}}(k) = \underline{\hat{d}}(k-1) - \frac{\Gamma\underline{\tilde{\Phi}}(k-r)\nu(k)}{1+\underline{\tilde{\Phi}}^T(k-r)\Gamma\underline{\tilde{\Phi}}(k-r)} \tag{7.11}$$

7.5 CONTROL ALGORITHM INITIALISATION

The realisation of an adaptive controller requires the numerical initialisation of certain parameters. Without the benefit of dealing with a specific application, the following discussion is couched in general terms.

7.5.1 REFERENCE MODEL

The reference model transfer function will already have been specified during the earlier stages of designing the adaptive control system. All that remains is to define its performance characteristics by assigning suitable values to its coefficients. In terms of general guidelines, it is important to specify a reference model with characteristics that can realistically be attained by the controlled process loop. As an example, consider the step response behaviour of the reference model. Its performance characteristics must not be such that too rapid a response is demanded of the controlled process. Otherwise, undesirable effects such as the phenomenon of control signal saturation, described in section 6.2 of chapter 6, will be incurred. Such a situation would be detrimental to the adaptive control scheme not least in terms of control system performance. Of equal importance is the likelihood of parameter adaptation being suspended for considerable periods of time, thereby defeating the objective of the adaptive control system.

Clearly, some prior knowledge about the controlled process will be of considerable assistance in initialising the reference model. Without a detailed examination of the controlled process however, the only information that is available concerns the structure of its transfer function. Beyond the self-apparent advice proposed above, initialisation of the reference model is very much an applications dependent problem. Therefore, it is only appropriate that it be dealt with in greater detail, during the course of chapters 8 and 9, which describe two applications of the adaptive control scheme.

7.5.2 ADAPTIVE GAIN

From chapter 5, the the expression for the parameter updating algorithm is given as,

$$\underline{\hat{d}}(k) = \underline{\hat{d}}(k-1) - \frac{\Gamma\underline{\tilde{\Phi}}(k-r)\nu^o(k)}{1+\underline{\tilde{\Phi}}^T(k-r)\Gamma\underline{\tilde{\Phi}}(k-r)} \tag{7.12}$$

The vector quantities, $\underline{\hat{d}}$ and $\underline{\tilde{\Phi}}$, are both of the same order, n, say. Γ is a diagonal, adaptive gain matrix of order n*n. Consequently, each term in this matrix can be used to affect the rate of adaptation associated with coefficients of the adjustable parameter vector, $\underline{\hat{d}}$.

In dealing with high order adaptive schemes, where n is likely to be large, the task of initialising the adaptive gain matrix appears to be quite daunting. However, the following modification can be made to the parameter updating algorithm to overcome this difficulty. Consider the use of an unique value for the adaptive gains. The choice of a particular value, γ_0 , for example, results in the following expression for the adaptive gain matrix.

$$\Gamma = \gamma_0 I \tag{7.13}$$

where, I is an n*n identity matrix. The expression for the parameter updating algorithm of equation (7.12) can thus be rewritten as,

$$\underline{\hat{d}}(k) = \underline{\hat{d}}(k-1) - \frac{\gamma_0 I\,\underline{\tilde{\Phi}}(k-r)\nu^o(k)}{1+\underline{\tilde{\Phi}}^T(k-r)\gamma_0 I\,\underline{\tilde{\Phi}}}$$

$$= \underline{\hat{d}}(k-1) - \frac{\underline{\tilde{\Phi}}(k-r)\nu^o(k)}{\gamma+\underline{\tilde{\Phi}}^T(k-r)\underline{\tilde{\Phi}}(k-r)} \tag{7.14}$$

with, $\gamma = 1/\gamma_0$.

The simplification proposed above might appear to be detrimental to the adaptive control scheme since it reduces the number of designer tunable parameters associated with the adaptation algorithm. Nevertheless, it is retained because it displays the following attributes. The benefits obtained are essentially twofold. The first of these concerns the simplification to the initialisation procedure. Now,

only one adaptive gain has to be selected, irrespective of the size of the adjustable parameter vector. The second, less apparent advantage, concerns the reduction in computational effort that results from using a single value for the adaptive gain. This fact can be appreciated by comparing the initial and the simplified updating algorithms of equations (7.12) and (7.14). Clearly, the number of multiplications has been drastically reduced. This will have a consequential effect on the length of the adaptive controller sampling period.

When addressing the question of selecting a value for γ, the following interpretation proves to be useful, when applied to the parameter updating algorithm. To begin with, consider the denominator of equation (7.14). The factor $\underline{\tilde{\Phi}}^T(k-r)\underline{\tilde{\Phi}}(k-r)$ is a positive, time-varying entity. Likewise, γ is also positive, though of a fixed value. Hence, rather than view the adaptive gain, γ , as an isolated element, greater insight can be obtained from considering the entire denominator as an expanded, time-varying adaptive gain. Henceforth, this will be referred to as the combined gain term. The fixed part, γ, acts to provide a lower bound on the size of the combined gain. Such a level will be attained in the unlikely case of all elements in the filtered observation vector, $\underline{\tilde{\Phi}}(k-r)$, being zero. The effect of $\underline{\tilde{\Phi}}^T(k-r)\underline{\tilde{\Phi}}(k-r)$ in the combined adaptive gain can be interpreted as that of a signal scaling factor [60]. As discussed in section 7.4 above, it provides a means of desensitising the parameter updating algorithm to variations in the magnitude of signals in the filtered observation vector.

In assigning a value for γ, it is instructive to consider some of the factors which affect the influence of the signal scaling factor. For the simplest of control schemes, there are likely to be only a few coefficients in the adjustable parameter vector. There will clearly be an identical number of elements in the filtered observation vector. Conversely, in a more complex adaptive control scheme, there will be a greater number of adaptive coefficients in the adjustable parameter vector. This will result in a correspondingly large observation vector. During adaptive control system operation, an examination of the behaviour of the signal scaling component is likely to reveal two fairly distinct modes of behaviour. For the simple adaptive scheme described above, the time response of the magnitude of the signal scaling component is likely to change in an irregular fashion (clearly, this will be governed by the form of the input command signal). By contrast, a more 'fluent' response is expected from the complex adaptive scheme. A convenient analogy can be made with the relationship between the number of cylinders in an internal

combustion engine and the relative smoothness of its power delivery. In this case, the relationship is drawn between the number of cylinders and the number of parameters in the observation vector. Considering the combined adaptive gain, the fluctuating contribution of the signal scaling component will be superimposed on some base value, as specified by γ.

In an attempt to prevent the parameter updating algorithm from being excessively perturbed by sudden, large fluctuations in the signal scaling factor, the following important factors should be borne in mind when initialising the fixed gain, γ. For simple adaptive schemes, γ should be made large; to a certain extent, the contribution of the signal scaling factor should effectively be ignored as it is expected to experience sizable fluctuations. For complex systems, a low value for γ is considered sufficient. This is because a significant portion of the combined gain would be made up by the time varying component. A minimum threshold, of significant magnitude, should nevertheless be imposed for even very high order schemes. This is advisable since it would help to deal with the possibility of a significant number of signals in the observation vector being zero.

7.5.3 ERROR FILTER COEFFICIENTS

The need for an error filter is one outcome of a hyperstability based analysis of the adaptive control scheme. Consideration of the linear, time-invariant part of the scheme leads to the requirement that the transfer function $C(z^{-1})/A_m(z^{-1})$, should be strictly positive real (S.P.R). In the frequency domain, this condition is characterised by a Nyquist locus which is constrained to the first and fourth quadrants. The precise nature of $A_m(z^{-1})$ is known once the reference model transfer function has been specified. It only remains to select an error filter transfer function, $C(z^{-1})$, of sufficiently high order and then specify its coefficients to meet the S.P.R. criterion. A graphical technique is employed in choosing suitable values for these coefficients. This procedure consists of the following series of steps. To begin with, the error filter is defined with a general transfer function of the form given below.

$$C(z^{-1}) = 1+c_1z^{-1}+c_2z^{-2}+\cdots+c_n z^{-n}+... \qquad (7.15)$$

As a starting point, for a given application, the order of the $C(z^{-1})$ filter is chosen

to be less than the order of $A_m(z^{-1})$ by a difference of one. Should it be discovered subsequently that this choice does not provide adequate flexibility to satisfy the S.P.R. condition then the order of the error filter can be increased as required. The converse is true should there be more error filter coefficients than is absolutely necessary. Application of the Nyquist locus test requires the discrete transfer function to be transformed to the frequency domain. To this end, the following ω_w, bi-linear transformation is employed.

$$z = \frac{1+j\omega_w}{1-j\omega_w} \tag{7.16}$$

The transfer function that results will satisfy the S.P.R. condition if its real part is non-zero and positive over all frequencies, ω_w.

A set of inequalities, in terms of the error filter coefficients, is obtained when the S.P.R. condition is applied to the ω_w transfer function. A graphical representation of these inequalities helps to delineate an allowable set of error filter coefficients [24,34]. The fact that a range of values is possible for the error filter coefficients appears to complicate matters. A procedure was developed to aid the selection of suitable coefficient values. This was achieved through experimental investigation on a real system with different values of error filter coefficients. Qualitatively, it was discovered that a high level of adaptive system behaviour could be obtained if the error filter coefficients were selected according to the following instructions.

1) the magnitude of the phase response of $C(z^{-1})/A_m(z^{-1})$ should be selected to be close to 90°, in the region of the Nyquist frequency (half the sampling frequency).

2) in the low frequency region, the phase response of $C(z^{-1})/A_m(z^{-1})$ must be asymptotically zero. In the case of the work reported in this thesis, this region corresponds to frequencies which are at and lower than a tenth of the Nyquist frequency.

In chapter 8, a comprehensive description is provided on an experimental investigation into the choice of error filter coefficients from the allowable set.

7.5.4 COMPENSATOR INITIAL CONDITIONS

Initialisation of the $F(z^{-1})$ and $G(z^{-1})$ compensator coefficients can be carried out in a multitude of different ways. Some advantage could be gained from prior knowledge of the dynamics of the controlled process. In such a situation, it would be possible to carry out an explicit solution of the pole-placement control law, of equation (4.3) in chapter 4, for the 'f' and 'g' compensator coefficients. These could then be used as the initial values in the adjustable parameter vector, $\underline{\hat{d}}$. Without prior knowledge such as this however, due attention should be paid to the general guidelines outlined below.

With regard to the $F(z^{-1})$ compensator, two observations can be made. The first of these relates to the roots of this polynomial. From a stability viewpoint, these must lie inside the unit z-plane disc. The following suggestion furnishes one means of achieving this goal; the roots of $F(z)$ could be equispaced around the perimeter of a disc, centered on (0,0j), and with a radius smaller than unity. A balance has to be struck between placing the roots too close to the perimeter of the unit disc and sufficiently far apart from each other and the origin. The second factor to be borne in mind concerns the initial value for the $\hat{f}_0$ coefficient. An appreciation of its importance can be gained by recalling that it acts as a forward path gain in the controlled process loop. Referring to equation (7.3), it is actually implemented as a $1/\hat{f}_0$ term. Hence, the choice of too small an initial value is likely to result in the process being driven with a control signal that is initially very large. Conversely, a very large $\hat{f}_0$ coefficient is likely to provoke a sluggish initial response from the controlled system. Some indication on the choice of an acceptable value can be obtained either by examining the existing process control system or by carrying out a set of closed loop step response tests with different forward path gains.

Whereas the $F(z^{-1})$ compensator has to be initialised in a manner which causes its roots to lie within a constrained region, no such restriction applies to the $G(z^{-1})$ compensator. In fact, the only general piece of information of any advantage in its initialisation relates to the steady state gain of the filter. The reference model transfer function is formulated on the basis of a given servo-system operating under closed loop, unity feedback control. As shown in chapter 5, the same condition applies to the controlled process loop. Hence, in using this information to initialise the $G(z^{-1})$ polynomial, the designer has to aim to satisfy

the following (steady state) condition,

$$G(1) = \hat{g}_0 + \hat{g}_1 \ldots + \hat{g}_g \cdots = 1 \qquad (7.17)$$

This condition ensures that the controlled process loop, like the reference model, has unity steady state gain.

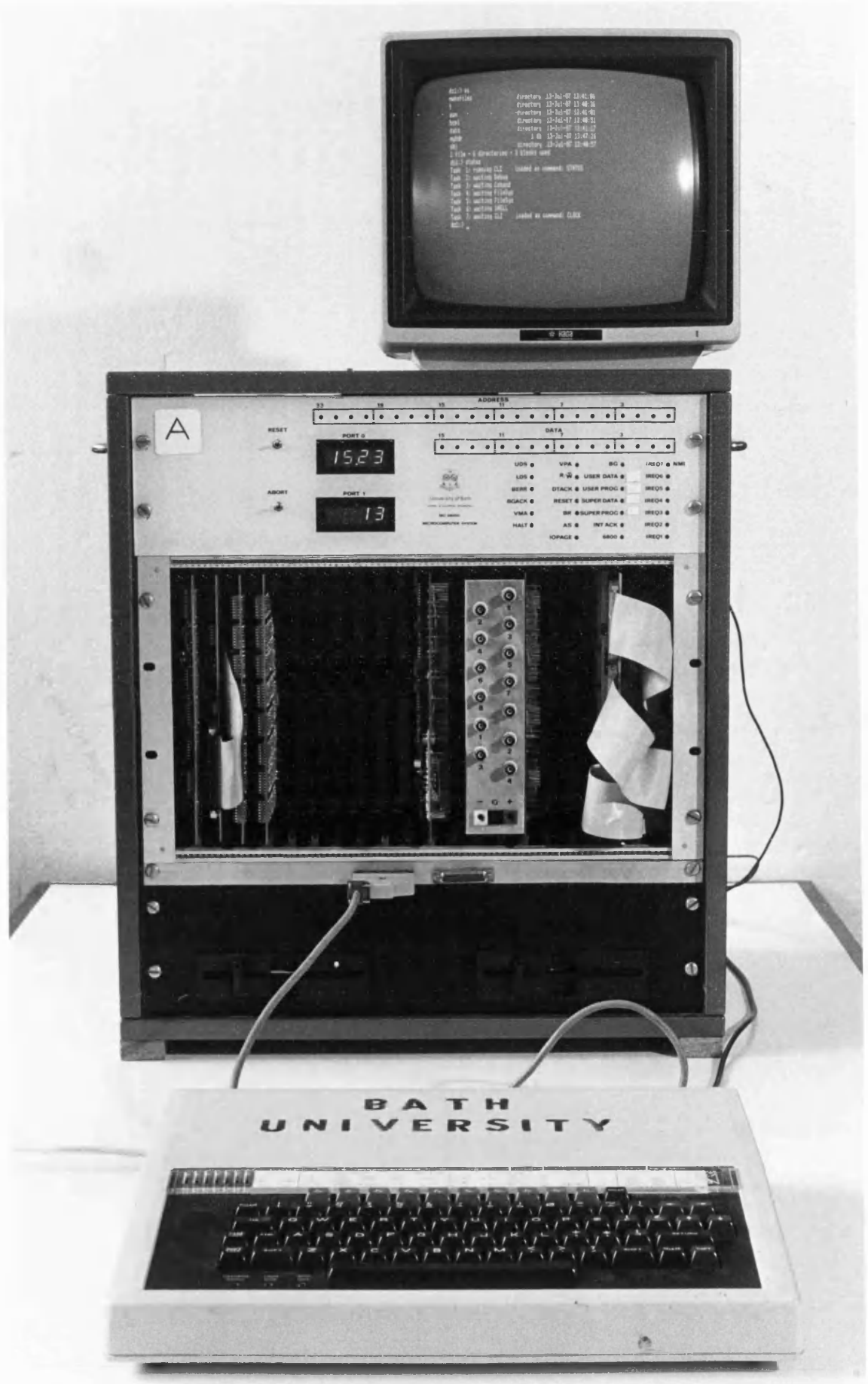

FIGURE 7:1 The DARKSTAR Computer System

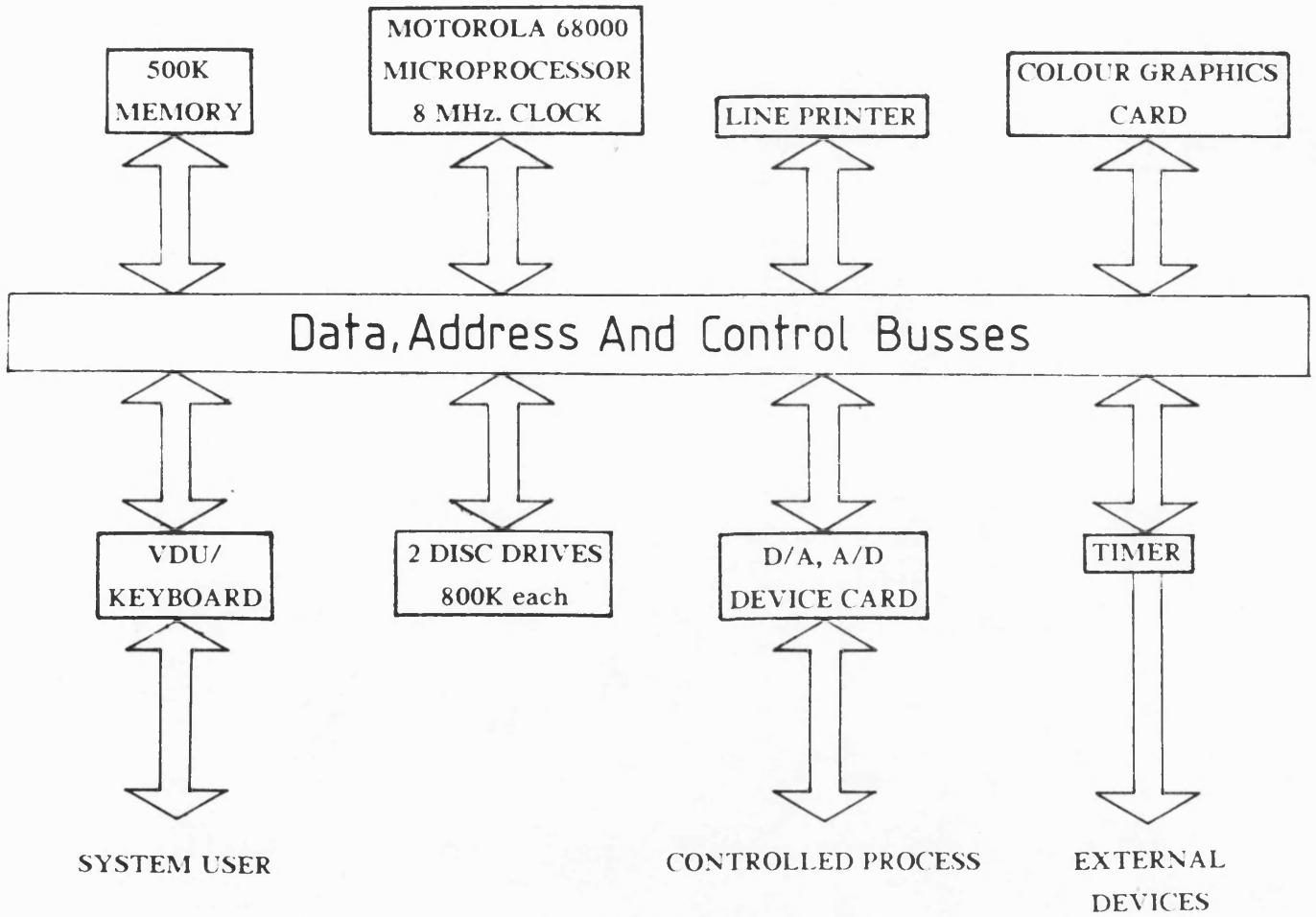

FIGURE 7:2 Schematic Representation Of The Darkstar Computer System

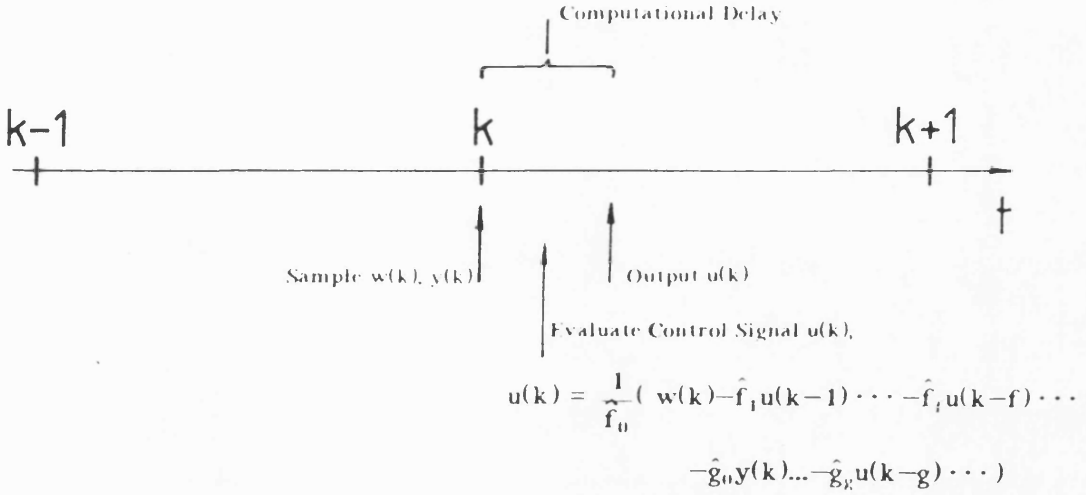

FIGURE 7:3 Diagrammatic Representation Of The Process Control Signal Evaluation Procedure

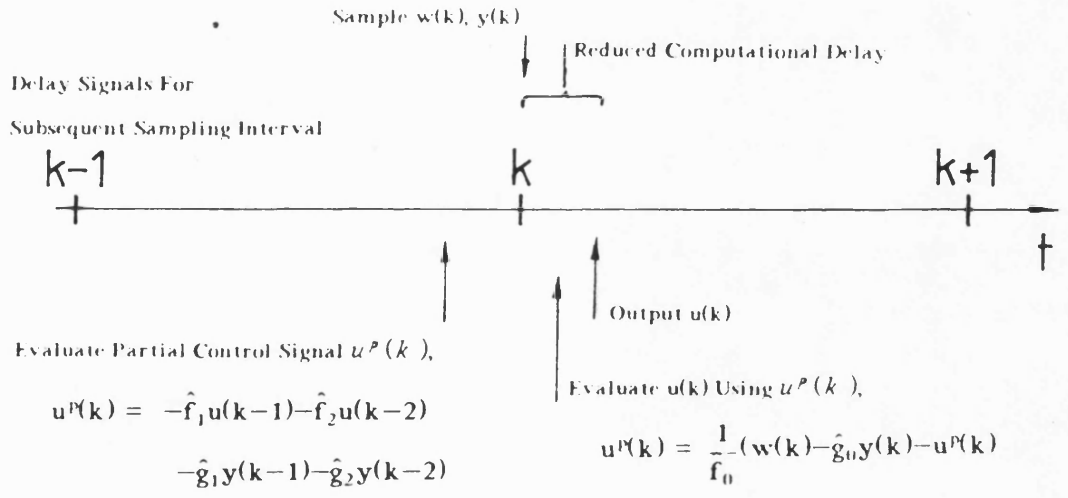

FIGURE 7:4 Enhanced Procedure For Evaluating The Process Control Signal

Original Scheme

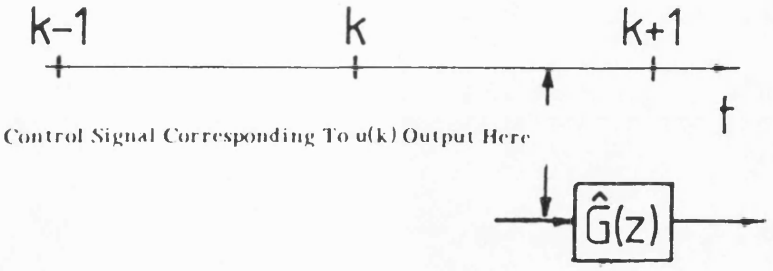

FIGURE 7:5a Timing Diagram For Original Control Scheme

Modified Scheme 1

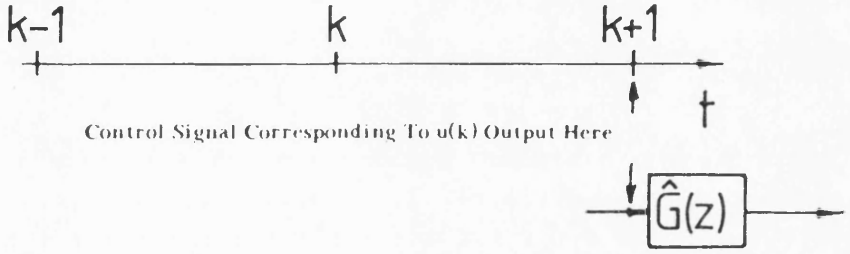

FIGURE 7:5b Timing Diagram For Modified Control Scheme

Modified Scheme 2

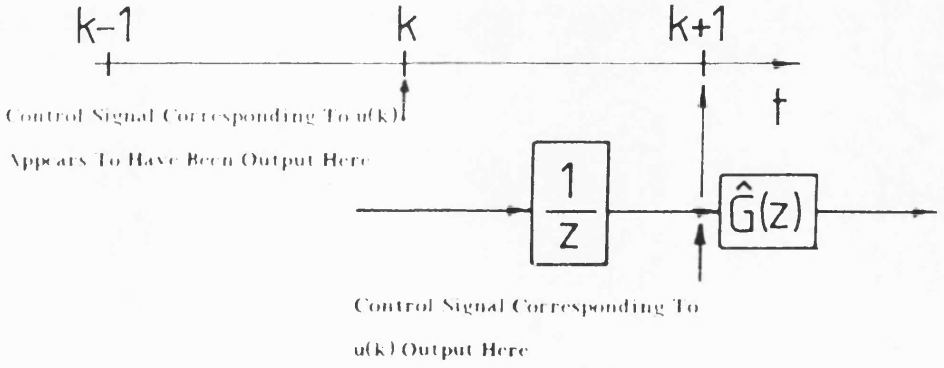

FIGURE 7:5c Alternative Interpretation Of Modified Control Scheme

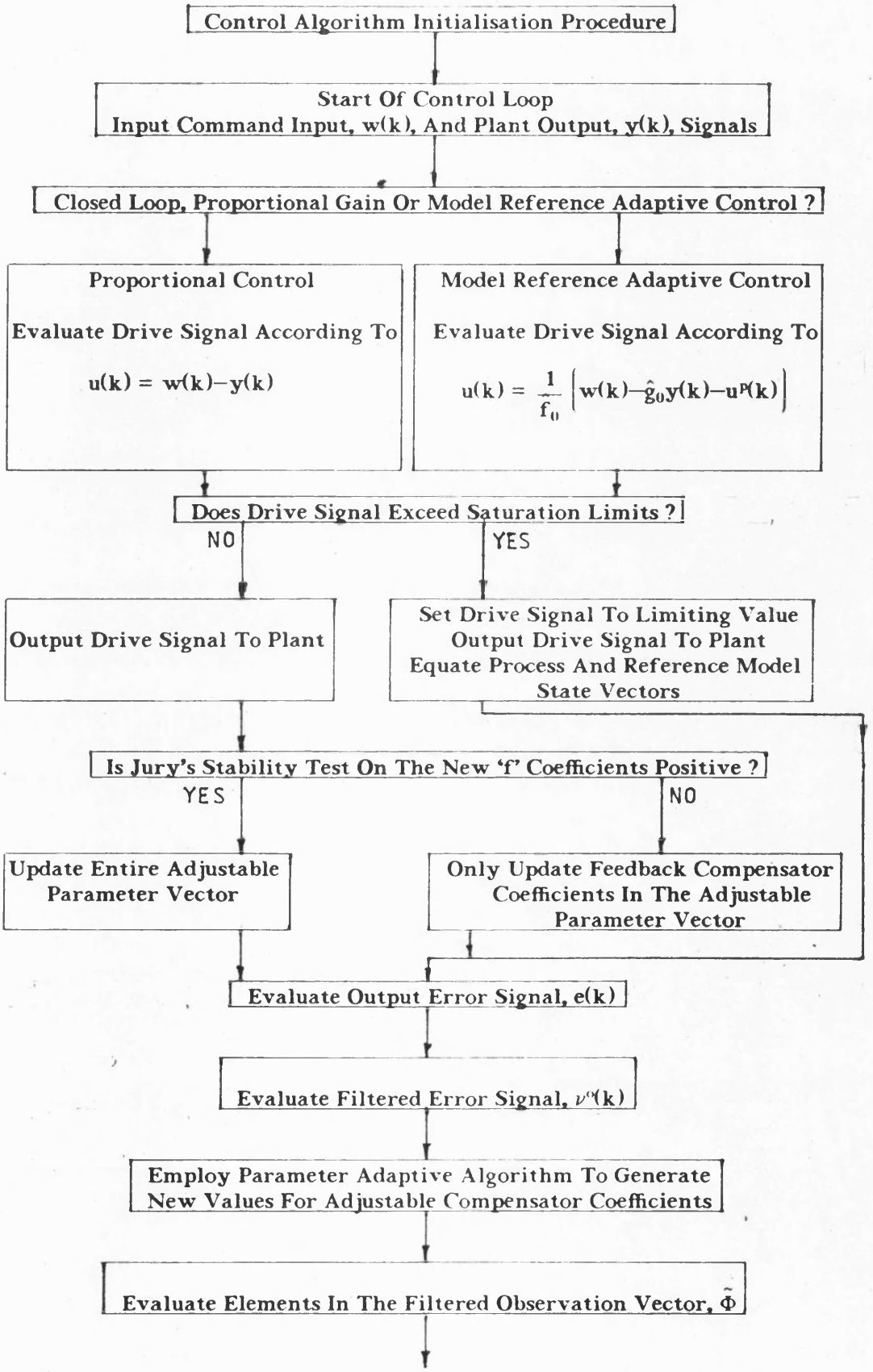
Control Algorithm Initialisation Procedure
Start Of Control Loop
Input Command Input, w(k), And Plant Output, y(k), Signals
Closed Loop, Proportional Gain Or Model Reference Adaptive Control ?
Proportional Control
Evaluate Drive Signal According To
u(k) = w(k)−y(k)
Model Reference Adaptive Control
Evaluate Drive Signal According To
u(k) = 1/f0 [w(k)−ĝ0y(k)−uP(k)]
Does Drive Signal Exceed Saturation Limits ?
NO
YES
Output Drive Signal To Plant
Set Drive Signal To Limiting Value
Output Drive Signal To Plant
Equate Process And Reference Model
State Vectors
Is Jury's Stability Test On The New 'f' Coefficients Positive ?
YES
NO
Update Entire Adjustable
Parameter Vector
Only Update Feedback Compensator
Coefficients In The Adjustable
Parameter Vector
Evaluate Output Error Signal, e(k)
Evaluate Filtered Error Signal, ν'(k)
Employ Parameter Adaptive Algorithm To Generate
New Values For Adjustable Compensator Coefficients
Evaluate Elements In The Filtered Observation Vector, Φ̃

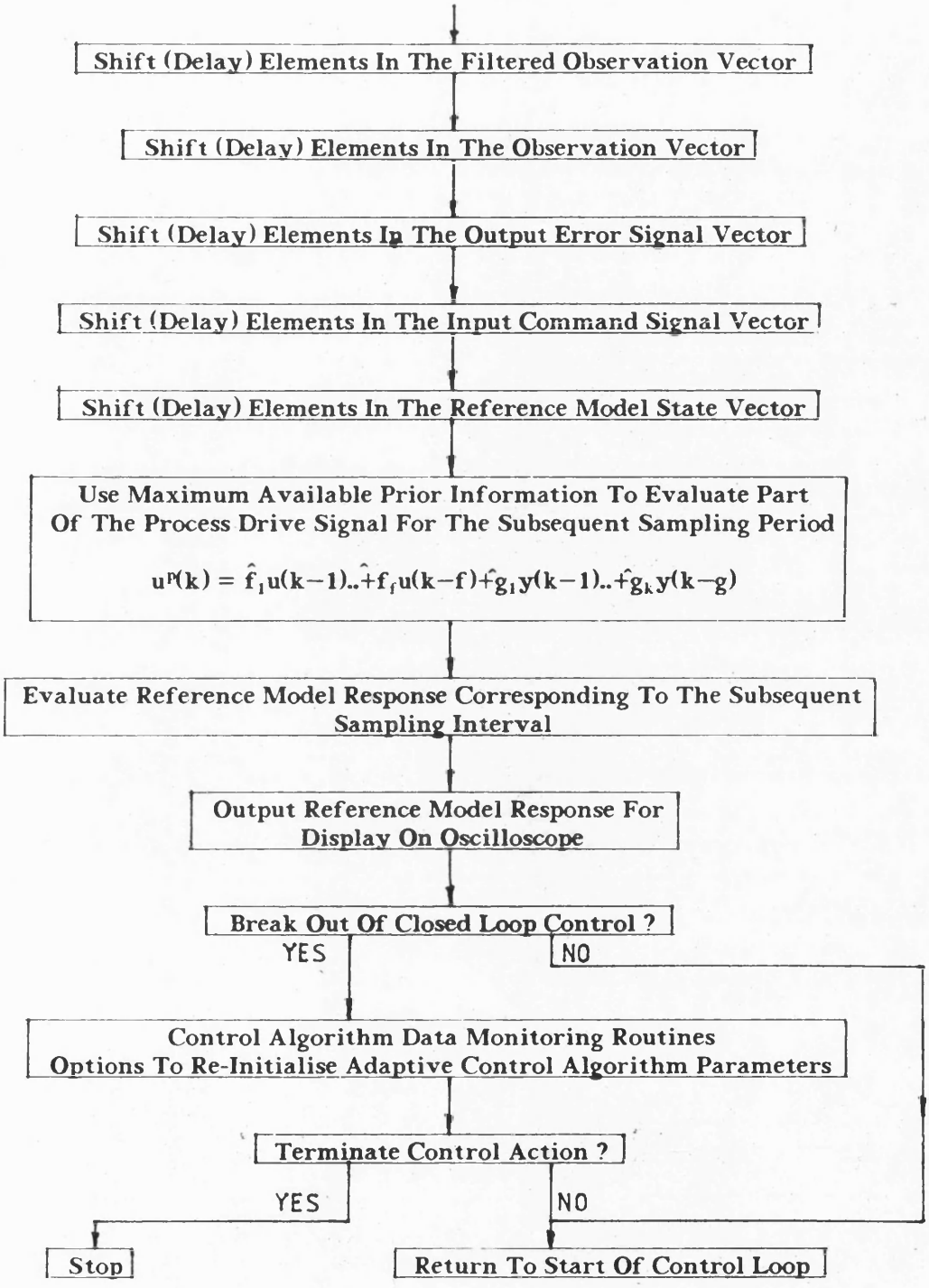

Flow Diagram 7:1 Fractionally Delayed Process Control Signal Algorithm

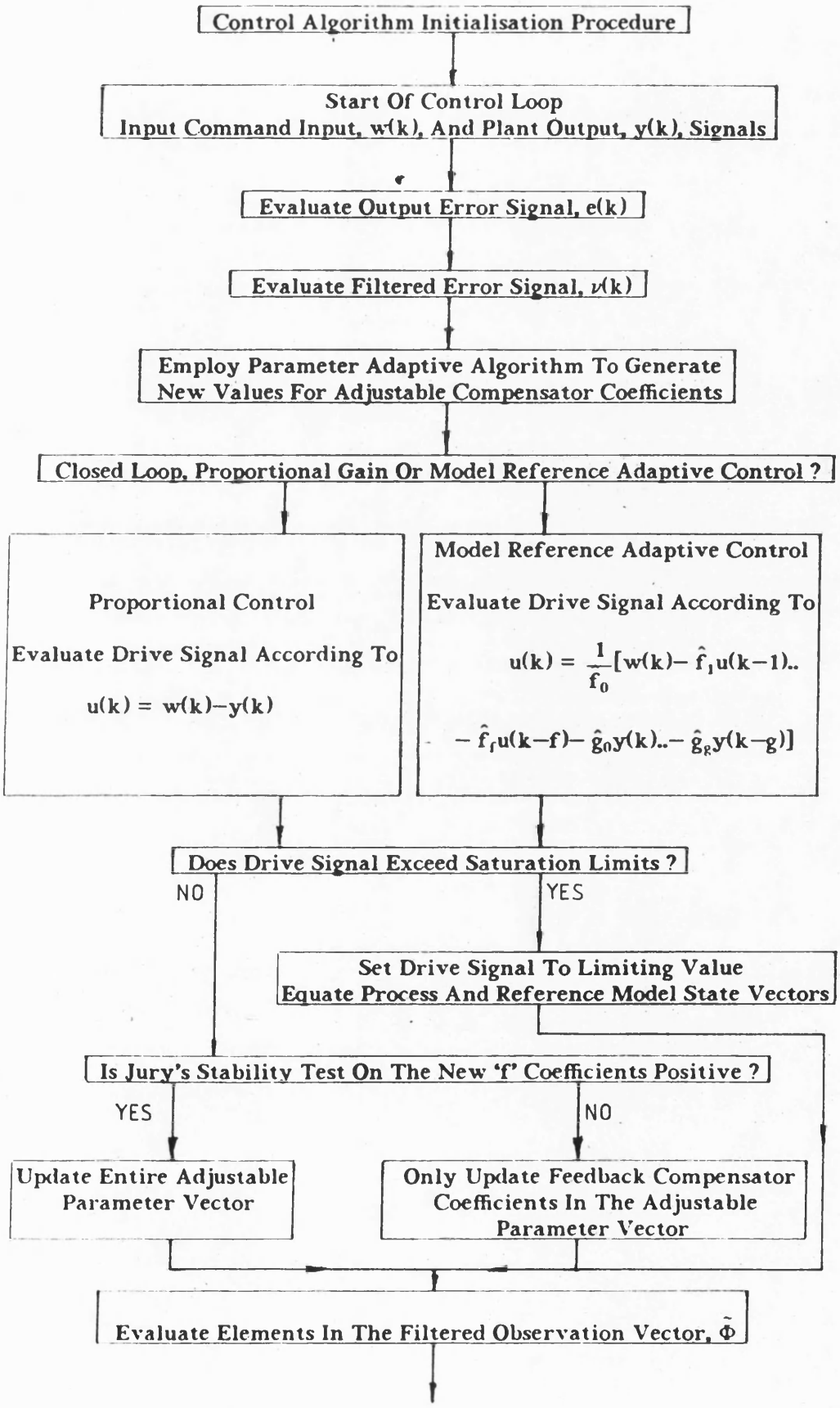
Control Algorithm Initialisation Procedure
Start Of Control Loop
Input Command Input, w(k), And Plant Output, y(k), Signals
Evaluate Output Error Signal, e(k)
Evaluate Filtered Error Signal, ν(k)
Employ Parameter Adaptive Algorithm To Generate New Values For Adjustable Compensator Coefficients
Closed Loop, Proportional Gain Or Model Reference Adaptive Control ?
Proportional Control
Evaluate Drive Signal According To
u(k) = w(k)−y(k)
Model Reference Adaptive Control
Evaluate Drive Signal According To
u(k) = 1/f0 [w(k)− f̂1u(k−1).. − f̂fu(k−f)− ĝ0y(k)..− ĝgy(k−g)]
Does Drive Signal Exceed Saturation Limits ?
NO
YES
Set Drive Signal To Limiting Value
Equate Process And Reference Model State Vectors
Is Jury's Stability Test On The New 'f' Coefficients Positive ?
YES
NO
Update Entire Adjustable Parameter Vector
Only Update Feedback Compensator Coefficients In The Adjustable Parameter Vector
Evaluate Elements In The Filtered Observation Vector, Φ̃

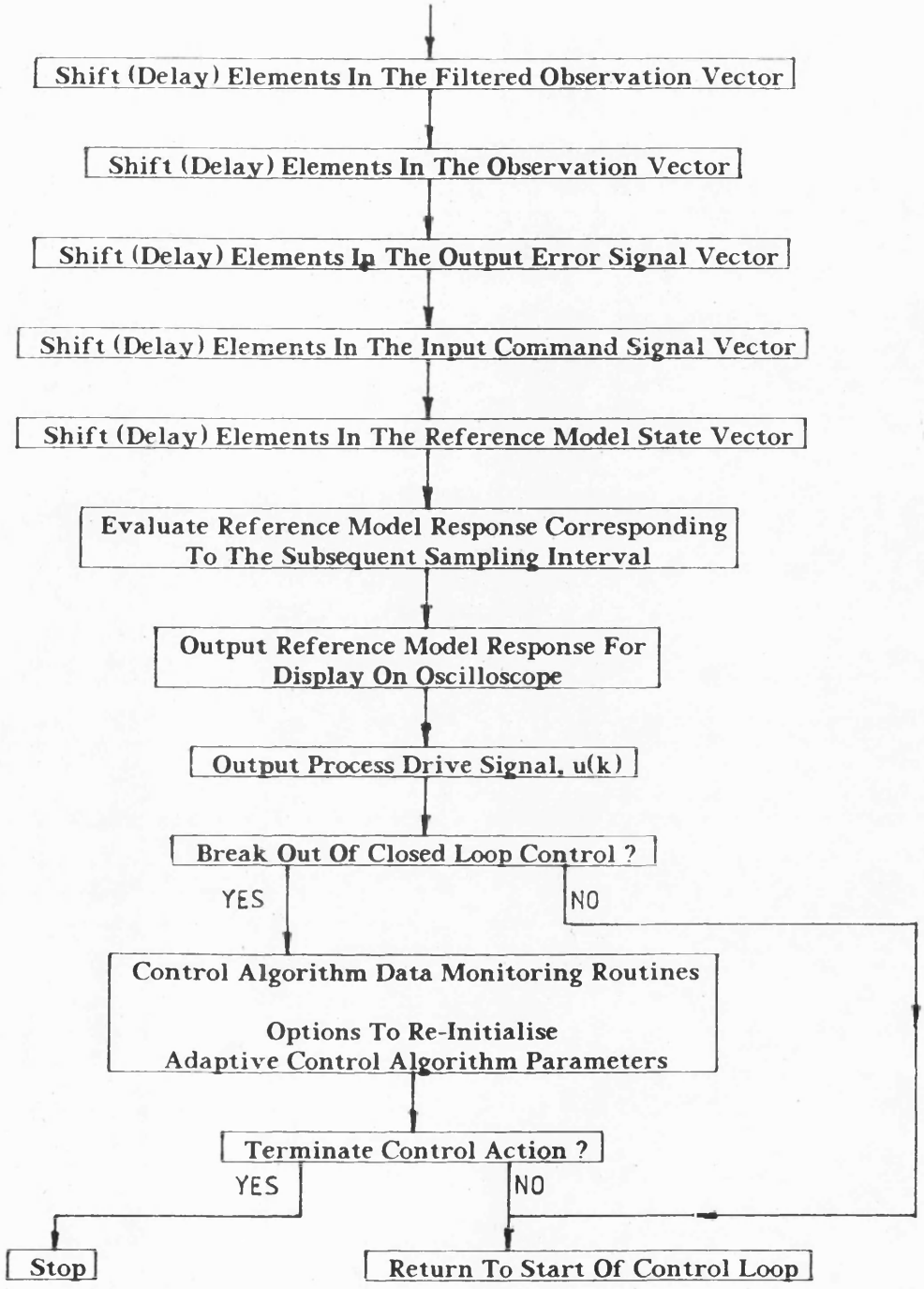

Flow Diagram 7:2 Algorithm For Process Control Signal Delayed By A Full Sampling Interval

CHAPTER 8

AN ADAPTIVELY CONTROLLED ELECTRO-MECHANICAL SERVOMECHANISM

8.1 INTRODUCTION

This chapter is the first of two on applying the adaptive controller design methodology to specific systems. The first application, considered in this chapter, places the essentially theoretical presentation of earlier chapters into a practical context. The presentation also aims to reduce the abstractness of the main components of the adaptive system. To achieve these goals, an adaptive control algorithm is designed around a relatively simple electro-mechanical position control system, centering on a d.c. servomotor. Devices such as this are fairly commonly encountered; they offer a compact medium for the transmission of electrical energy, with subsequent conversion to mechanical motion. Variations in design and the use of a wide range of construction materials mean that there exists a plethora of different machines. For this study however, individual motor characteristics are ignored in order that greater attention may be devoted to the adaptive control scheme itself.

Following the controller design and initialisation stages, a number of tests are carried out on the test rig. These demonstrate the behaviour of the adaptive control scheme under a variety of operating conditions.

Due to the relative simplicity of the controlled process, it is possible to highlight distinctive traits in adaptive system performance. These can be attributed to certain individual features in the parameter adaptive part of the control algorithm. An entire section of this chapter is devoted to studying one important set of characteristics.

To complete the presentation of this chapter, a final section is devoted to the design and testing of an integral action, adaptive control scheme.

8.2 ADAPTIVE CONTROLLER DESIGN

An orderly approach to designing adaptive control schemes can be developed by following the sequence of operations outlined below. The design task can be viewed in two parts. Initially, the main components of the adaptive algorithm have to be specified. During the second stage, attention is given to the numerical initialisation of various components within the control scheme.

8.2.1 CONTROL SYSTEM DESCRIPTION

Process Modelling

A photograph of the controlled system is shown in figure 8:1. The main components consist of an armature controlled d.c. motor and a tachogenerator. The motor is rated at 25 W and is capable of supplying a continuous torque of 10 Ncm. A rotary potentiometer is linked to the output shaft of the d.c. motor. A generalised schematic, of the form shown in figure 8:2, is used to represent the controlled process. The load term, J, accounts for the inertia of all the rotating components while c' relates to the viscous damping inherent in the controlled process. The d.c. motor is provided with an analogue, minor loop form of tachogenerator feedback. This allows the effective damping of the controlled process to be altered by varying the tachogenerator feedback gain. With regard to the adaptive control scheme, this feature offers a simple means with which to effect changes in the controlled process dynamics.

A block diagram representation of the controlled process is provided in figure 8:3. The bandwidth of the power amplifier and motor stage is considered to be significantly wider than the mechanical part of the system; hence, it is described by a simple gain term. The torque provided by the motor has to overcome the inertial and damping loads. The output shaft from the motor is connected to a rotary potentiometer, via a reduction gear train. A simplified block diagram representation of the ensemble is shown in figure 8:4. Changes in the tachogenerator feedback gain,

K_4, of figure 8:3 mean that it is possible to perturb the coefficients K and τ in the controlled process of figure 8:4.

According to figure 8:4, the controlled process is modelled with a continuous-time transfer function of the following form.

$$\frac{y}{V_i} = \frac{K}{s(1+\tau s)} \tag{8.1}$$

A discrete approximation for the controlled process can be obtained by applying the pole-zero mapping procedure outlined in chapter 3. The transfer function that results is given by,

$$\frac{y(z)}{V_i(z)} = \frac{b_0(1+z)^2}{(z-1)(z-a')} \tag{8.2}$$

The continuous-time and discrete transfer functions both have second order denominators. The latter also has two zeros at z=-1. These arise from mapping two continuous-time infinite zeros from equation (8.1). The transfer function of equation (8.2) represents just the electro-mechanical system. It is now necessary to take the D/A converter preceding it into account. Following the guidelines outlined in chapter 4, one infinite continuous-time zero is mapped as an infinite z-plane zero. This results in the following transfer function for the controlled plant.

$$\frac{y(z)}{V'_i(z)} = \frac{b_0(1+z)}{(z-1)(z-a')}$$

Hence,

$$\frac{y(z^{-1})}{V'_i(z^{-1})} = \frac{b_0 z^{-1}(1+z^{-1})}{1+a_1 z^{-1}+a_2 z^{-2}} \tag{8.3}$$

The signal, V'_i, stands for the input to the D/A converter cascaded with the d.c. motor.

Computational Delay

Prior experience indicates that an adaptive control scheme designed around the process model of equation (8.3) would be computationally undemanding. In part, this is a result of having relatively few adaptive parameters to generate. An important consequence of factors such as this is a control algorithm having a short sampling period. For reasons outlined in section 7.4 of chapter 7, such a scheme is best implemented with the following modification whereby the process transfer function is deliberately augmented with a unit sampling delay. This modification is shown, schematically, in figure 8:5. The justification for this delay is that it overcomes the need to evaluate and send out the process control signal with a minimum amount of delay.

The introduction of a z^{-1} term in the control scheme means that the effective transfer function of the controlled process becomes,

$$\frac{y(z^{-1})}{u(z^{-1})} = \frac{1}{z}\frac{z^{-1}(1+z^{-1})}{(1-a'z^{-1})(1-z^{-1})} = \frac{b_0 z^{-2}(1+z^{-1})}{1+a_1 z^{-1}+a_2 z^{-2}}$$

$$= \frac{b_o z^{-2} B(z^{-1})}{A(z^{-1})} \qquad (8.4)$$

Reference Model

A closed loop reference model transfer function is specified on the basis of the process open loop transfer function of equation (8.4). As discussed in chapter 3, the use of a unity feedback form of closed loop system results in the following reference model transfer function.

$$\frac{x(z^{-1})}{w(z^{-1})} = \frac{b_m z^{-2}(1+z^{-1})}{1+a'_{m,1}z^{-1}+a'_{m,2}z^{-2} + b_m z^{-2}(1+z^{-1})}$$

$$= \frac{b_m z^{-2}(1+z^{-1})}{1+a_{m,1}z^{-1}+a_{m,2}z^{-2}+a_{m,3}z^{-3}}$$

$$= \frac{b_m z^{-2} B(z^{-1})}{A_m(z^{-1})} \tag{8.5}$$

Compensator Network Specification

With the assistance of the process transfer function of equation (8.4), appropriate orders can be selected for the $F(z^{-1})$ and $G(z^{-1})$ compensators of figure 8:5. The model following objective will be satisfied when the closed loop reference model and controlled process loop share the same characteristic equation. The orders of the relevant polynomials in the controlled process and closed loop reference model transfer functions are readily obtainable from equations (8.4) and (8.5) respectively. Hence, from chapter 4, satisfaction of the control law becomes possible when the $F(z^{-1})$ and $G(z^{-1})$ compensators are specified to be of the following forms,

$$F(z^{-1}) = f_0 + f_1 z^{-1} + f_2 z^{-2} \tag{8.6}$$

$$G(z^{-1}) = g_0 + g_1 z^{-1} \tag{8.7}$$

Parameter Adaptive Algorithm Specification

The P.A.A. for this scheme can be written automatically, on the basis of the generalised results developed in chapter 5. The following set of equations define the foundations of the algorithm, prior to its modification with a variable dead-band filter.

The adjustable parameter vector is constructed from the compensator coefficients, thus,

$$\underline{\hat{d}}(k) = [\ \hat{f}_0(k)\ \ \hat{f}_1(k)\ \ \hat{f}_2(k)\ \ \hat{g}_0(k)\ \ \hat{g}_1(k)\ ]^T \tag{8.8}$$

Likewise, the observation vector is given by,

$$\underline{\Phi}(k) = [\ u(k)\ u(k-1)\ u(k-2)\ y(k)\ y(k-1)\ ]^T \tag{8.9}$$

The filtered observation vector is dependent upon the numerator dynamics as shared by the controlled process and reference model transfer functions. From equation (8.4), these can be seen to include the $B(z^{-1})$ polynomial and a second order, free-delay term. Hence, the filtered observation vector becomes;

$$\begin{aligned}\tilde{\underline{\Phi}}(k) &= z^{-2}B(z^{-1})\underline{\Phi}(k) \\ &= B(z^{-1})\underline{\Phi}(k-2)\end{aligned} \tag{8.10}$$

Finally, an amalgamation of the important definitions given above results in a P.A.A. of the following form;

$$\hat{\underline{d}}^T(k) = \hat{\underline{d}}^T(k-1) - \frac{\tilde{\underline{\Phi}}(k-2)\nu^o(k)}{\gamma + \tilde{\underline{\Phi}}^T(k-2)\tilde{\underline{\Phi}}(k-2)} \tag{8.11}$$

where, ν^o is the 'a priori' filtered output error signal and γ is an adaptation gain.

8.2.2 CONTROL SYSTEM INITIALISATION

Reference Model

The reference model transfer function can be initialised in a number of different ways. This is an inevitable outcome of dealing with a range of different devices and variations in the performance requirements expected in different situations.

The availability of some prior information about the controlled process is of considerable assistance in specifying the reference model characteristics. For this case study, it was possible to carry out a number of tests on the controlled process, using closed loop digital control. Preliminary tests were carried out with the software written for the adaptive scheme. However, the control algorithm was operated as a proportional action scheme as indicated in flow-diagram 7.2. The reasons for this were two-fold. Firstly, it made it possible to examine the controlled process under digital control using virtually the same sampling period that would be used subsequently during adaptive control. Secondly, these tests were carried out with the process control signal being delayed to the end of each sampling period. This made it possible to study the behaviour of the effective controlled process rather than the d.c. servo-system itself.

The series of tests that was carried out consisted of examining the step response behaviour of the controlled process. This was done in order to gauge its response speed. The procedure that was followed in specifying the reference model was based on these observations. To begin with, the reference model was initialised with a set of numerical values; this procedure is explained in greater detail below. The reference model was then operated in parallel with the controlled process, as allowed by the adaptive controller software [77]. This facilitated a visual comparison of the reference model and controlled process step responses. The reference model coefficient values were then adjusted until a level of performance that was judged to be capable of being met by the controlled process was attained.

Numerical initialisation of the reference model proceeded along the following lines. The reference model transfer function was obtained from the basis of an open loop transfer function operating under unity feedback conditions. Consequently, it is possible to express the closed loop transfer function in terms of a set of open loop parameters, thus,

$$\frac{x(z^{-1})}{w(z^{-1})} = \frac{1}{\dfrac{(1-z^{-1})(1-a'_m z^{-1})}{b_m z^{-2}(1+z^{-1})}+1}$$

$$= \frac{b_m z^{-2}(1+z^{-1})}{1-(1+a'_m)z^{-1}+(a'_m+b_m)z^{-2}+b_m z^{-3}} \qquad (8.12)$$

Clearly, this form of expression only calls for the initialisation two parameters, as opposed to four in the general reference model transfer function of equation (8.5). The a'_m coefficient in equation (8.12) represents a pole at $z = a'_m$ in the open loop transfer function. A value of 0.6 was arbitrarily assigned to it. A low initial value was then selected for the b_m gain. This was substituted in equation (8.12) and a check was carried out on its characteristic equation. This was done in order to ensure that no roots fell outside the unit disc. The control algorithm software was then operated with a number of different values for b_m until a satisfactory level of performance was obtained. This corresponded to the following numerical transfer function.

$$\frac{x(z^{-1})}{w(z^{-1})} = \frac{0.02z^{-2}(1+z^{-1})}{1-1.6z^{-1}+0.62z^{-2}+0.02z^{-3}} \qquad (8.13)$$

Error Filter

An error filter, $C(z^{-1})$, has to be specified such that the transfer function $C(z^{-1})/A_m(z^{-1})$ is strictly positive real. Adopting the suggestion proposed in chapter 7, section 7.5.3, the error filter was specified to be of one order lower than the reference model denominator polynomial, $A_m(z^{-1})$. This resulted in $C(z^{-1})$ being of the form given below,

$$C(z^{-1}) = 1+c_1z^{-1}+c_2z^{-2} \qquad (8.14)$$

The S.P.R. condition was then applied to the following transfer function,

$$\frac{C(z^{-1})}{A_m(z^{-1})} = \frac{1+c_1z^{-1}+c_2z^{-2}}{1-1.6z^{-1}+0.62z^{-2}+0.02z^{-3}} \qquad (8.15)$$

The detailed evaluation of conditions on the 'c' coefficients is considered in appendix 3. Determination of these conditions is eased, to a considerable extent, by the use of MACSYMA, a symbolic computation computer program. Appendix 3 provides a

comprehensive demonstration of its use with reference to the S.P.R. condition considered here. The main results to emerge from this analysis can be expressed as a series of inequalities in terms of the 'c' coefficients. These are listed below.

$$c_2 > -c_1 - 1 \tag{8.16}$$

$$c_2 > c_1 - 1 \tag{8.17}$$

$$c_2 < -4.179c_1 + 1.154 \tag{8.18}$$

$$c_2 < -0.695c_1 - 0.424 \tag{8.19}$$

Figure 8:6 is a graphical representation of these inequalities. The enclosed, triangular region corresponds to those sets of c_1–c_2 values which satisfy the S.P.R. requirement.

Clearly, according to figure 8:6, the error filter coefficients are capable of being initialised in a large number of ways. The consequences of choosing certain pairings from the available region are explored at greater length in section 8.4 of this chapter. For the purpose of this application however, coefficient initialisation was carried out on the basis of the guidelines suggested in chapter 7. The values chosen for the error filter coefficients are indicated in the following expression.

$$C(z^{-1}) = 1 - 0.5z^{-1} - 0.34z^{-2} \tag{8.20}$$

If the error filter of equation (8.20) is considered as a means of obtaining a weighted error signal then this selection implies a gradually decreasing weighting factor on older information.

Figure 8:7 shows the frequency response characteristics for the transfer function, $C(z^{-1})/A_m(z^{-1})$ using the aforementioned error filter coefficients. The important feature to note in this figure is the phase response characteristic, which is of the requisite form; in the low frequency region, it is asymptotically zero. At its greatest, the magnitude of the phase response attains 60^{o}.

Adaptive Gain

For the series of experiments reported here, the value chosen for the adaptive gain, λ, was 10000. This value was obtained during preliminary testing of the adaptive control scheme; experiments were carried out by substituting a representative analogue circuit for the d.c. servomotor. It was therefore possible to experiment with the control software in complete safety. The analogue circuit was designed to have adjustable dynamics. This was done in order to gauge the parameter adaptive properties of the adaptive control scheme under idealised operating conditions. It was observed that use of the gain value indicated above resulted in a satisfactory level of system behaviour. Adaptive system behaviour did not appear to vary noticeably with different values of adaptive gain; values differing by a factor of ten, in either direction, were tried.

Compensator Networks

For stability reasons, the $F(z^{-1})$ compensator must have its roots inside the unit z-plane disc. The likelihood of a very oscillatory initial process control signal can be avoided by initialising the compensator coefficients such that its roots are located well away from the perimeter of the unit disc. An extremely safe initialisation procedure would be to place its roots at the origin of the unit disc. The choice made here however involved placing the two roots of $F(z^{-1})$ at the points $z = \pm 0.3$.

To complete the initialisation procedure for the $F(z^{-1})$ polynomial, it is also necessary to assign a value to f_0, a forward path gain. This task was carried out with some assistance from step response tests conducted on the d.c. servo-system. Under closed loop digital control, with a unit forward path gain, the controlled system displayed an acceptable level of performance; examples of these responses are discussed at a more relevant stage, later in this section. In order to build in some margin of safety, the f_0 coefficient was assigned a value of 2. This results in the closed loop system having a lower forward path gain. The following expression specifies the initial $F(z^{-1})$ filter condition.

$$F(z^{-1}) = 2f_0 - 0.18z^{-2} \tag{8.21}$$

With no stability requirements for the $G(z^{-1})$ compensator, its initialisation is open to an extremely wide range of options. Some assistance is available from the requirement that the controlled process should have unit steady state gain. This condition means that G(1) has to be equal to 1. To avoid having to choose a particular root position for the $G(z^{-1})$ polynomial, the problem was circumvented by assigning it to infinity. This resulted in an initial $G(z^{-1})$ filter of the form given below.

$$G(z^{-1}) = z^{-1} \tag{8.22}$$

Variable Dead-Band Filter

The variable dead-band filter was implemented according to the manner described in section 6.2 of chapter 6. As part of the initialisation procedure, it is necessary to select values for the following three coefficients: σ, the variable dead-band filter pole location; ϵ_0, the constant input signal to the filter; and, ϵ, the filter gain.

The prime objective of introducing a variable dead-band characteristic in the P.A.A. is to enhance its robustness properties by desensitising it to unmodelled dynamics in the controlled process. For the d.c. servo-system used here, the process is considered to be modelled to a high degree of accuracy. The level of confidence thus engendered led to the variable dead-band filter being initialised in a manner geared more in favour of preserving the alertness of the P.A.A. The following parameter values were chosen; $\sigma = 0.7$, $\epsilon_0 = 10.0$ and $\epsilon = 0.003$. These correspond to the variable dead-band filter having sluggish performance characteristics as a result of having a filter pole located at z=0.7. The characteristic also possesses a small minimum dead-band size. These factors help to temper the action of the variable dead-band characteristic and place a close tolerance on the level of model following expected.

8.3 EXPERIMENTAL EVALUATION OF THE ADAPTIVE CONTROL SCHEME

Prior to presenting the results of testing the adaptive control algorithm, a few comments are made on the test procedure that was employed.

8.3.1 TEST METHOD

The majority of experimental tests reported here were carried out with 2V peak-to-peak input command signals. This corresponds to a servo-system output displacement of 60°. During the course of experimentation, command signals of different amplitudes did not result in widely differing levels of control system performance. The waveform and frequency of the command signals were varied for reasons which will become apparent during the course of the subsequent presentation.

In order to study the reactions of the adaptive scheme, the dynamics of the controlled process were perturbed by altering the d.c. servo-system tachogenerator feedback gain. Such changes were only carried out by certain prescribed amounts. The reason for this was to try and maintain some degree of consistency in tests with the adaptive controller. Two possibilities were catered for. These comprised a sudden reduction in the tachogenerator feedback gain, by a given amount, and a sudden increase to return to the original condition. Figure 8:8 shows the step

response behaviour of the controlled process for the two modes of operation; these correspond to proportional action control, as allowed by the adaptive control algorithm software. The sampling period was measured as 8 ms. The initial set of step responses correspond to the lower of the two tachogenerator feedback gain settings. The bandwidths of the closed loop system, for the two operating conditions, are 7 Hz. and 1 Hz. respectively. This compares with a reference model bandwidth of 3.1 Hz.

8.3.2 PRESENTATION OF TEST RESULTS

Figure 8:9 is a typical example of the way in which the adaptive system behaves when responsibility for control action is switched from ordinary closed loop proportional digital control to model reference adaptive control. The intervening pause during this changeover results from the way in which the control algorithm software is implemented. The action of transferring control action causes a break in the control algorithm. This causes control action to be suspended in order that a set of user guidance instructions can be output to the v.d.u. [77].

The situation shown in figure 8:9 corresponds to the case where the controlled process is characterised by a heavily damped step response. An acceptable level of model following behaviour is attained within a relatively short time span. Within a few more signal cycles excellent model following, as typified by the response shown in figure 8:10, is produced.

An example of corrective adaptive behaviour, following a sudden change in the dynamics of the controlled process, is shown in figure 8:11. This corresponds to the case where the d.c. servo-system tachogenerator feedback gain is suddenly reduced. Initially, the controlled process reacts with quite a large overshoot. However, this is soon corrected and successful model following behaviour resumed. The reverse situation, where the tachogenerator feedback gain is suddenly returned to its original setting is shown in figure 8:12. Once again, adaptive action is acceptably quick. The transient step response of the controlled process is exceptionally consistent. However, the overall trend is somewhat marred by the overshoot in the process response, although this is seen to be gradually diminishing. Nevertheless, this is considered to be an acceptable penalty which can be offset against the generally consistent level of control system performance that is

maintained.

The responses recorded thus far have been obtained with what can be considered as fairly low frequency command inputs. Figures 8:13 and 8:14 differ through the use of a 5Hz. square wave input. The beginning and end parts of each recording are testimony to the quality of model following that is maintained. However, in addition to this feature, figure 8:13 represents the case where the tachogenerator feedback gain is suddenly reduced. The reverse situation is shown in figure 8:14. Although consistent model following is eventually obtained in both examples, the time taken is marginally different for the two cases, in favour of the response of figure 8:13. An explanation for this phenomenon can be given in terms of the quality of the signals being fed to the P.A.A. An examination of the parameter updating expression indicates that it is some function of the process input-output signals. In figure 8:13, the servo-system is initially operating with a high inherent damping. This would imply that the process control signal is periodically large, especially at the start of each step change in the command signal. When the sudden change in process dynamics occurs, the process output, y, becomes very large. Thus, both the control signal, u, and the process output, y, are temporarily relatively large. The incremental part of the parameter updating algorithm can therefore be expected to echo this phenomenon. The likely outcome is that corrective parameter adaptation initially occurs fairly rapidly. A similar line of argument can be formulated for the situation described by figure 8:14. For this set of operating conditions, it is realistic to consider that the process control signal and the output signal are of relatively small magnitudes. This description is especially valid immediately following a sudden increase in tachogenerator feedback gain. In the light of the argument developed for the observations made in figure 8:13, the line of reasoning that follows for the new situation is self-apparent.

Following an initial period of parameter adaptation, it can be argued that a small model-process error is maintained for a lengthier period in figure 8:14 when compared with figure 8:13. The response of figure 8:14 corresponds to the controlled process operating with a high level of damping. This implies a control signal that is periodically large. When translated into its implications for the variable dead-band characteristic a case can be made for a relaxation on model following performance. This situation is typified by the response during the latter stages of figure 8:14. Although apparent to a lesser extent, it is still possible to discern a similar set of trends at the lower input command frequencies of figures 8:11 and 8:12. An

important point highlighted by these observations is that adaptive behaviour should not be judged purely in terms of the length of time taken for good model following to resume; this would represent a gross oversimplification of the situation.

Thus far, the control system has only been tested with different frequency square wave inputs. It is unlikely that this type of command signal will always be encountered in all applications. Hence, the behaviour of the adaptive algorithm will now be examined with sinusoidal command signals. By comparison with square wave inputs, this type of signal has a considerably poorer frequency content. Moreover, this type of situation has been shown to be a source of considerable problems in explicit identification self tuning control schemes [13,20].

Figure 8:15 shows the situation that results when the d.c servo-system is subjected to a sudden reduction in its effective damping. Adaptation appears to be remarkably quick and the desired level of model following performance is soon reattained.

The aim of the adaptation mechanism is to regulate the controlled process loop. This goal requires the model following objective to be satisfied and results in the model-process output error being reduced to zero. However, as indicated in [36], this does not necessarily imply parameter convergence to that set of compensator coefficients which satisfies the pole-placement control law. Consequently, it is possible to argue that the compensator coefficients have only been adjusted to a sufficient degree that ensures a respectable level of model following behaviour. This aspect of the adaptive control algorithm was examined in the following manner. Following the change in the controlled process dynamics and recorded in figure 8:15, the command signal, still a sinusoid, was instantaneously switched to a square wave. The behaviour of the adaptive system to this change is shown in figure 8:16. From it, slight differences in square wave model following behaviour are apparent, though these are soon corrected. It is possible to argue that parameter convergence, during the sinusoidal phase of operation as typified in figure 8:15, was good enough to bring the compensator coefficients close to the converged set as values as required by the pole-placement control law. Complete convergence no longer became necessary once the desired level of model following performance had been attained.

The test procedure described in figures 8:15 and 8:16 corresponds to a sudden increase in the tachogenerator feedback gain. For completeness, the reverse situation was also examined. The respective counterparts of figures 8:15 and 8:16 are figures 8:17 and 8:18. As before, figure 8:17 shows how control system behaviour is maintained, following a sudden change in process dynamics, with a sinusoidal input signal. As expected, corrective adaptation ensures a rapid return to the desired level of model following performance. Figure 8:18 can however be viewed as an indicator of the quality of adaptation that occurred during the sinusoidal excitation phase. When a square wave inputs is selected, a slightly degraded level of model following ensues. As before however, this is soon improved upon. Clearly, there appears to be some link between the 'correctness' of parameter convergence and the spectral richness of the input command signal.

The situation described above corresponds to a case of parameter adaptation satisfying a model following requirement rather than a pole-placement control law. This resulted in a degraded level of system response when the command input was changed to a signal having a richer spectral content in comparison to its predecessor. This type of phenomenon was also observed in terms of the coefficient values of the $G(z^{-1})$ filter for the following operating conditions. These coincided with parameter adaptation occurring while the response of the reference model was of a certain form; with regard to square wave inputs, for example, the reference model response was continuously changing, as in figures 8:13 and 8:14. Other cases resulting in similar parameter adaptive behaviour include sinusoidal and triangular shaped command inputs. All of these conditions are typified by the lack of any static behaviour in the output of the reference model. During such operating conditions, it was noted that parameter adaptation, following a change in the dynamics of the controlled process, resulted in an acceptable level of model following performance. Figures 8:13, 8:14, 8:15 and 8:17 support this statement. However, it was also observed that the steady state gain of the $G(z^{-1})$ feedback compensator differed significantly from unity. By temporarily interrupting the control algorithm and monitoring the values of relevant parameters, divergences of the order of 30% were noted on a number of occasions. This implies that the controlled process closed loop transfer function does not have unity steady state gain. Such a situation is remarkable because it appears to be totally at variance with the control law objective. This subject was touched on in section 5.6.2 of chapter 5. A typical example of control system behaviour in such circumstances is shown in figure 8:19. This recording was obtained by first exciting the control system with a 5Hz. square

wave command input. During this period, the dynamics of the d.c. servo-system were suddenly altered by adjusting its tachogenerator feedback gain. The effect of the ensuing adaptation on the feedback compensator steady state gain is apparent in figure 8:19 when the frequency of the input command signal is suddenly reduced to 0.5Hz. Initially, there is a slight overshoot caused by the $G(z^{-1})$ filter having a steady state gain less than unity. This aberration is soon corrected. The controlled process loop is forced to have unity steady state gain in order to match the steady state response of the reference model.

An explanation for this type of behaviour can be made in terms of the model following control objective. (To begin with, the explanation is developed with reference to the simple case of a sinusoidal command input signal.) Following a change in the dynamics of the controlled process, the adaptation algorithm aims to retune the compensator coefficients to restore model following behaviour. Convergence to the correct (tuned) set of compensator coefficients, as defined by the pole-placement control law, would result in the reference model and controlled process closed loop transfer functions having identical frequency response characteristics. The implication of this is that perfect model following would be obtained at all frequencies. However, this is a far stronger requirement than is necessary to ensure a high degree of model following, at the single sinusoidal frequency. Hence, the compensator coefficients are only altered by a sufficient amount to assure the resumption of acceptable model following behaviour, at the given frequency.

A slightly more complex extension of this argument can be formulated in terms of low frequency square wave command inputs. Now, sufficiently good model following can be expected when the reference model and controlled loop closed loop transfer functions share the following properties:

1) similar frequency response characteristics at the dominant sinusoidal component frequencies in the reference model output.

2) unity steady state gain

Clearly, these conditions are considerably weaker than those imposed by the pole-placement control law which calls for identical frequency response characteristics at all frequencies.

Command signals fed to controlled process are unlikely to be highly complex, from a frequency spectrum viewpoint. Hence, it is likely that they will only include a few dominant frequencies. Whilst still assuring a satisfactory level of model following behaviour, it is likely that the adjustable compensator coefficients will adopt values somewhere in the proximity of their converged counterparts. The parametric difference between actual and converged values is expected to become gradually smaller as the number of significant spectral lines in the reference model output increases. Such an explanation readily accommodates the phenomenon of the $G(z^{-1})$ filter steady state gain not always being equal to unity. A similar argument was recently developed in a more detailed examination of this aspect of adaptive system behaviour [36].

The controlled process loop should ideally possess a feedback compensator with unity steady state gain. This is a necessary condition if the closed loop system is itself to have unity steady state gain. Unless the reference model response contains a steady component, there is no overriding requirement on the $G(z^{-1})$ compensator coefficients for the unity steady state gain condition to be met. A solution to this phenomenon is desirable if the action of the adaptive system is to be enhanced. It is clear that by superimposing a d.c. offset on the input command signal, the spectral content of the reference model response can be improved. This should lead to the coefficients of the $G(z^{-1})$ filter meeting the unity steady state gain requirement. If it is not possible to modify the command signal in this direct fashion then the following alternative can be employed. This involves altering the control system measurement coordinate framework to a uni-polar one. This lends the appearance of a constant offset superimposed on the input command signal, and hence, the reference model output.

In an attempt to verify the outcome of the changes suggested above, the adaptive system was excited with a range of sinusoidal and high frequency square waves. Unlike the earlier examples however, these were superimposed on a constant d.c. signal. Following the line of argument made above, the response of the reference model now includes an additional spectral component, in the form of its steady response to the offset signal component. For the controlled process to be able

to attain an acceptable level of performance, it has to match the reference model behaviour at one or more critical frequencies and have unity steady state gain. Occasional examination of the $G(z^{-1})$ filter coefficients, by interrupting the control algorithm software [77], showed this to be true with only minor excursions of the order of 1%.

This discussion, allied to the responses recorded in figures 8:15 to 8:19, highlights one of the many interesting aspects of direct model reference adaptive control. From one standpoint, the adaptive system has shown itself to be capable of maintaining a consistent level of model following behaviour under a variety of operating conditions. This is true in respect of the dynamics of the controlled process transfer function and the waveform and frequency of input command signals. In contrast to this however, it can also be argued that doubts exist over the accuracy of parameter adaptation when insufficiently rich command input signals are used. Although this factor might appear to detract from the adaptive system in one particular area, its ability to maintain a given level of model following performance is considered to be of much greater importance. To emphasise this point, a series of tests was carried out with a pseudo-random command signal; this was generated by a Hewlett-Packard 3582A spectrum analyser. The signals were band limited to a maximum frequency of 1 Hz. and were considered to be representative of command signals likely to be encountered in real applications. Figure 8:20 is typical of the quality of control system behaviour that was observed; the reference model response is not shown as it is identical to that of the controlled process.

The pseudo-random noise source was also used to test the noise-immunity properties of the adaptive scheme. To simulate realistic conditions, the noise signal was band limited to a maximum frequency of 50 Hz. and a maximum amplitude of 20 mV. This signal was superimposed on the process output and adaptive system behaviour observed over a period of time with a wide range of command input signals. Control system behaviour was not noticeably different under the new operating conditions. Two reasons explain this quality of behaviour. Firstly, the variable dead-band characteristic is responsible for setting a tolerance on model following. This attenuates the presence of noise signals. Secondly, the process output signals are high-pass filtered by $B(z^{-1})$ prior to their use in the adaptation algorithm. This helps to isolate the P.A.A. from the high frequency components in the noise signal.

8.4 ERROR FILTER INFLUENCE ON ADAPTIVE BEHAVIOUR

One of several stages in the adaptive controller design process consists of initialising the coefficients of an error filter, $C(z^{-1})$. In earlier discussions on this subject, a number of guidelines were proposed. The material presented in this section aims to provide some justification for the suggested guidelines. This is facilitated by means of a series of experiments using a number of different sets of error filter coefficients.

8.4.1 EXPERIMENTAL SYSTEM DESCRIPTION

The adaptive control scheme used in section 8.2 was retained for this set of tests. However, the sole modification made to the control algorithm was the elimination of the variable dead-band filter. This was considered to be a justifiable alteration since its influence runs the risk of masking out some of the interesting behavioural characteristics arising from the use of different sets of error filter coefficients. The removal of this function from the control algorithm was carried out by setting the variable dead-band filter gain to zero. This meant that the algorithm sampling period remained unchanged from before.

In order to retain the same control system performance specification as above, the choice of reference model remained unchanged from earlier. Consequently, the S.P.R. region, for an error filter of the form specified in equation (8.14), is as shown in figure 8:6. One of the suggested guidelines for initialising the error filter coefficients makes use of a particular phenomenon related to the phase response characteristics of the transfer function $C(z^{-1})/A_m(z^{-1})$. The desired form of phase behaviour is one where the phase locus is asymptotically zero in the low frequency region. The dotted line passing through the S.P.R. space of figure 8:6 corresponds to those sets of c_1–c_2 values which result in a phase response that is characterised by this condition. This line was drawn through a sample set of points which were found to satisfy the low frequency phase response condition.

The sets of c_1–c_2 pairs that were examined in this investigation are listed in table 8.1. The following procedure was followed in their selection. Initially, three points, S1, S2 and S3 in table 8.1, were selected; these were specifically chosen because they lie on the dotted line of figure 8:6. The transition from S1 to S3 involves traversing from left to right along the c_1 axis. Selection of the remaining points was carried out with the aim of examining the influence of the c_2 coefficient when c_1 was kept fixed. The next two sets of points, S4 and S5, were selected on the basis of certain features relating to the points S1 and S2 and the steady state gain of the error filter. Without going through the full process of applying the final value theorem [42], it can be stated that the following expression specifies the steady state gain of the $C(z^{-1})$ filter.

$$C(z^{-1})_{steadystate} = C(1) = 1+c_1+c_2 \tag{8.23}$$

At the points S1 and S2, the error filter has a steady state gain of 0.025 and 0.05 respectively. Using the c_1 value at point S3, the points S4 and S5 were selected such the resulting steady state filter gains matched these values respectively. The c_2 values that result from this approach lie below the dotted line in figure 8:6. For the sake of completeness, two additional points, S6 and S7, were chosen. These lie above the dotted line and the same c_2 distance away from S3 as the points S4 and S5.

Frequency response characteristics for the transfer function, $C(z^{-1})/A_m(z^{-1})$, using the seven sets of c_1–c_2 pairings are shown in figures 8:21 to 8:23. Considering the first three sets of points, S1 to S3, the main features of interest relate to the phase response characteristics as shown in figure 8:21. In all three, the low frequency behaviour is asymptotically zero. This is to be expected as it was a prerequisite for choosing these particular pairings. The other noteworthy feature is the value of the 'maximum' phase angle encountered. This can be seen to increase gradually in relation to a movement in the positive direction along the c_1 axis. The remaining frequency response diagrams, of the error filter coefficient pairings S4 to S7, need to be examined in the light of the S3 pairing since all five correspond to a single value for c_1. The two cases where the c_1–c_2 points lie below the dotted line result in positive valued phase angles in the low frequency region, as seen in figure 8:22. The further away that a particular point is from from its associated point on the dotted line, the greater is this phase difference. Remarkably, the maximum magnitude of phase angle encountered appears to remain relatively

constant. From figure 8.23, the same feature, but in terms of negative valued angles, applies to those sets of points lying on the opposite side of the dotted line. These patterns are of clear benefit is assisting the iterative procedure to find c_1—c_2 points with desirable low frequency characteristics.

8.4.2 EXPERIMENTAL PROCEDURE

The influence of the different error filter coefficients was carried out by subjecting the system to sudden alterations in the d.c. servomotor tachogenerator feedback gain. Perturbations to the dynamics of the controlled process were identical to those described and used in section 8.3 above.

8.4.3 EXPERIMENTAL RESULTS

Figures 8:24, 8:25 and 8:26 show the response of the adaptive system to a sudden increase in the effective damping of the controlled process. These responses correspond to the error filter pairings S1, S2 and S3 respectively. Without considering the quality of overall model following behaviour, differences in the speed with which corrective action occurs is highlighted. The corresponding cases for a reduction in effective damping are shown in figures 8:27, 8:28 and 8:29 respectively. Once again, a similar pattern emerges with regard to the speed of corrective action. From these six sets of results, the S3 error filter pairing can arguably be said to provide the best level of adaptive performance.

Although it might appear a relatively minor point, a note of caution needs to be injected in considering the magnitude of the initial overshoot in the responses of figures 8:27, 8:28 and 8:29. It appears that the move towards an improvement in the speed of adaptation is in some way penalised in terms of the relative quality of control system response.

The following observations can be made from the experimental data that has been presented thus far. In terms of the error filter coefficients, it appears, at this stage, that improved adaptive action corresponds to a move to the bottom-right region of the S.P.R. space of figure 8:6. Moreover, the c_1—c_2 pairings used to generate the results presented above possess a certain form of low frequency phase

response locus, as witnessed by the frequency response characteristics of figure 8:21.

The next step in this experimental investigation examines possible influences of the c_2 parameter. Adopting an orderly approach to this problem, two conditions, corresponding to the S4 and S5 pairings, are considered first. These correspond to a fixed value of -1 for the c_1 coefficient. The parameter pairs of S4 and S5 employ c_2 values of 0.025 and 0.05 respectively. In terms of the steady state gain of the error filter, these points correspond to S1 and S2 respectively.

Figures 8:30 and 8:31, corresponding to the error filter settings of S4 and S5, display the responses of the adaptive system to a sudden increase in the effective damping of the controlled process. By comparison with the response of figure 8:26, the apparent speed of corrective action is similar. The only difference concerns steady state response of the controlled process; this becomes progressively worse as the $C(z^{-1})$ filter steady state gain becomes smaller. A similar description of adaptive system behaviour can be applied to the case of a sudden increase in effective system damping; the responses of the S4 and S5 error filter coefficients to this perturbation are shown in figures 8:32 and 8:33 respectively. Apart from the steady state model following performance, the responses recorded for the S4 and S5 cases bear a greater resemblance with those due to the S3 setting, figure 8:29, than do the cases S1 and S2, figures 8:27 and 8:28.

On the basis of the observations made thus far, it is possible to distinguish a number of adaptive system behavioural patterns. The overall speed of response of the adaptive control scheme, to sudden changes in the dynamics of the controlled process, is influenced by the choice of error filter coefficients. From a qualitative viewpoint, the quickest levels of performance that were recorded correspond to c_1—c_2 pairings near the bottom-right of the S.P.R. space used in this study. Variations in the value of the c_2 coefficient, for a given value of c_1, appeared to have little effect on the way in which the adaptation algorithm regulated the transient portion of the controlled process step responses. However, it was clear that the choice of value for c_2 had a marked influence on the steady state process behaviour. From the c_1—c_2 pairings examined thus far, the best adaptive behaviour obtained corresponded to that value of c_2 which caused the $C(z^{-1})/A_m(z^{-1})$ transfer function to possess a readily identifiable low frequency phase response characteristic. This transfer function was also characterised with a maximum magnitude of phase approaching 90°.

In an attempt to build on the observations that have been made, two more sets of error filter coefficients, S6 and S7, were examined. Once again, the value of the c_1 coefficient was fixed at -1. The points S6 and S7 were selected to correspond to those of S4 and S5 respectively. The choice of c_2 values selected, were done so on the basis of a mirror image representation of the S4 and S5 pairings in the axis of reflection defined by the line $c_2 = 0.1$. This resulted in c_2 values of 0.175 and 0.15, for S6 and S7 respectively.

Adaptive responses to a sudden increase in effective system damping, for the error filter settings of S6 and S7, are shown in figures 8:34 and 8:35. As with the cases of S3, S4 and S5 (figures 8:26, 8:30 and 8:31 respectively), it can be argued that the general trend in the speed of corrective adaptation action is similar. However, the cases corresponding to the settings of S4 and S5 resulted in satisfactory model following over the transient part of the step responses. This was also coupled with a degradation in the quality of steady state setpoint and model following response. The converse appears to hold true of the c_1—c_2 coefficients of S6 and S7. This point is most forcibly made when a comparison is made between the two associated points, S4 and S6, in figures 8:30 and 8:34. To confirm this, figures 8:36 and 8:37 show the responses of the adaptive system, to a sudden reduction in the controlled process tachogenerator feedback gain, for the error filter settings of S6 and S7. The previously observed trend, of good steady state behaviour but less satisfactory transient model following, is once again evident. The apparently highly energetic way with which corrective adaptive action is achieved appears to bear some direct relationship to the size of the error filter steady state gain which, in this case, depends upon the choice of c_2 coefficient. This is shown in figures 8:34, 8:35 and, to a lesser degree, in figures 8:36 and 8:37.

In the light of these observations, the behaviour patterns that were highlighted earlier can now be re-examined and, in some cases, reinforced. For a given c_1 coefficient, it is apparent that variations in the value of the c_2 coefficient have a muted effect on the overall speed of adaptive action. However, it was observed that the choice of value for the c_2 coefficient affected adaptive system behaviour in a localised sense. Referring to the S.P.R. region of figure 8:6, this influence could be gauged with reference to the dotted line shown; this corresponds to S.P.R. transfer functions having asymptotically zero low frequency phase response characteristics. Where the choice of coefficient values resulted in a c_1—c_2 pair lying below the dotted line, steady state model following behaviour was

compromised, following a sudden change in the dynamics of the controlled process. Conversely, a point situated above the dotted line resulted in an apparently rapid level of corrective adaptive behaviour. This produced a highly oscillatory reaction in the controlled process response. The trend appeared to worsen as the steady state gain of the error filter increased. This point gains a greater measure of importance in the light of an examination of figures 8:27, 8:28 and 8:29. The three responses recorded correspond to c_1—c_2 pairs lying on the dotted line of figure 8:6 and resulting in error filters with a gradually increasing steady state gain. These responses indicate the magnitude of the initial overshoot increasing in line with the size of the error filter steady state gain. Figures 8:34 and 8:35 also provide further evidence of this pattern. This observation injects a cautionary note in initialising the error filter coefficients. It argues against choosing a c_1—c_2 pairing which has an asymptotically zero low frequency phase response and which is situated to the extreme bottom-right of the permitted S.P.R. space.

Identical trends in adaptive system performance, with changes in the error filter coefficients were observed when the reference model was initialised with a different set of coefficients. The experimental investigation conducted into the influence of the error filter coefficients offers considerable justification for the initialisation guidelines advanced in chapter 7.

8.5 INTEGRAL ACTION ADAPTIVE CONTROL SCHEME

The need for an integral action form of compensation arises when the controlled process is required to possess enhanced disturbance rejection qualities. Examples where this is likely to be needed are when the control system is oriented towards set-point tracking or, when it is known in advance that externally generated disturbances are likely to be present; the latter could take the form of opposing or assisting forces acting on the servomotor drive shaft. Problems of this nature affect the behaviour of the basic control system. In an adaptive scheme, these considerations have to be taken a step further.

The implications for the P.A.A. of disturbances impinging on the controlled process were discussed in section 6.6 of chapter 6. At that time, two alternatives were proposed for realising an integral action controller. The control algorithm presented below makes use of the first of the two approaches.

8.5.1 CONTROL SYSTEM DESCRIPTION

Process Model

Figure 8:38 is a schematic of the sampled data control system under discussion. The controlled plant is the same d.c. servo-system that was used previously. The transfer function of the controlled plant remains unchanged from that used in earlier parts of this chapter. However, the main differences in the control scheme involve the implementation of an integral term in the controlled process loop. This is carried out by introducing the term, $K_I(z-a_I)/(z-1)$, in its forward path. At this early stage, the integrator is defined in a general form. This will offer the designer a greater degree of flexibility over its specification, through the choice of a gain value, K_I, and the zero at $z = a_I$.

In the previous, integral-action-free scheme of figure 8:5, the control system was augmented with a z^{-1} unit delay element. This was introduced as a means of overcoming the problem of a computational delay in evaluating the process control signal. The effective controlled process transfer function for this scheme is of a higher order than in either of the two previous sections. This implies that there will be a greater number of adjustable parameters to be generated. The resulting increase in the sampling period of the control algorithm, taken with the advice of section 7.4 in chapter 7, obviates the need to model a computational delay. This line of reasoning will become more apparent as the design and implementation of the adaptive system develops. The format of the resulting control scheme is typified by flow-diagram 7:1.

From earlier in this chapter, equation (8.3) represents the discrete transfer function used to model the controlled d.c. servo-system and D/A converter. Once the integral term is accounted for, the effective transfer function for the controlled process is given by an expression of the following form,

$$\frac{y(z)}{u(z)} = \frac{K_I(z-a_I)}{(z-1)} \frac{b'_0(z+1)}{(z^2-a_1z-a_2)}$$

Hence,

$$\frac{y(z^{-1})}{u(z^{-1})} = \frac{b_0z^{-1}(1-a_Iz^{-1})(1+z^{-1})}{1-a_1z^{-1}-a_2z^{-2}-a_3z^{-3}}$$

$$= \frac{b_0z^{-1}B(z^{-1})}{A(z^{-1})} \qquad (8.24)$$

It should be noted that, unlike in previous schemes, the $B(z^{-1})$ polynomial of equation (8.24) contains a root at a point other than z=-1. The root position is known since it is intentionally introduced as part of the integrator design process.

Reference Model

Adopting the usual procedure outlined earlier, the reference model transfer function is derived on the basis of equation (8.24). In this way, the controlled process and open loop reference model transfer functions share the same structure. It is necessary to operate the open loop reference model under closed loop control, with unity feedback gain. This results in a reference system possessing unity steady state gain. The closed loop reference model transfer function is developed as follows.

$$\frac{x(z)}{w(z)} = \frac{b'_mK_I(z-a_I)(z+1)}{z^3+a'_1z^2+a'_2z+a'_3+b'_mK_I(z-a_I)(z+1)}$$

Therefore,

$$\frac{x(z^{-1})}{w(z^{-1})} = \frac{b_mz^{-1}(1-a_Iz^{-1})(1+z^{-1})}{1-a_{m,1}z^{-1}-a_{m,2}z^{-2}-a_{m,3}z^{-3}}$$

$$= \frac{b_mz^{-1}B(z^{-1})}{A_m(z^{-1})} \qquad (8.25)$$

The $B(z^{-1})$ polynomial of equation (8.25) is identical to that in the process transfer function of equation (8.24).

Compensator Network Specification

Suitable orders for the $F(z^{-1})$ and $G(z^{-1})$ compensators are derived according to the method outlined in chapter 4. For the control scheme considered here, the reference model has a third order characteristic equation. The process open loop transfer function is characterised by third order denominator and numerator polynomials. Application of equations (4.8) and (4.9) from chapter 4 result in $F(z^{-1})$ and $G(z^{-1})$ compensators of the following generalised forms.

$$F(z^{-1}) = f_0+f_1z^{-1}+f_2z^{-2} \tag{8.26}$$

$$G(z^{-1}) = g_0+g_1z^{-1}+g_2z^{-2} \tag{8.27}$$

A simple verification of these expressions can be made by considering the equation for the pole-placement control law. Using the compensator networks specified above, the process loop characteristic equation is of order 5. This leads to the formulation of six simultaneous equations, from the coefficients of the z-operator terms. This set of equations contains six 'unknowns', namely the six compensator coefficients of equations (8.26) and (8.27).

Parameter Adaptive Algorithm Specification

The parameter adaptive algorithm is specified in terms of an adjustable parameter vector, a filtered observation vector and a parameter updating algorithm. For this adaptive system the following two expressions define the adjustable parameter and observation vectors respectively.

$$\underline{\hat{\mathbf{d}}}^T = [\ \hat{f}_o(k)\ \hat{f}_1(k)\ \hat{f}_2(k)\ \hat{g}_0(k)\ \hat{g}_1(k)\ \hat{g}_2(k)\ ] \tag{8.28}$$

$$\underline{\Phi}(k) = [\ u(k)\ u(k-1)\ u(k-2)\ y(k)\ y(k-1)\ y(k-2)\ ]^T \tag{8.29}$$

The parameter updating algorithm is some function of a filtered version of the observation vector of equation (8.29) with the filtering effect depending on the numerator dynamics in the process transfer function. Hence, from equation (8.24), the filtered observation vector, $\underline{\tilde{\Phi}}$ is written as,

$$\underline{\tilde{\Phi}}(k) = z^{-1}B(z^{-1})\underline{\Phi}(k) \tag{8.30}$$

with,

$$B(z^{-1}) = 1+(1-a_1)z^{-1}-a_1 z^{-2} \tag{8.31}$$

8.5.2 CONTROL SYSTEM INITIALISATION

Reference Model

The reference model transfer function contains a third order characteristic equation. In addition, there is a gain, b_m, and a zero at $z=a_1$, all of which have to be initialised. In carrying out this task, some degree of assistance can be gained by examining a hypothetical, reference model root locus diagram.

On the basis of the derivation of the closed loop reference model transfer function of equation (8.25), it can be stated that the open loop transfer function contains the following.

1) two poles, one of which is an integrator, associated with the d.c. servo-system.

2) a second integrator due to the integral action controller.

3) a zero at z=-1 derived from the d.c. servo-system.

4) a zero at $z = a_I$ arising from the integral action controller.

Omitting to draw in this last zero, the initial root locations of a hypothetical root locus diagram are as shown in figure 8:39; this corresponds to a zero forward path gain in the open loop transfer function. The procedure for drawing root locus diagrams involves examining the behaviour of the roots of the characteristic equation, for controlled variations in a single transfer function parameter. The usual choice for this manipulated variable is the forward path gain, b_m. Using this approach, a root locus diagram of the general form shown in figure 8:39 is expected. The fact that two branches of the loci move immediately outside the unit disc means that the closed loop system is unstable. Hence, no practical reference model could be specified for the control scheme. Bearing this in mind, the previously neglected zero, from the integral action term, can be used to improve the situation. This zero can be placed anywhere on the real axis. To be effective, it needs to be located to the left of the (1,0j) point. This is because it exerts an attraction on loci passing in its vicinity. Therefore, the loci emanating from the (1,0j) point can be drawn inside the unit disc and a stable reference model be specified. A hypothetical root locus diagram is shown in figure 8:40. The precise location of this zero is a choice for the designer. The following comments provide some assistance in this task. The further away that the zero is placed from the (1,0j) point the less will be its attractive influence on the problematic loci. If however, the zero is placed too close to the (1,0j) point it will have an adverse affect on the quality of the reference model step response behaviour. This phenomenon causes the step response to display an overshoot. The magnitude of this overshoot increases the nearer the zero location approaches the (1,0j) point [42].

Drawing on the guidelines highlighted above, the reference model was initialised with the integral term zero at z=0.5 and the following set of closed loop poles.

$$\frac{x(z)}{w(z)} = \frac{b_m(z-0.5)(z+1)}{(z-0.85-0.1j)(z-0.85+0.1j)(z-0.4)} \tag{8.32}$$

The final step in the initialisation procedure consists of evaluating a suitable value for the reference model gain, b_m. Under steady state operating conditions, the reference system is required to have unity steady state gain. Application of the final value theorem [42] to the reference model of equation (8.32) results in the following expression for its steady state output to a unit step input.

$$\lim_{k\to\infty} x(k) = \left[\frac{b_m(z-0.5)(z+1)}{z^3-2.1z^2+1.4125z-0.293}\right]_{z=1}$$

$$= \frac{b_m}{0.0195}$$

Hence, the desired value for b_m is 0.0195.

Compensator Networks

The $F(z^{-1})$ and $G(z^{-1})$ compensators are both of order 2. As with the adaptive algorithm presented at the start of this chapter, the $F(z^{-1})$ polynomial of equation (8.26) was initialised with its roots at z=±0.3. In addition, the f_0 coefficient was assigned a value of 2. This results in the following expression for the $F(z^{-1})$ compensator.

$$F(z^{-1}) = 2.0-0.18z^{-2} \tag{8.33}$$

The root locus examination of a hypothetical reference model indicated the stabilising nature of placing a zero near the (1,0j) point. This argument is just as applicable to the controlled process, since it too includes two integrators in its open loop transfer function. The $G(z^{-1})$ is responsible for introducing two zeros in the controlled process loop. The beneficial effect of placing a zero near the (1,0j) point is taken into account by placing one of compensator roots at z=0.8. The following choice of initial values for the $G(z^{-1})$ polynomial satisfies this condition.

$$G(z^{-1}) = 5z^{-1} - 4z^{-2} \tag{8.34}$$

It should also be noted that the feedback filter is initialised in a manner which makes its steady state gain equal to unity.

Integral Action Gain

The integral term introduced in the forward path of the controlled process includes a gain, K_I. This facilitates an additional degree of flexibility when initialising the control system. It is generally accepted that the introduction of an integrator in a control loop tends to reduce its stability margins. In order to alleviate this condition, the effect of the integrator was moderated by selecting $K_I = 0.5$.

Variable Dead Band

By comparison with the adaptive control schemes discussed earlier in this chapter, this new scheme has simply been augmented with an integral action controller; this is obviously a known term. The degree of confidence that was previously expressed in the discrete model of the d.c. servo-system is still held. Hence, the same variable dead-band filter settings as before were retained.

Error Filter

Employing the design guidelines outlined in chapter 7, the error filter was specified on the basis of the following transfer function.

$$\frac{C(z^{-1})}{A_m(z^{-1})} = \frac{1+c_1z^{-1}+c_2z^{-2}}{1+a_{m,1}z^{-1}+a_{m,2}z^{-2}+a_{m,3}z^{-3}}$$

$$= \frac{z^3+c_1z^2+c_2z}{z^3+a_{m,1}z^2+a_{m,2}z+a_{m,3}} \qquad (8.35)$$

The use of MACSYMA to examine the S.P.R. problem with reference to this transfer function led to the following set of inequalities:

$$c_2 > -c_1-1 \qquad (8.36)$$

$$c_2 > c_1-1 \qquad (8.37)$$

$$c_2 < -4.444c_1+3.889 \qquad (8.38)$$

$$c_2 < -0.767c_1-0.560 \qquad (8.39)$$

A graphical representation of these inequalities makes it possible to visualise the allowable c_1–c_2 S.P.R. region. This is shown in figure 8:41.

Using the error filter selection guidelines suggested in section 7.5.3 of chapter 7 and drawing on the observations made in section 8.4.3 above, the following values were chosen for the 'c' coefficients, c_1=-1.0 and c_2=0.09. This pairing is not too close to the far bottom-right of the S.P.R. parameter region.

The frequency response characteristics of the S.P.R. transfer function, with this set of error filter coefficients, are shown in figure 8:42. As expected, the low frequency phase response characteristics are of a desirable form. The maximum phase angle is approximately -70^{o}.

8.6 EXPERIMENTAL EVALUATION OF THE ADAPTIVE CONTROL SCHEME

8.6.1 TEST METHOD

For reasons outlined in chapter 6 and more recently in section 8.3.2, it is possible for the feedback compensator, $G(z^{-1})$, to have a non-unity steady state gain. It is evident that should this phenomenon occur to a significant degree then the whole objective of using an integral action control scheme is likely to be jeopardised. Considering simply the set-point tracking objective, it is essential to have unity steady state feedback if the input signal to the integral term is to become zero when the desired set-point is reached. With any other value of steady state gain, the consequences of a null input to the integrator mean that set-point tracking is not being met. To alleviate this problem, the system was tested with command input signals containing a steady offset. This was arbitrarily selected as 1V while the basic command signal waveforms were restricted to a peak-to-peak value of 2V, as before. As discussed in section 8.3.2, the inclusion of an offset signal constrains the $G(z^{-1})$ polynomial to have unity steady state gain. This is of obvious benefit in assisting the disturbance rejection properties of this control scheme.

Referring back to figure 8:2, it can be seen that the test rig includes an adjustable potentiometer which feeds a signal to the input of the d.c. servomotor. This potentiometer was used to introduce a sudden offset disturbance in the controlled process loop. The magnitude of its value was arbitrarily selected as 1V.

8.6.2 PRESENTATION OF TEST RESULTS

The adaptive control algorithm designed for this scheme differs from that of section 8.2 in a number of different aspects. One of these concerns the decision not to include a computational delay term in the controlled process model. The algorithm considered here was found to operate with a sampling period of 11.5 ms. The fractional delay in evaluating and sending out the control signal took approximately 12% of this time. This value falls well inside the 20% mark proposed in chapter 7 and beyond which the type of solution employed in section 8.2 would have been advised.

The performance of the adaptive system is examined from two aspects. The first of these concerns its parameter adaptive capabilities and the second its disturbance rejection properties. To begin with, model following behaviour was observed for the switch from ordinary closed loop to adaptive control. Following this initial experiment, the effect of perturbing the dynamics of the controlled process was studied. This was achieved by using the adjustable tachogenerator feedback gain as before.

Figure 8:43 is representative of the start-up performance upon switching to adaptive control action. This response was obtained with the d.c. servo-system operating at the higher of the two tachogenerator feedback gain settings. In spite of being located well away from the (1,0j) point, the influence of the zero at z=0.5 is noticeable in the reference model step response. It appears as a small overshoot which, by the standards of this control scheme, is considered to be quite acceptable.

The influence of the extra integral term in the controlled process loop is apparent from the initially highly oscillatory process response in figure 8:43. The relatively poor level of response is attributed to a poor choice of initial conditions for the compensator coefficients. In an attempt to improve this, the experiment was repeated with a sinusoidal input signal. This places a less stringent set of requirements on model following performance since the command signal does not possess as 'rich' a spectral content. This should help to provide a more relaxed form of parameter adaptation. The results obtained are shown in figure 8:44. Although there is still some oscillatory behaviour, this does not last for as long as in the response of figure 8:43. Figure 8:45 shows what occurs when the input command signal is suddenly altered to a square wave. The quality of response is very good.

This suggests that, where possible, an improvement in overall adaptive system behaviour can be obtained by commencing adaptive control with a relatively 'unexciting' input signal. In this case, a sinusoidal waveform superimposed on an offset signal was found to be adequate. The sinusoidal input causes the compensator coefficients to be adjusted to an improved set of values, by comparison with their initial selections. In addition, the offset component imposes a steady state gain constraint on the feedback path compensator, $G(z^{-1})$. The benefits of this are apparent in the response shown in figure 8:45. Here, very good model following is obtained over the static part of the reference model response. This compares favourably when examined against a similar test carried out in section 8.3.2 and typified by the response in figure 8:19.

Figures 8:43 and 8:44 showed two cases of adaptive start-up behaviour. The latter was considered to be the superior of the two. The improved quality of response that was observed is explained with the following argument. Consider the situation whereby the adaptive system has to adjust the compensator coefficients from a given set of initial values to a different one. It is argued that the transition between these two states can occur along a number of different trajectories. This concept is schematically shown in figure 8:46, for the case of a two parameter adaptive system. Convergence to a unique pairing is not shown for every trajectory. This is because it might not always be called for, especially with an undemanding reference model response characterised by a relatively poor spectral content. The particular trajectory that is followed is likely to depend on a number of factors, including the type of signal used to excite the adaptive system. The simpler the spectral content of this signal, the greater the number of trajectories which can accommodate this transition is likely to be. Therefore, the use of a relatively simple command signal, such as a sinusoid, will offer a greater number of opportunities for approaching within a short distance of the desired set of compensator values while still maintaining a high level of model following action. Greater rapprochement to the desired set of compensator coefficients can be expected to follow upon switching to a spectrally-richer driving signal.

Attention is now turned to the question of adaptive system behaviour following changes in the dynamics of the controlled process transfer function. Figure 8:47 shows the case of a sudden reduction in the tachogenerator feedback gain. The parameter adaptive algorithm reacts quickly to maintain the previous trend of the process transient response. Some overshoot is also obtained though this

is gradually improved upon. The reverse situation, whereby the effective damping coefficient is returned to its original setting, results in the form of response recorded in figure 8:48. There is some initial oscillatory behaviour before excellent model following resumes. The oscillatory response is characteristic of an integrator with a high gain. On the evidence of this behaviour, a case can be made for using a lower value for the integrator gain, K_I.

For the purpose of comparison, the adverse influence of a disturbance acting on a non-integral-action control scheme is presented. Figure 8:49 was obtained with the adaptive scheme discussed in section 8.3. The disturbance signal causes the controlled process response to be offset by some mean amount. However, the parameter adaptive system still attempts to maintain a semblance of steady state model following; this is not correct because the model-process error is not the result of a model-process parametric error. A secondary feature to note in figure 8:49 is the initial response of the reference model on the rise stroke following a step input. This condition causes the process control signal to become saturated. As a result, the series-parallel mode of operation becomes effective and the reference model is locked onto controlled process. Returning to the integral-action adaptive control scheme, figures 8:50 and 8:51 are typical examples of control system behaviour that were observed when offset signals were were introduced in the controlled process loop. Figure 8:50 corresponds to the case of a high effective damping coefficient while figure 8:51 represents the lower of the two tachogenerator feedback settings used throughout this chapter. In both cases the disturbance is overcome and consistent model following resumes. Slight differences are however apparent in the transient responses to the disturbance. These are attributed to the prevailing dynamics of the controlled process. In figure 8:50, for example, the d.c. servo-system is heavily damped. Therefore, it responds quite sluggishly to the sudden disturbance. The opposite is true of the system configuration employed in figure 8:51. With reference to this recording, it is worth noting that parameter adaptation does take place during the transient occasioned by the disturbance signal. This is only natural as the model-process output error becomes non-zero for a short period of time. The parameter adaptation that ensues is undesirable since it is provoked by an unmodelled phenomenon; it is not the consequence of a model-process parametric error. The adverse nature of this adaptation is witnessed in the quality of the process step responses following the disturbance.

	Compensator Coefficients	
Pairing	c_1	c_2
S1	-1.8	0.825
S2	-1.5	0.55
S3	-1.0	0.1
S4	-1.0	0.025
S5	-1.0	0.05
S6	-1.0	0.175
S7	-1.0	0.15

TABLE 8:1 COEFFICIENT PAIRS USED TO STUDY ERROR FILTER INFLUENCE ON ADAPTIVE SYSTEM BEHAVIOUR

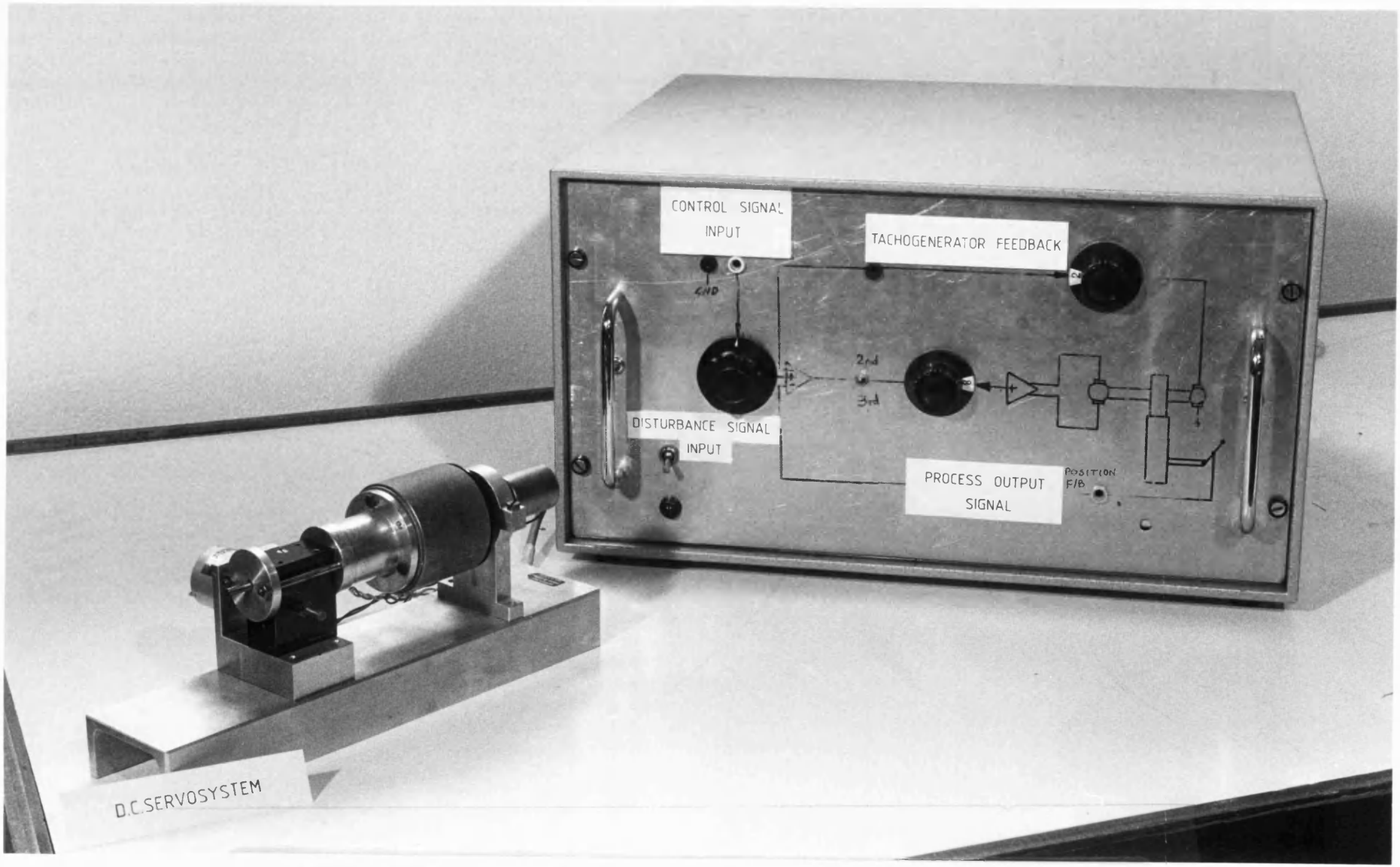

FIGURE 8:1 Electro-Mechanical Servomechanism Test Rig

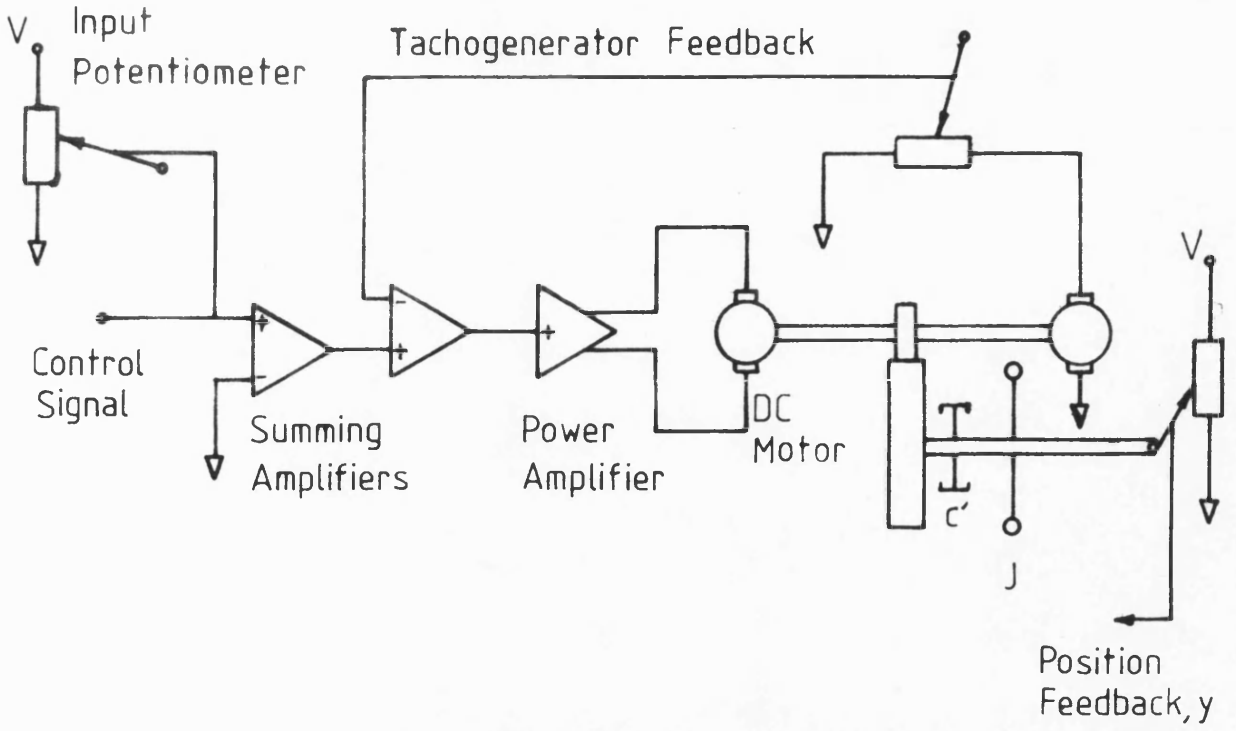

FIGURE 8:2 Schematic Representation Of D.C. Servosystem

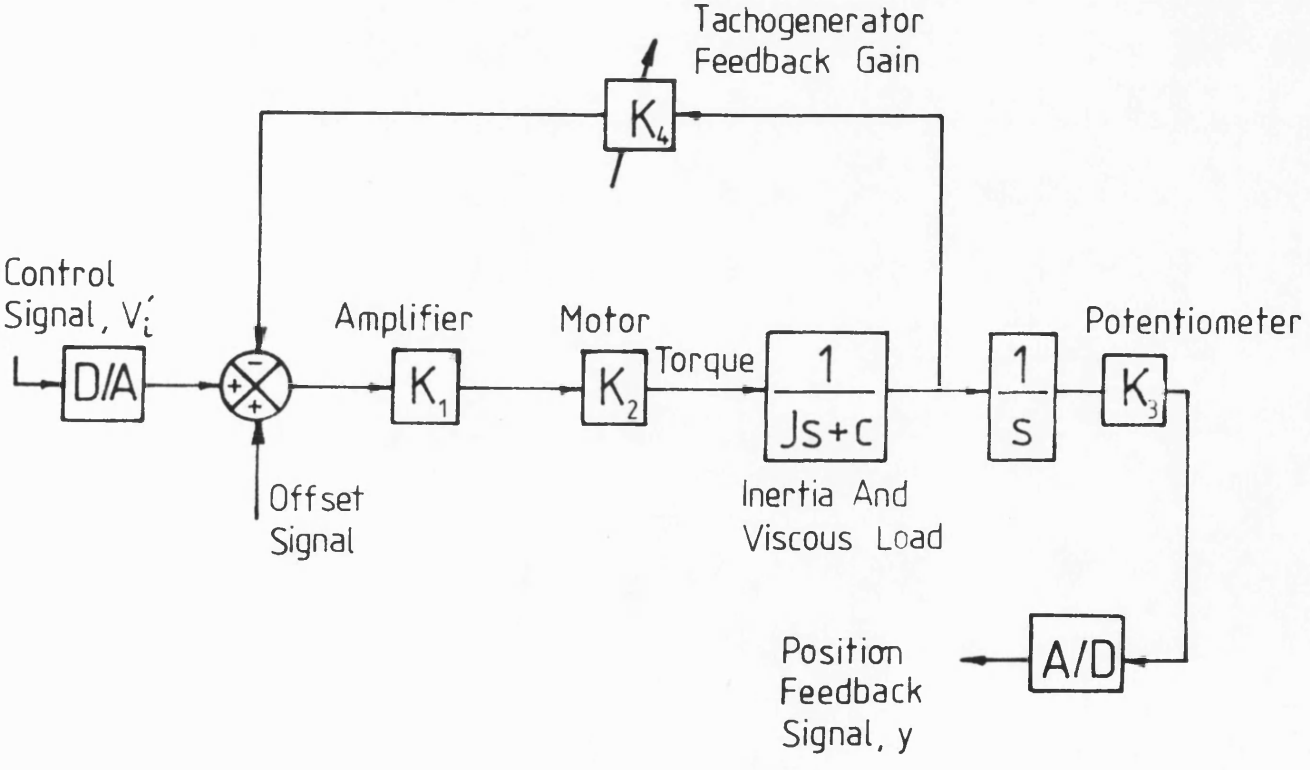

FIGURE 8:3 Block Diagram Representation Of Controlled Process

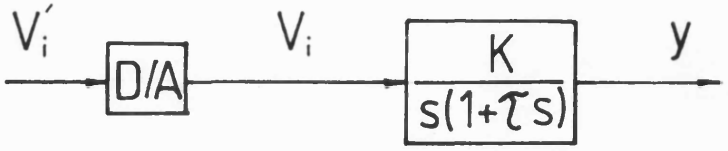

FIGURE 8:4 Simplified Representation Of Controlled Process

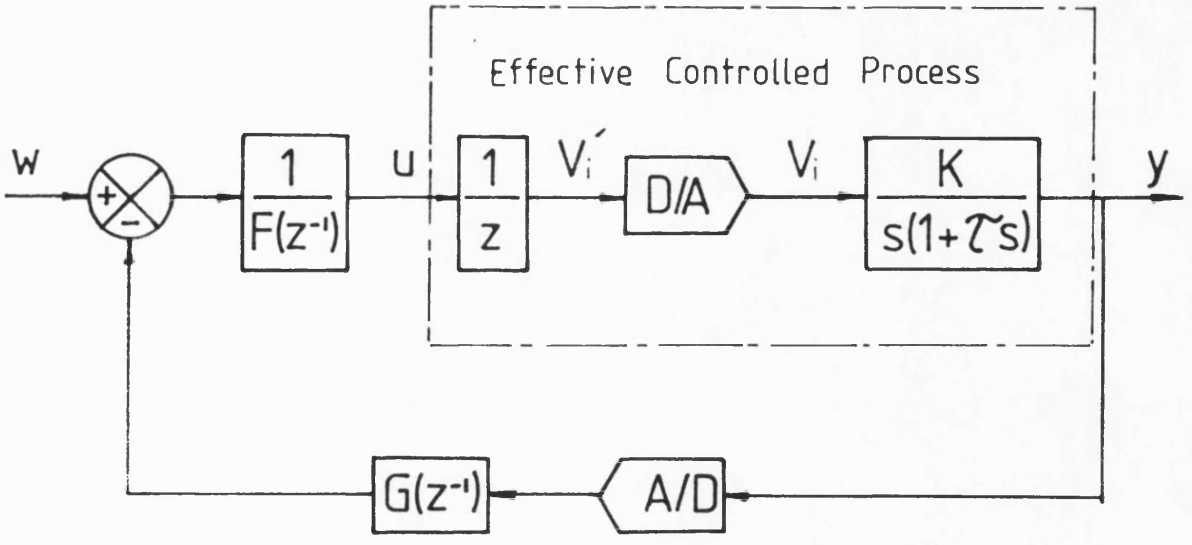

FIGURE 8:5 D.C. Servosystem Closed Loop Control Scheme

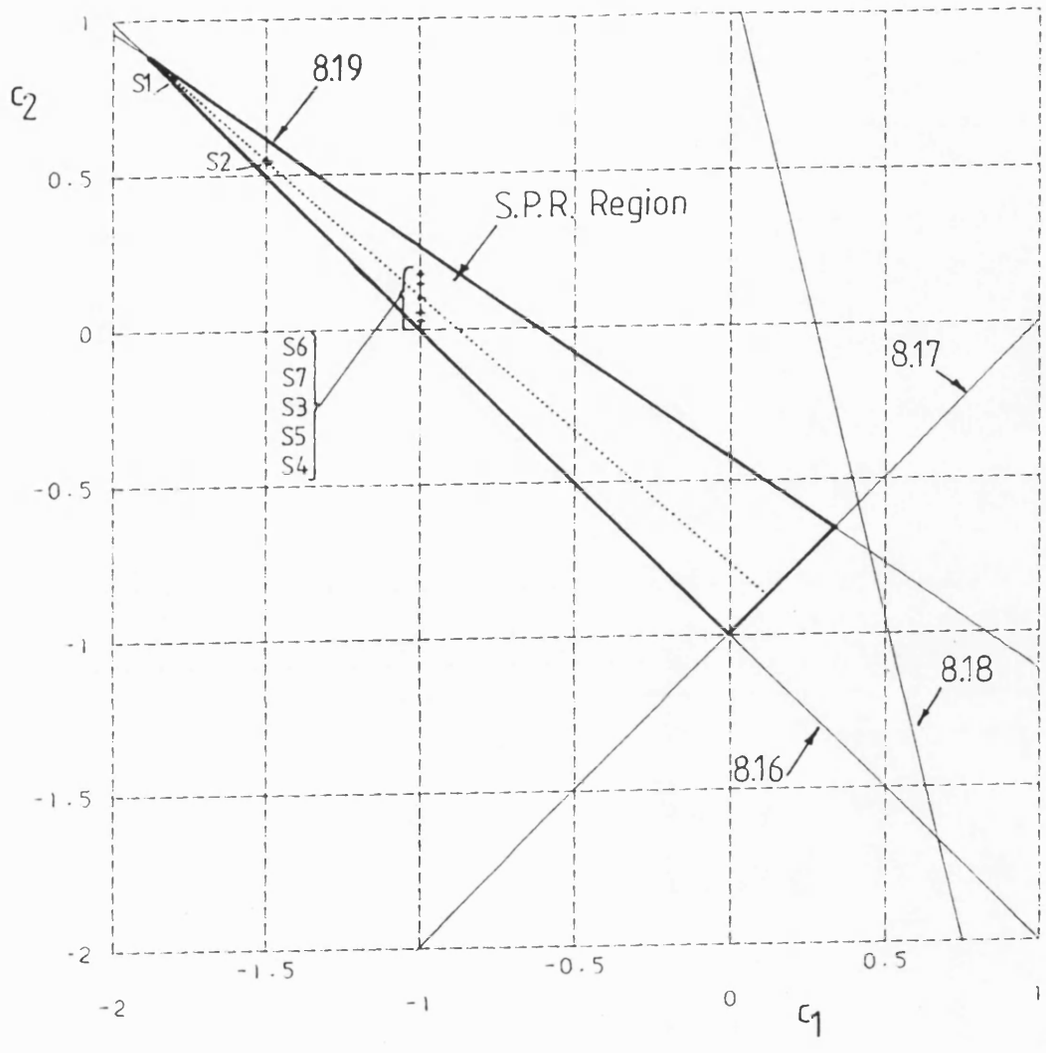

FIGURE 8:6 c_1–c_2 Parameter Space Satisfying S.P.R. Condition

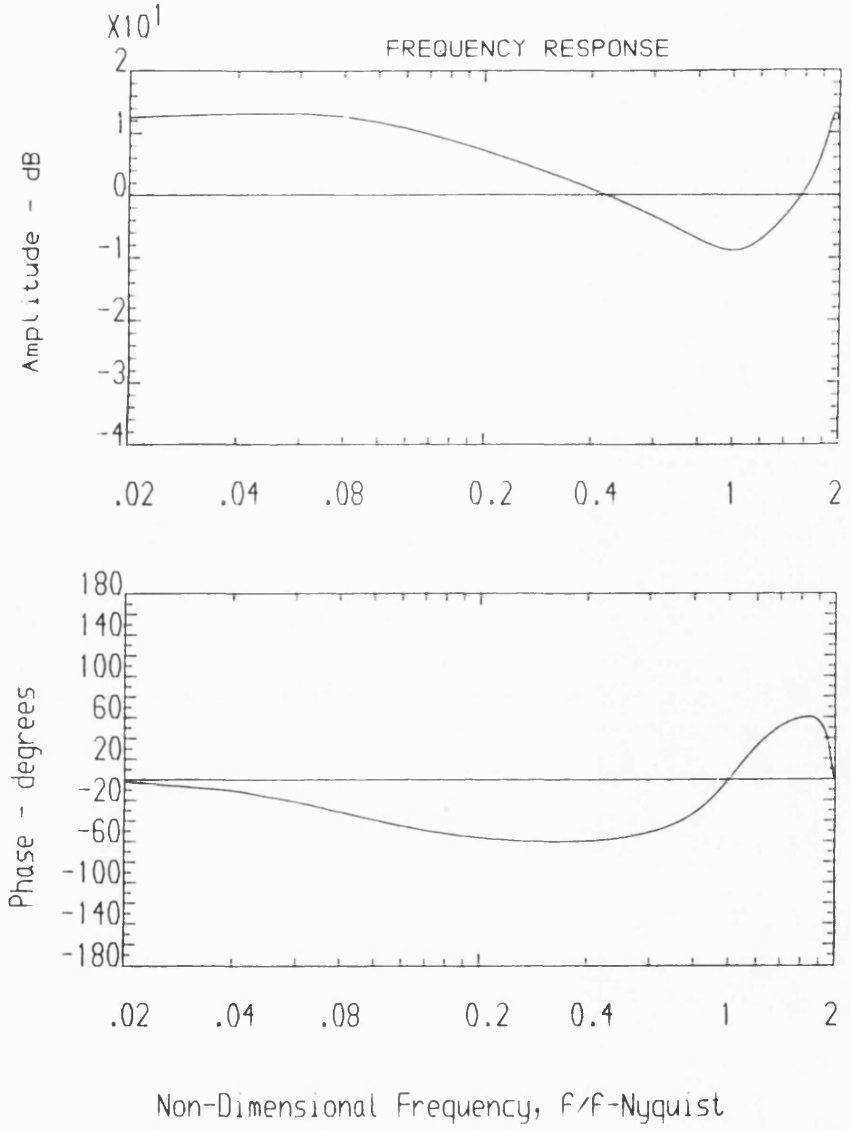

FIGURE 8:7 S.P.R. Transfer Function Frequency Response Characteristics

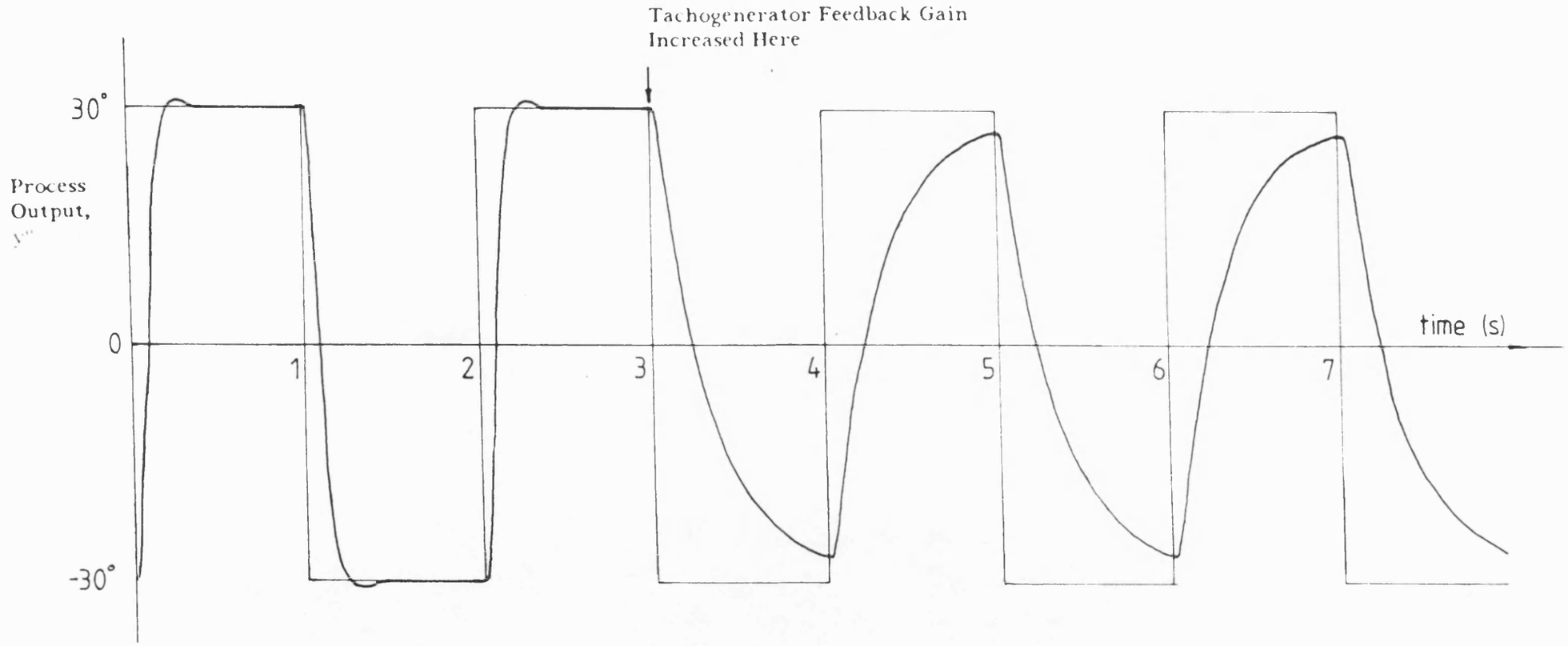

FIGURE 8:8 Comparison Of D.C. Servosystem Response For Different Tachogenerator Feedback Gains

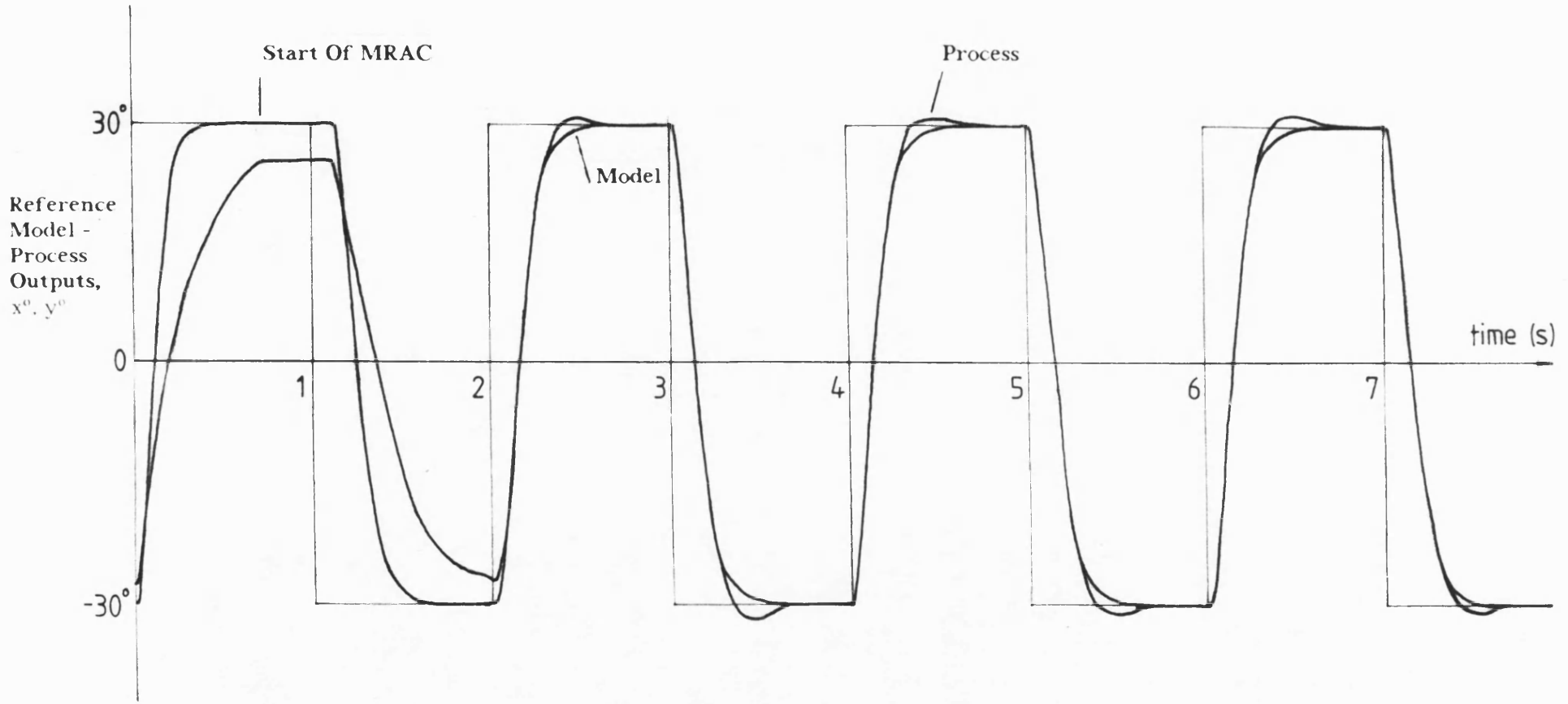

FIGURE 8:9 Start Of Model Reference Adaptive Control

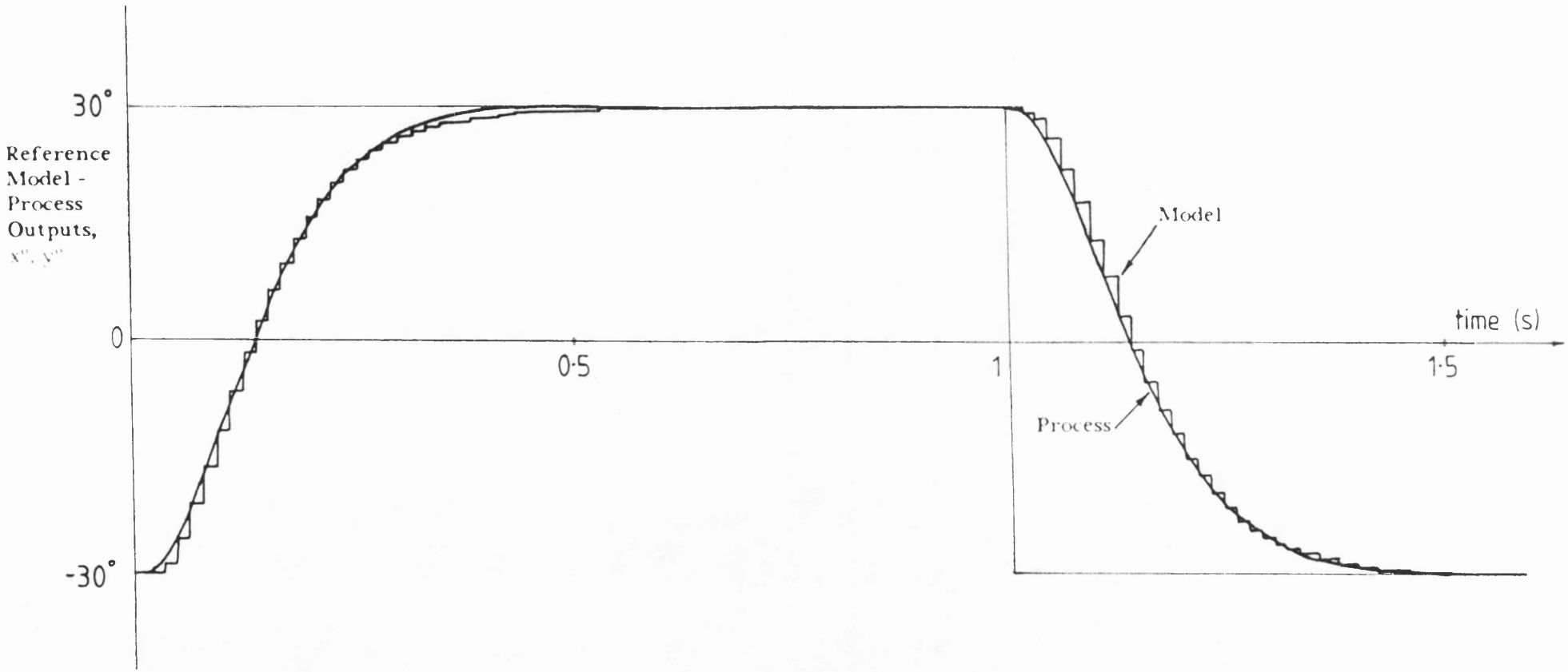

FIGURE 8:10 A Typical Example Of Model Following Behaviour

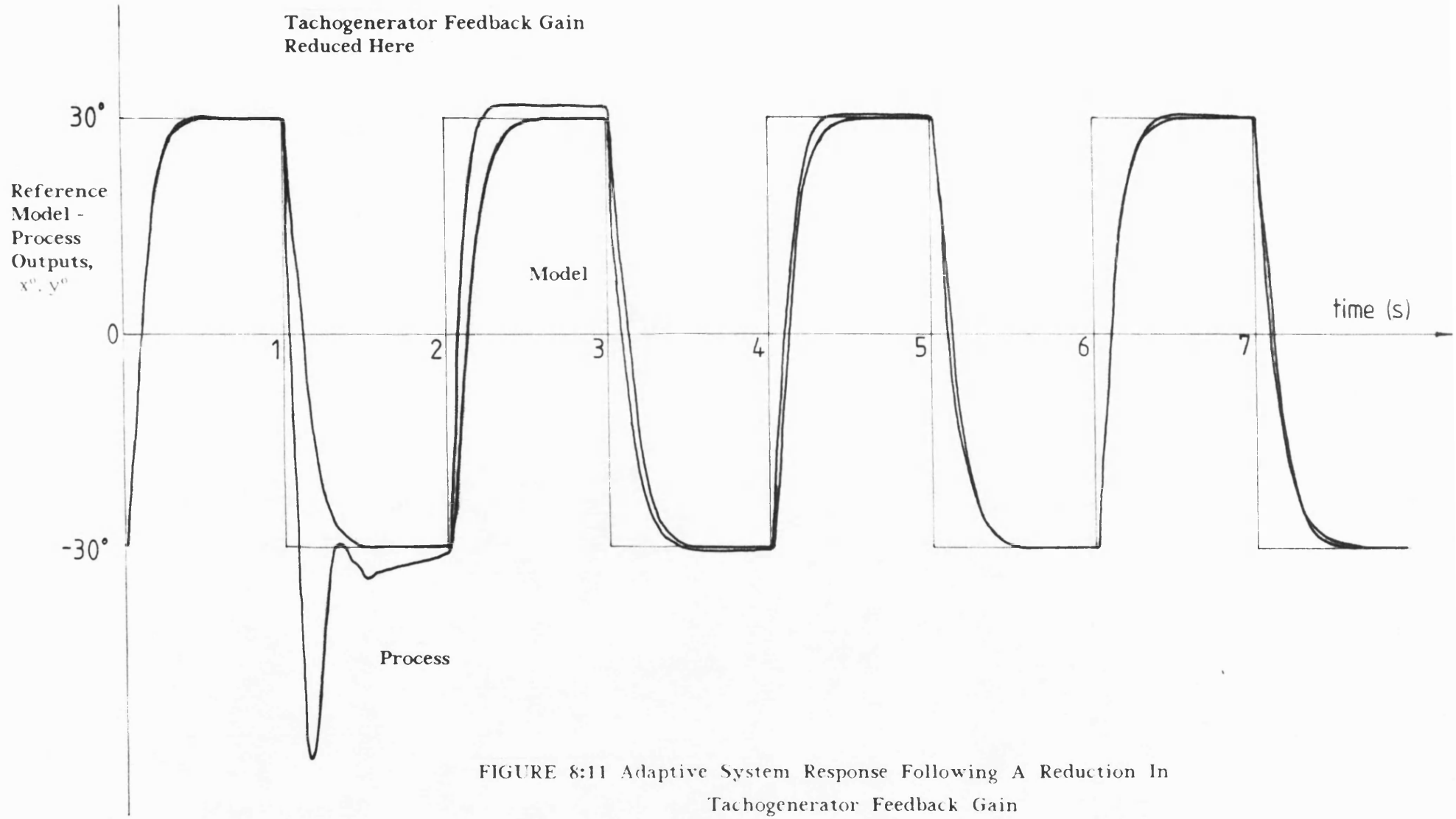

FIGURE 8:11 Adaptive System Response Following A Reduction In Tachogenerator Feedback Gain

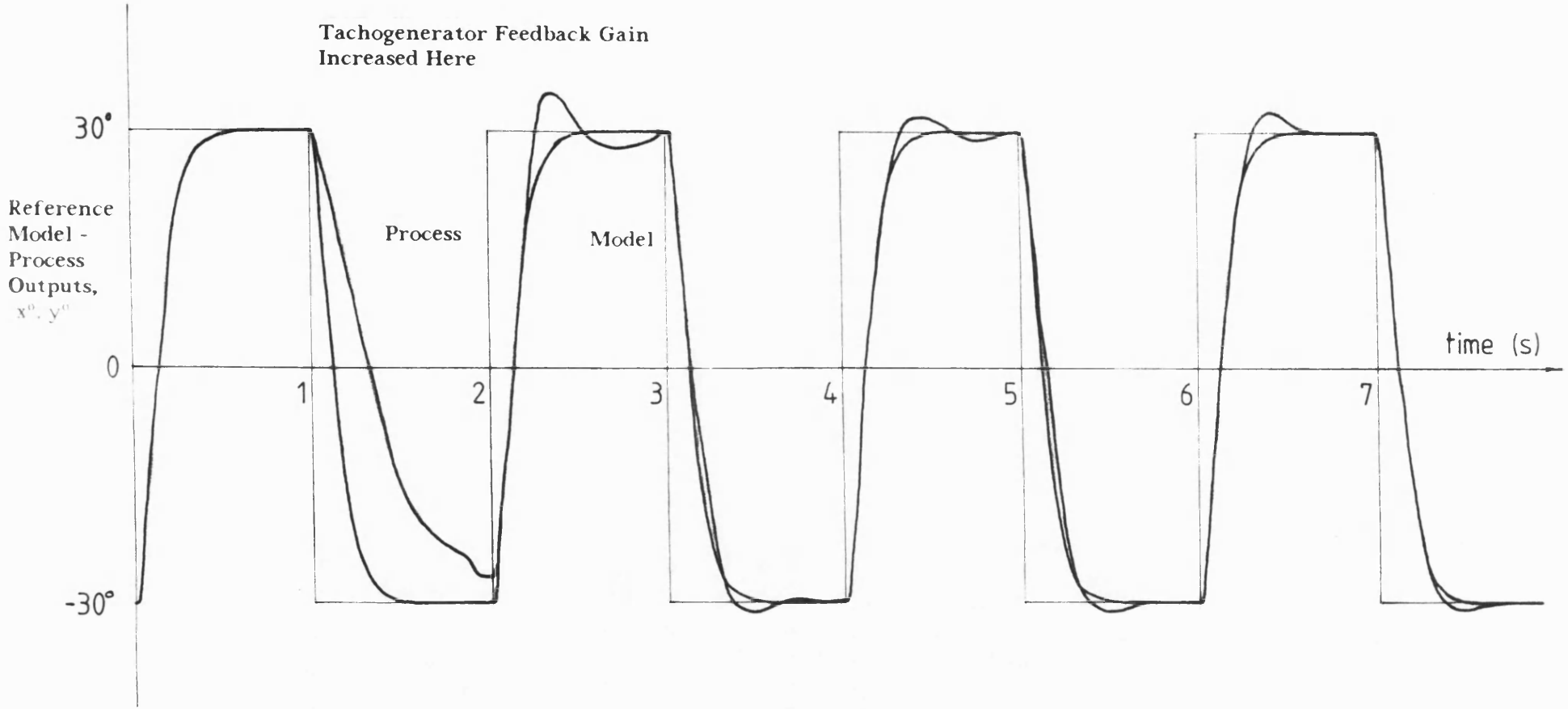

FIGURE 8:12 Adaptive System Response Following An Increase In Tachogenerator Feedback Gain

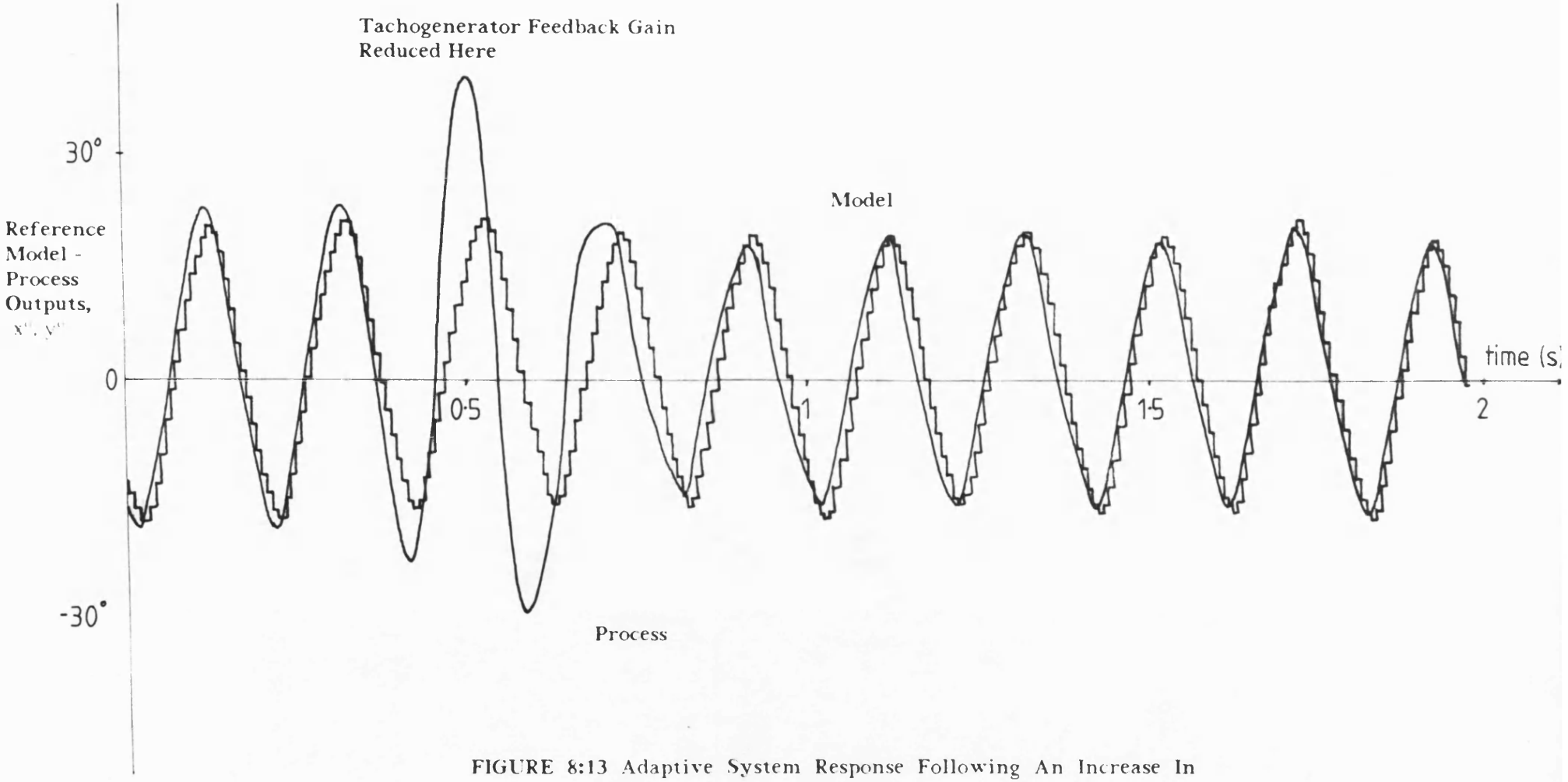

FIGURE 8:13 Adaptive System Response Following An Increase In Tachogenerator Feedback Gain
(5 Hz. Square Wave Command Signal)

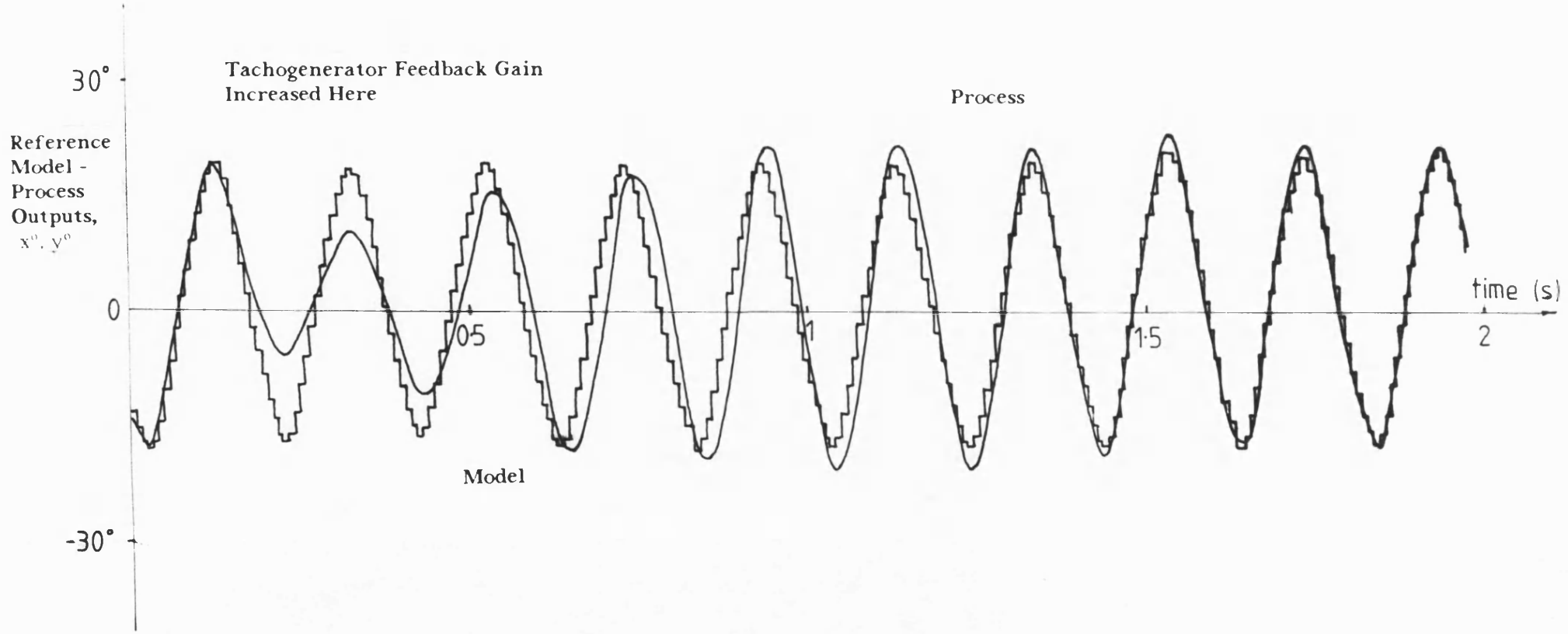

FIGURE 8:14 Adaptive System Response Following A Reduction In Tachogenerator Feedback Gain (5 Hz. Square Wave Command Signal)

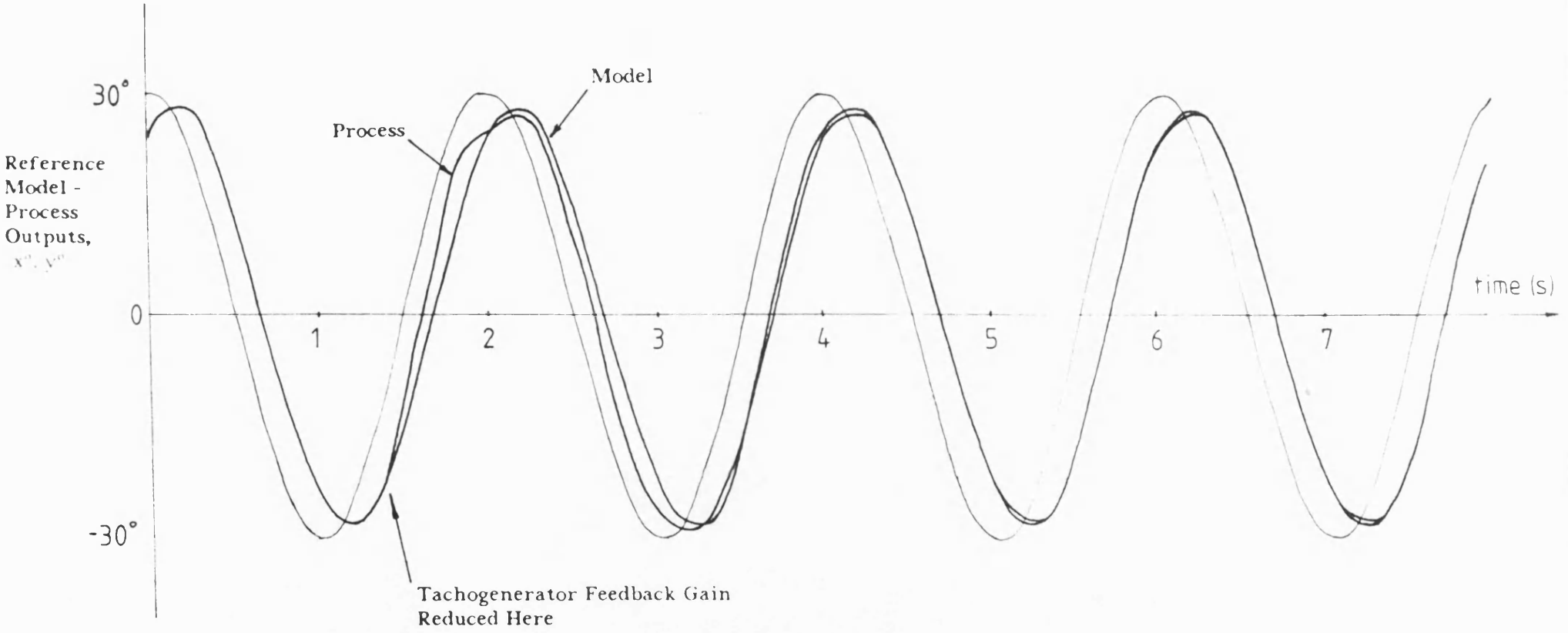

FIGURE 8:15 Adaptive System Response Following A Reduction In Tachogenerator Feedback Gain (Sinusoidal Command Signal)

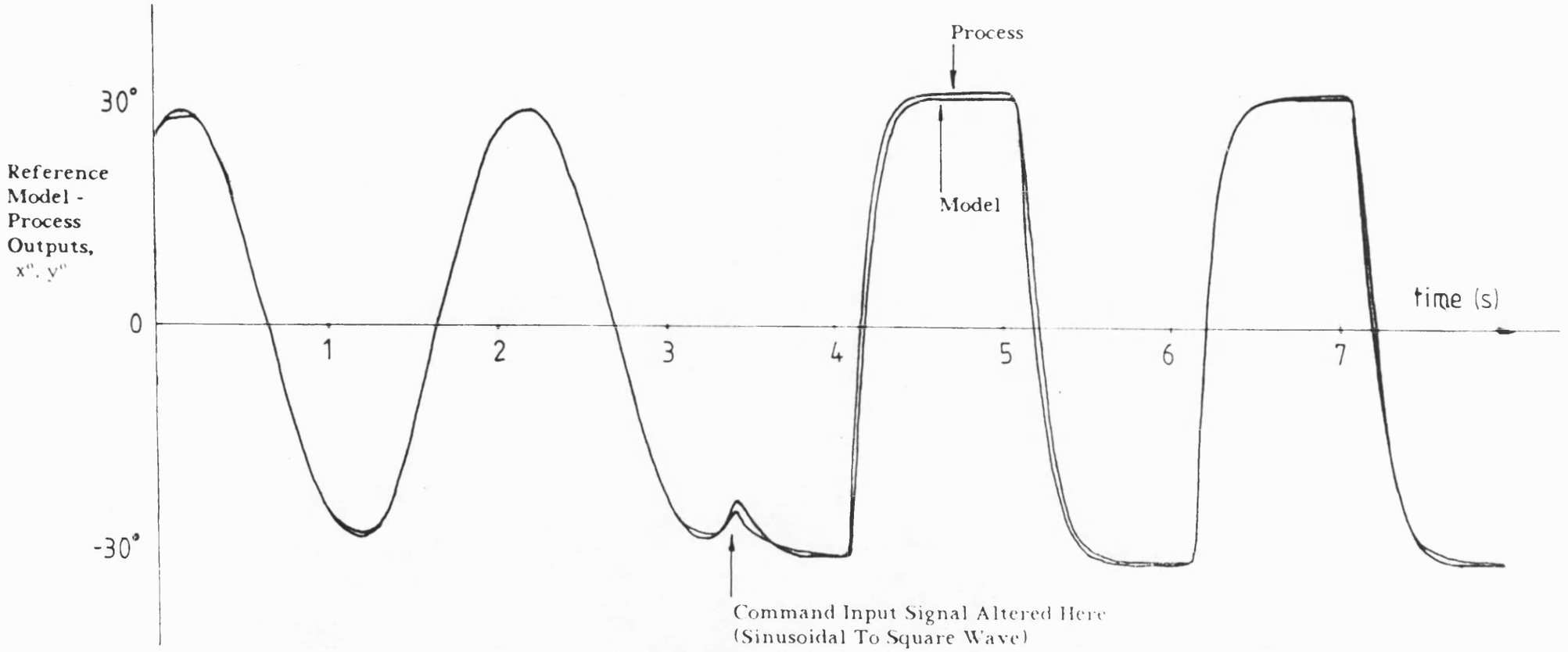

FIGURE 8:16 Adaptive System Behaviour For Different Waveform Command Signals

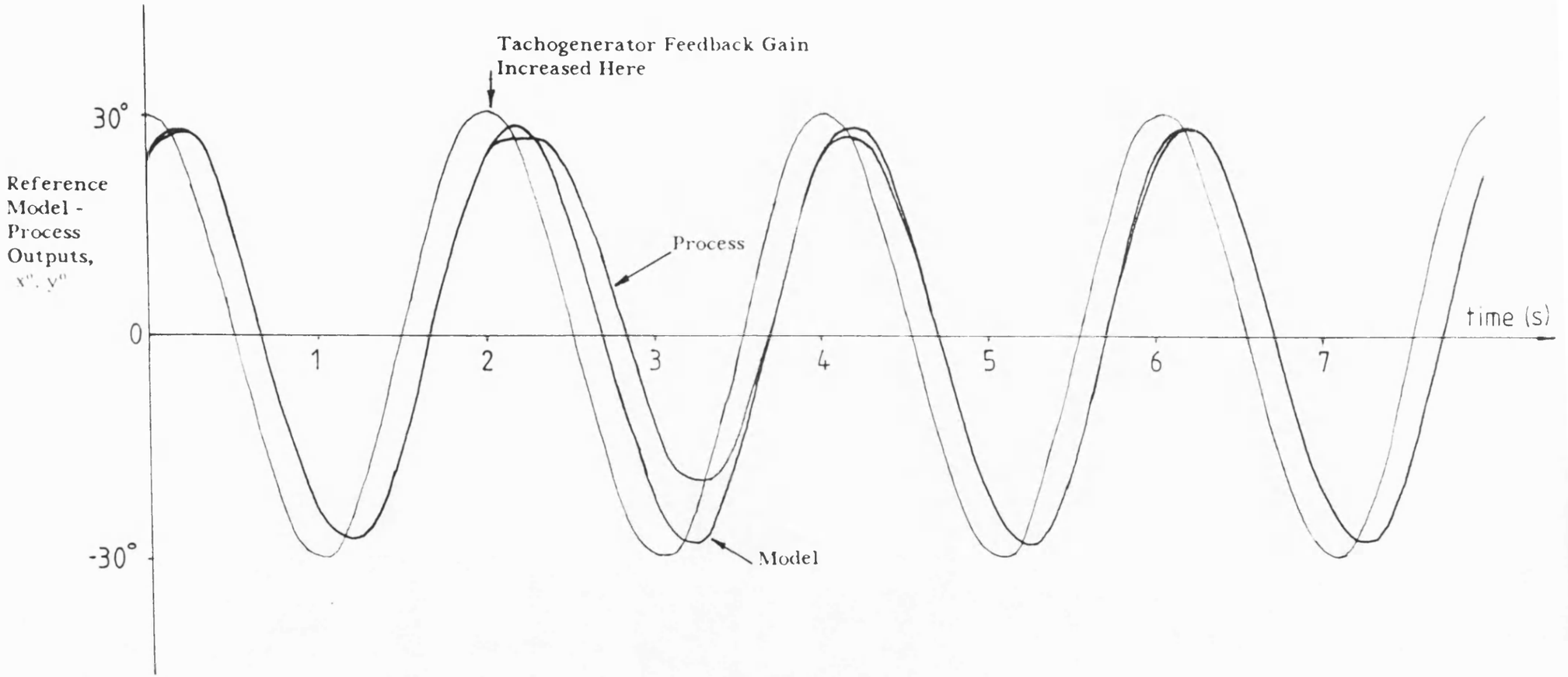

FIGURE 8:17 Adaptive System Response Following An Increase In Tachogenerator Feedback Gain (Sinusoidal Command Signal)

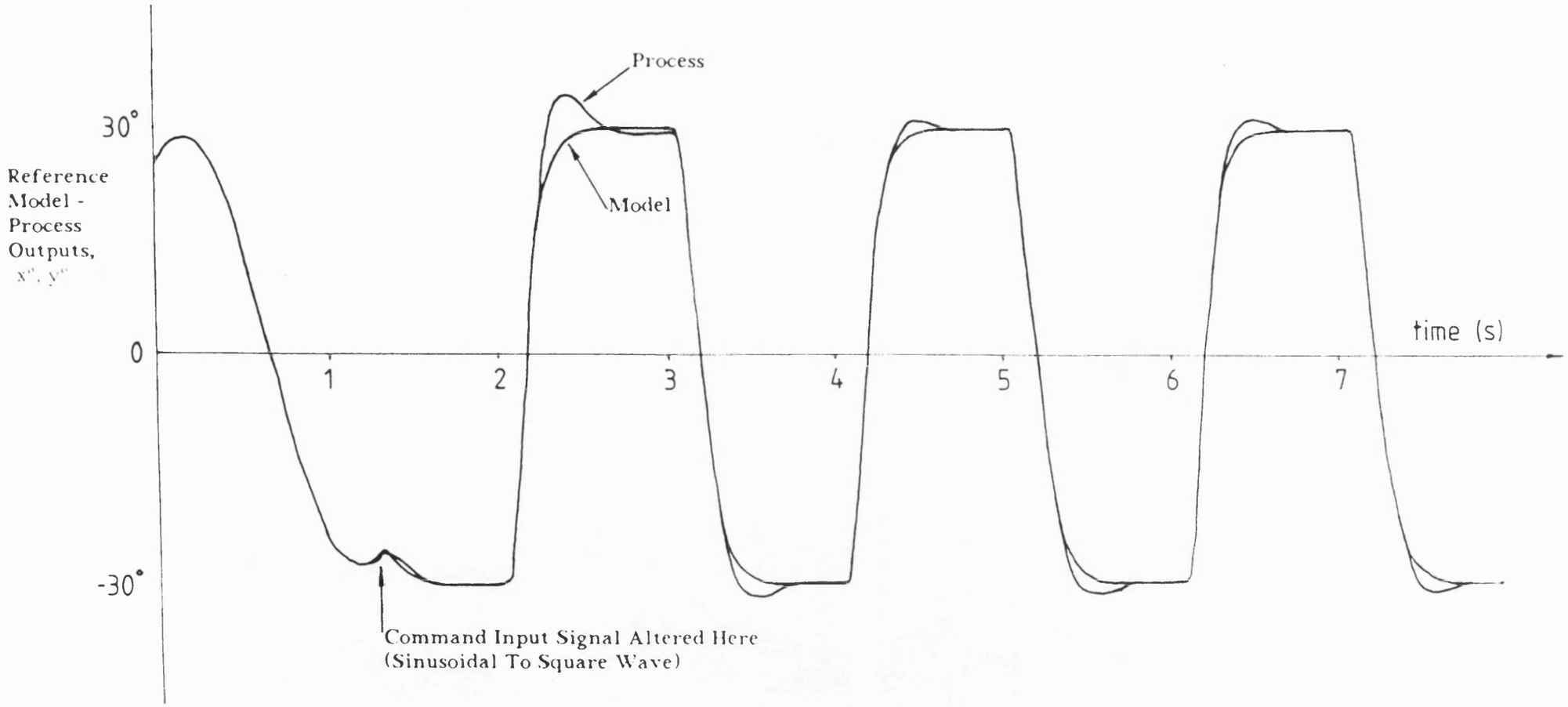

FIGURE 8:18 Adaptive System Behaviour For Different Waveform Command Signals

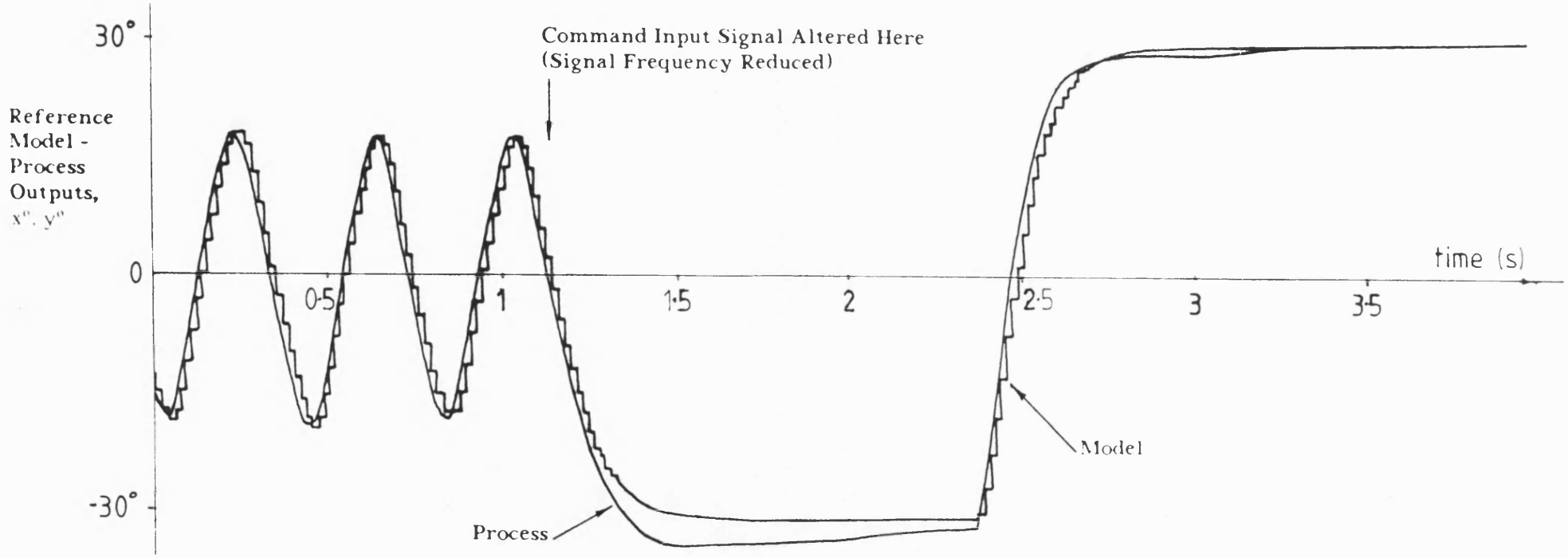

FIGURE 8:19 Adaptive System Behaviour For Different Frequency Command Signals

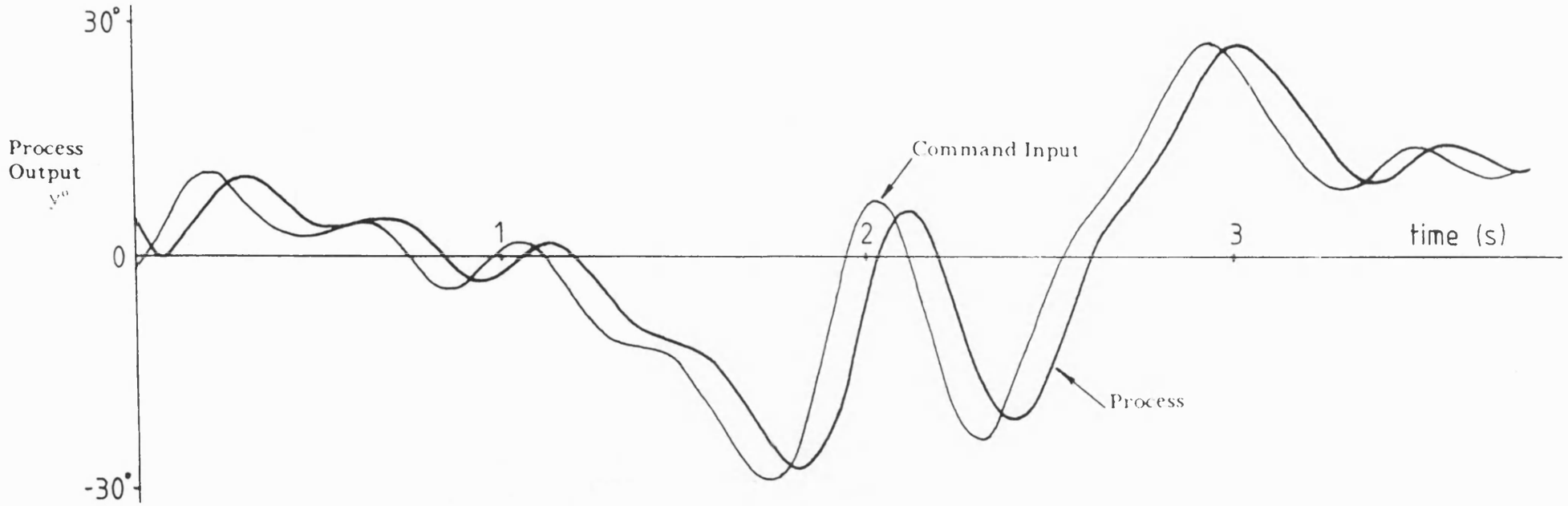

FIGURE 8:20 A Typical Example Of Control System Behaviour
With A P.R.B.S. Command Signal

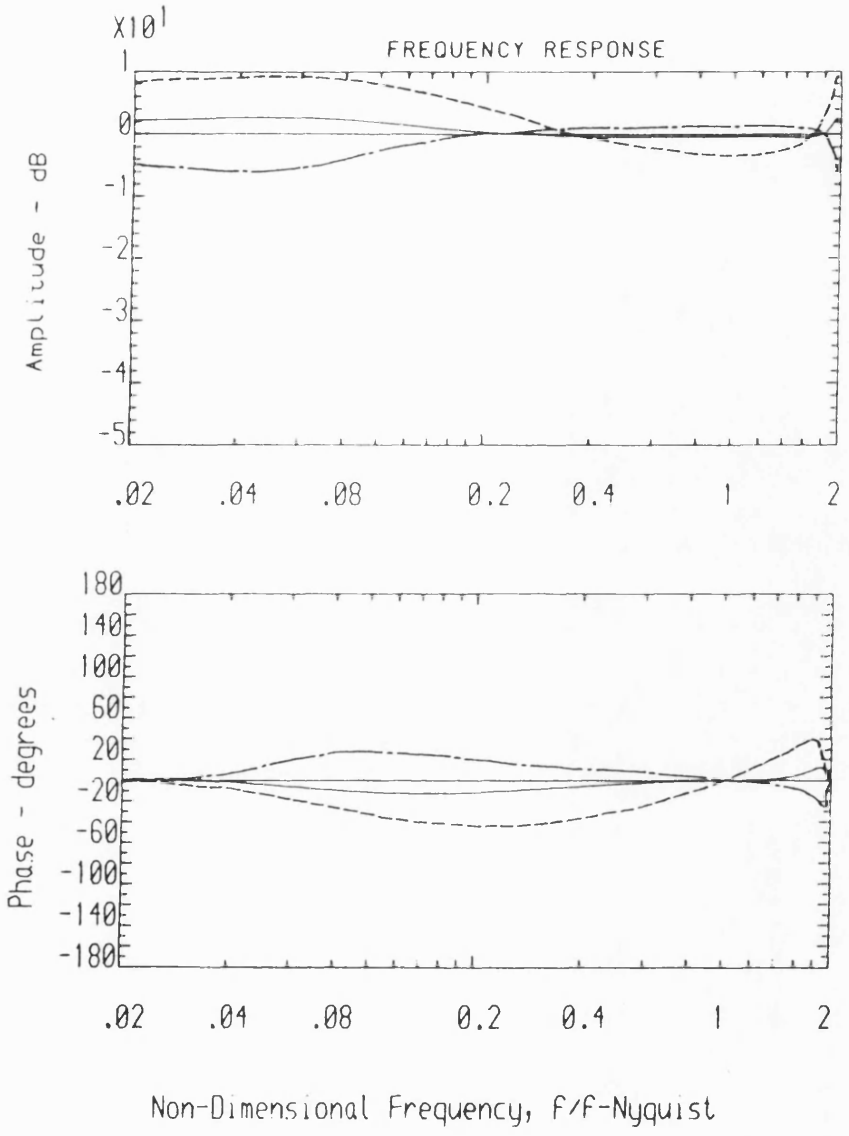

FIGURE 8:21 Frequency Response Characteristics Of S.P.R. Transfer Functions With Different Error Filter Coefficients

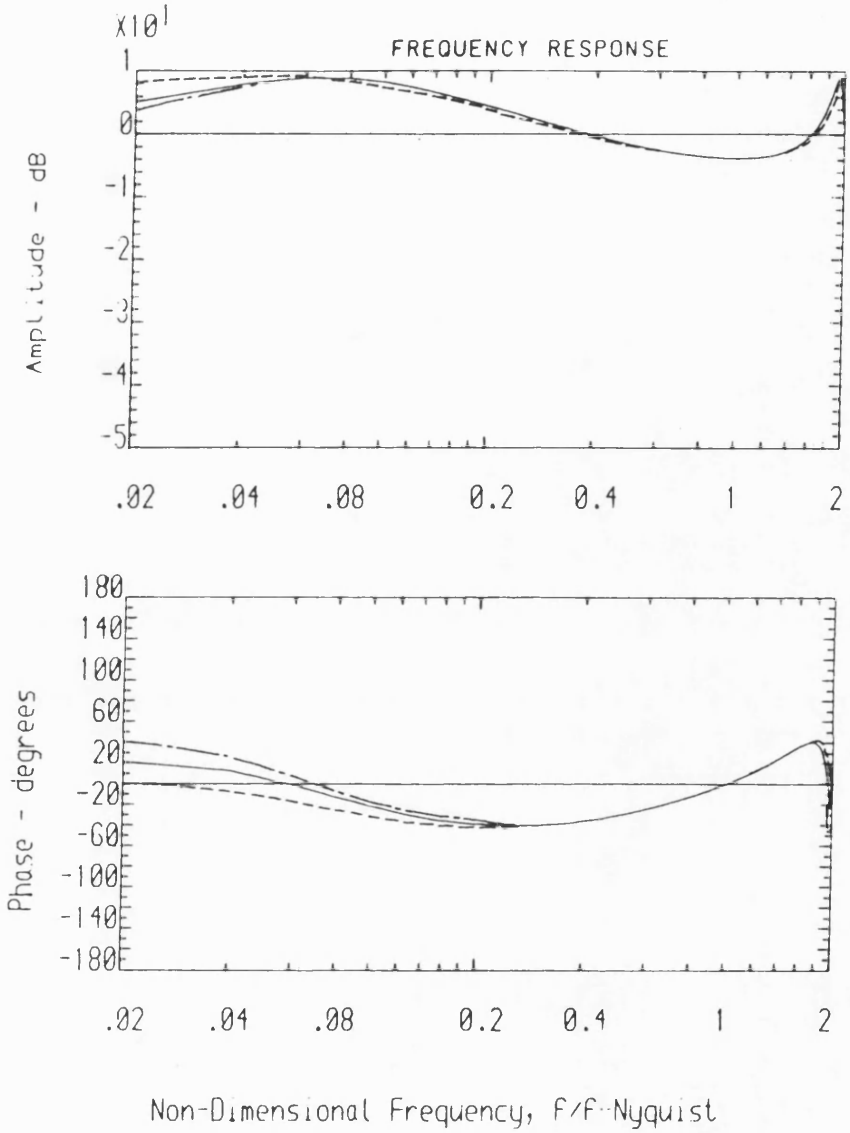

-------- S3 Pairing $c_1 = -1{\cdot}0$, $c_2 = 0{\cdot}1$

——·—— S4 Pairing $c_1 = -1{\cdot}0$, $c_2 = 0{\cdot}025$

———— S5 Pairing $c_1 = -1{\cdot}0$, $c_2 = 0{\cdot}05$

FIGURE 8:22 Frequency Response Characteristics Of S.P.R. Transfer Functions With Different Error Filter Coefficients

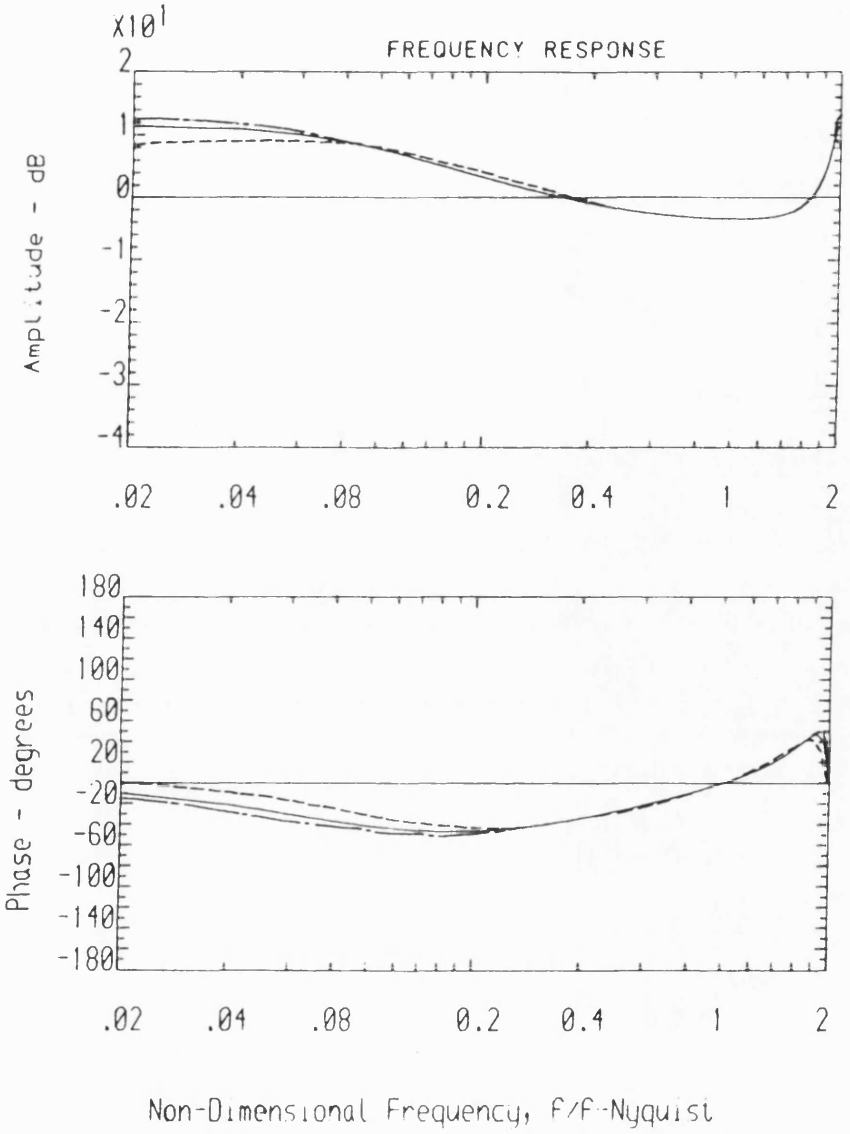

---------- S3 Pairing $c_1 = -1{\cdot}0$, $c_2 = 0{\cdot}1$

——·—— S6 Pairing $c_1 = -1{\cdot}0$, $c_2 = 0{\cdot}175$

———— S7 Pairing $c_1 = -1{\cdot}0$, $c_2 = 0{\cdot}15$

FIGURE 8:23 Frequency Response Characteristics Of S.P.R. Transfer Functions With Different Error Filter Coefficients

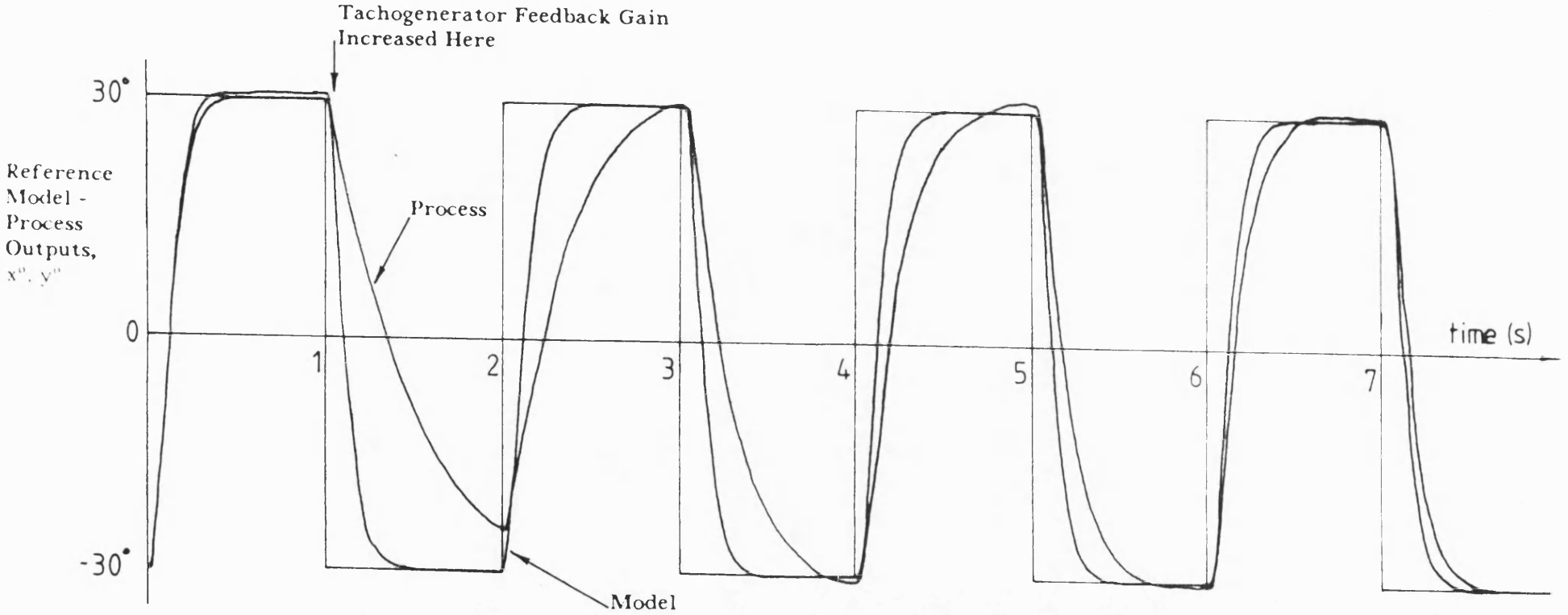

FIGURE 8:24 Adaptive System Behaviour For Error Filter Setting S1

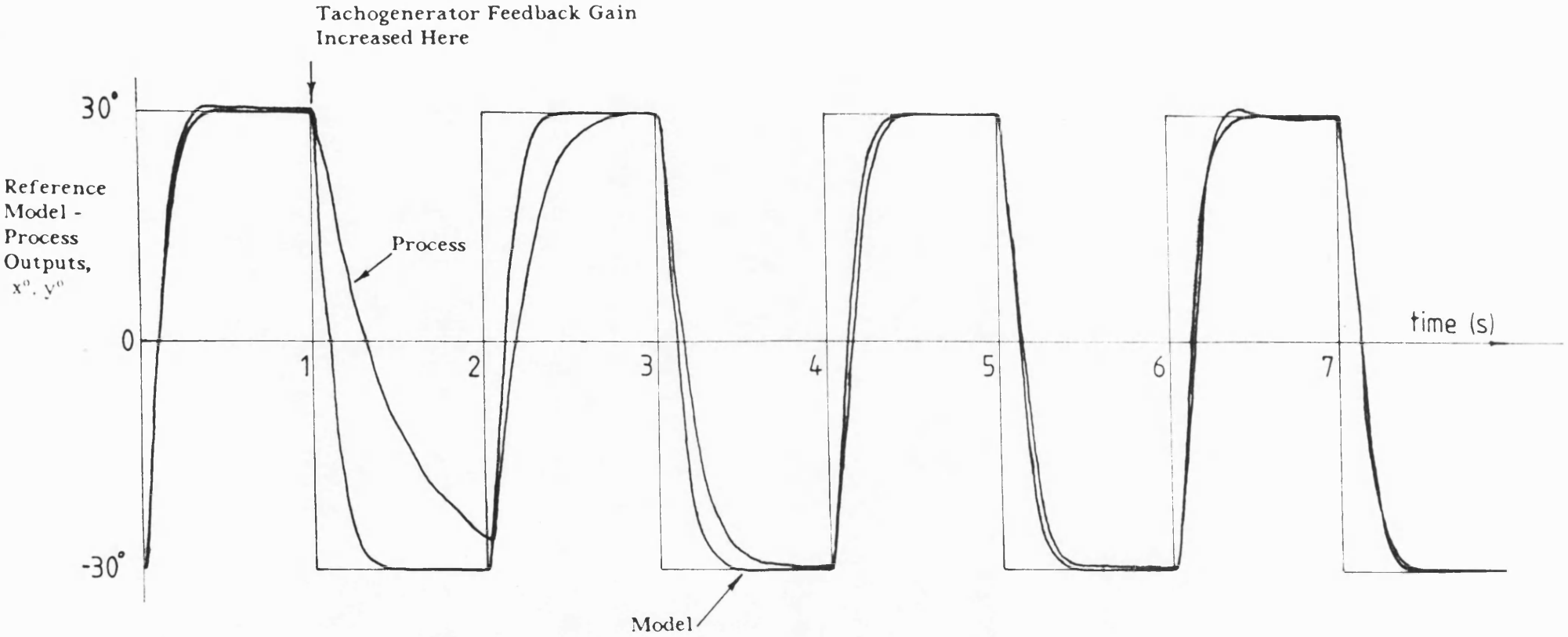

FIGURE 8:25 Adaptive System Behaviour For Error Filter Setting S2

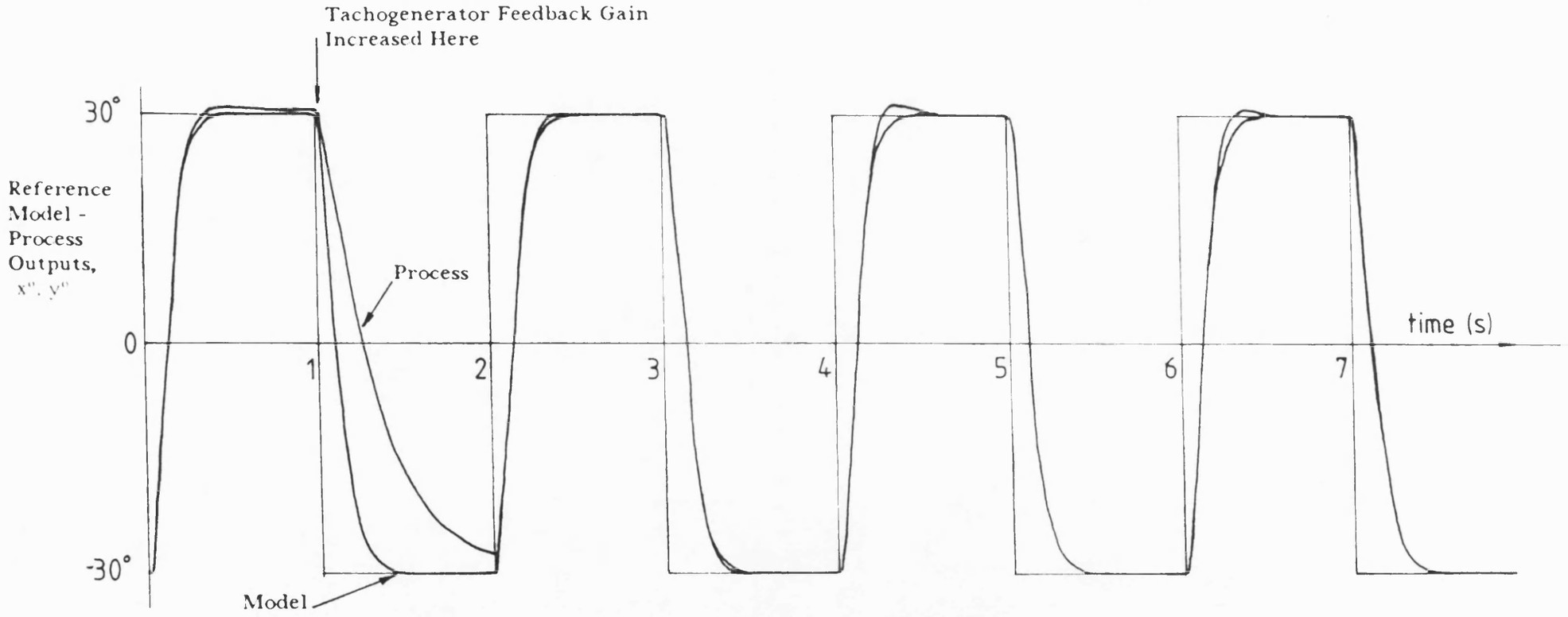

FIGURE 8:26 Adaptive System Behaviour For Error Filter Setting S3

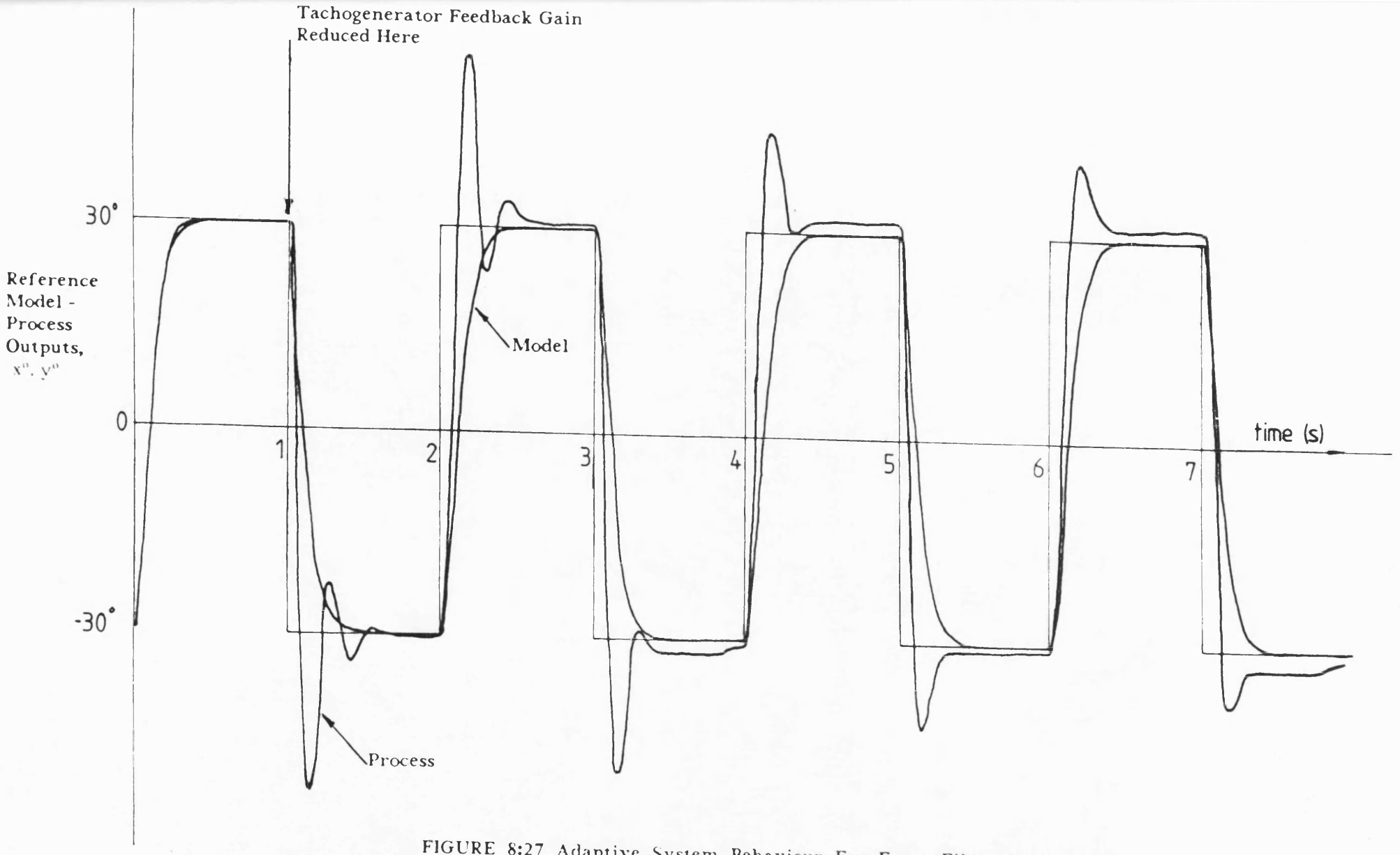

FIGURE 8:27 Adaptive System Behaviour For Error Filter Setting S1

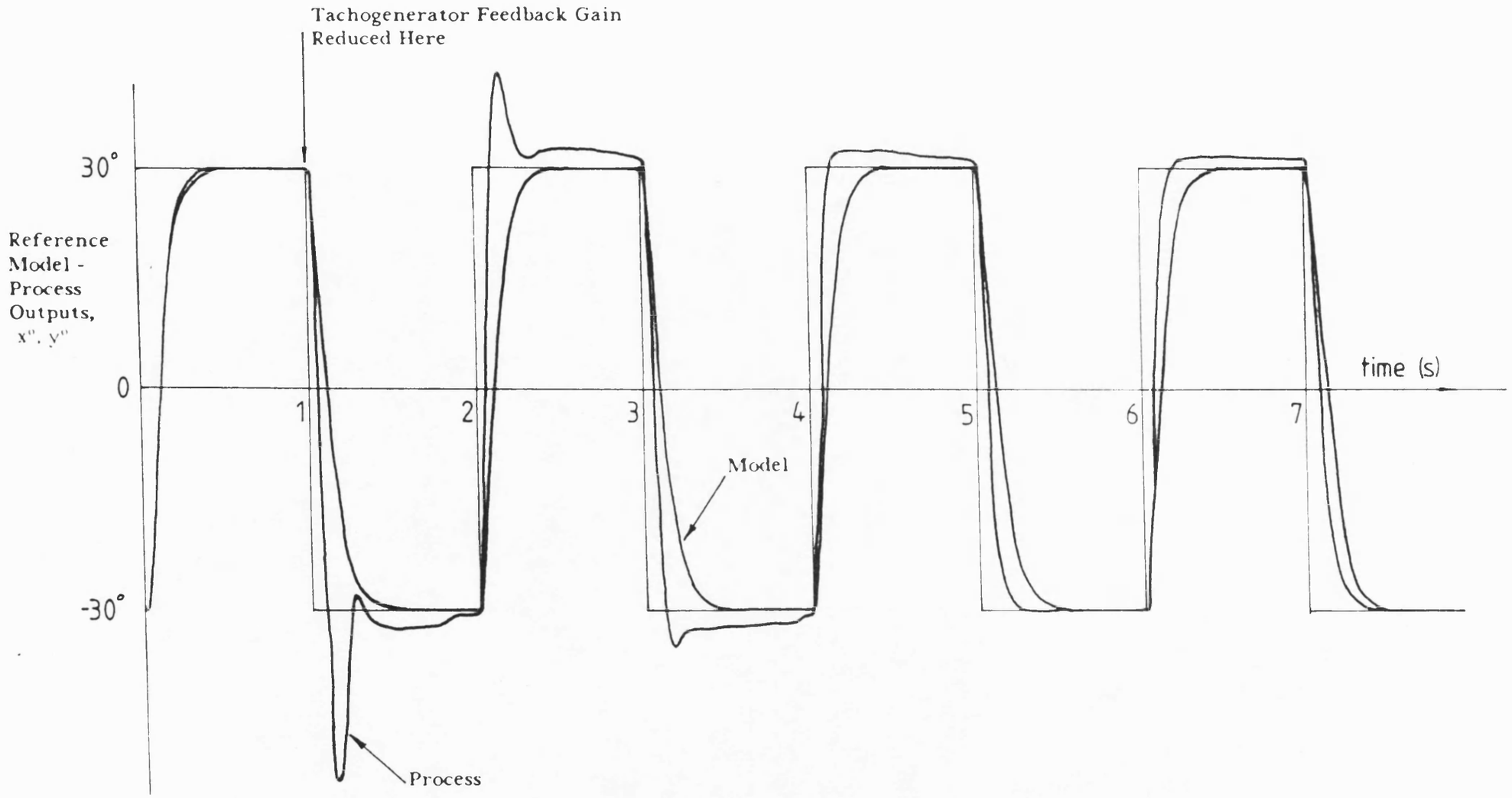

FIGURE 8:28 Adaptive System Behaviour For Error Filter Setting S2

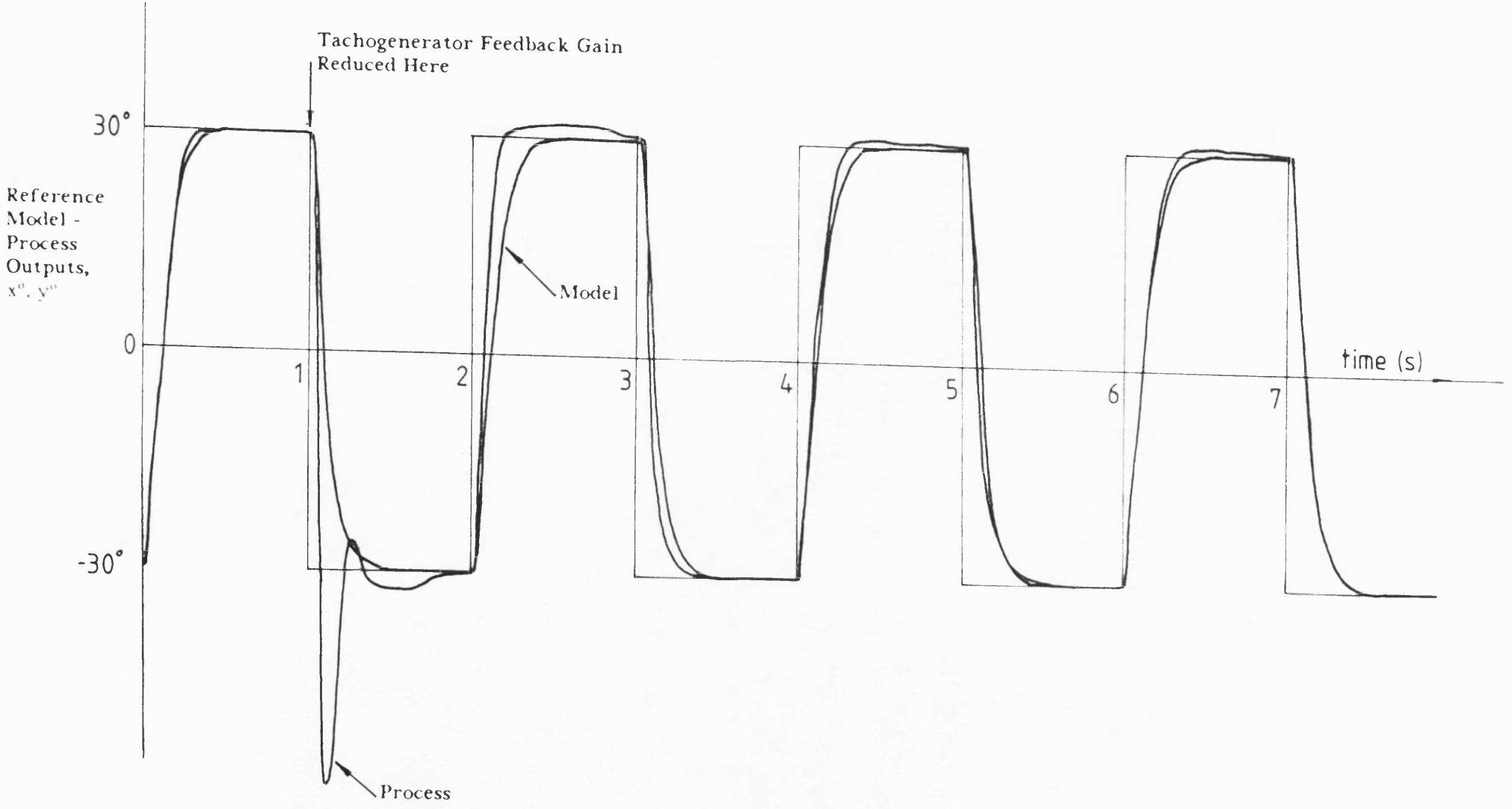

FIGURE 8:29 Adaptive System Behaviour For Error Filter Setting S3

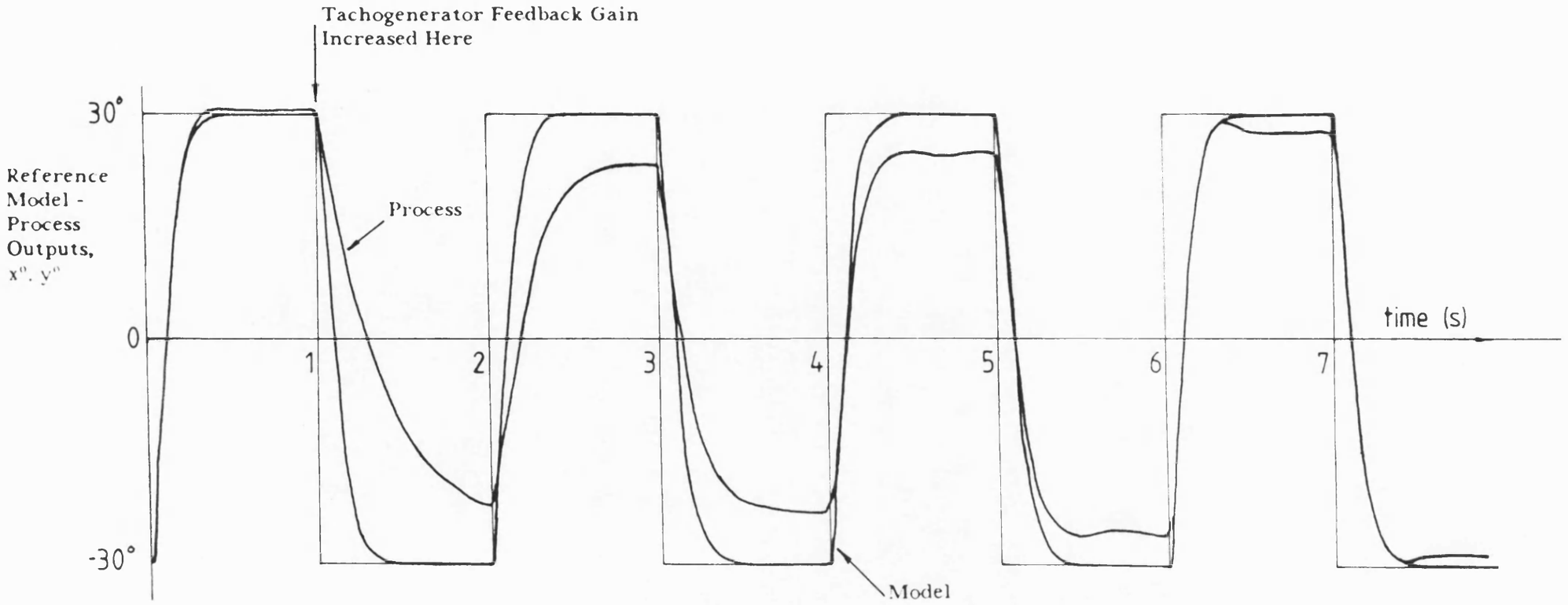

FIGURE 8:30 Adaptive System Behaviour For Error Filter Setting S4

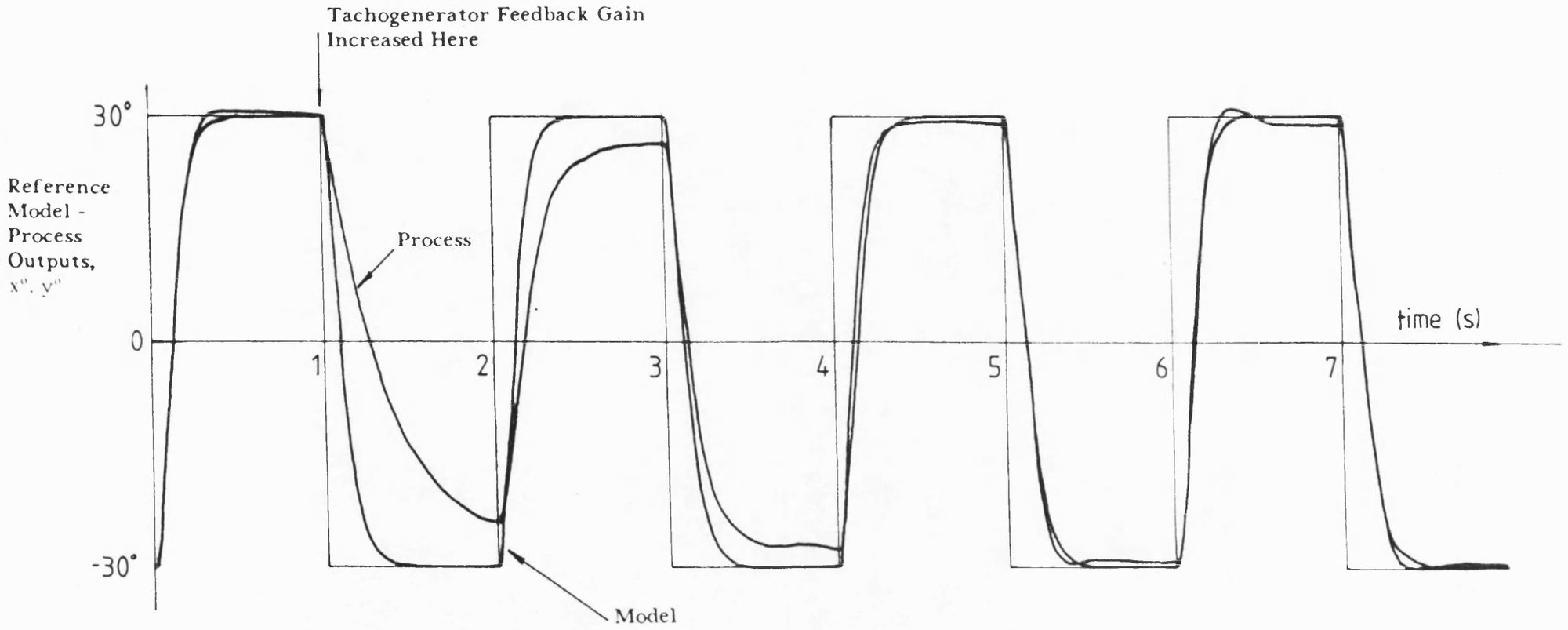

FIGURE 8:31 Adaptive System Behaviour For Error Filter Setting S5

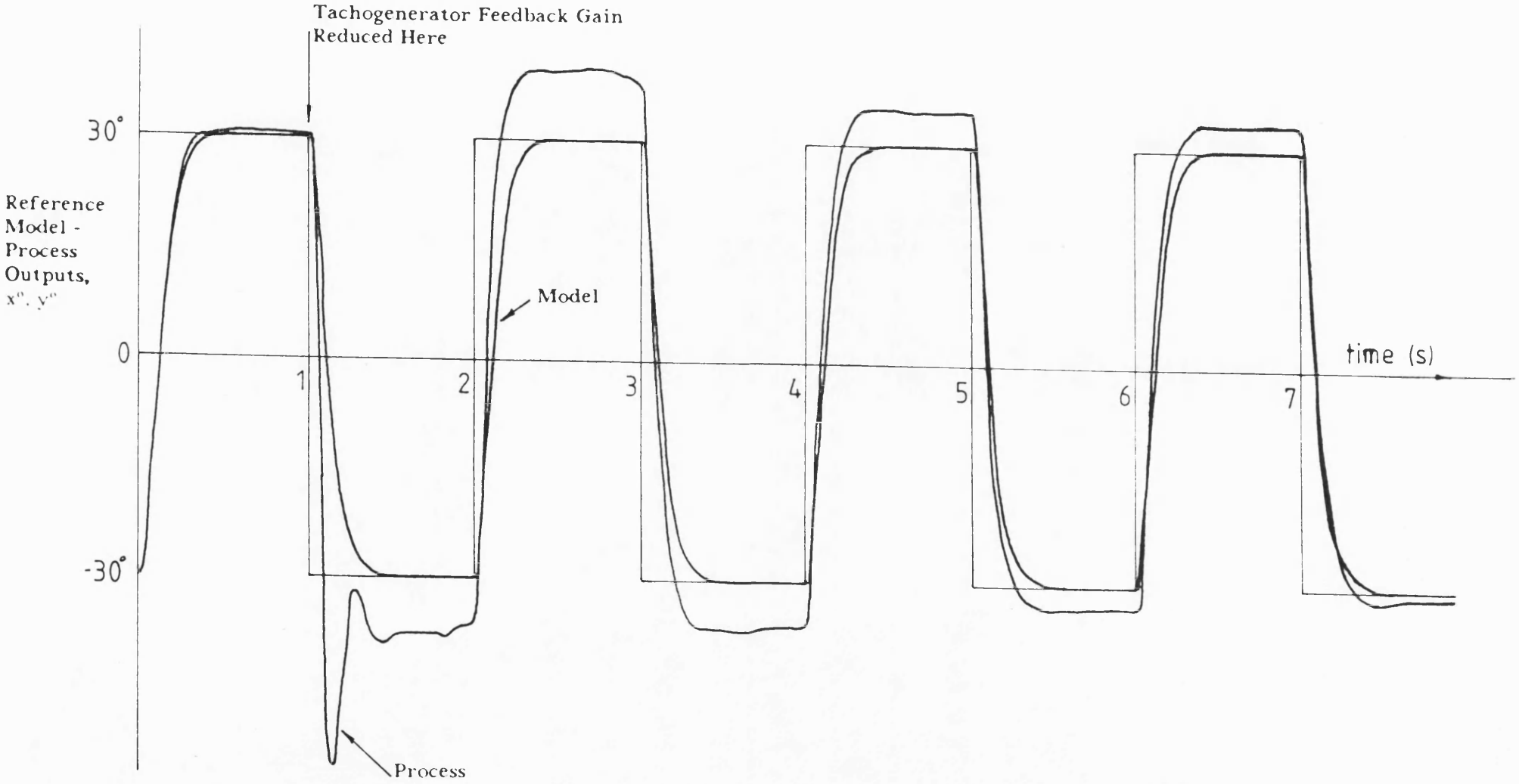

FIGURE 8:32 Adaptive System Behaviour For Error Filter Setting S4

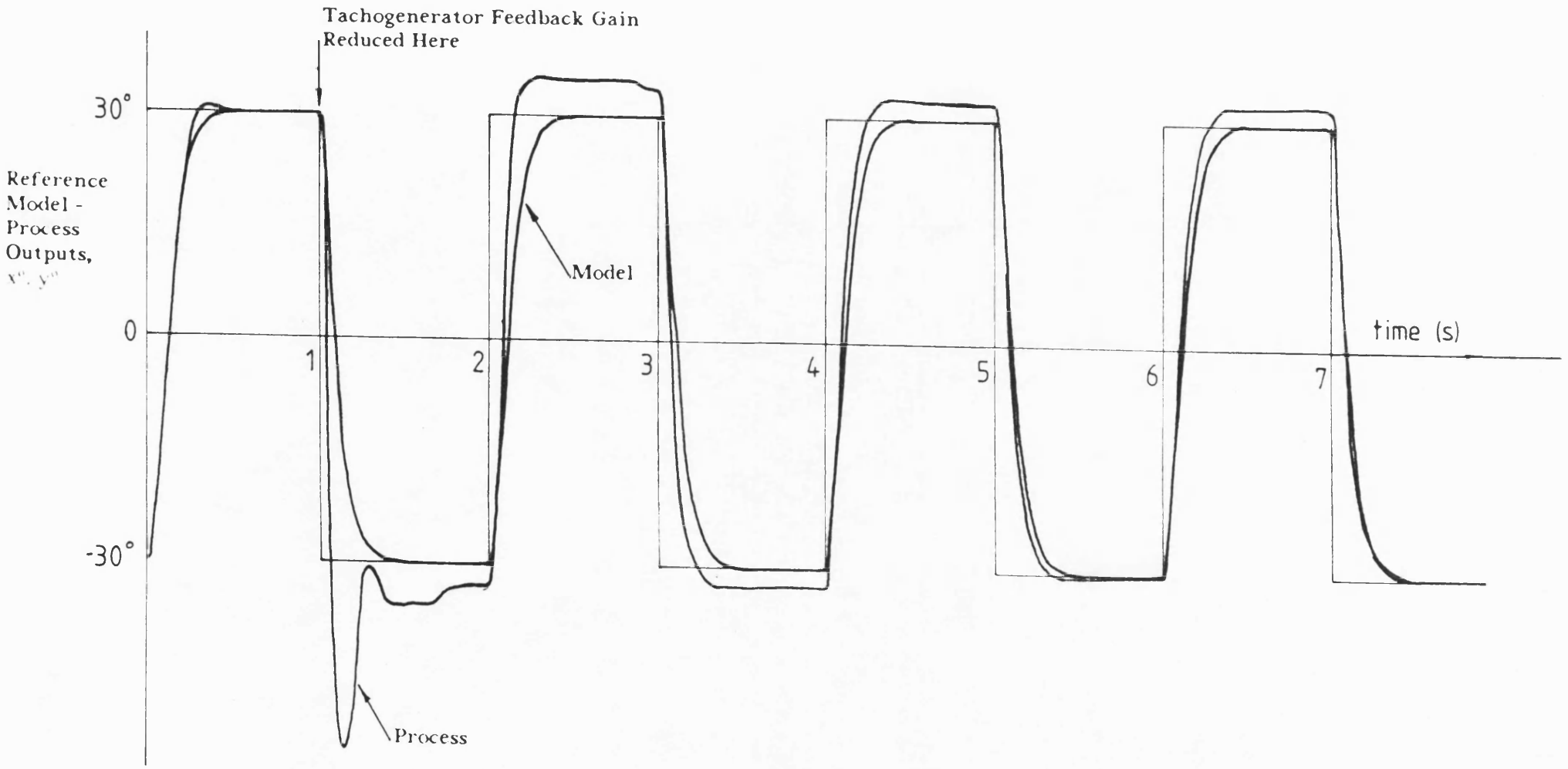

FIGURE 8:33 Adaptive System Behaviour For Error Filter Setting S5

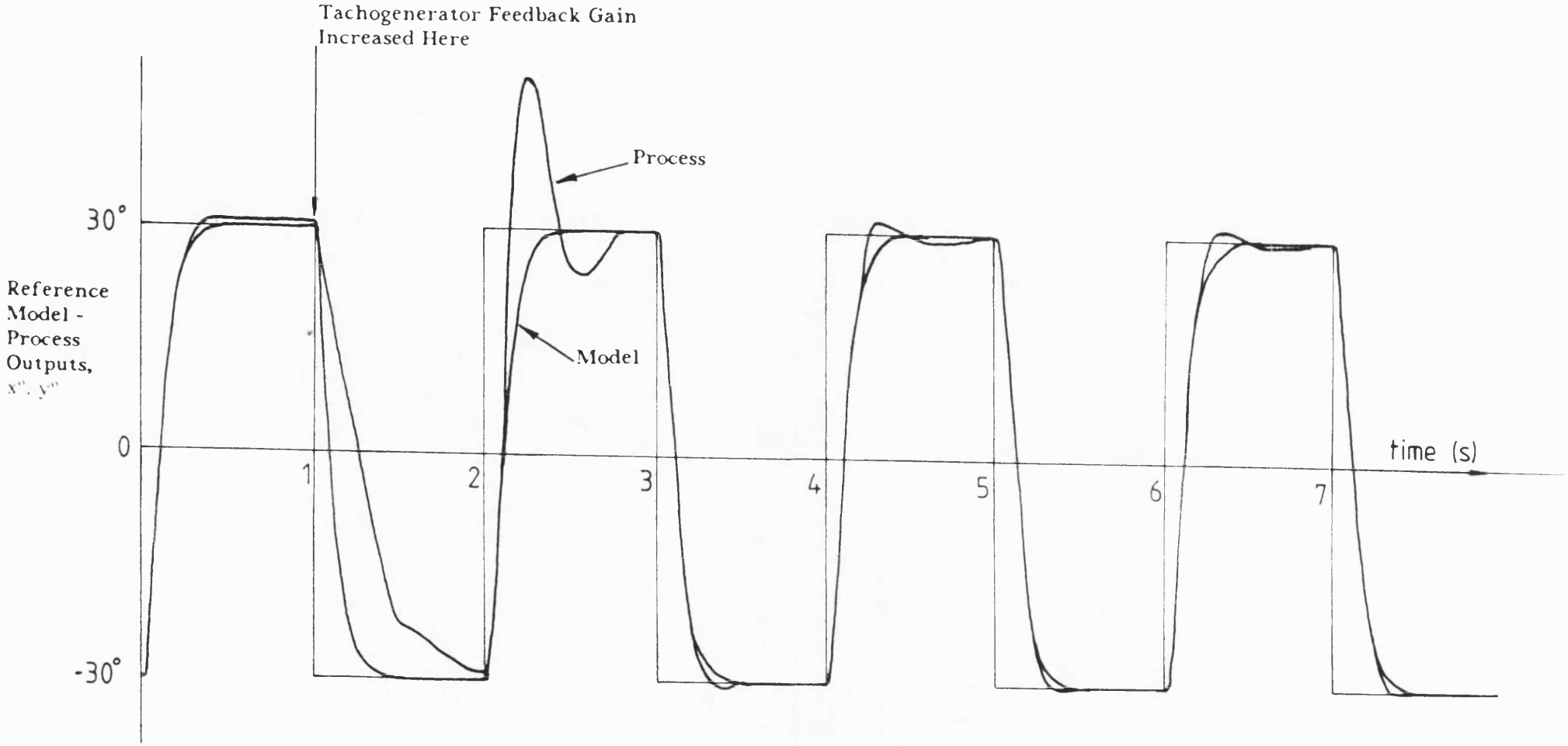

FIGURE 8:34 Adaptive System Behaviour For Error Filter Setting S6

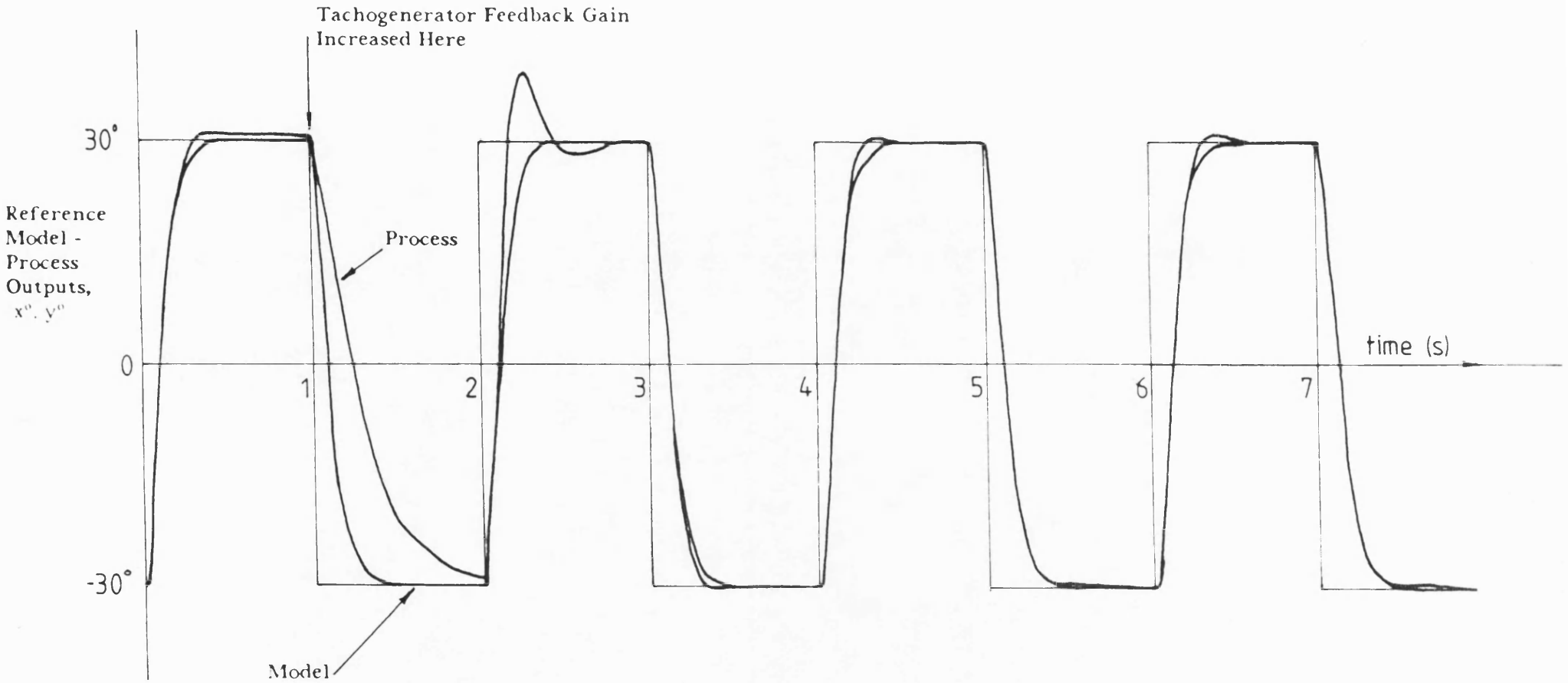

FIGURE 8:35 Adaptive System Behaviour For Error Filter Setting S7

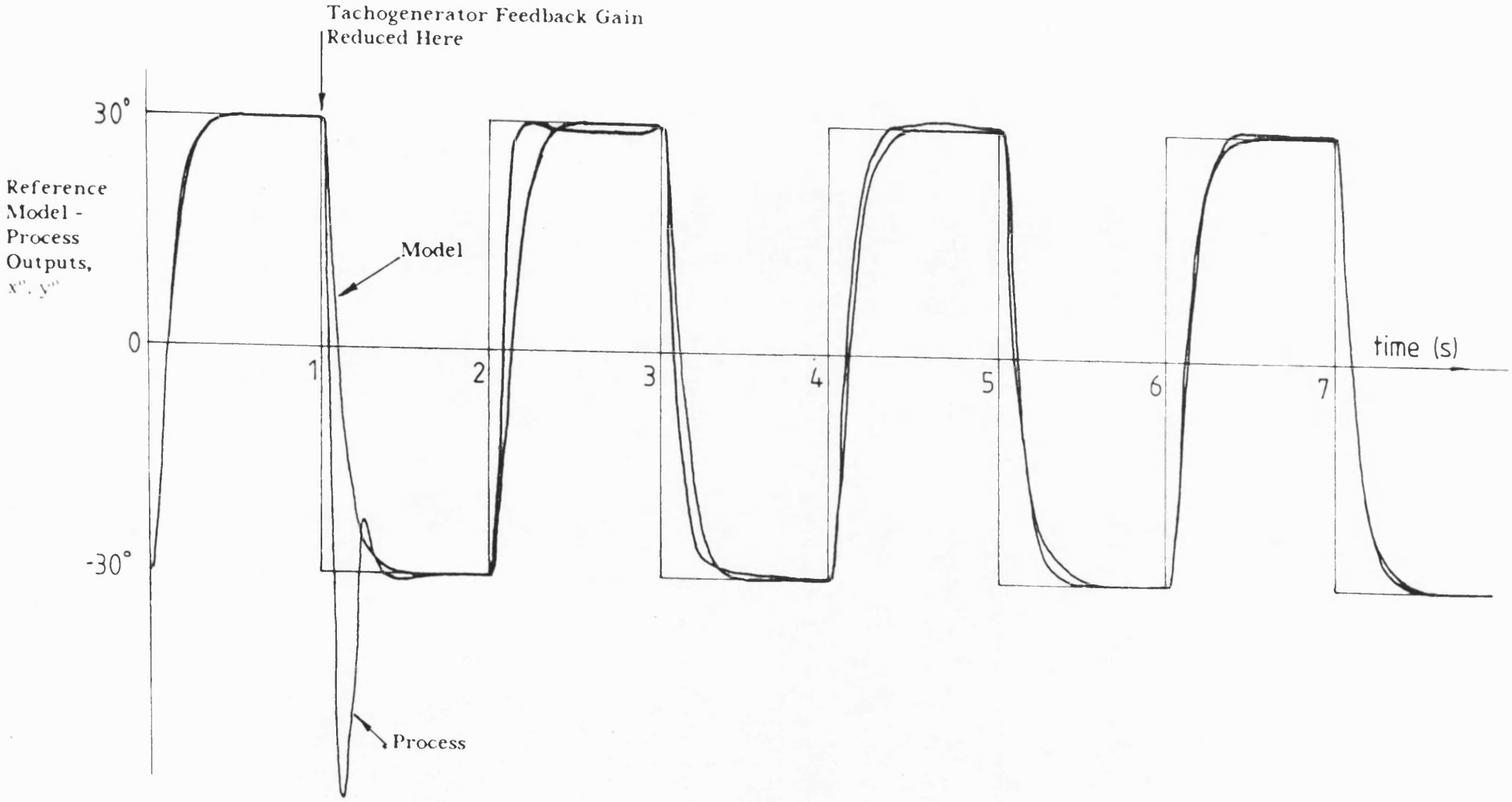

FIGURE 8:36 Adaptive System Behaviour For Error Filter Setting S6

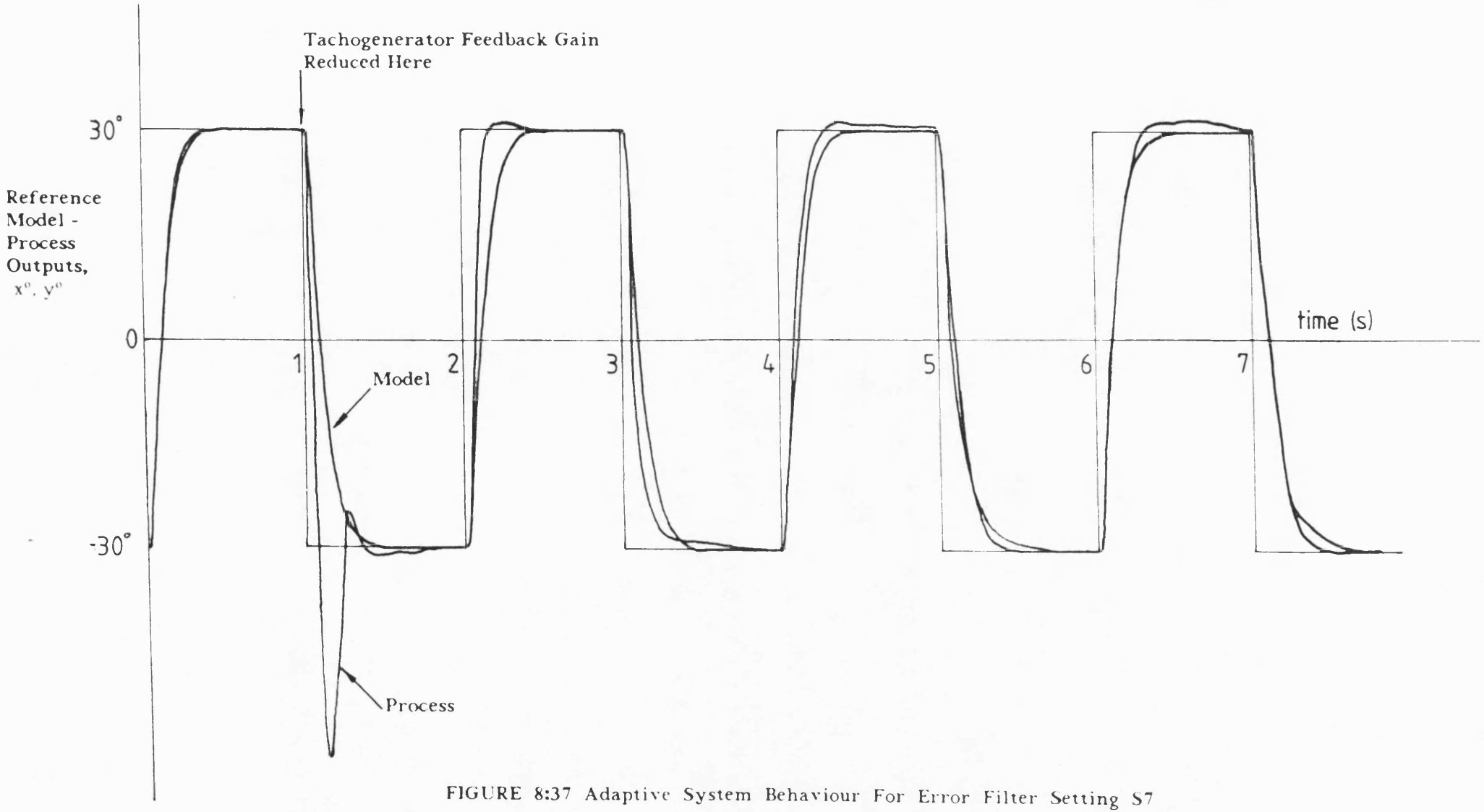

FIGURE 8:37 Adaptive System Behaviour For Error Filter Setting S7

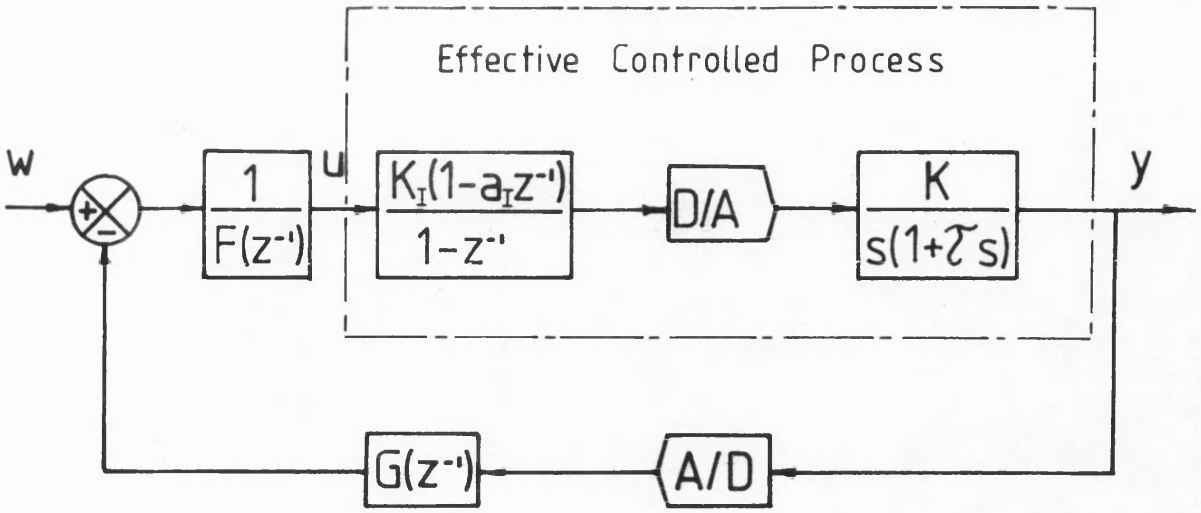

FIGURE 8:38 D.C. Servosystem Integral Action Closed Loop Control Scheme

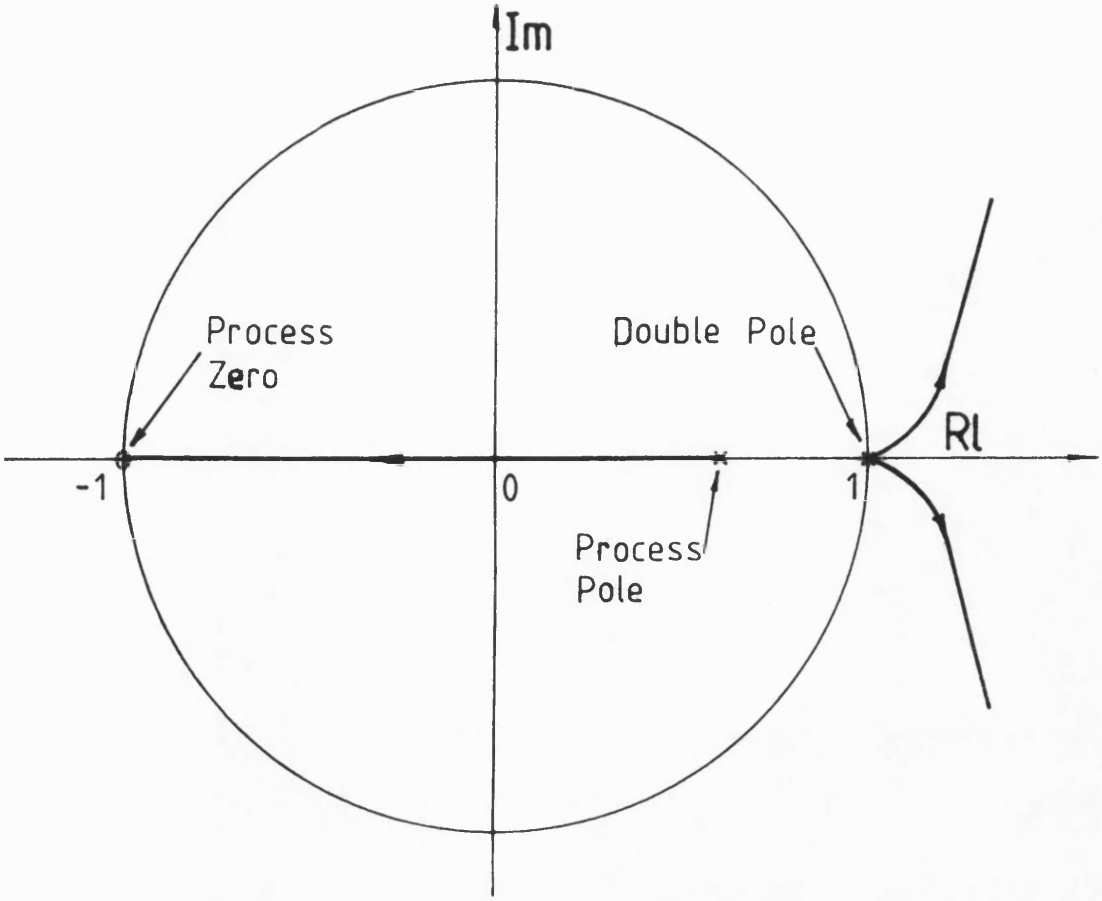

FIGURE 8:39 Root Locus Diagram For A Simple Integral Action Controller

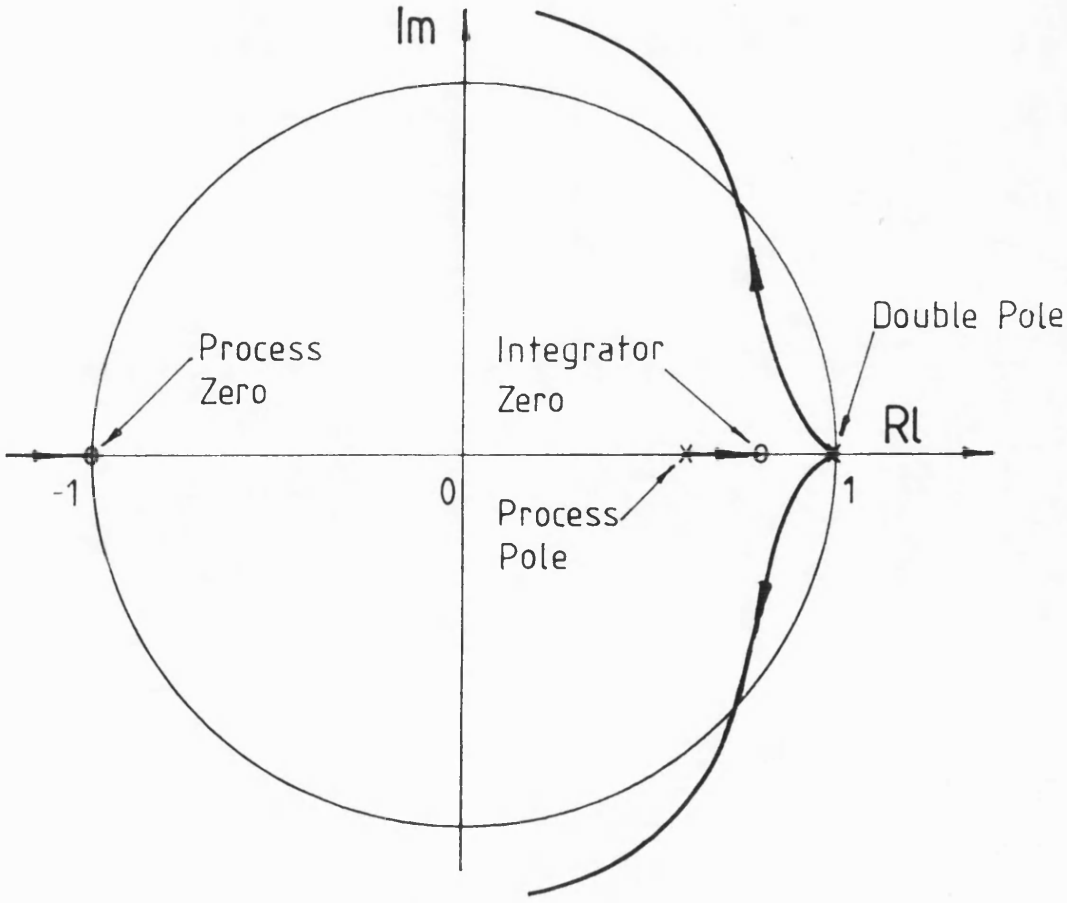

FIGURE 8:40 Modified Root Locus Diagram Incorporating A Zero Associated With The Integral Action Controller

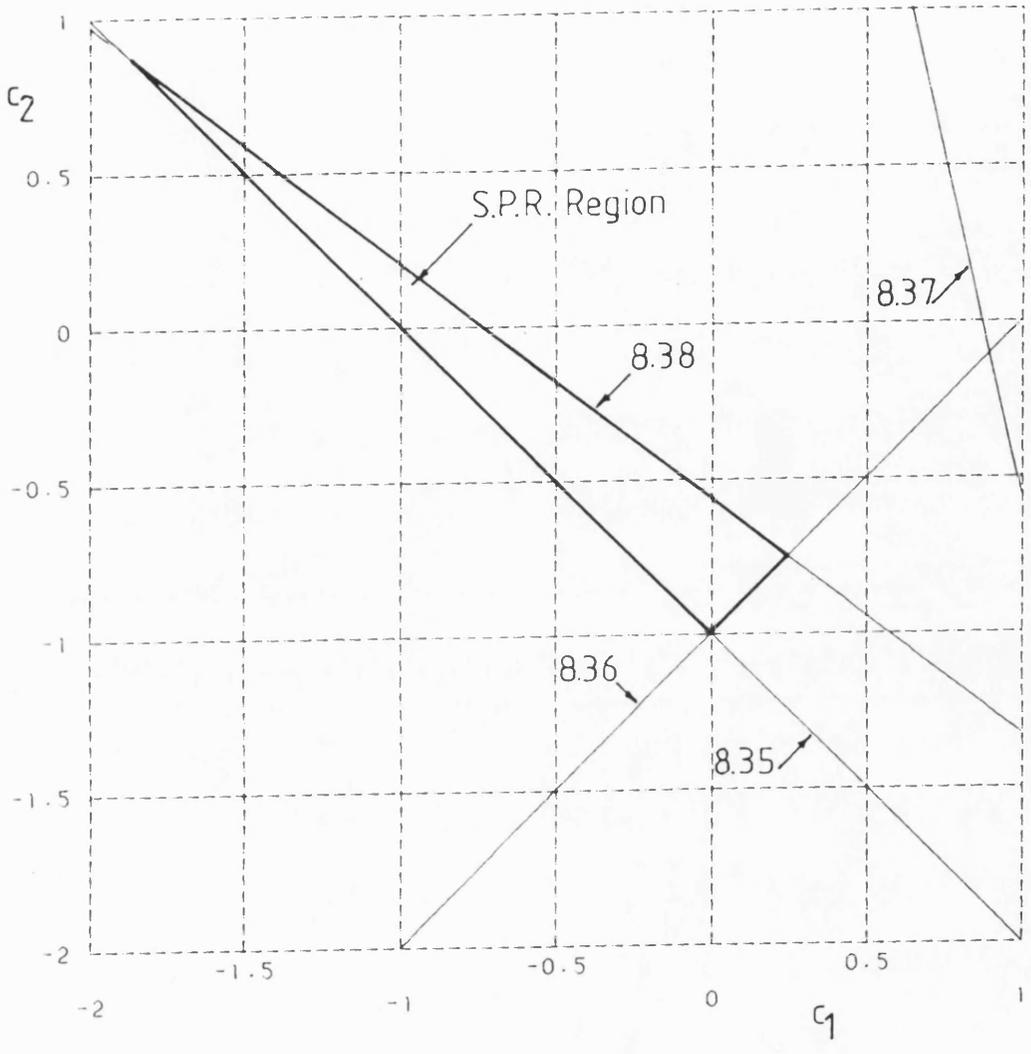

FIGURE 8:41 c_1–c_2 Parameter Space Satisfying S.P.R. Condition

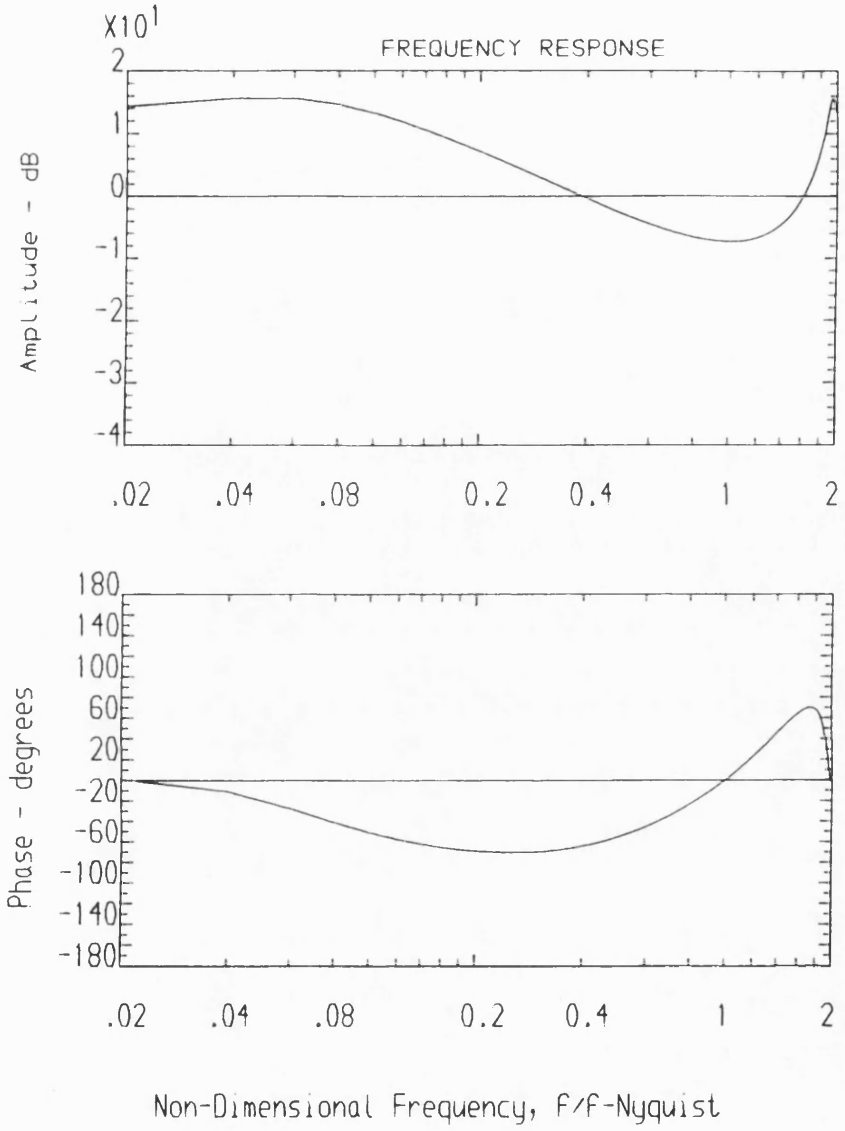

FIGURE 8:42 S.P.R. Transfer Function Frequency Response Characteristics

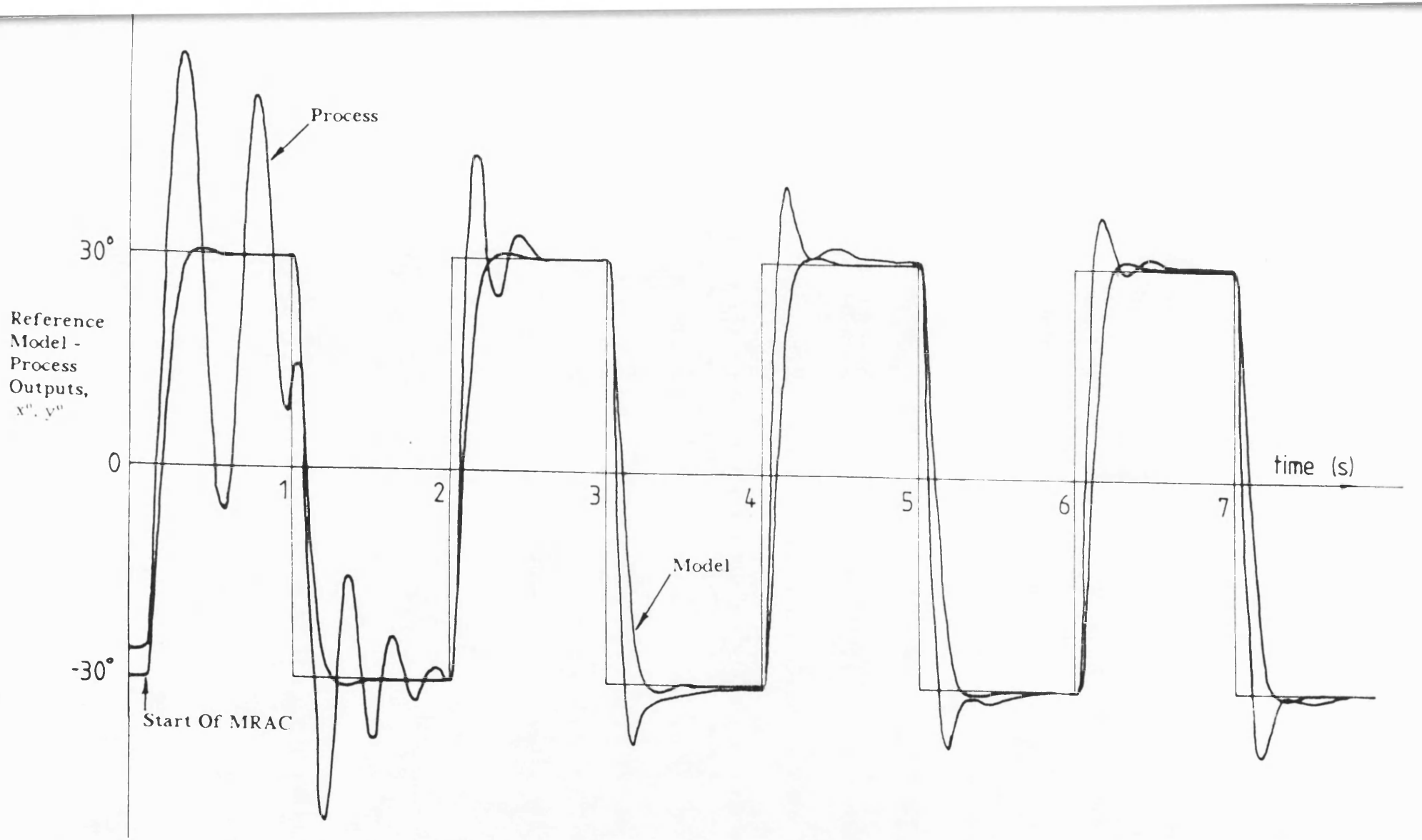

FIGURE 8:43 Start Of Model Reference Adaptive Control Using A Square Wave Command Input

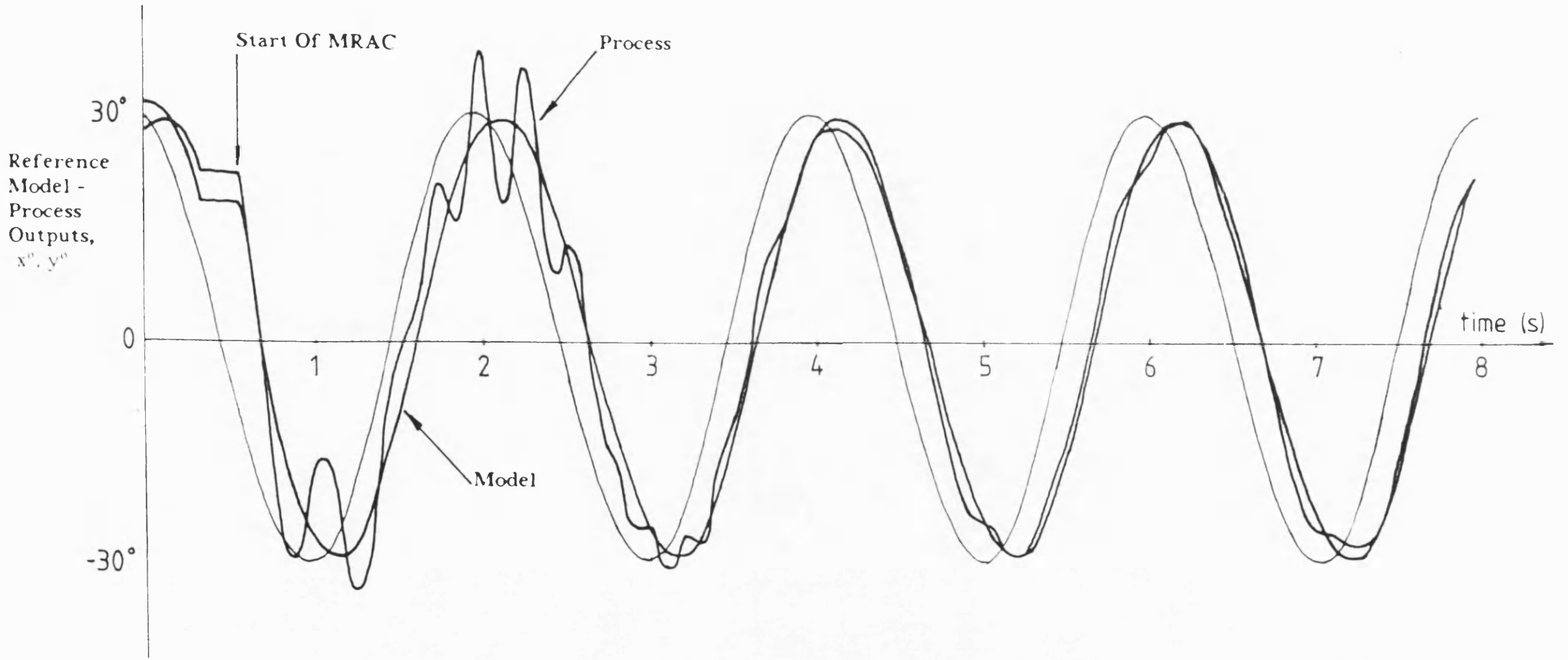

FIGURE 8:44 Start Of Model Reference Adaptive Control Using A Sinusoidal Command Input

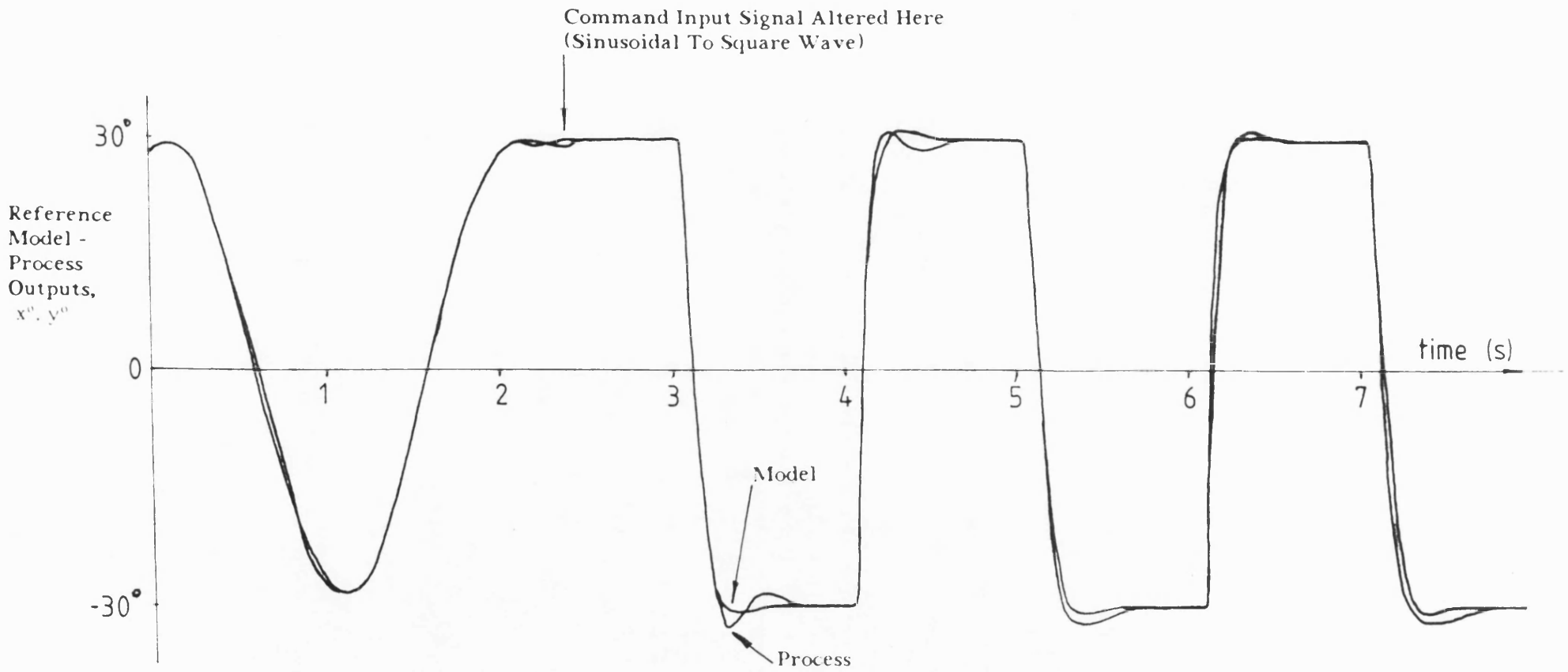

FIGURE 8:45 Adaptive System Behaviour Following A Change In Command Signal Waveform

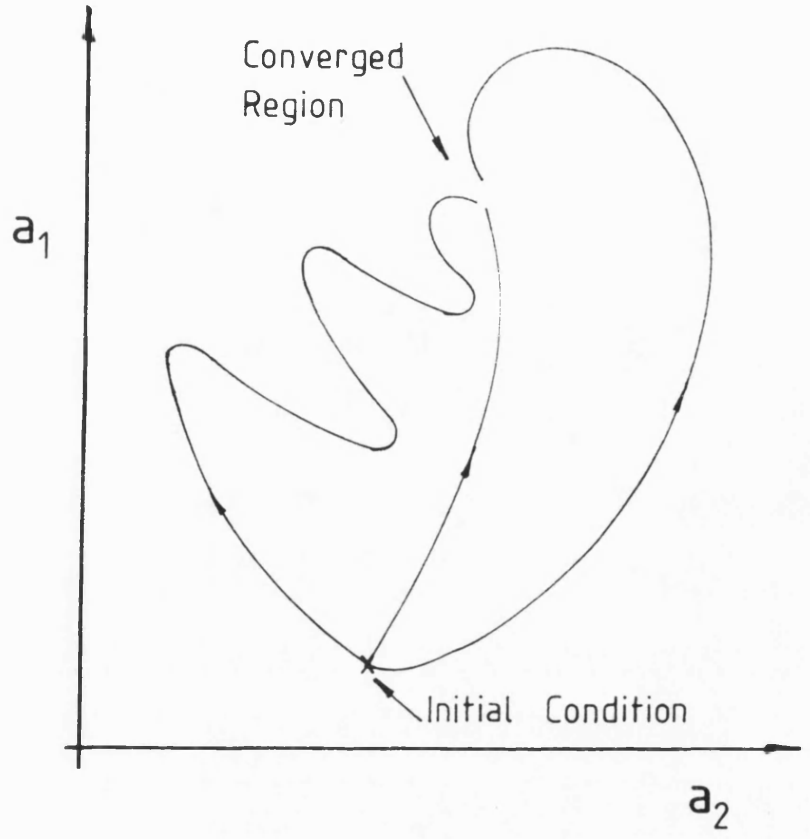

FIGURE 8:46 Hypothetical Convergence Paths For A Two-Parameter Adaptive Scheme a_1, a_2

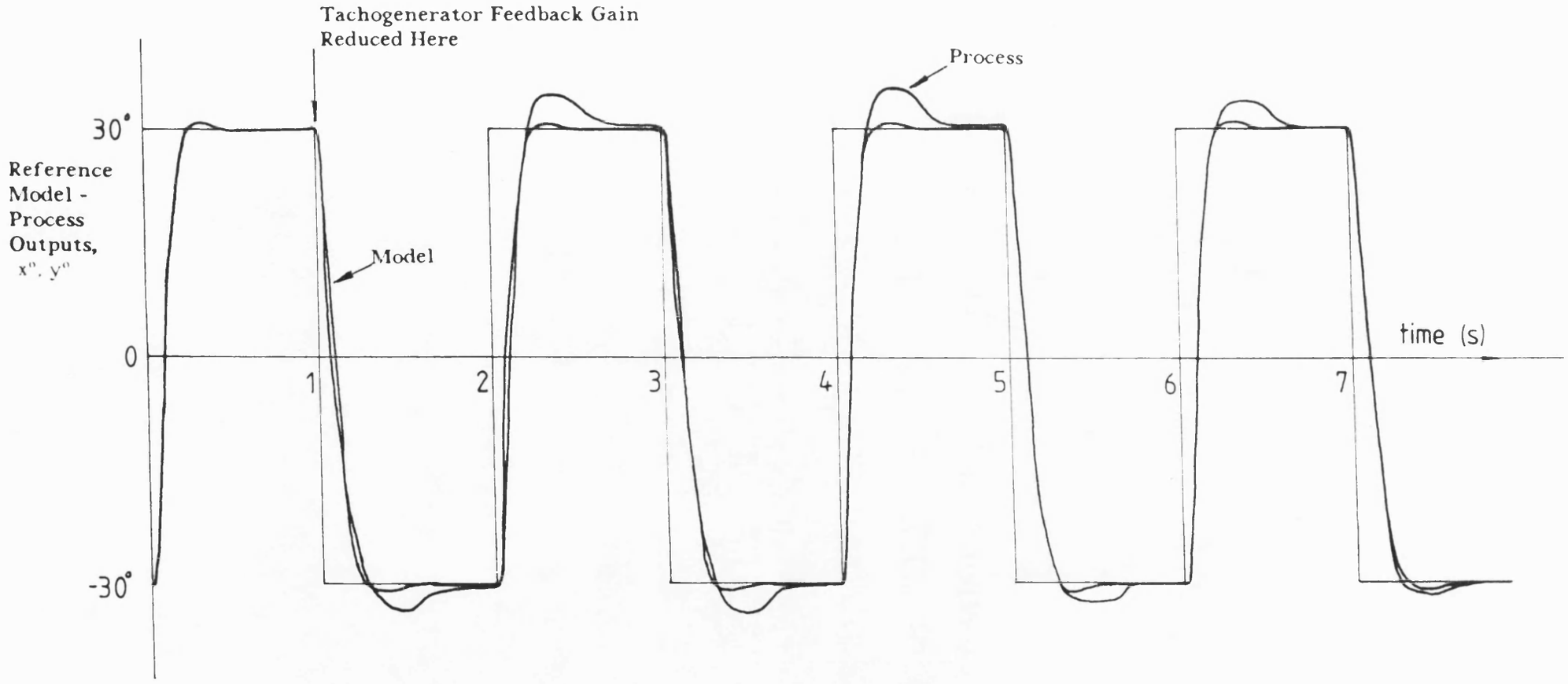

FIGURE 8:47 Adaptive System Behaviour Following A Reduction In Tachogenerator Feedback Gain

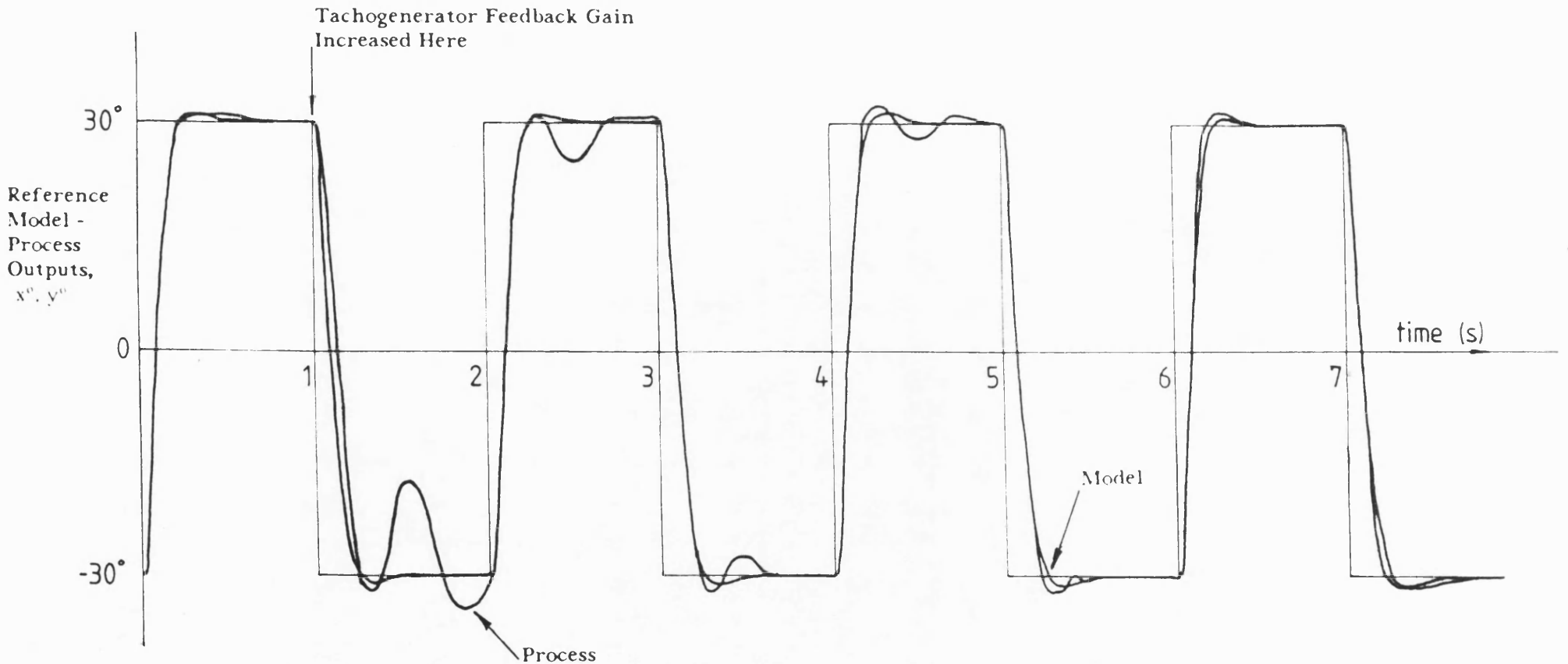

FIGURE 8:48 Adaptive System Behaviour Following An Increase In Tachogenerator Feedback Gain

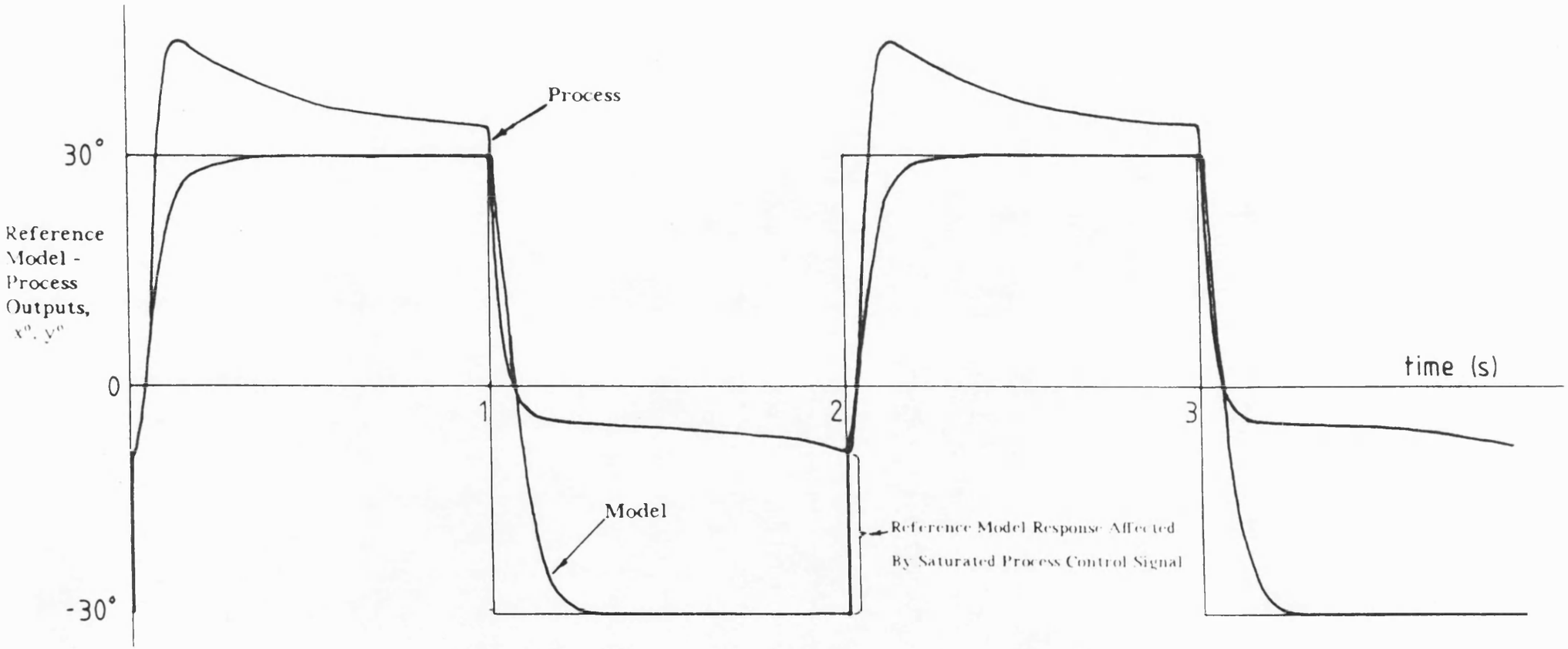

FIGURE 8:49 Example Of Offset Disturbance Signal Acting On The Non-Integral Action M.R.A.C. Scheme

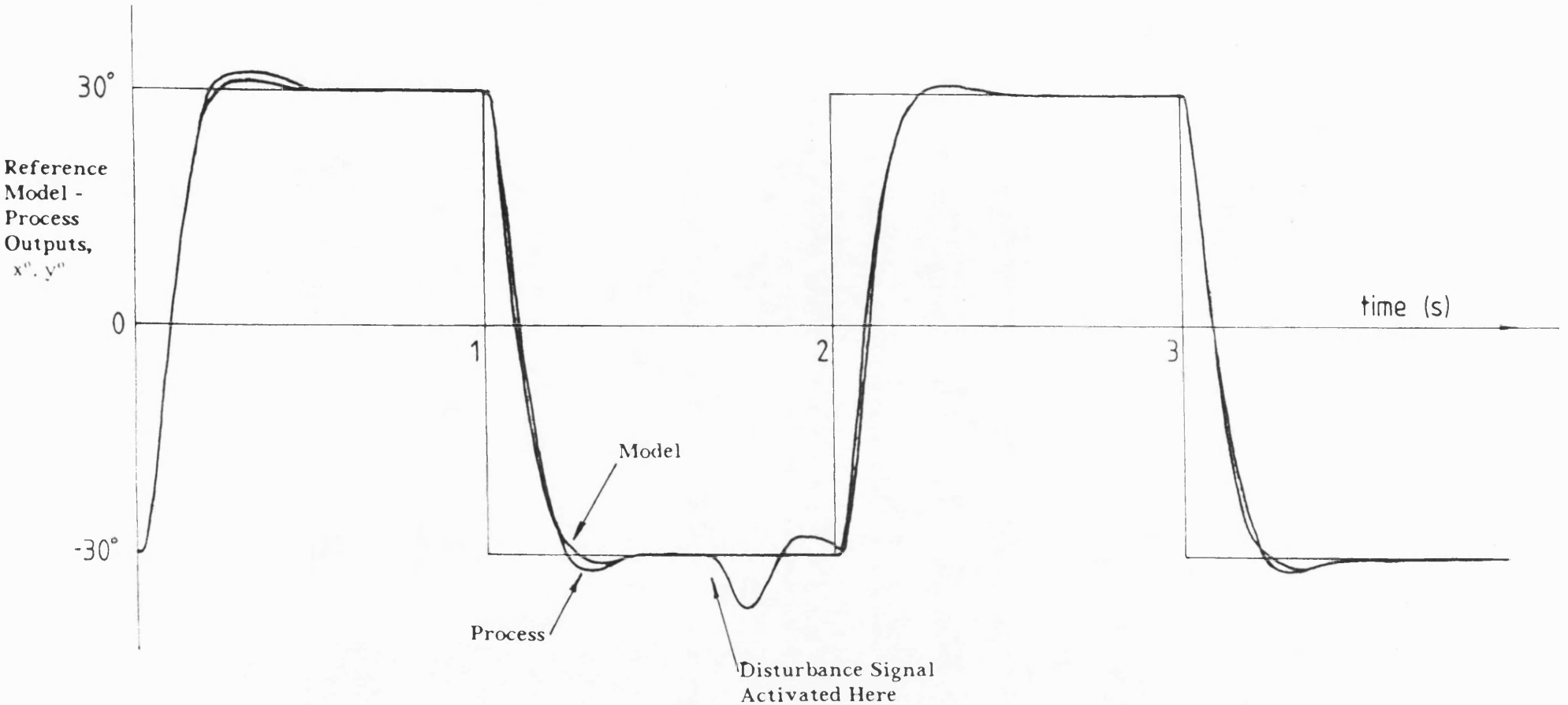

FIGURE 8:50 Disturbance Rejection Response Of The Integral-Action Scheme (High Tachogenerator Feedback Gain Setting)

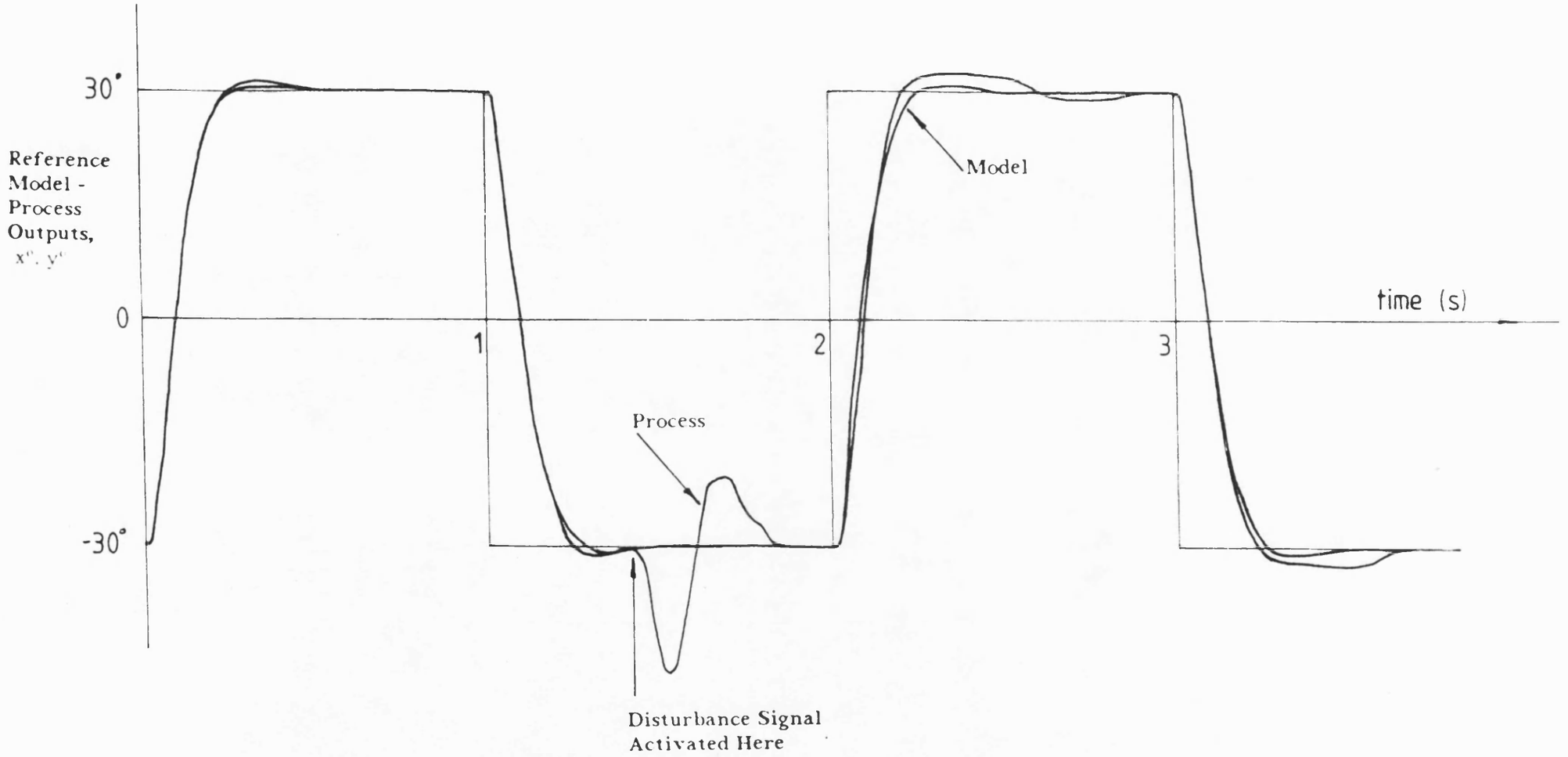

FIGURE 8:51 Disturbance Rejection Response Of The Integral-Action Scheme (Low Tachogenerator Feedback Gain Setting)

CHAPTER 9

AN ADAPTIVELY CONTROLLED ELECTRO-HYDRAULIC SERVOMECHANISM

9.1 INTRODUCTION

The material presented in this chapter outlines the development of an adaptive control scheme for an electro-hydraulic servomechanism. One of the underlying objectives of this presentation is to reinforce the controller design methodology of earlier chapters.

An important aspect of modern fluid power systems concerns the relative ease of their marriage with electronic components. The outcome of this association has resulted in mechanisms with high power-to-weight ratios which are capable of being controlled with compact, low-power electronic hardware. Such devices are also notable for the flexibility that they offer in terms of energy transmission and rapid system response. The versatility of their application is witnessed by their use as linear and rotary positioning mechanisms. Other applications encompass speed control and dynamometer circuits. The electro-hydraulic system dealt with in this chapter is just one example of the numerous possibilities that exist. Although the control scheme designed around it will unavoidably be device specific the underlying theme of its design is applicable to a broader spectrum of such mechanisms.

The servo-system used for this study is employed to a similar effect as the d.c. servomotor in chapter 8. Essentially, it involves the transmission of energy, through a fluid medium, with subsequent conversion into useful work. The main differences that can be highlighted involve a change in the scale of the two mechanisms and a more complex transfer function. With regard to the control objective, the electro-hydraulic system is a linear position control system, the d.c. servo-system being an angular position control scheme.

The presentation of this chapter follows an established pattern. Initially, the adaptive scheme is specified in terms of the control system constituent parts. This is followed by the numerical initialisation of relevant controller parameters. A series of secondary routines are subsequently developed as a means of overcoming non-linear characteristics associated with the electro-hydraulic system hardware. The adaptive control algorithm to emerge from this process was then investigated experimentally, using two different servo-valves.

9.2 ADAPTIVE CONTROLLER DESIGN

By following the controller design methodology, this stage of the procedure is separated into two sections; control system description and its subsequent initialisation.

9.2.1 CONTROL SYSTEM DESCRIPTION

Process Model

Figure 9:1 is a photograph of the electro-hydraulic servomechanism test rig. The lower half of this photograph shows a horizontally mounted actuator-mass combination. Hydraulic flow to and from the actuator is controlled by an electro-hydraulic servo-valve. This is located above the actuator in figure 9:1. The micro-processor part of the closed loop system can be seen in the top-left of this photograph.

Figure 9:2 is a schematic representation of the control scheme depicted in figure 9:1. A pump supplies hydraulic fluid to the servo-valve via an electronically operated pressure reducing valve. This device was incorporated into the hydraulic circuit for two reasons. Firstly, it can be used as an easily operable safety device which acts to divert flow away from the electro-hydraulic servo-valve. Its second benefit is in being able to regulate the supply pressure to the electro-hydraulic system. As such, it offers one possibility for effecting parametric perturbations in the dynamics of the controlled process.

The mechanical part of the controlled process begins with the electro-hydraulic servo-valve; for the series of experiments reported in this chapter, two devices were tested in succession. Table 9:1 provides relevant information on their performance characteristics. A comparison of the two highlights the severe, non-linear characteristics in the MOOG valve; this servo-valve was the first one used in experimenting with the adaptive control algorithm. Hydraulic fluid, supplied through the servo-valve, is used to drive an asymmetric actuator; its physical dimensions are summarised in table 9:1. The use of this type of actuator is representative of many practical applications of electro-hydraulic position control systems and in this study serves to highlight the problem of a direction-of-travel related performance characteristic.

The actuator rod is connected to an inertial load which is mounted on a free running trolley. The mass of this system is 890 Kg. Position feedback from the trolley is obtained by means of a wire-wound potentiometer with a sensitivity of 31mV/mm.

The final part of the electro-hydraulic test rig constitutes two volumes of trapped oil. These are depicted on either side of the servo-valve in figure 9:2. By opening the appropriate set of valves it is possible to vent these trapped volumes into the hydraulic lines between the servo-valve and actuator. The effect of their introduction is to simulate an increase in the size of the inertial load [13]. This change clearly implies a sudden change in the dynamics of the controlled process and can be used to test the parameter adaptive control scheme.

For the purpose of this control scheme, the transfer function of initial interest is that relating y, the process output, to u', the servo-valve drive signal in figure 9:2. A small perturbation analysis is used in part 1 of appendix 4 to develop a linearised, continuous-time transfer function of this system. The result of this analysis is a fourth order, type one transfer function with a finite numerator zero. This transfer function was considered to be of far greater complexity than warranted for this control scheme. In addition, the controller design methodology developed earlier is only applicable to continuous-time transfer functions that are free of finite zeros. Hence, a reduced order model was sought. In part 2 of appendix 4, the results derived in part 1 are extended to a special situation. This concerns the case of a symmetrical actuator. A small perturbation analysis of this device, with the actuator piston lying at the mid-stroke position, results in the following form

of third order, type one transfer function.

$$\frac{y}{u'} = \frac{K\omega_n^2}{s(s^2+2\zeta\omega_n s+\omega_n^2)} \tag{9.1}$$

The transfer function of equation (9.1) is of an acceptable form for deriving a discrete approximation that can be used in the adaptive controller design process. The discrete derivation is carried out through the use of the pole-zero mapping rules presented in chapter 3. The continuous-time transfer function of equation (9.1) contains a third order denominator and three infinite zeros. This results in the following discrete approximation of the continuous-time system,

$$\frac{y(z)}{u'(z)} = \frac{b'_0(1+z)^3}{(z-1)(z^2+a'_1z+a'_2)}$$

$$= \frac{b'_0(1+z)^3}{z^3+a_1z^2+a_2z+a_3} \tag{9.2}$$

Within the context of the adaptive scheme, the transfer function of interest concerns the effective controlled process; this represents a combination of the electro-hydraulic servomechanism and the D/A converter preceding it. The transfer function of this system is derived on the basis of equation (9.2). In accounting for the D/A converter, the procedure adopted here is to model one continuous-time infinite zero as a discrete infinite zero. This alteration to equation (9.2) results in the following discrete transfer function,

$$\frac{y(z)}{u(z)} = \frac{b_0(1+z)^2}{z^3+a_1z^2+a_2z+a_3} \tag{9.3}$$

It should be noted that equation (9.3) relates the sampled process output, y(z), to the control signal u(z) which is generated by the micro-processor system and then fed to the D/A converter.

During the early stages of controller design, some preliminary testing was carried out on the electro-hydraulic servomechanism. This involved examining its step response behaviour under closed loop proportional action digital control [34]. Figure 9:3 is a typical example of the level of response recorded. An important

feature to note in this figure is the presence of a time delay in the response of the controlled process. An average value for the duration of the time delay was evaluated as 13 ms. This is close to the 15 ms. sampling period of the adaptive control algorithm. As a consequence, the controlled process transfer function of equation (9.3) was adjusted by introducing a z^{-1} term to reflect this phenomenon. The following expression represents the transfer function used to model the controlled process.

$$\frac{y(z)}{u(z)} = \frac{1}{z}\frac{b_0(1+z)^2}{z^3+a_1z^2+a_2z+a_3}$$

Employing the delay operator convention, this expression reduces to the following,

$$\frac{y(z^{-1})}{u(z^{-1})} = \frac{b_0z^{-2}(1+z^{-1})^2}{1+a_1z^{-1}+a_2z^{-2}+a_3^{-3}}$$

$$= \frac{b_0z^{-2}B(z^{-1})}{A(z^{-1})} \qquad (9.4)$$

The process model of equation (9.4) is of a sufficiently high order to imply high order compensator networks; this deduction follows from a comparison of the two control schemes developed in chapter 8. The presence of high order compensator networks indicates a large number of coefficients in the adjustable parameter vector and hence an adaptive algorithm with a relatively long sampling period. The computational delay in evaluating the process control signal for such a scheme represents a small fraction of the algorithm sampling period. This deduction follows from the discussion of section 7.4 in chapter 7. For this reason the control algorithm developed here was based on the scheme depicted in flow-diagram 7:1. This means that no steps are taken to account for the computational delay phenomenon and the process model remains unaltered.

Reference Model

The basic structure of a reference model for this control scheme is derived from the controlled process transfer function of equation (9.4). This algebraic expression is used to represent an open loop reference model. A closed loop reference model, which will eventually be employed in the control algorithm, is developed by

operating the open loop system in a unity feedback control loop. Accordingly, the following set of steps leads to the derivation of a closed loop reference model transfer function.

$$\frac{x(z^{-1})}{w(z^{-1})} = \frac{b_m z^{-2}(1+z^{-1})^2}{1+a'_{m,1}z^{-1}+a'_{m,2}z^{-2}+a'_{m,3}z^{-3} + b_m z^{-2}(1+z^{-1})^2}$$

$$= \frac{b_m z^{-2}(1+z^{-1})^2}{1+a_{1,m}z^{-1}+a_{m,2}z^{-2}+a_{m,3}z^{-3}+a_{m,4}z^{-4}}$$

$$= \frac{b_m z^{-2}B(z^{-1})}{A_m(z^{-1})} \qquad (9.5)$$

Compensator Network Specification

After the controlled process and reference model, the third essential component in the model reference control scheme comprises the compensator networks. Drawing on the important results from chapter 4, it can be stated that the two compensator filters, $F(z^{-1})$ and $G(z^{-1})$ of figure 9:2, need to be of the following forms.

$$F(z^{-1}) = f_0+f_1z^{-1}+f_2z^{-2}+f_3z^{-3} \qquad (9.6)$$

$$G(z^{-1}) = g_0+g_1z^{-1}+g_2z^{-2} \qquad (9.7)$$

Parameter Adaptive Algorithm Specification

The set of equations that define the parameter adaptive algorithm can be readily specified by applying the results of chapter 5. To begin with, the coefficients of the compensators in the controlled process loop are grouped together in an adjustable parameter vector thus,

$$\underline{\hat{d}}(k) = [\,\hat{f}_0(k)\;\hat{f}_1(k)\;\hat{f}_2(k)\;\hat{f}_3(k)\;\hat{g}_0(k)\;\hat{g}_1(k)\;\hat{g}_2(k)\;\hat{g}_3(k)\,]^T \qquad (9.8)$$

An observation vector associated with this parameter vector is similarly defined as,

$$\underline{\Phi}(k) = [\, u(k)\, u(k-1)\, u(k-2)\, u(k-3)\, y(k)\, y(k-1)\, y(k-2)\, y(k-3)\,]^T \qquad (9.9)$$

The updating algorithm used to adjust coefficients in the parameter vector of equation (9.8) depends on a filtered version of the observation vector. The filtering effect is a function of the numerator dynamics in the controlled process transfer function. From equation (9.4) this results in the following procedure for evaluating the filtered observation vector, $\tilde{\underline{\Phi}}$.

$$\tilde{\underline{\Phi}}(k) = z^{-2}B(z^{-1})\underline{\Phi}(k)$$

$$= B(z^{-1})\underline{\Phi}(k-2) \qquad (9.10)$$

The parameter updating expression of equation (5.30) in chapter 5 can now be specified for this control scheme in terms of the component parts specified above. Thus, the seven-element adjustable parameter vector of equation (9.8) is updated according to the following procedure.

$$\hat{\underline{d}}(k) = \hat{\underline{d}}(k-1) - \frac{\tilde{\underline{\Phi}}(k-2)\nu^{o}(k)}{\gamma + \tilde{\underline{\Phi}}^{T}(k-2)\tilde{\underline{\Phi}}(k-2)} \qquad (9.11)$$

9.2.2 CONTROL SYSTEM INITIALISATION

Reference Model

The specification of a suitable reference model for this control scheme calls for the initialisation of a fourth order characteristic equation and a gain, b_m as indicated by equation (9.5). Some assistance in this procedure can be gained by considering the closed loop step response behaviour of the controlled process in conjunction with a root locus analysis of the reference model transfer function as explained below.

Figure 9:3 is representative of the step response of the controlled process under closed loop proportional proportional control. A control engineering interpretation of this response suggests an exponential form of first order system response superimposed with an oscillatory second order factor. In addition, this response includes a time delay. Since the controlled process and open loop reference

model share similar structural properties, it is possible to deduce a certain form for the reference model characteristic equation from these observations: the oscillatory part of the step response corresponds to a complex pair of roots; the two remaining roots are real with one exerting a dominant influence. One of these real roots is associated with the integral term in the open loop reference model transfer function. The unit time delay term is responsible for the remaining one. A root locus analysis will help to clarify these observations.

Figure 9:4 shows a root locus diagram for an example transfer function of the form given in equation (9.5). The loci are drawn for increasing values of forward path gain, b_m, beginning with zero. As the value of b_m increases, a pair of loci moves towards the perimeter of the unit disc and eventually outside it. Simultaneously, loci emanating from the points, z=0 and z=1, approach one another before separating and eventually converging to the double zeros at z=-1. The initial roots at z=0 and z=1 are associated with a unit time step delay and an integrator respectively. Figure 6:8 shows loci of constant damping and natural frequency in the z-plane. The oscillatory component of the step response in figure 9:3 occurs at less than half the Nyquist frequency. Moreover, the degree of oscillation is highly persistent and indicates a low damping coefficient. Hence, the characteristic equation contains a pair of complex roots, close to the perimeter of the unit disc, and in its first and fourth quadrants. The remaining two roots of the characteristic equation are real with one lying close to the point z=1; this is the rightmost of the the four roots and causes it to have a dominant effect on the step response of the system. This explains the underlying exponential form of step response.

Selection of a suitable reference model transfer function can now be considered in the light of the above observations. Clearly, a desirable level of performance can be described in terms of a reference model with a relatively fast, oscillatory-free step response. This procedure was carried out by arbitrarily specifying a characteristic equation with one real root close to the point z=0.1 and a complex pair at $z=0.3 \pm 0.3i$. The former thus becomes the leftmost root along the real axis while the latter pair of roots are sufficiently well damped to ensure an oscillatory-free reference model step response. This is because they are located well away from the perimeter of the unit disc [42]. The remaining root was selected to lie nearest to the point z=1; this ensures that it exerts a dominant influence on the reference model response. By altering its position, it was possible to affect the step response rise time. In order to select a suitable root position, the controlled process

was first operated under closed loop, proportional control using the same software as for the adaptive control algorithm [77]. This meant that the step response tests, an example of which is shown in figure 9:3, were conducted at the same sampling rate as would subsequently be used for the adaptively controlled system. Reference to flow-diagram 7:1 indicates how this is achieved. By operating the reference model in parallel with the controlled process, it was possible to choose different locations for the last characteristic equation root and compare the response of the two systems. A suitable root position was selected when the speed of the reference model transient response was judged almost to match that of the controlled process. More importantly, this choice was considered to be capable of being met by the controlled process at other operating conditions. The characteristic equation of the reference model that was eventually selected is given by the following expression.

$$(z-0.1)(z-0.75)(z-0.3+0.3i)(z-0.3+0.3i) = 0 \tag{9.12}$$

Substitution of equation (9.12) in the reference model transfer function of equation (9.5) yields the following expression,

$$\frac{x(z^{-1})}{w(z^{-1})} = \frac{b_m z^{-2}(1+z^{-1})^2}{1-1.45z^{-1}+0.765z^{-2}-0.198z^{-3}+0.0135z^{-4}} \tag{9.13}$$

Operation of the reference model in the adaptive control algorithm as part of its initialisation procedure required the selection of a value for its forward path gain, b_m. This was evaluated by recalling that the reference model is required to have unity steady state gain. This can be determined by making use of the final value theorem [42]. When this procedure is applied to the transfer function of equation (9.13), the following expression results,

$$\lim_{k\to\infty} x(k) = \left. \frac{b_m z^{-2}(1+z^{-1})^2}{1-1.45z^{-1}+0.765z^{-2}-0.198z^{-3}+0.0135z^{-4}} \right|_{z=1} \tag{9.14}$$

$$= \frac{4b_m}{0.1305}$$

Clearly, a value of 0.032625 for b_m satisfies the steady state operating requirements.

The bandwidth of the reference model specified in equation (9.13) is 3 Hz. By comparison, the corresponding value for the electro-hydraulic system under closed loop proportional control is 1.1 Hz.

Error Filter

The procedure for designing the error filter follows a standard procedure based on the strict positive realness of a particular transfer function. For this control scheme, the denominator of this transfer function involves the reference model characteristic equation given in equation (9.12). This is a fourth order polynomial. On this basis, the design guidelines outlined in chapter 7 call for a third order error filter polynomial. This results in the following form of S.P.R. transfer function,

$$\frac{C(z^{-1})}{A_m(z^{-1})} = \frac{1+c_1z^{-1}+c_2z^{-2}+c_3z^{-3}}{1-1.45z^{-1}+0.765z^{-2}-0.198z^{-3}+0.0135z^{-4}} \tag{9.15}$$

The use of MACSYMA (appendix 3) results in the following set of constraints on the error filter coefficients if the S.P.R. condition is to be satisfied.

$$c_2 > c_1+c_3-1 \tag{9.16}$$

$$c_2 > -c_1-c_3-1 \tag{9.17}$$

$$c_2 > 3.63c_1-7.58c_3-0.30 \tag{9.18}$$

$$c_2 > -1.21c_1+2.40c_3-0.13 \tag{9.19}$$

$$c_2 > -0.39c_1-1.73c_3-0.10 \tag{9.20}$$

To ease the task of specifying the three error filter coefficients, the problem was simplified to one involving the specification of only two parameters. The error filter initialisation guidelines were formulated for the c_1 and c_2 coefficients. Consequently, it was decided to assign a numerical value to the c_3 parameter. The choice of a value for c_3 was based on an approximate method for specifying the error filter coefficients suggested in [24]. The method proposed is as follows: for a

given power of z, the value of the error filter polynomial coefficient should be chosen such that its magnitude is smaller than its corresponding z-coefficient in the S.P.R. transfer function denominator polynomial. For this scheme, the coefficient of the z^{-3} term in the denominator polynomial is -0.198. On this basis, a value of 0.15 was arbitrarily selected for c_3. Upon making this substitution the set of inequalities (9.16-20) reduces to a two parameter system. A graphical representation of their common region is shown in figure 9:5.

The coefficient specification procedure outlined in section 7.5.3 of chapter 7 was used to evaluate suitable values for the remaining error filter coefficients. The values selected were $c_1 = -0.4$ and $c_2 = -0.5$. Figure 9:6 shows the frequency response characteristics of the S.P.R. transfer function resulting from this choice. The low frequency phase response is asymptotically zero while the maximum magnitude of phase is lower than the maximum allowable value of 90°.

Figure 9:7 shows the frequency response characteristics of the error filter, $C(z^{-1})$. It is possible to highlight an interesting engineering related feature from this information [34]. In developing the adaptive controller design procedure one simplification that was made involved the use of an approximate model of the controlled process. In specifying a discrete transfer function, using the pole-zero mapping procedure, it can be argued that a degree of modelling error is introduced, particularly in the region of the Nyquist frequency; this is attributed to the procedure of automatically mapping continuous-time infinite zeros to the point z=-1 in the discrete domain. However, the use of an error filter with the set of coefficients specified above acts to desensitise the parameter adaptive algorithm to modelling errors associated with this factor. This results from the approximate stop-band filtering effect that the error filter possesses in the region of the Nyquist frequency.

Adaptive Gain

The discussion of section 7.5.2 in chapter 7 examined the combined influence of the adaptive gain, γ, and the observation vector related scaling factor on the performance of the parameter updating algorithm. It was argued that in the case of a complex control scheme, with a considerable number of terms in the observation vector, the influence of the fixed adaptive gain, γ, is weak. The control scheme

proposed in this chapter can be classed as this type of system since it has a seven element adjustable parameter vector.

The adaptive algorithms developed in chapter 8 employed a value of 10^4 for the adaptive gain, γ. The extended parameter vector for the electro-hydraulic control scheme suggests a lower value. A value of 10^3 was judged to be adequate.

Compensator Networks

Initialisation of the $F(z^{-1})$ compensator requires the specification of four coefficients. This procedure was commenced by selecting three root locations for the compensator polynomial: one root was positioned at the point z=0.3; by maintaining an equivalent magnitude for the real part, the two remaining roots were chosen to be complex and located at $z=-0.3\pm0.3j$.

The step response behaviour of the controlled process, as shown in figure 9:3, indicates a fast level of initial response. This response was obtained with a forward path gain of unity. By choosing to retain this value of gain, the set of values used to initialise the forward path compensator was as follows,

$$F(z^{-1}) = 1-0.9z^{-1}+0.28z^{-2}-0.04z^{-3} \tag{9.21}$$

The process of initialising the feedback compensator, $G(z^{-1})$, is complicated by the extremely wide choice of options available. For this application the second order filter was initialised with the following expression,

$$G(z^{-1}) = 0.5z^{-1}+0.5z^{-2} \tag{9.22}$$

This choice corresponds to a quadratic expression with two infinite roots. It should also be noted that the steady state gain of this filter is unity.

Variable Dead-Band Filter

Two reasons can be given to justify the use of a variable dead-band characteristic in this adaptive control scheme. The first concerns the use of a reduced order continuous-time transfer function to represent the controlled process. The second reason arises from the derivation of a representative discrete model of the controlled process using the pole-zero mapping technique.

The following prior information about the control scheme provides some assistance in initialising the variable dead-band characteristic. In section 5.6.1 of chapter 5, one possible influence of the $B(z^{-1})$ polynomial was discussed. Its filtering effect was considered to introduce a degree of modelling error immunity in the parameter adaptive algorithm. The $B(z^{-1})$ polynomial for this control scheme includes two zeros at z=-1; this implies a notable degree of high frequency attenuation in the signals that constitute the filtered observation vector. Moreover, this type of filtering action will be compounded by the effect of the error filter; its frequency response characteristics approximate to a stop-band filtering effect in the region of the Nyquist frequency, as shown in figure 9:7. A consequence of these phenomena leads to the conclusion that the variable dead-band filter should be initialised in favour of a parameter adaptive algorithm that is biased more towards alertness than robustness. To this end, the following set of values was specified for the respective parameters in the dead-band filter: the filter pole, σ, was assigned to the point 0.8; the filter gain, ϵ, was selected as 0.002 and the constant input signal, ϵ_0, was chosen to be 10.0.

9.3 CONTROL SYSTEM ENHANCEMENT FEATURES

An important benefit of employing a micro-processor system to implement control algorithms concerns the relative ease with which it is possible to implement compact, non-linear forms of control action. This is demonstrated with the following developments aimed at enhancing the performance of this control algorithm.

9.3.1 ASYMMETRIC ACTUATOR GAIN

The electro-hydraulic servo-system considered in this application employs an asymmetric actuator as shown in figure 9:2. Its influence on the step response behaviour of the closed loop system is evident in figure 9:3. This type of behaviour can be associated with a change in the gain of the controlled process depending on the direction of actuator travel. A specific routine based on prior information about the actuator was developed to overcome this phenomenon. The procedure involved multiplying the process control signal with a corrective gain according to the direction of actuator travel. This would act to cancel the change in gain due to the controlled process. According to the analysis of appendix 5, the directional gain factor is equal to the square root of the piston/annulus area ratio (1.21 for the actuator used here).

9.3.2 SERVO-VALVE PERFORMANCE LINEARISATION PROCEDURE

A MOOG servo-valve was used for the initial set of experiments reported in this chapter; its performance characteristics are summarised in table 9.1. The important features of this device are its dual flow-gain characteristics and a dead-band around the null point. These are graphically represented in figure 9:8. Their influence on the step response behaviour of the controlled process can be seen in figure 9:3. Following a step change in the command signal, the servo-system displays an extremely rapid initial response. This is due to a large drive signal which causes the servo-valve to operate over its high flow-gain region. The poor level of steady of steady state behaviour exhibited is related to the servo-valve dead-band characteristic. In an attempt to linearise and improve upon these performance features, the series of control actions described below were developed.

To begin with, the servo-valve characteristics were parametrised on the basis of manufacturer supplied data and experimental verification. The software routine that was devised from this information is explained with the aid of flow diagram 9:1 and figure 9:9. Essentially, the routine was required to check for two conditions. If the process control signal corresponded to the high flow-gain operating region then it was reduced by an appropriate amount as shown by the characteristic in figure 9:9. The aim of this modification was to provide a constant flow-gain characteristic. This objective can be appreciated by visualising the result of combining the servo-

valve dual gain characteristic and its software linearising procedure.

The second monitored condition was used to check for the case of a control signal falling inside the servo-valve dead-zone. Two actions were triggered when this occurred. The first of these consisted of assigning the control signal an appropriate positive or negative value, corresponding to the respective dead-band threshold. This action is signified by the lack of a mapping function for the dead-zone in figure 9:9. One advantage of this procedure is that it overcomes the delay associated with the control signal traversing the dead-zone after a change in the command input signal. The second action that is instigated when the process control signal enters the dead-zone causes the model-process output error to be set to zero. This is necessary because the controlled process is operating in a non-linear mode; this could give rise to undesirable parameter adaptation because the controlled process appears to have zero gain.

The two routines that have been developed in this section act on the process control signal, u. This is the output from the $1/F(z^{-1})$ compensator block in figure 9:2. The order in which the operations are carried out is indicated in flow diagram 9:1.

9.4 EXPERIMENTAL EVALUATION OF THE ADAPTIVE CONTROL SCHEME

9.4.1 TEST METHOD

The adaptive control algorithm was tested under a variety of operating conditions. These comprised the use of different waveform command signals and perturbations to the dynamics of the controlled process. Regarding the latter, two possibilities were catered for. The first made use of the two extra volumes of oil in figure 9:2. The effect of their introduction into the hydraulic circuit can be seen in figure 9:10. This shows the step response of the controlled process under proportional control. The two modes of operation simulate low and high inertial load conditions respectively [13]. They are characterised by a change in the natural frequency from 12.6 to 7.6 Hz. It is more important to note that the latter case represents a system that is nearly critically stable.

The second means of perturbing the dynamics of the controlled process employed the pressure reducing safety mechanism in figure 9:2 to affect the system hydraulic supply pressure.

Unless specified otherwise, all tests were carried out about the actuator mid-stroke position. This station is defined as y=0 in the following set of test results.

9.4.2 PRESENTATION OF TEST RESULTS

Figure 9:11 shows the reaction of the adaptive control algorithm as control action is transferred from proportional control to model reference adaptive control. This experiment was carried out with a system supply pressure of 100 bar and low simulated load. The speed with which a reasonably acceptable level of model following is achieved is commendable. Two other features are worthy of mention. The first of these concerns the actual step response of the controlled process. Unlike those of figure 9:3, where the transient can be separated into two distinct modes, those of figure 9:11 display a greater degree of consistency coupled with a significant improvement in steady state behaviour. The second improvement to be highlighted in figure 9:11 relates to the nearly complete disappearance of oscillatory behaviour in the process step response. This experiment was repeated with the routine for the direction of travel related gain temporarily suspended. Control system behaviour was not noticeably different from that shown in figure 9:10. This implies a rapid level of adaptive control action to maintain consistent model following. The corrective gain procedure was nevertheless retained for subsequent tests as it represents a simple means of relieving the burden on the parameter adaptive algorithm.

The effects of alterations to the dynamics of the controlled process are first examined in terms of simulated changes to the driven load inertia. Figure 9:12 shows how well the adaptive control algorithm responds after a switch to the high simulated load condition. Although the process response includes a small amount of oscillation around the set point the transient part of its step response remains as before. A reverse in the simulated load condition is shown in figure 9:13. This corresponds to a return to the original mode of system dynamics. Once again, the quality of model following is very good. Although the results presented above were obtained with a supply pressure of 100 bar they are representative of

observations made at other working pressures.

The above tests were repeated under a worse case situation. This corresponds to the use of a sinusoidal input command signal. Figure 9:14 is typical of the quality of model following that resulted after a simulated increase in the load inertia. Model following is maintained within a small tolerance band. The persistence of an oscillatory component in the response of the controlled process is not overcome for a number of reasons. Since the oscillations are of a relatively high frequency, their presence in the signals reaching the parameter adaptive algorithm will be attenuated. This is a consequence of the high pass filtering effect arising from the $B(z^{-1})$ polynomial when it is used to generate the filtered observation vector. Another factor to be taken into account concerns the magnitude of the oscillations. Their small size makes it likely that the model-process error that they cause will be reduced by the variable dead-band characteristic. A check on the quality of parameter adaptation for the response recorded in figure 9:14 was carried out by altering the command input to a square wave signal. Control system performance is shown in figure 9:15. This indicates a reasonable level of model following although the quality of parameter adaptation continued to be improved as a result of using the 'richer' square wave input.

The pair of responses recorded in figures 9:14 and 9:15 are matched by their respective counterparts of figures 9:16 and 9:17. These show the results obtained for the reverse situation of a simulated reduction in the load inertia. Under sinusoidal command input operation, the effect of parameter adaptation does not appear to vary significantly; a comparison of figures 9:14 and 9:16 highlights the continued presence of an oscillatory component in the response of the controlled process. The slightly larger magnitude of the initial oscillations, in figure 9:16, result in a greater degree of parameter adaptation. When the command input is altered to a square wave, as shown in figure 9:17, model following resumes in a slightly improved manner when compared with figure 9:15.

The second set of experiments devised to test the adaptive control scheme is also considered to be representative of the type of problem likely to be encountered in real applications. The tests involved observing the quality of control system behaviour following sizable changes in the system hydraulic supply pressure. Figure 9:18 shows the case where the supply pressure was suddenly increased from 80 to 160 bar. The apparent increase in the gain of the controlled process provokes a step

response with an overshoot although this is gradually corrected. An even better level of response was obtained for the case of a sinusoidal command input signal as shown in figure 9:19. Examples of the reverse situation, where the supply pressure was reduced from 160 to 80 bar, are shown in figures 9:20 and 9:21. The effect of this perturbation is clearly discernible in the initially sluggish behaviour of the controlled process. These tests were carried out at the low simulated load condition. They are similar to those obtained at the high simulated load condition.

9.5 INTEGRAL ACTION ADAPTIVE CONTROL SCHEME

The discussion in section 6.6 of chapter 6 highlighted the adverse effects that a steady disturbance signal would have on the parameter adaptive algorithm. A parallel case, concerning the likely degradation in set-point tracking behaviour, was also pointed out. For the electro-hydraulic servo-system considered here, there are a number of situations which could give rise to disturbances acting on the system. Simple examples include the presence of a d.c. offset in the servo-valve current drive circuitry or a servo-valve with an incorrectly centred spool. Disturbances acting on the load inertia, such as a steady or spring generated force, will exert an equally undesirable effect on set-point tracking and parameter adaptation. The use of some form of integral action in the control loop is a common procedure for improving its disturbance rejection properties.

Two different approaches for introducing integral action control in the model reference adaptive control scheme were presented in section 6.6 of chapter 6. The application of the first of these has already been reported in chapter 8. The material presented in this section offers a practical example of implementing the second form of integral action control.

The test rig used for this presentation was essentially the same as that used for the previous set of experiments. The only difference is in the use of a different servo-valve in place of the MOOG unit employed earlier. This alteration highlights the versatile nature of the adaptive control algorithm and the ease with which it can be altered on a micro-processor system. The important characteristics of the new servo-valve are summarised in table 9:1. The DOWTY unit clearly possesses less complex performance characteristics than the MOOG servo-valve. This has certain implications for altering that section of the adaptive algorithm developed in section

9.3.2. These modifications will be discussed at an appropriate stage later in this presentation.

An important characteristic of the DOWTY servo-valve is that it incorporates a zero-lapped spool. Under steady state operating conditions, there exists an equilibrium force balance on the load inertia. The same applies to the actuator jack. This situation requires different pressures to be maintained in the actuator chambers on either side of the jack. For this to be possible, the servo-valve spool has to lie off its null position. This implies the presence of a non-zero control signal, u, in figure 9:2. In a non-adaptive control scheme, it would be necessary for the $1/F(z^{-1})$ compensator block in figure 9:2 to contain an integral term. This would allow a non-zero control signal, u, for a zero input to the compensator block and would imply that set-point tracking was being met. The adaptive control scheme reported in [34] managed to achieve an acceptable level of set-point tracking by causing the feedback compensator, $G(z^{-1})$ of figure 9:2, to have a non-unity steady state gain. Although this helps in attaining the desired control objective it represents an incorrect case of parameter adaptation. One aim of introducing an integral action controller is to overcome this problem, thereby enhancing the quality of parameter adaptation.

9.6 CONTROL SYSTEM DESCRIPTION

The hardware elements that constitute the controlled process are virtually identical to those used in section 9.2.1. As a consequence, the controlled process and reference model were still represented with the transfer functions of equations (9.4) and (9.5) respectively; the compensator networks were defined by equations (9.6) and (9.7). This results in the parameter adaptive part of the control scheme containing seven element adjustable parameter and filtered observation vectors, equations (9.8) and (9.10) respectively. Equation (9.11) provides the algorithm for generating the adjustable compensator coefficients. Two additional expressions are introduced to complete the description of the adaptive control scheme. The first of these is the integral action controller. Its presence in the control scheme is shown schematically in figure 6:11. The transfer function of this filter is given as,

$$\frac{ie(z)}{e(z)} = \frac{K_E}{z-1} \tag{9.23}$$

where e is the 'a priori' model-process output error.

The transfer function of equation (9.23) can be written as an evaluation procedure; the output from the integrator, at a given sampling instant, k, is given by,

$$ie(k) = ie(k-1) + K_E e(k-1) \tag{9.24}$$

The contribution of the integral action controller is fed to the controlled process by being added to the process control signal. This results in a calculation procedure expressed with the following equation.

$$u(k) = \frac{1}{\hat{f}_0}(w(k) - \hat{f}_1 u(k-1) - \hat{f}_2 u(k-2) - \hat{f}_3 u(k-3)$$

$$- \hat{g}_0 y(k) - \hat{g}_1 y(k-1) - \hat{g}_2 y(k-2)) + ie(k) \tag{9.25}$$

Since the contribution of the integral term, ie(k), depends on previously delayed information, it can be evaluated during the sampling interval prior to its use. This is indicated by the expression of equation (9.24).

9.6.1 CONTROL SYSTEM INITIALISATION

Since the controlled process remains essentially the same as that used in section 9.2.1, the initialisation procedure followed here is as detailed in section 9.2.2. The use of a different servo-valve clearly obviates the need for the servo-valve performance linearising procedure presented in section 9.3.2. The only other alteration to the initialisation procedure concerns the choice of an integral gain, K_E. This matter is discussed below.

The integral action controller operates on the model-process error. Under usual operating conditions, this signal is meant to provide an indication of the parametric error between the controlled process loop and reference model transfer functions. However, the situation becomes complicated when disturbances act on the controlled process. In such cases, the model-process error contains a parametric error and a disturbance signal related component. The integral action controller is targeted at the latter constituent. Therefore, it was considered necessary to employ a low value for the integral gain, K_E in order to attenuate perturbations to the controlled process as a result of integrating the parametric component of the model-process error signal.

In section 8.5, a different form of integral action control was used; it was initialised with a gain of 0.5. Subsequent experimentation with the control scheme indicated that this value was too large. Although it is not strictly correct to make a direct comparison of the two integral terms, the experience that had been gained prompted the selection of a value of 0.05 for integral gain in the electro-hydraulic scheme.

9.7 PRESENTATION OF TEST RESULTS

An identical set of tests to that reported in section 9.4 above was carried out on the integral action adaptive control scheme. The results obtained were virtually the same as those observed with the control algorithm for the MOOG servo-valve. To avoid undue repetition, they are not discussed here.

Two additional sets of experiments were carried out in order to emphasise the robustness properties of the adaptive control algorithm. The reasons for devising these tests are outlined below.

The experimental work reported in section 9.4 and [34] involved operating the electro-hydraulic servomechanism about a mean position that corresponds to the actuator mid-stroke position; this is shown in figure 9:22. This position most closely approaches the condition employed in part 2 of appendix 4 during which a reduced order model was developed for the controlled process. The assumptions made during this analysis are likely to be violated significantly when the servomechanism is operated at extreme regions of the actuator stroke. The ability of

the adaptive control algorithm to assure a satisfactory level of model following under such circumstances was examined by operating the servomechanism at two extremities of the actuator stroke. The first mean position selected corresponds to 25% of the actuator stroke as indicated in figure 9:22. Typical examples of the levels of model following that were observed are shown in figures 9:23 and 9:24. The two cases shown correspond to the low and high simulated load conditions respectively and a supply pressure of 100 bar. Both figures represent a high level of 'close' model following. Moreover, they support the modelling simplifications made in developing a reduced complexity adaptive control scheme.

The second set of experiments used to examine the robustness qualities of the adaptive scheme effectively compounded the difficulties of the previous test. For this series of experiments, the servo-system was operated about a mean position corresponding to 75% of the actuator stroke as shown in figure 9:22. In addition, however, the load was also in contact with a horizontally mounted spring. The spring rate was 48.5 KN/m and the spring was compressed by a mean value of 4 cm. for the tests reported below. The process step response recorded in figure 9:25 shows the behaviour of the control scheme under adaptive control; the gain of the integrator acting on the model-process error was set to zero for this experiment. This helps to highlight the influence of the spring generated disturbance. The higher spring force at the end of the extract stroke is witnessed by a significant deterioration in static accuracy. When this test was repeated with the integral gain, K_E initialised with a value of 0.05 a much improved level of behaviour was observed. Figures 9:26 and 9:27, for example, show the cases corresponding to the low and high simulated load conditions respectively. In both cases model following behaviour is highly acceptable. More importantly however, the quality of steady state performance exhibits a considerable improvement over that shown in figure 9:25.

The command signals used in the previous series of experiments are of a fixed form and repetitive. As such, it can be argued that they are not representative of the operating signals that would be encountered with real applications. A series of tests was therefore conducted with a band limited pseudo-random command signal; this was generated using a standard output from a Hewlet Packard 3582A spectrum analyser. The frequency content of the command signal was restricted to a maximum of 1 Hz. and was not considered to be an unrealistic limitation. The quality of model following that was obtained is typified by the response shown in

figure 9:28. This only shows the command input and the response of the controlled process. The response of the reference model is not shown because it was indistinguishable from that of the controlled process. This represents an excellent degree of model following. It was maintained consistently over a variety of operating conditions and following perturbations to the dynamics of the controlled process. An additional observation that was made during this series of tests is shown in figure 9:29. This response demonstrates a case of the electro-hydraulic servomechanism being slew rate limited. The check procedure developed in section 6.3 of chapter 6 intervenes to suspend parameter adaptation and lock the reference model onto the controlled process without unduly disrupting the behaviour of the controlled process. Its effectiveness can be gauged by the smooth transition out of a saturated control signal operating condition.

SERVOVALVE 1	SERVOVALVE 2
MOOG Series 76 -3 dB Bandwidth > 50 Hz. Flow Gain At 70 bar 1.26 L/min/mA, spool travel < 25% 5.4 L/min/mA, spool travel > 25%	DOWTY Series 4551 -3 dB Bandwidth > 50 Hz. Flow Gain At 70 bar 3.8 L/min/mA
CYLINDER DRIVE	
Stroke: 610 mm, y=0 At Actuator Mid-Position Piston Area: 2025 mm^2 Annulus Area: 1380 mm^2 Additional Dead Volume: 2L On Each Side	
LOAD SYSTEM	
890 Kg Mounted On A Free Running Trolley Very Low Damping	
SUPPLY PRESSURE CONTROL	
Continuously Variable From 60 To 160 bar	
SPRING	
Spring Force Coefficient: 48.5 KN/m	

TABLE 9:1 ELECTRO-HYDRAULIC SERVO-SYSTEM TEST RIG DATA

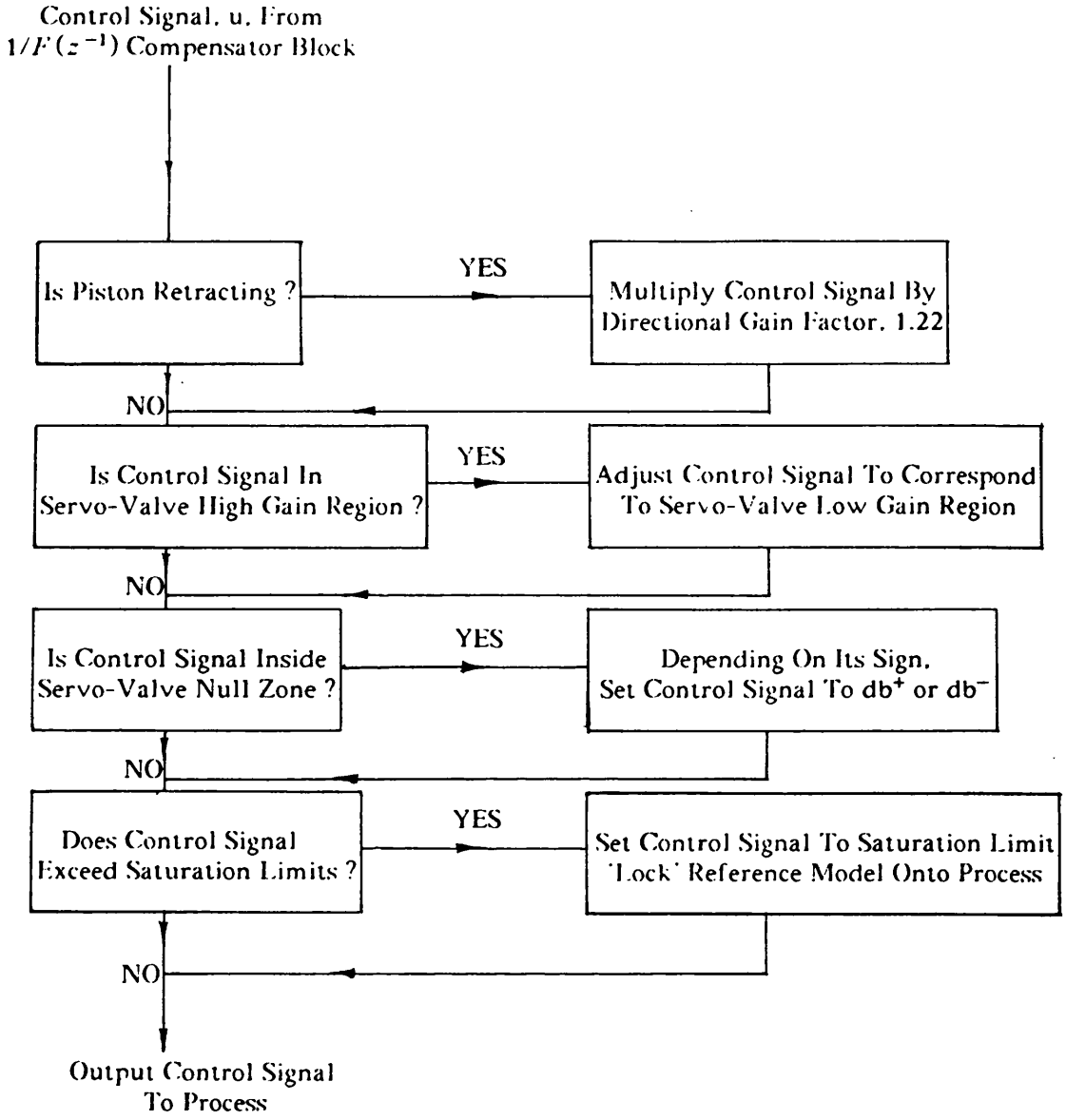

FLOW DIAGRAM 9:1 ELECTRO-HYDRAULIC SERVOMECHANISM

PERFORMANCE LINEARISATION PROCEDURE

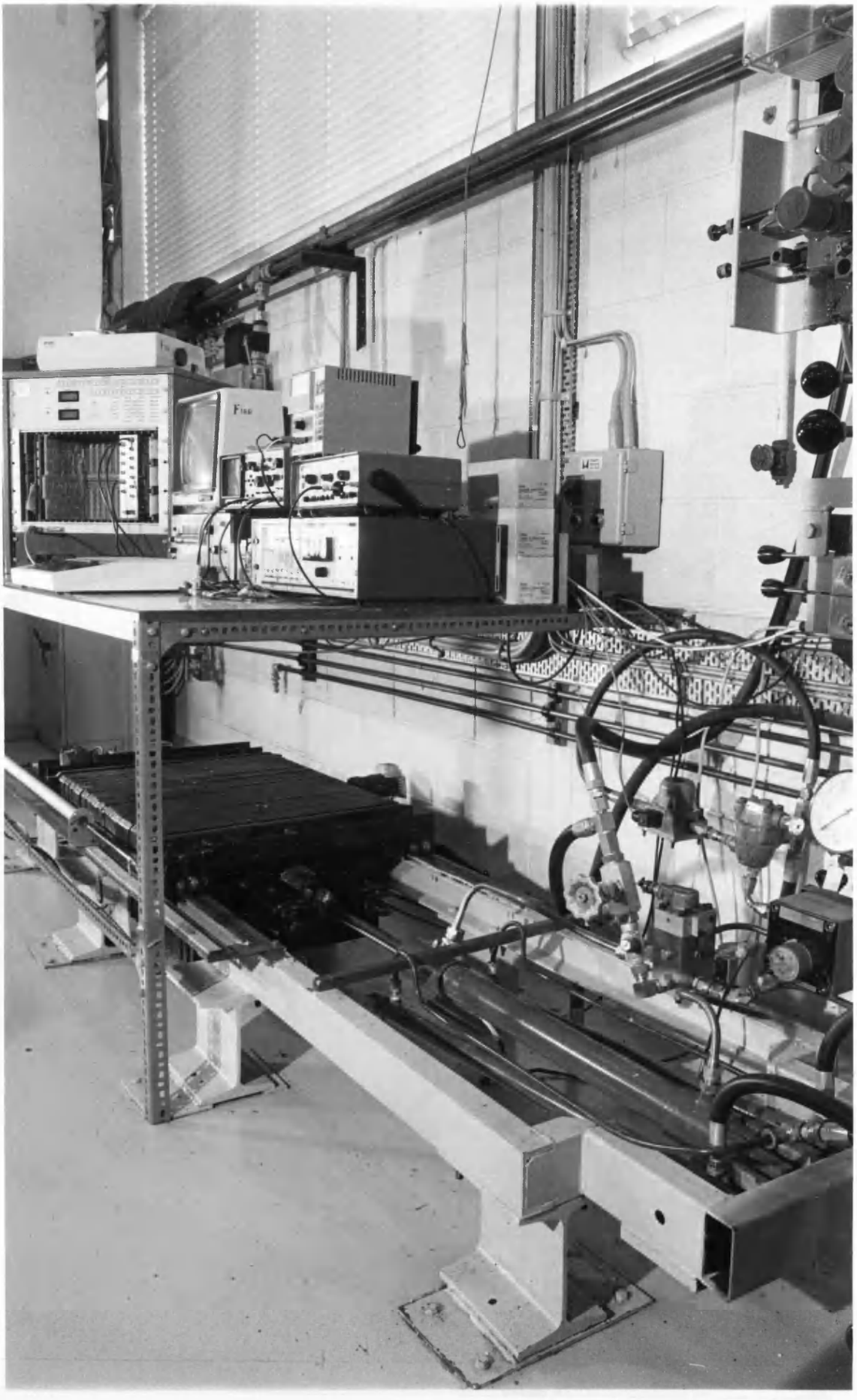

FIGURE 9:1 Electro-Hydraulic Servomechanism Test Rig

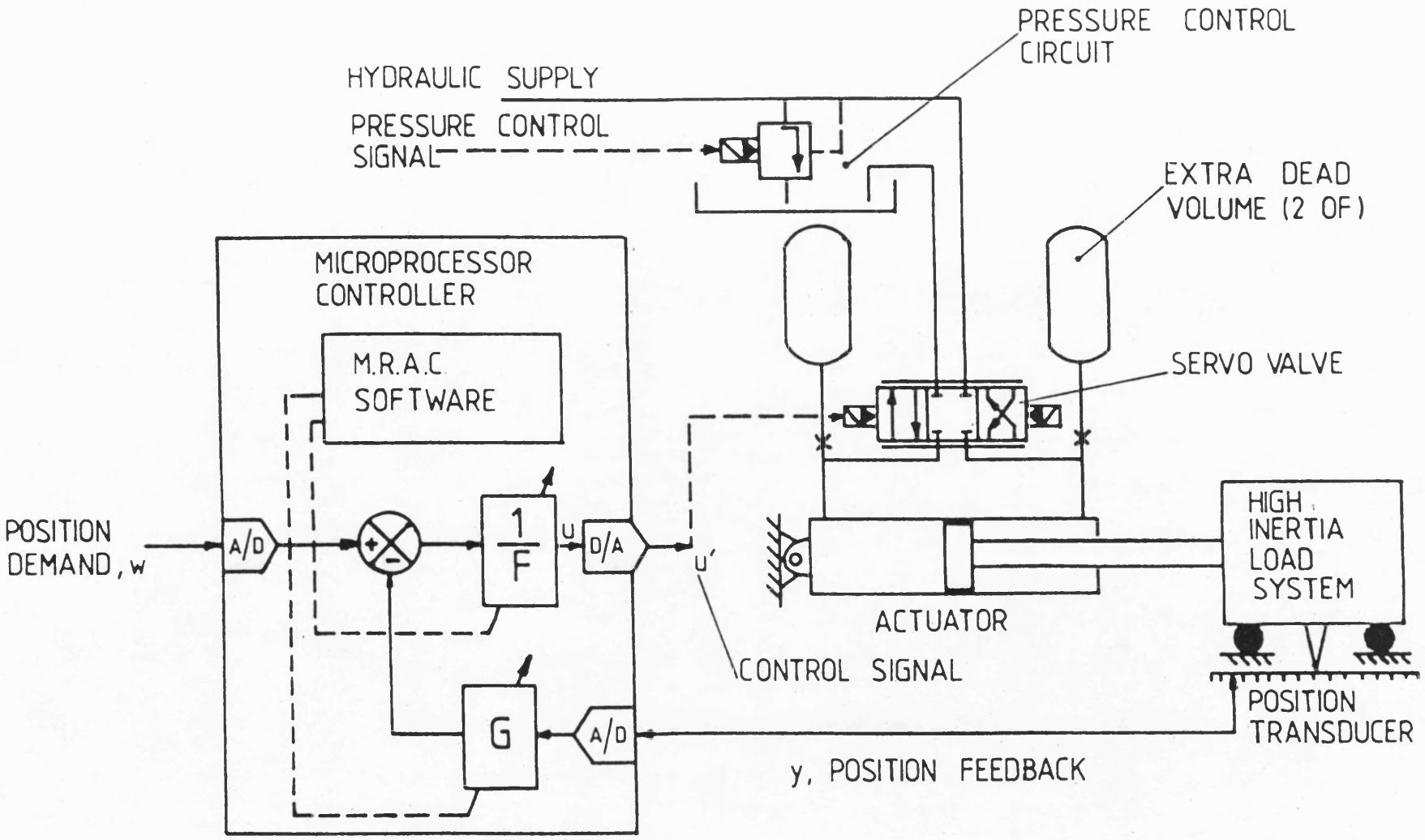

FIGURE 9:2 Electro-Hydraulic Position Control Servomechanism

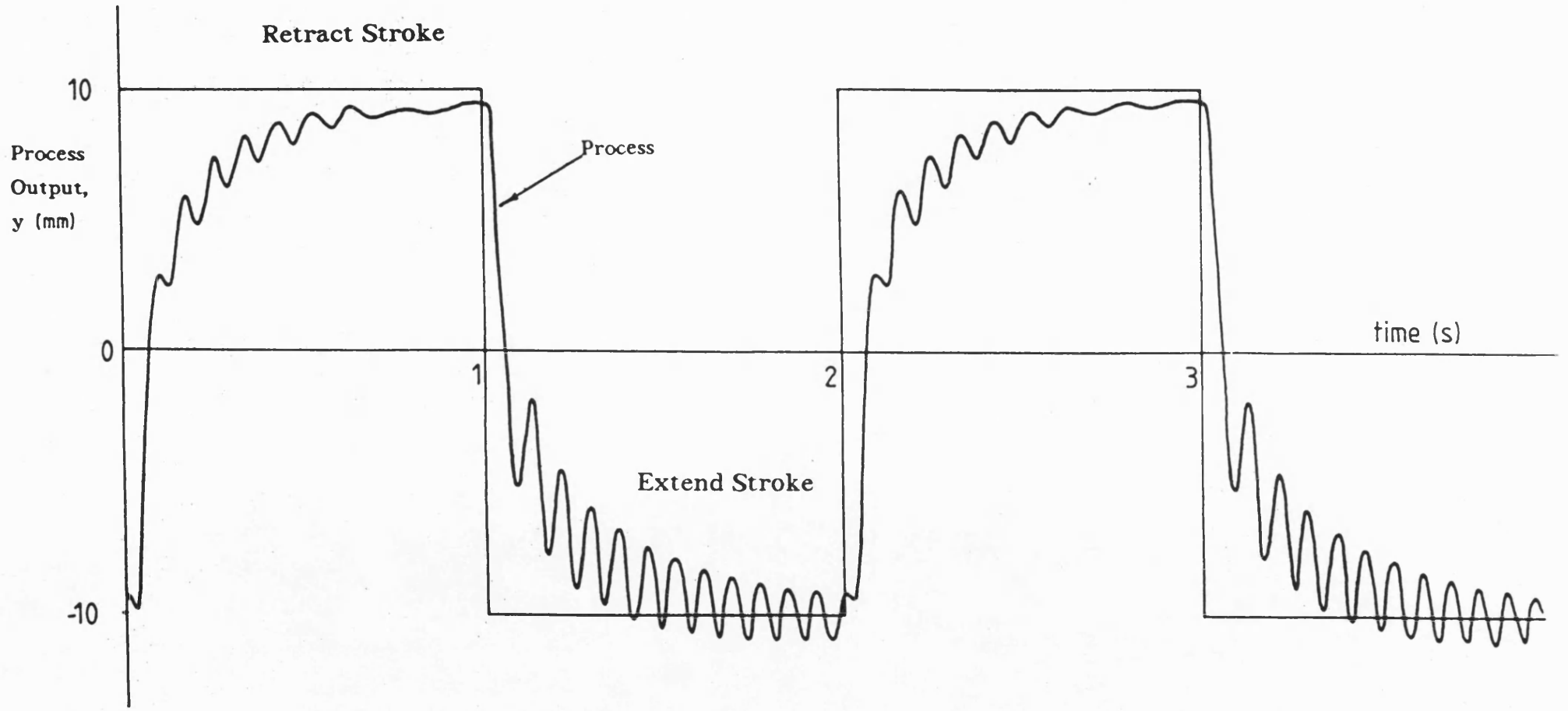

FIGURE 9:3 Electro-Hydraulic Servo-System Closed Loop Step Response Behaviour

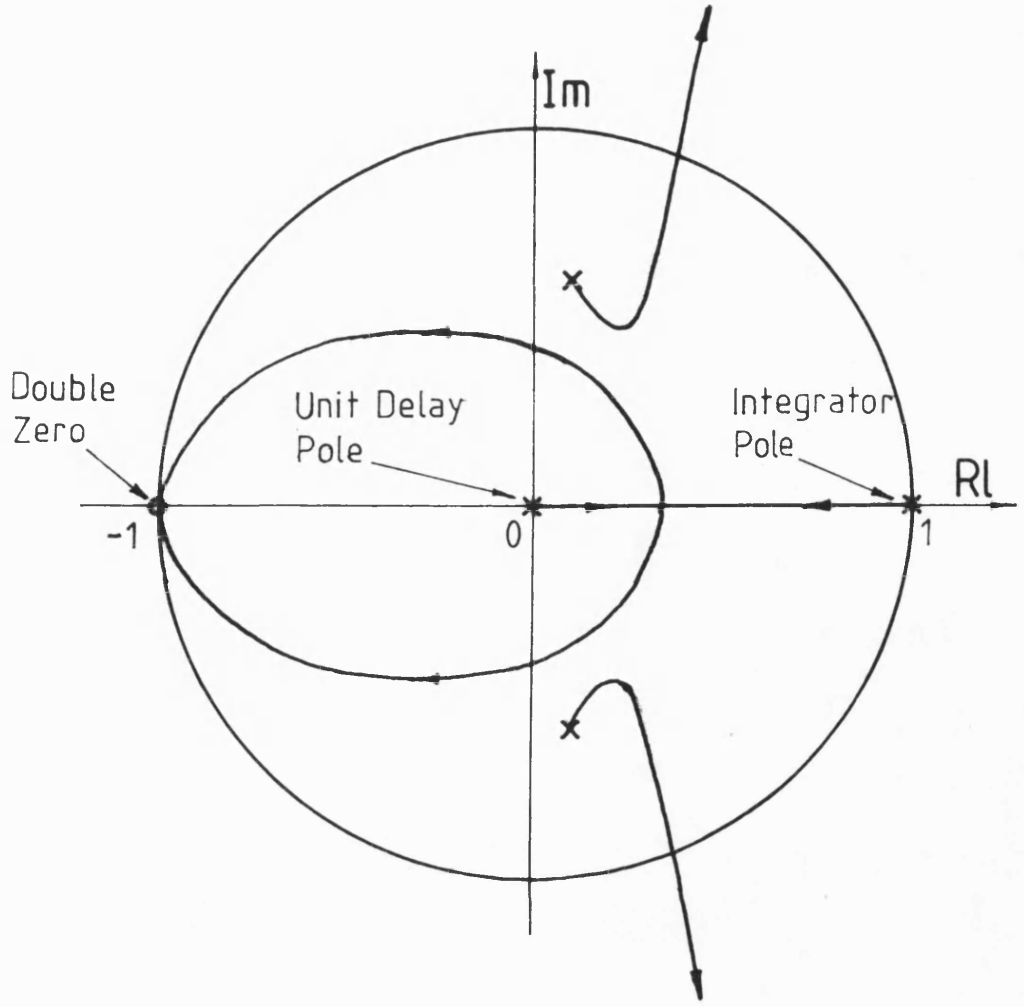

FIGURE 9:4 Root Locus Diagram For Electro-Hydraulic Control Scheme

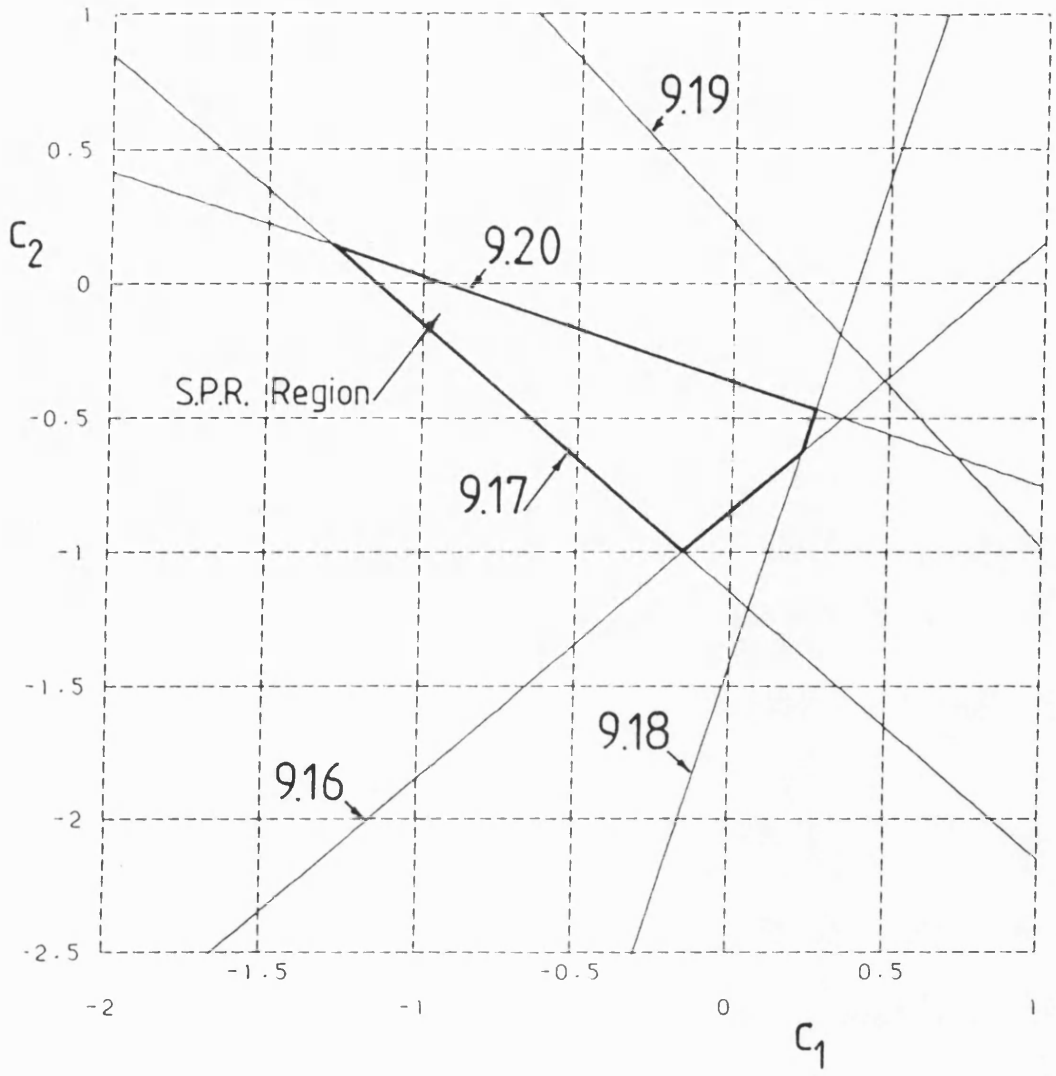

FIGURE 9:5 c_1–c_2 Parameter Space Satisfying S.P.R. Condition

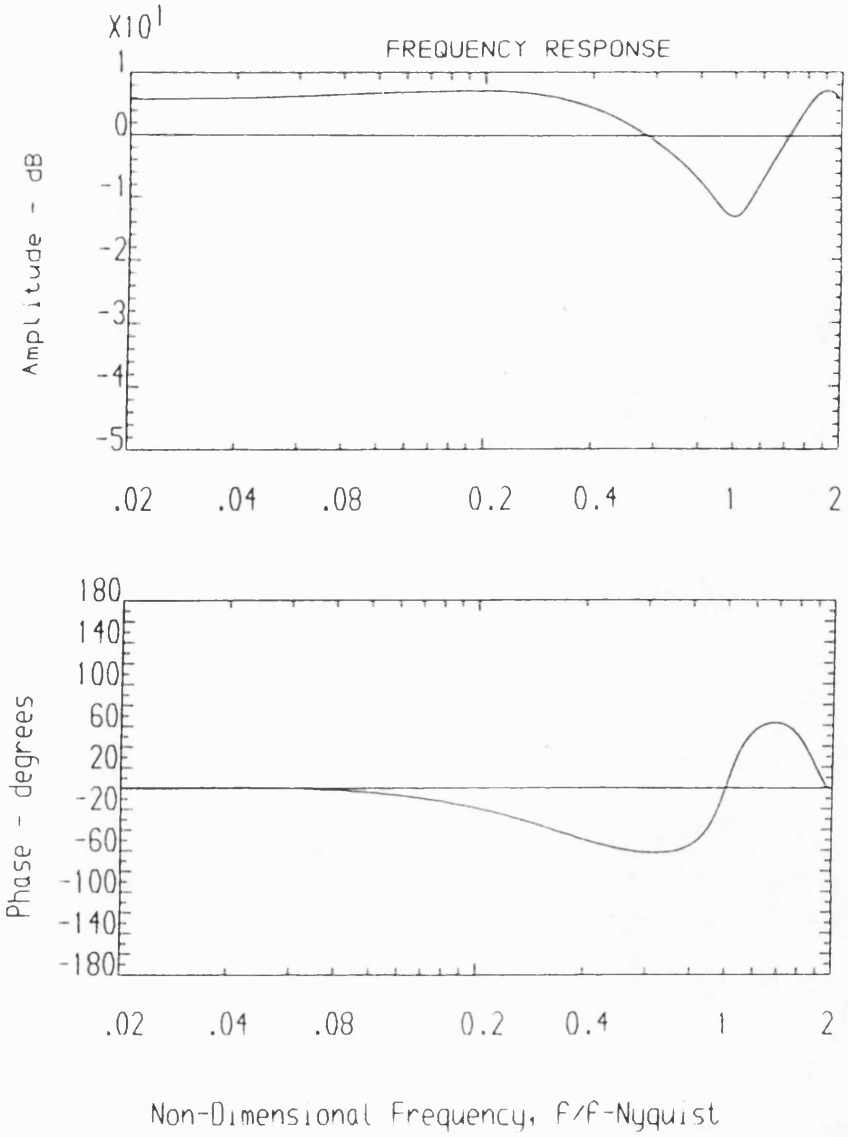

FIGURE 9:6 S.P.R. Transfer Function Frequency Response Characteristics

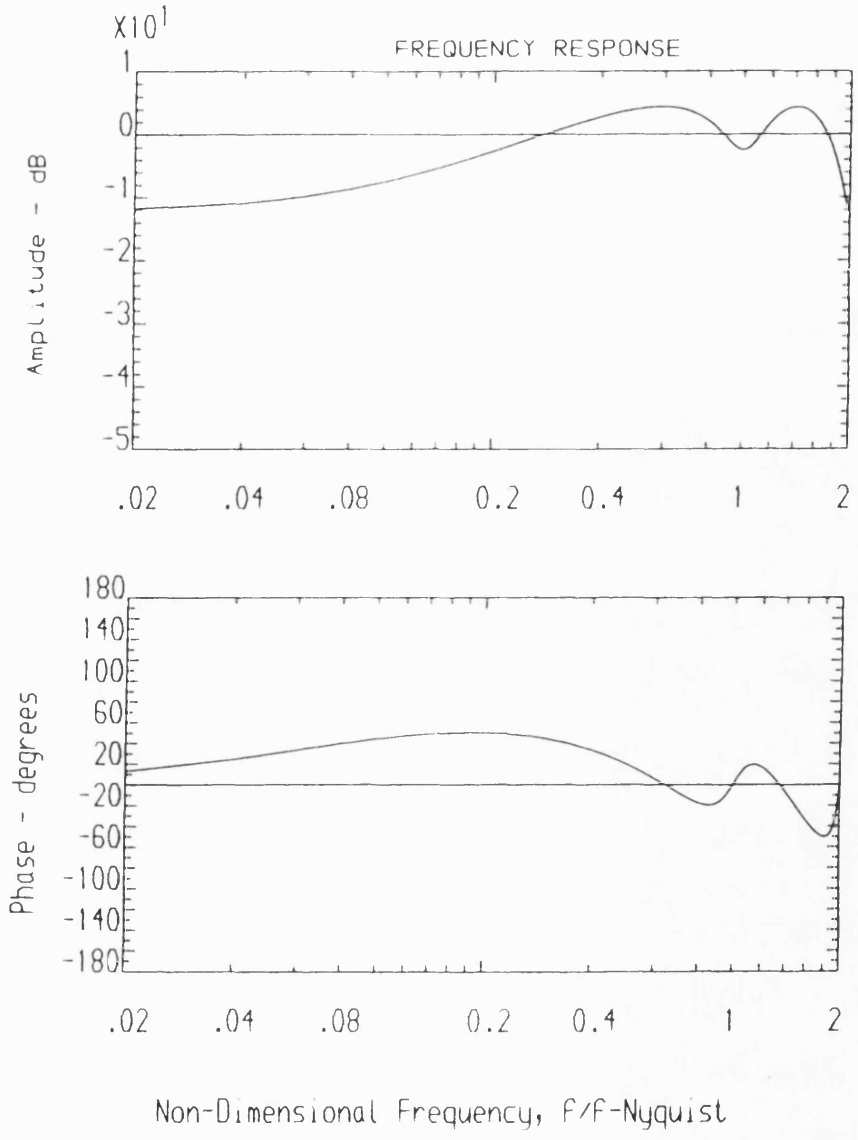

FIGURE 9:7 Error Filter Transfer Function Frequency Response Characteristics

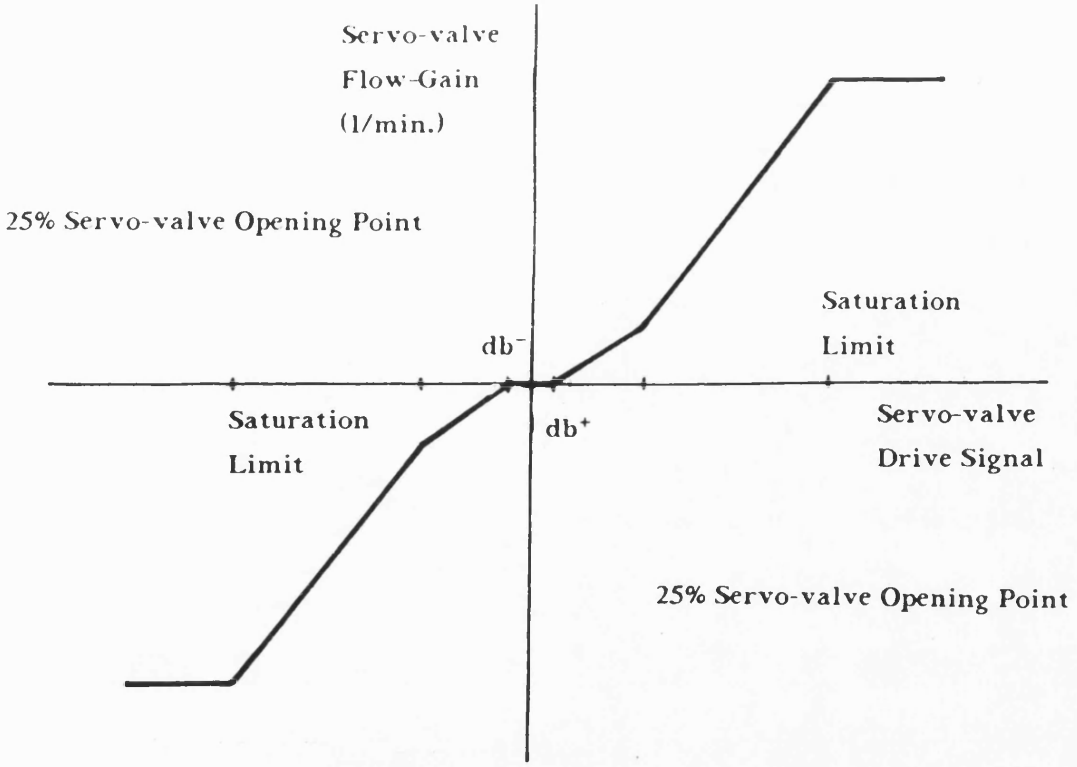

FIGURE 9:8 Servo-Valve Non-Linear Performance Characteristics

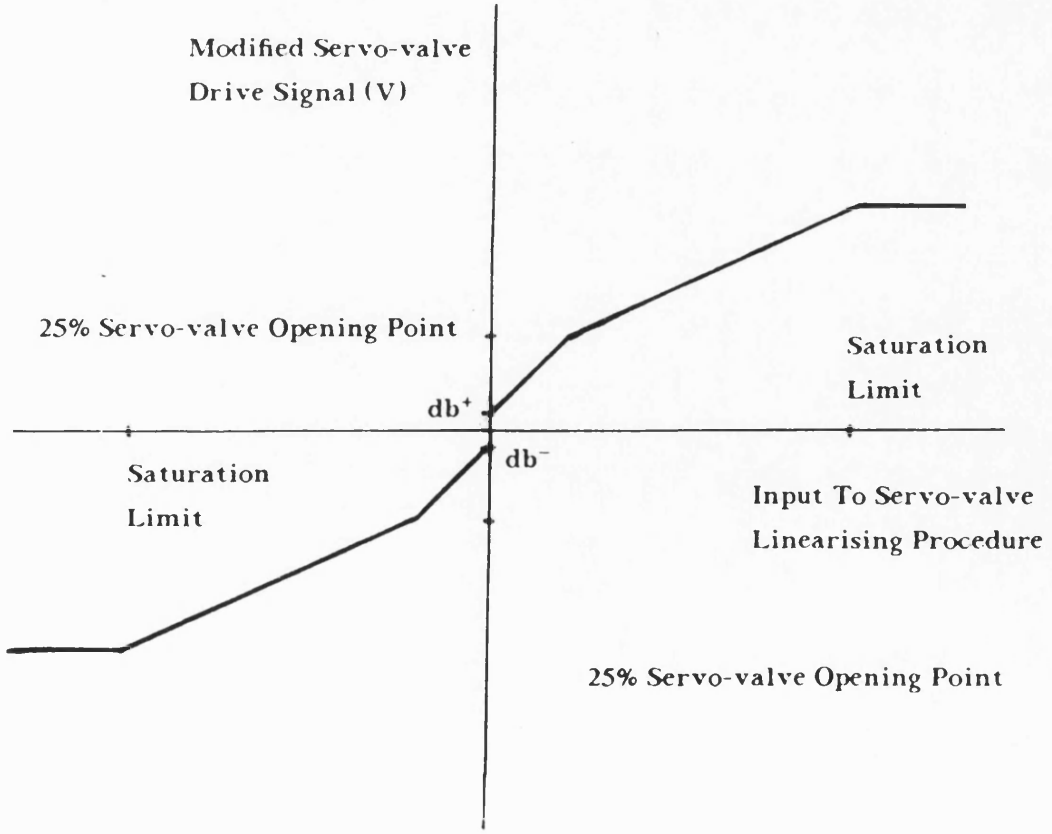

FIGURE 9:9 Software Filter Procedure Designed To Linearise Servo-Valve Non-Linear Characteristics

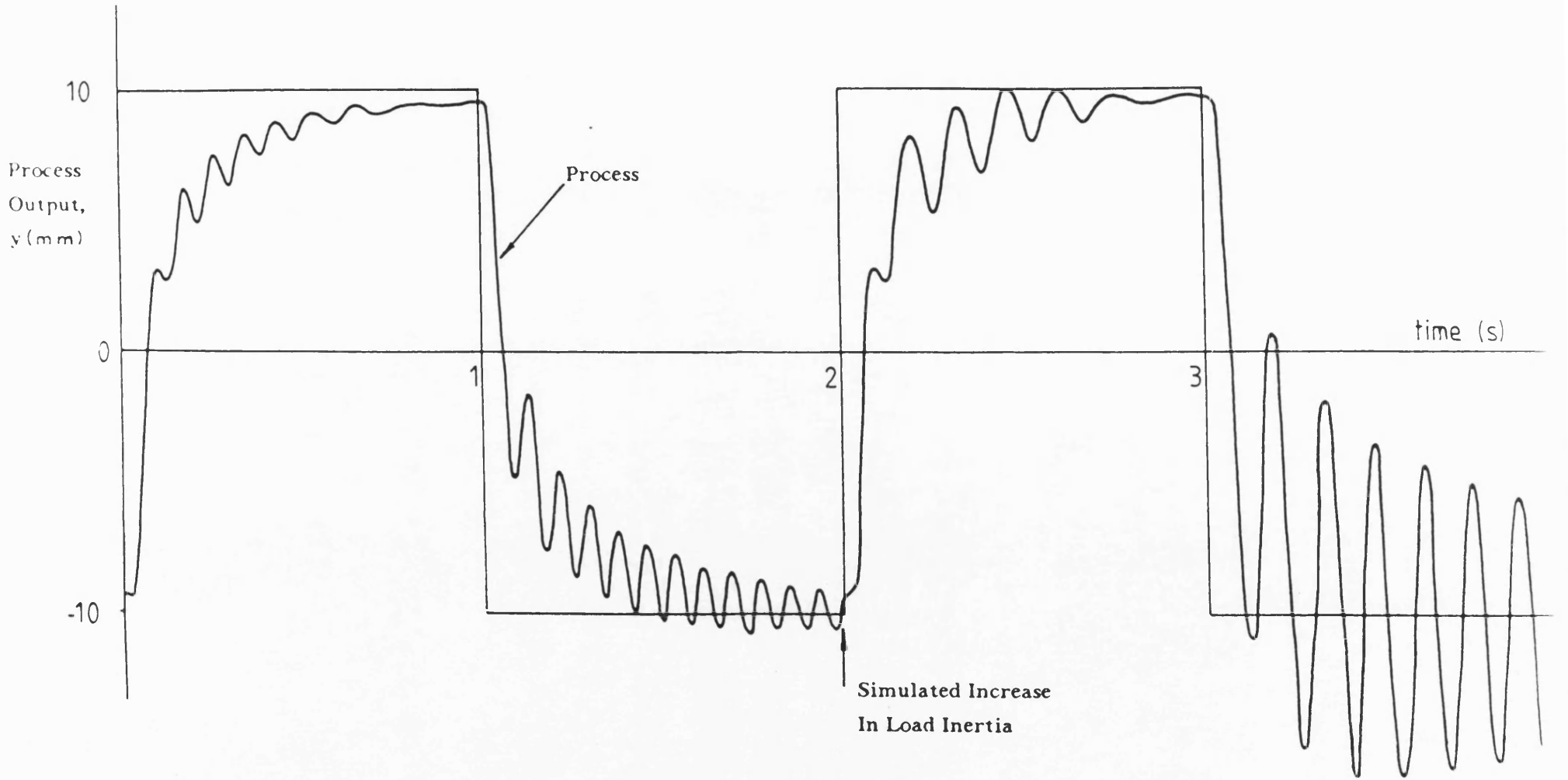

FIGURE 9:10 Comparison Of Electro-Hydraulic System Response For Different Simulated Load Conditions

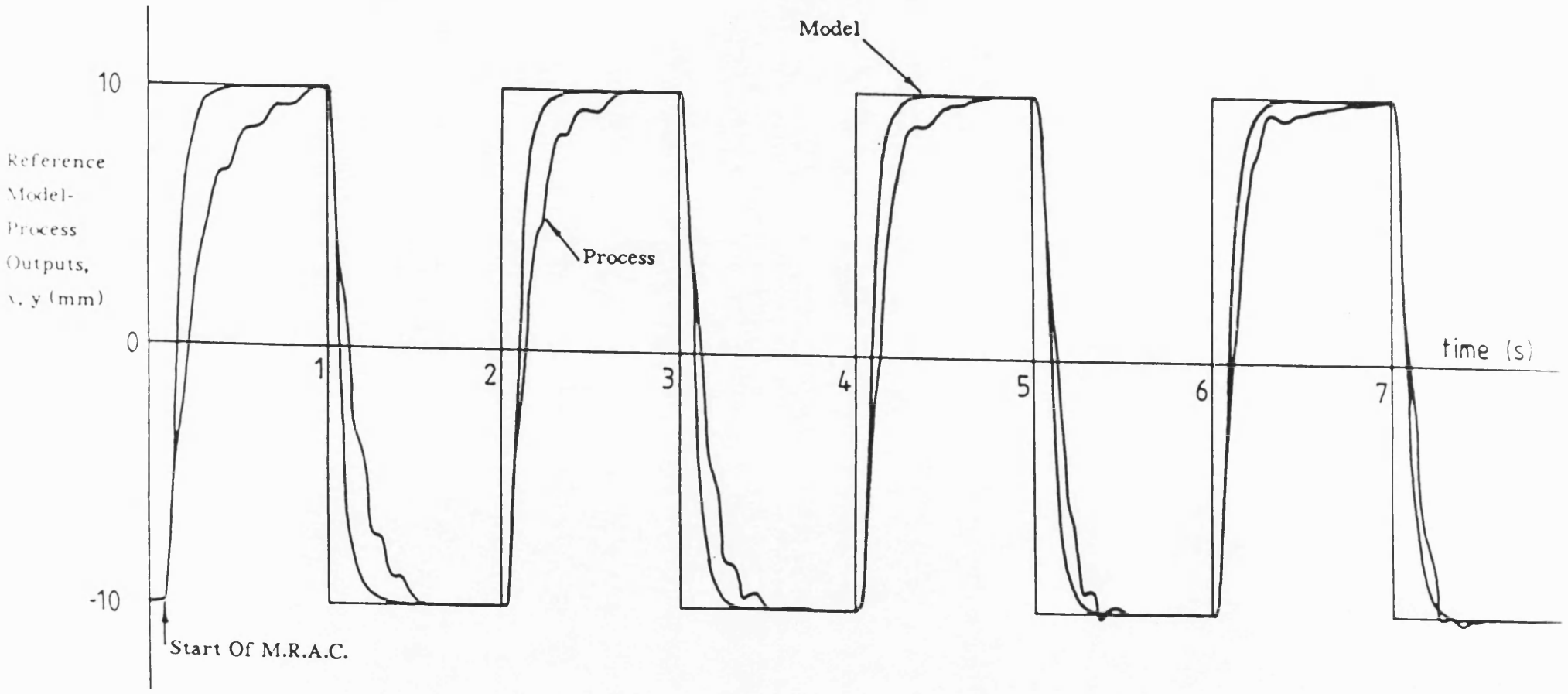

FIGURE 9:11 Start Of Model Reference Adaptive Control

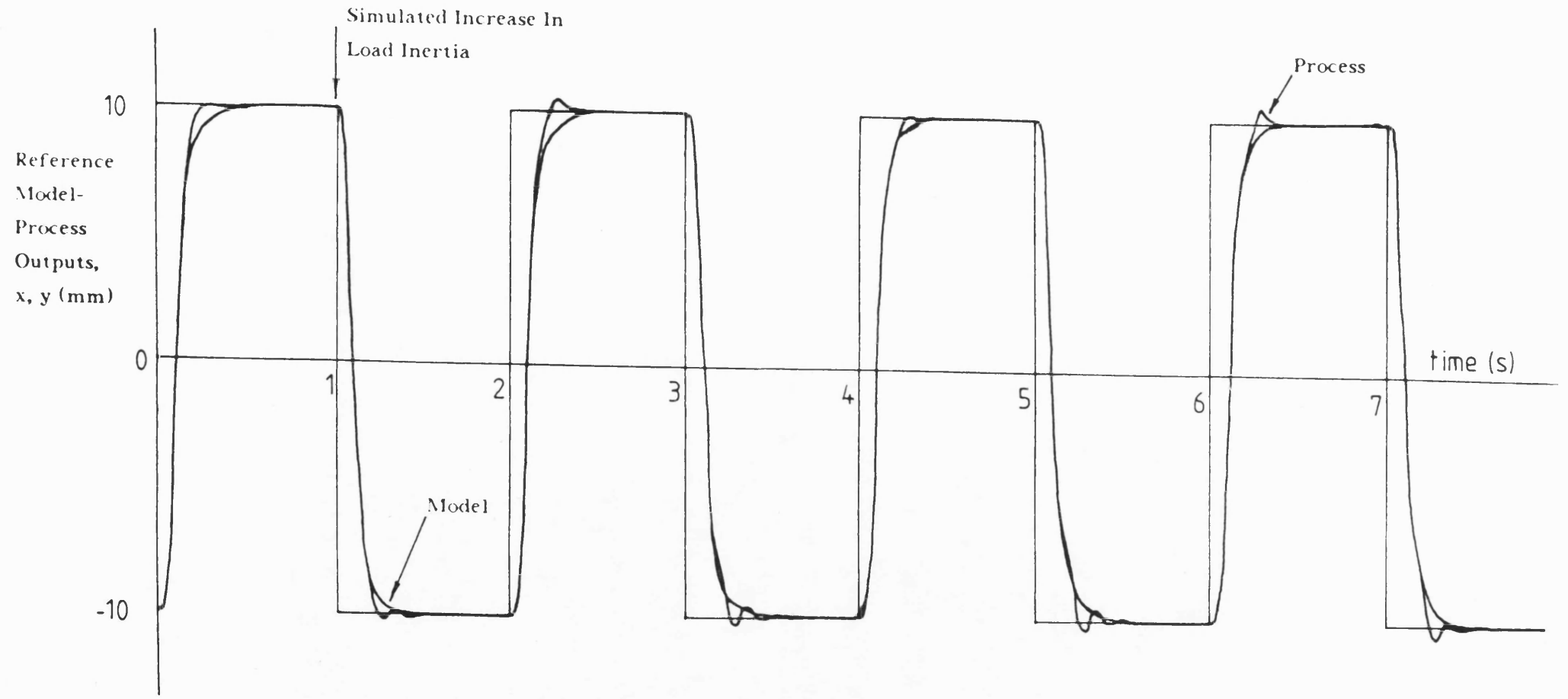

FIGURE 9:12 Adaptive System Response Following A Simulated Increase In Load Inertia

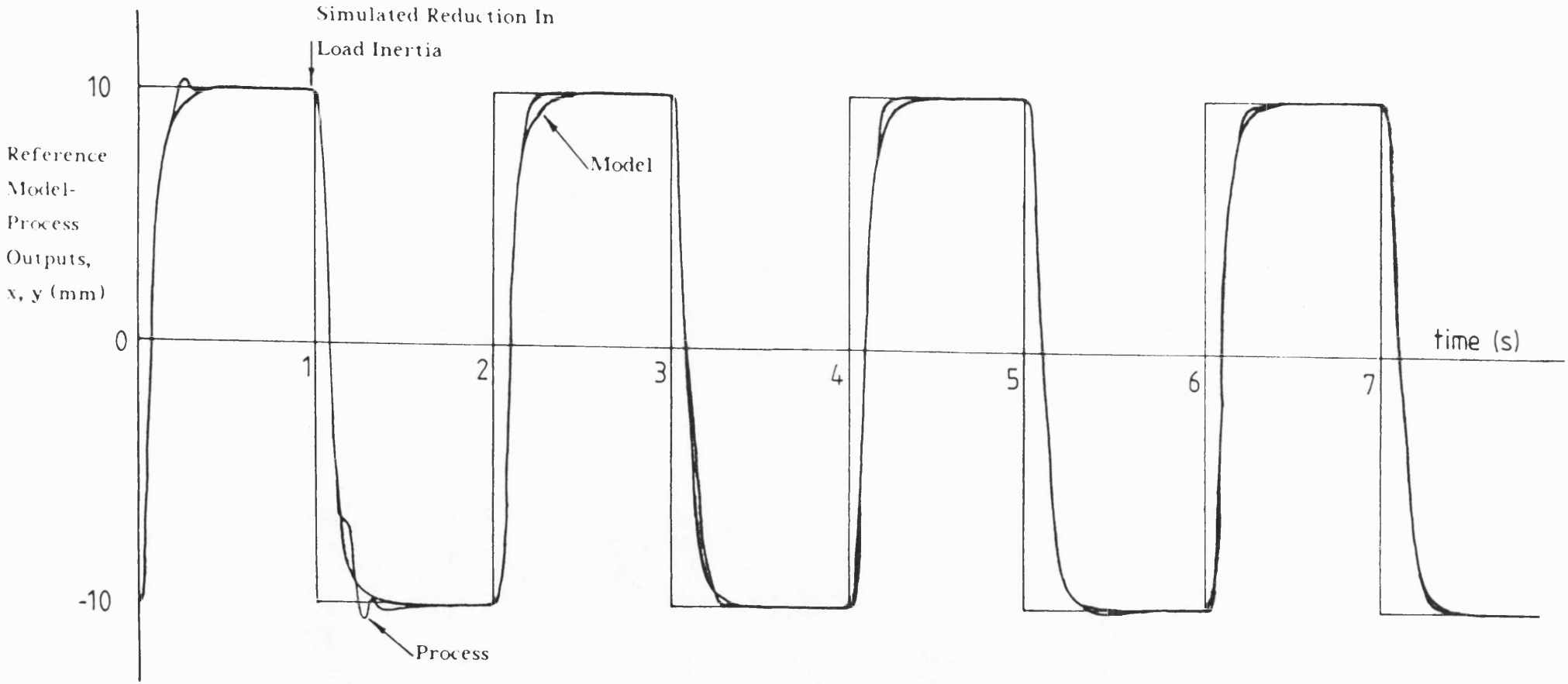

FIGURE 9:13 Adaptive System Response Following A Simulated Reduction In Load Inertia

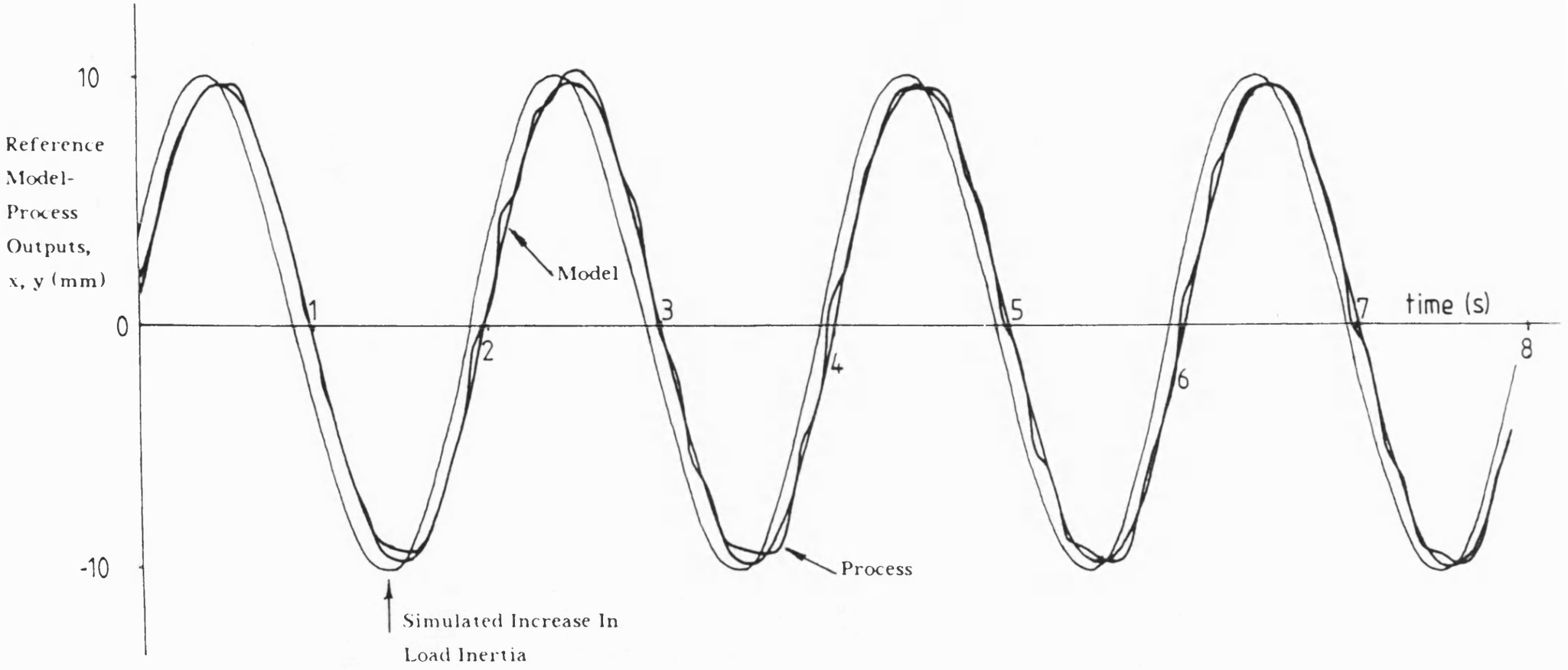

FIGURE 9:14 Adaptive System Response Following A Simulated Increase In Load Inertia (Sinusoidal Command Signal)

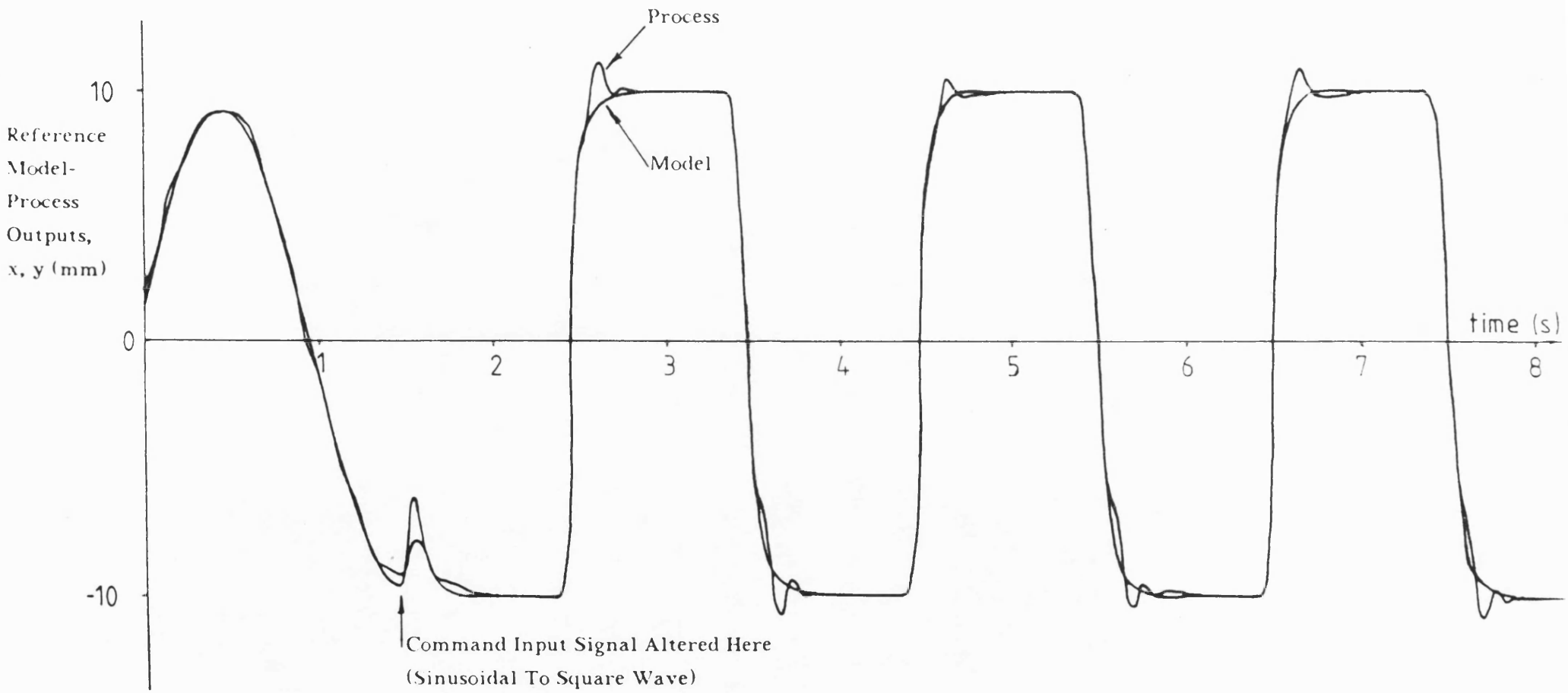

FIGURE 9:15 Adaptive System Behaviour For Different Waveform Command Signals

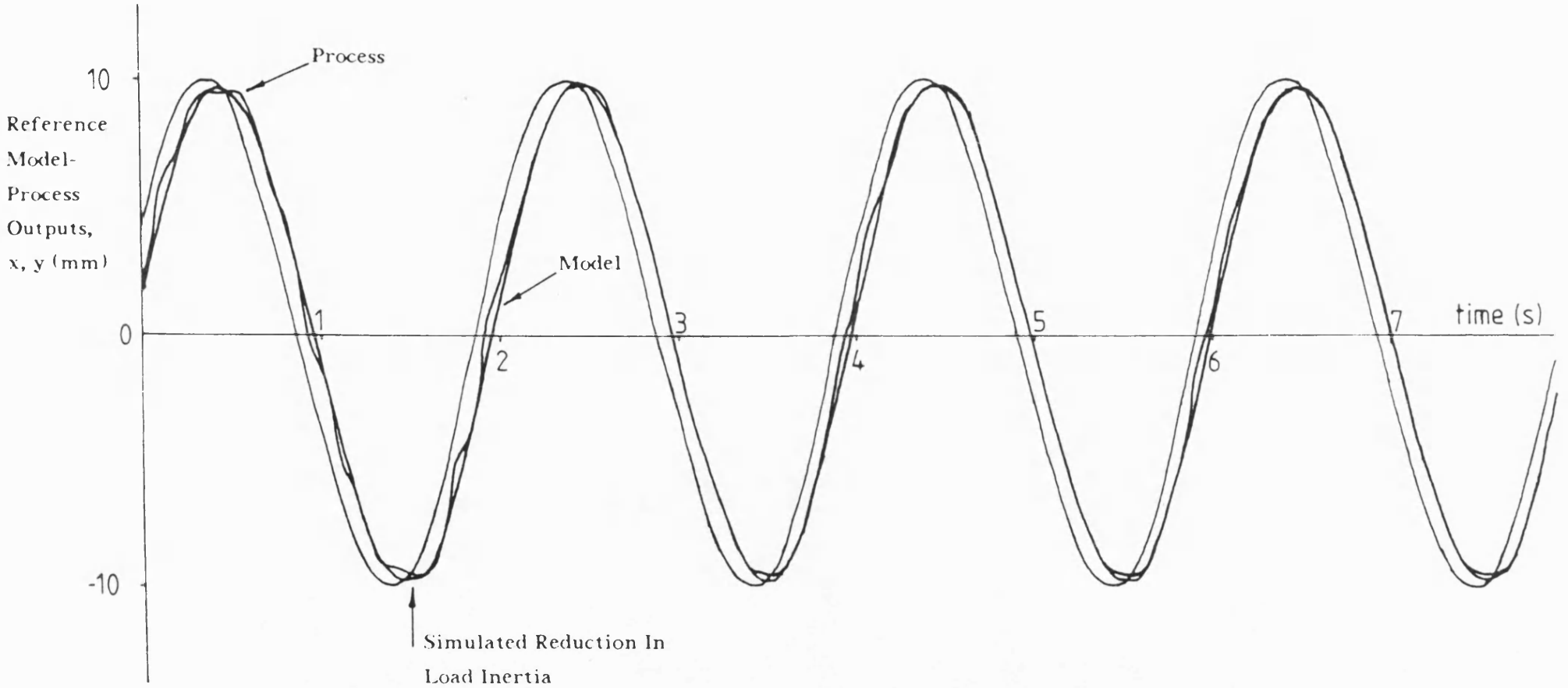

FIGURE 9:16 Adaptive System Response Following A Simulated Reduction In Load Inertia (Sinusoidal Command Signal)

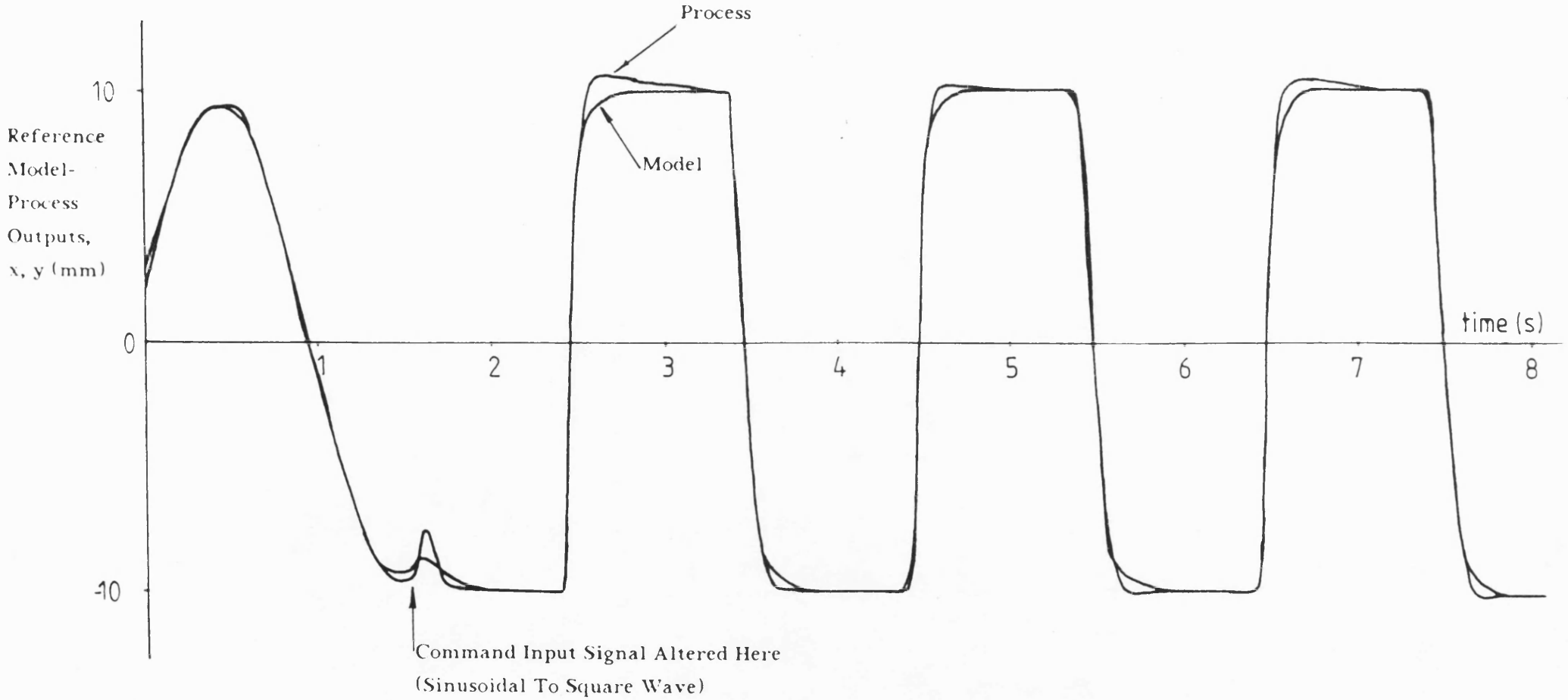

FIGURE 9:17 Adaptive System Behaviour For Different Waveform Command Signals

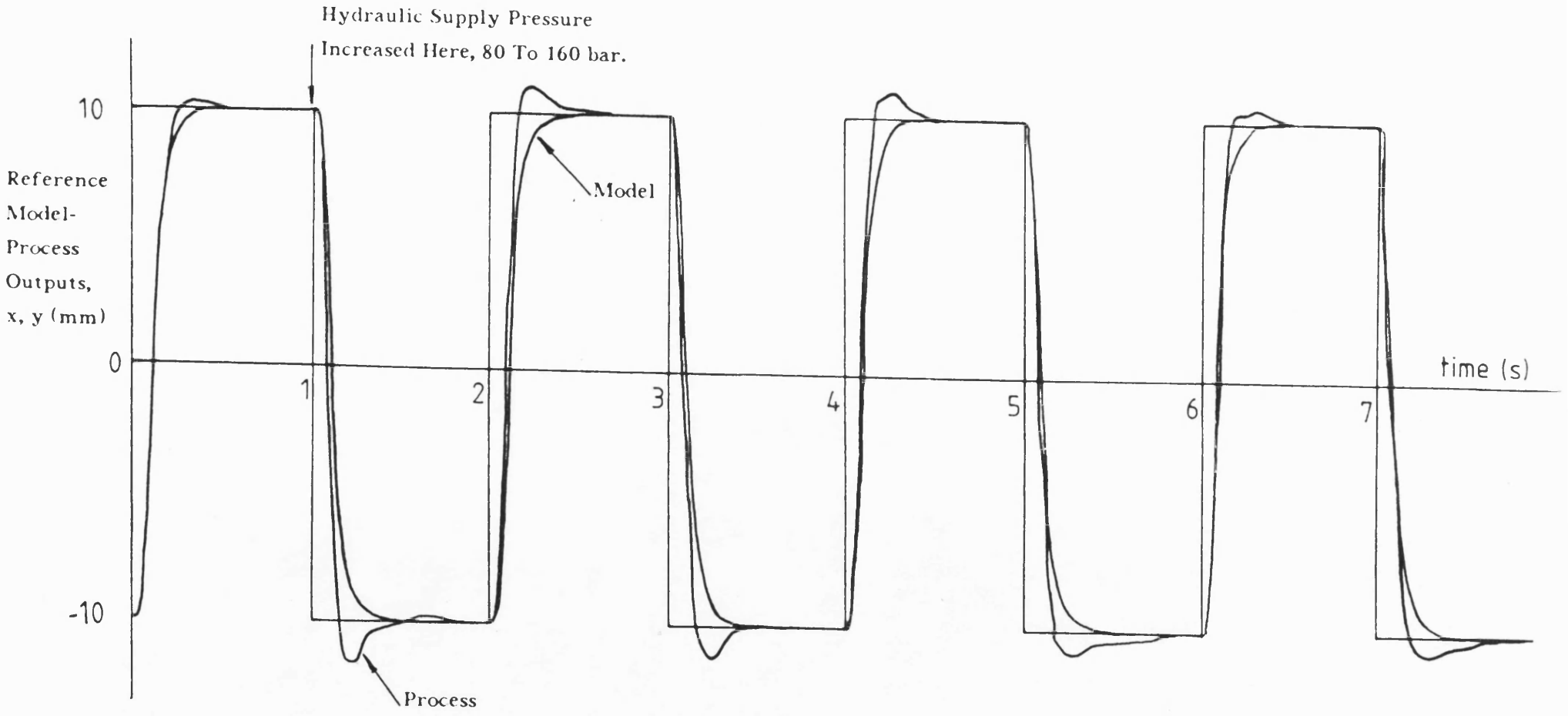

FIGURE 9:18 Adaptive System Response Following An Increase In Hydraulic Supply Pressure

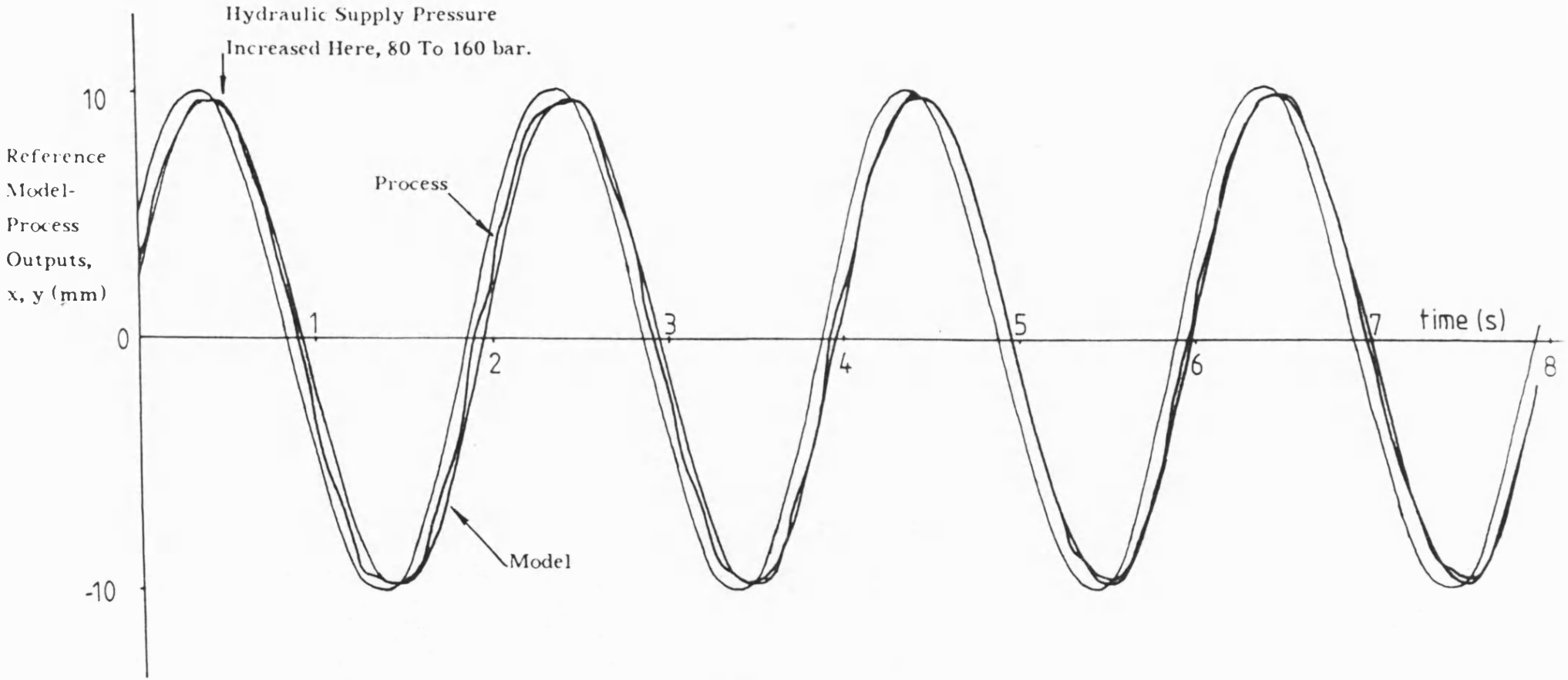

FIGURE 9:19 Adaptive System Response Following An Increase In Hydraulic Supply Pressure (Sinusoidal Command Signal)

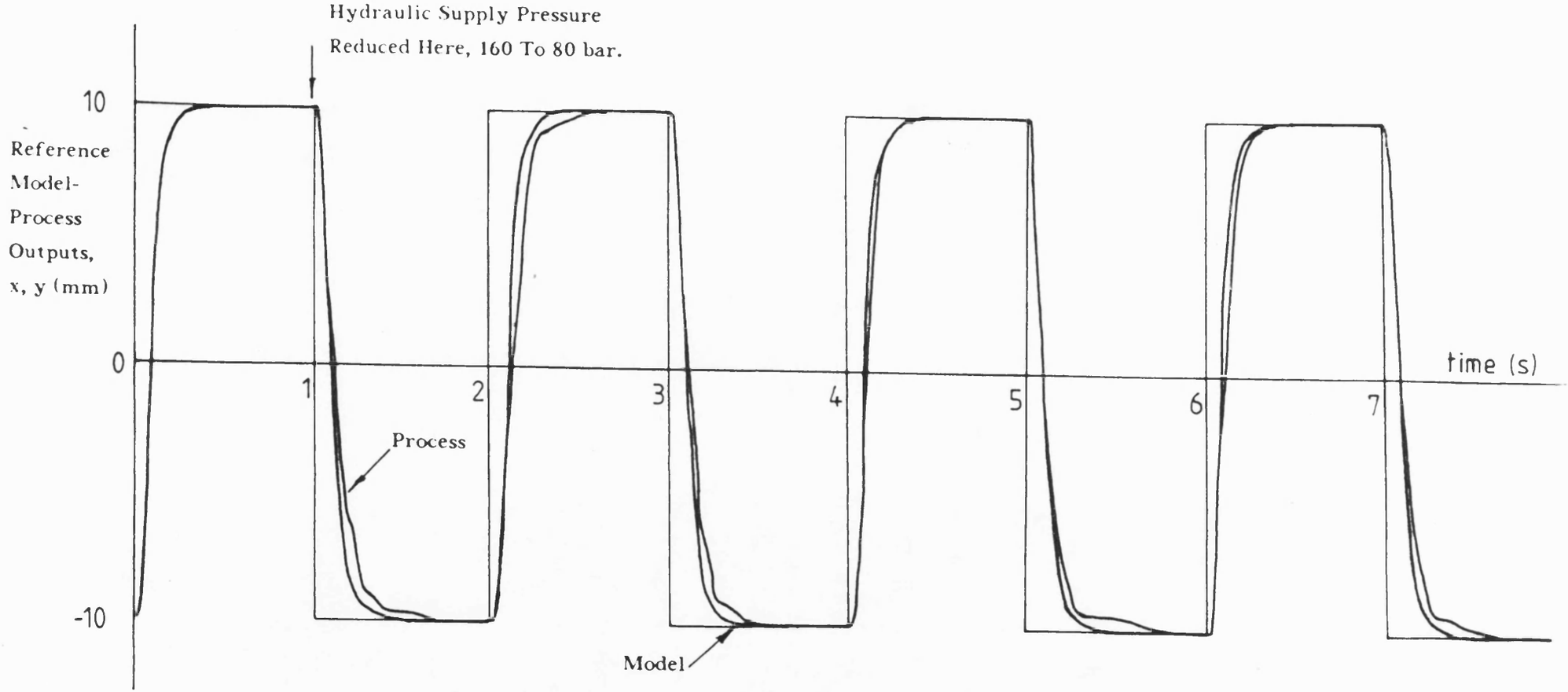

FIGURE 9:20 Adaptive System Response Following A Reduction In Hydraulic Supply Pressure

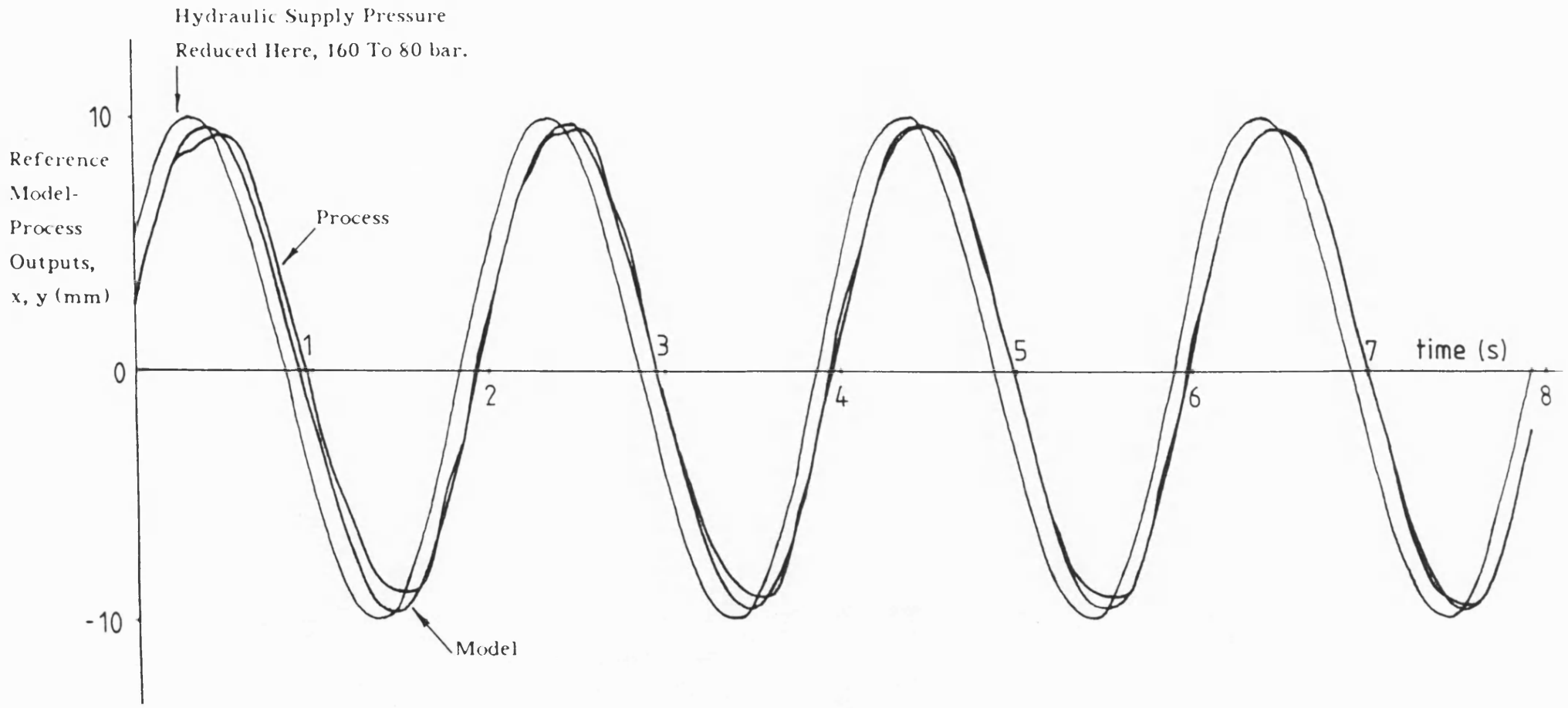

FIGURE 9:21 Adaptive System Response Following A Reduction In Hydraulic Supply Pressure (Sinusoidal Command Signal)

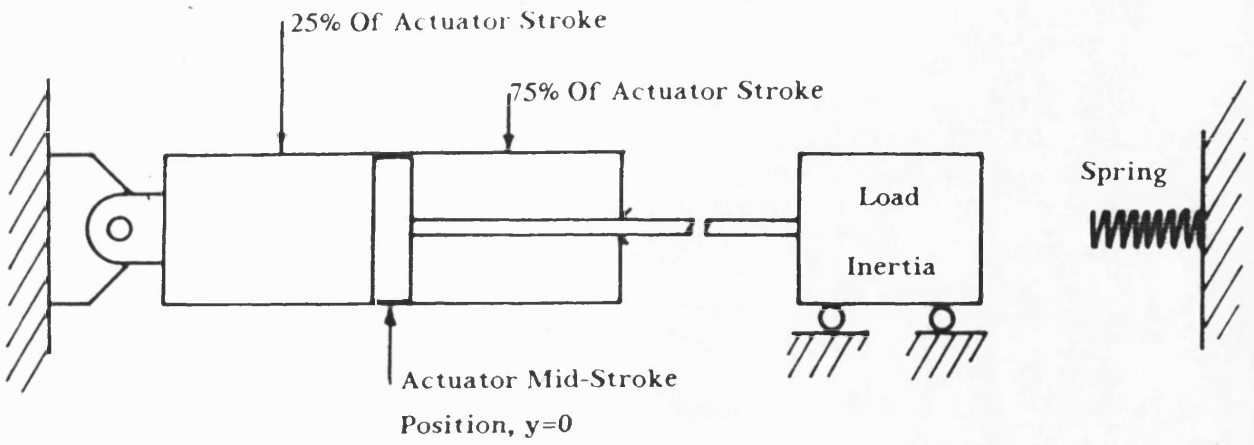

FIGURE 9:22 Actuator Reference Points And Spring Loading Arrangement

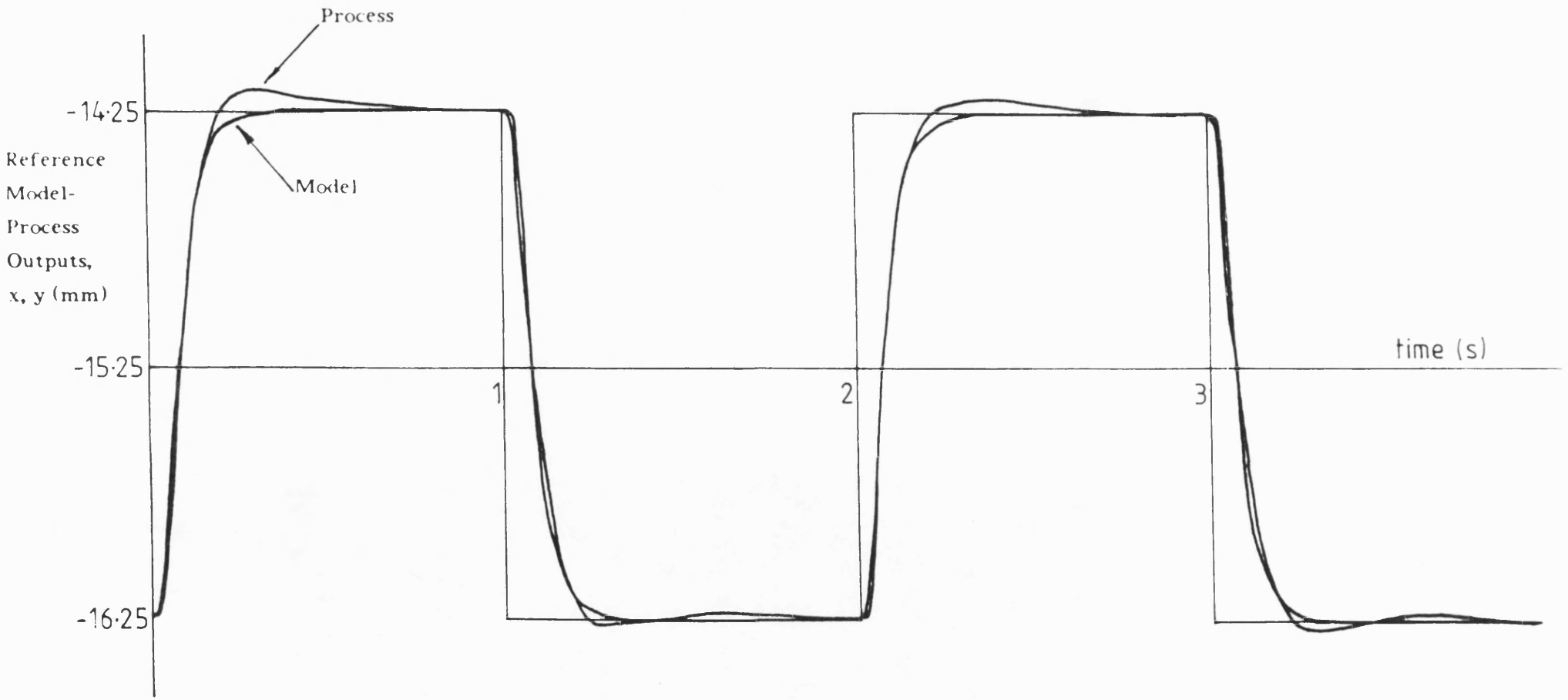

FIGURE 9:23 A Typical Example Of Model Following Behaviour
25% Of Actuator Stroke Operating Point
Low Simulated Load Condition

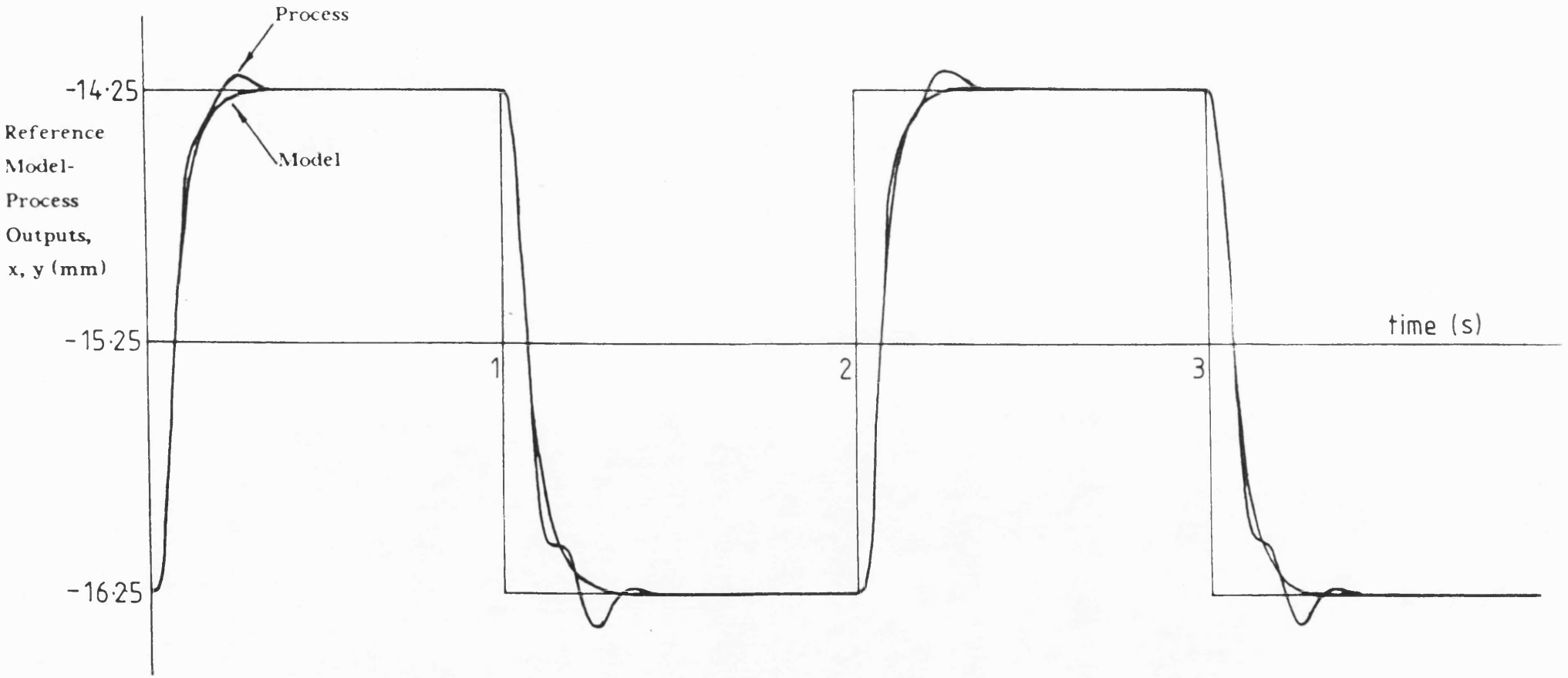

FIGURE 9:24 A Typical Example Of Model Following Behaviour
25% Of Actuator Stroke Operating Point
High Simulated Load Condition

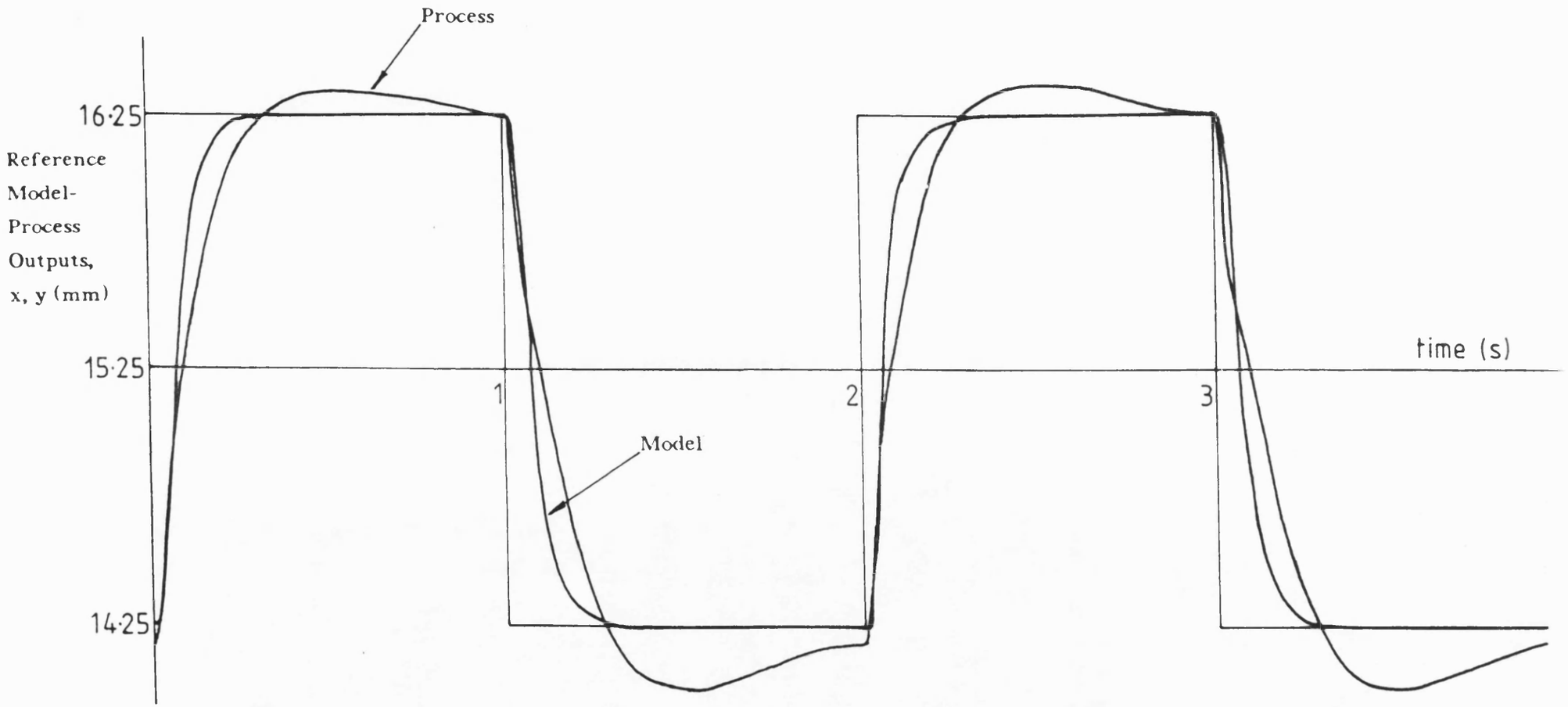

FIGURE 9:25 Model Following Behaviour With Integral-Action Controller Redundant Load Inertia In Contact With Spring

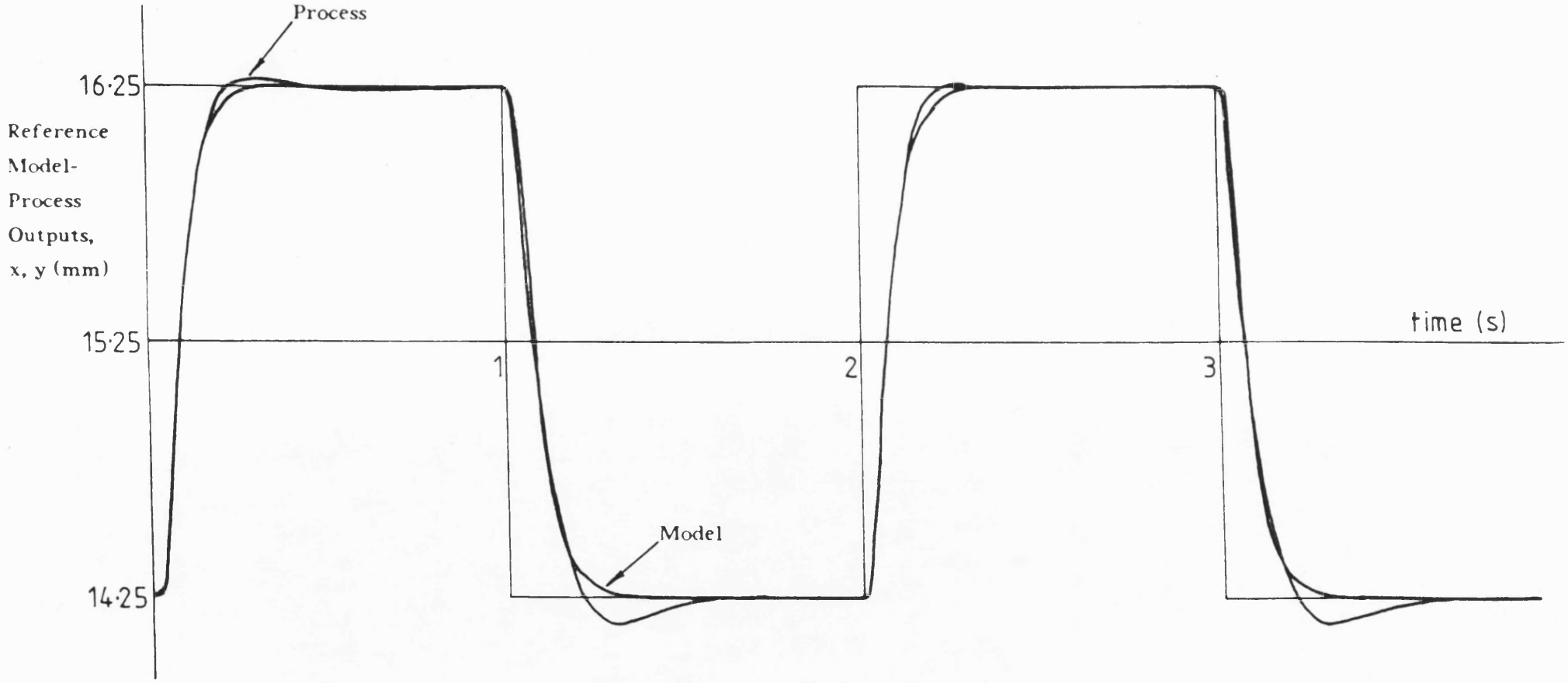

FIGURE 9:26 A Typical Example Of Model Following Behaviour
75% Of Actuator Stroke Operating Point
Load Inertia In Contact With Spring (Low Simulated Load Condition)

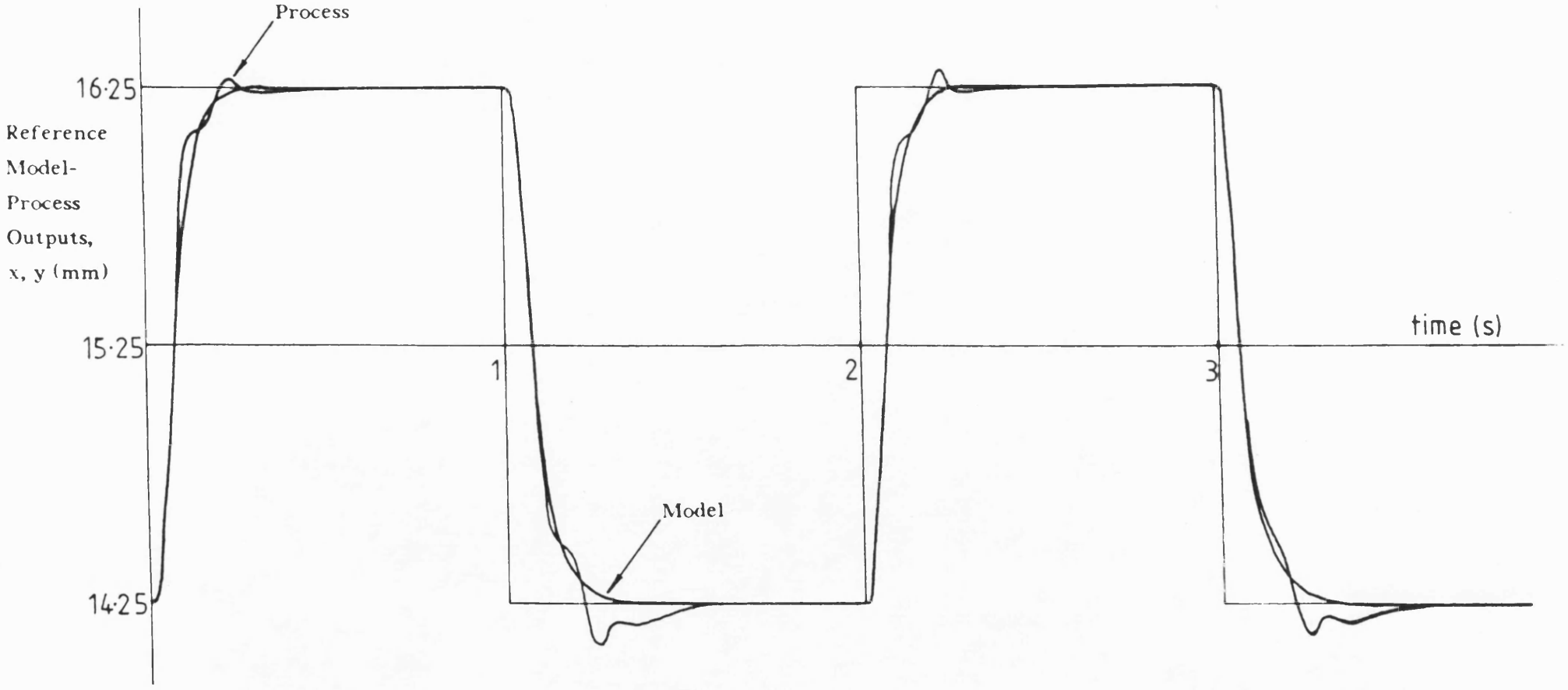

FIGURE 9:27 A Typical Example Of Model Following Behaviour
75% Of Actuator Stroke Operating Point
Load Inertia In Contact With Spring (High Simulated Load Condition)

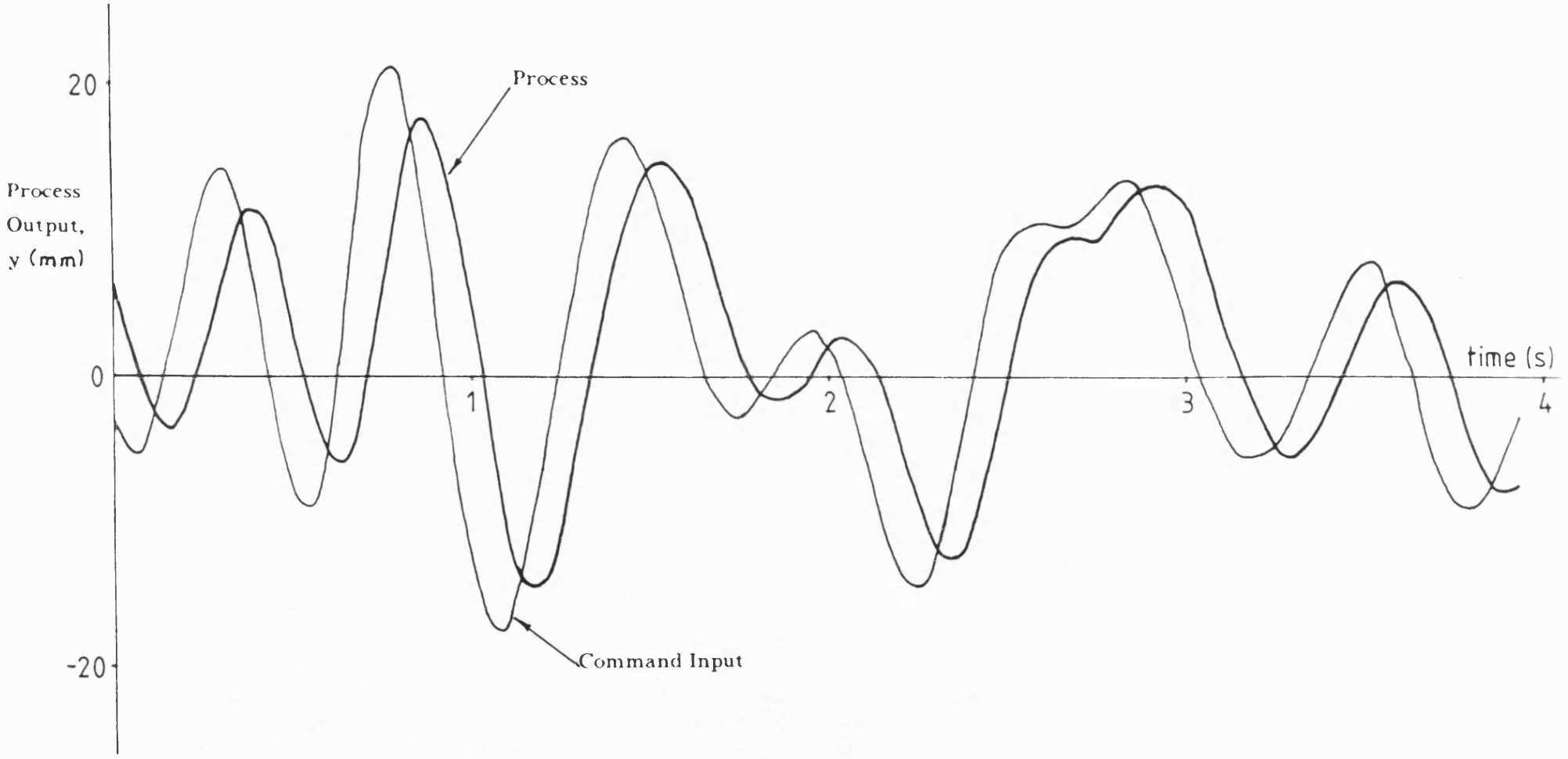

FIGURE 9:28 A Typical Example Of Control System Behaviour With A P.R.B.S. Command Signal

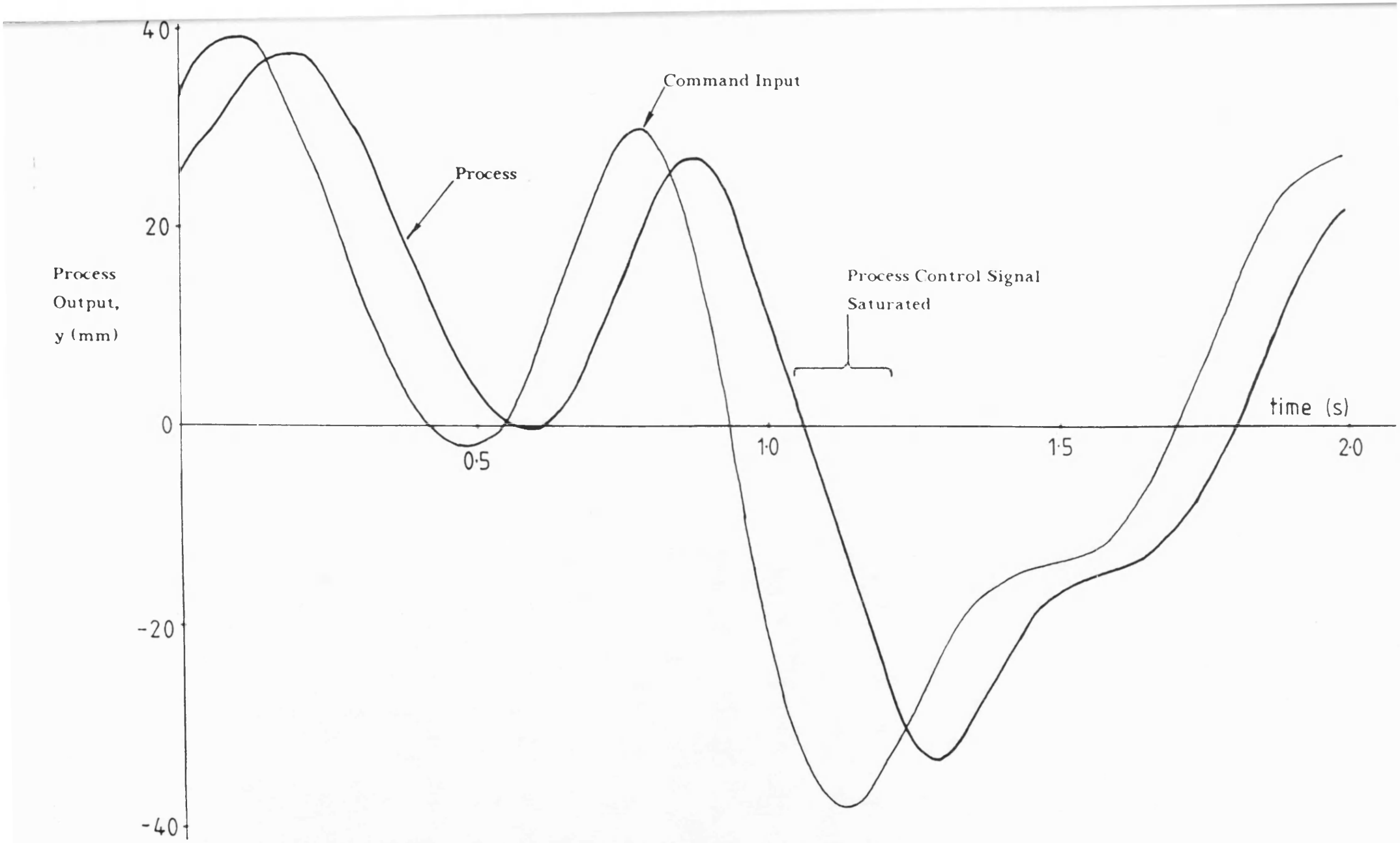

FIGURE 9:29 Demonstration Of The Process Control Signal Saturation Limiting Procedure (P.R.B.S. Command Signal)

CHAPTER 10

CONCLUSIONS AND RECOMMENDATIONS FOR FUTURE WORK

10.1 CONCLUSIONS

The work reported in this thesis has contributed a systematic approach to adaptive control system design. The control scheme was based on fundamental concepts from the field of model reference adaptive control. In addition, it was developed within the framework of a sampled data system. As a consequence, the results of the design procedure emerge in a form that requires no alteration in order to be implemented on a micro-processor system.

Detailed design of the adaptive control algorithm commenced with the specification of individual elements within the control scheme; namely, reference model, controlled process and compensator network transfer functions. A parameter adaptive algorithm was developed by augmenting the basic process control loop and reference model with an additional outer feedback loop. This generated the coefficients of the compensator networks in the process control loop. The design of a parameter adaptive algorithm employed recognised concepts and results from hyperstability theory. A detailed analysis was presented in order to demonstrate the relative ease of its use. In addition, this also served to highlight the wide choice of parameter updating algorithms that can be developed.

The basic adaptive control algorithm was tailored to enhance its application to real systems involving non-linear components. This involved supplementing it with the following features: a variable dead-band characteristic responsible for activating and affecting the degree of parameter adaptation; a saturation monitoring routine to ensure that parameter adaptation could only proceed while the process control signal fell within a pre-determined, linear operating region; and, a procedure to monitor the stability properties of the forward path compensator network in the process control loop. The first two alterations were directed at the parameter adaptive part of the control scheme; the third was a precautionary addition which would assure the stability of the controlled process loop.

The relative ease of applying the adaptive controller design procedure was demonstrated through the development of control schemes for two servo-systems. The design procedure comprised two stages namely, control algorithm specification and, numerical initialisation.

The first application that was examined involved an angular position control d.c. servo-system. Two distinct control algorithms were proposed. The first of these is termed a 'basic' adaptive control scheme. Apart from drawing on important elements from the controller design procedure, the algorithm also incorporated an important feature to overcome the problem of a fractional delay in computing the process control signal. This was achieved by modelling the computation period as a unit delay. This term was linked to the controlled process model to form an effective controlled process model.

The second algorithm designed around the d.c. servo-system incorporated an integral-action controller in the controlled process loop. This is necessary where set-point tracking is important and where external disturbances are liable to act on the controlled process.

Experimentation with the two adaptive control algorithms for the d.c. servo-system provided exceptionally good results regarding reference model following performance. These were obtained in the face of deliberate perturbations to the dynamics of the controlled process and for a wide range of command signals.

As part of the series of experiments on the d.c. servo-system, careful attention was given to the influence of the error filter in the parameter adaptive algorithm. For a given application, specification of the coefficients of this filter is carried out by ensuring that a particular transfer function was strictly positive real; this transfer function is formed by combining the error filter transfer function and the reference model characteristic equation. A graphical technique was developed for initialising the error filter coefficients. This gives rise to a very large number of options. Guidelines were established to assist the task of selecting a suitable set of error filter coefficients from the wide choice available. This was done on the basis of a series of experiments. The observations made were used to demonstrate an association between a desirable level of adaptive system behaviour and specific frequency response characteristics for the S.P.R. transfer function.

The general nature of the adaptive controller design procedure was demonstrated through its application to an electro-hydraulic position control servomechanism. The same basic design procedure was followed in developing and initialising the adaptive control algorithm. One of several important features with this control scheme was the use of a reduced order model to represent the controlled process. Other notable features included the implementation of device specific routines to enhance the behaviour of the control scheme. One example of this was the use of software aimed at overcoming certain non-linear characteristics in the electro-hydraulic servo-valve.

The portability of the adaptive scheme for the electro-hydraulic system was highlighted through its application to a slightly modified test rig. This involved the use of different servo-valve from that of the previous scheme. In addition, the control algorithm was also used to demonstrate the implementation of an integral action form of control. This worked on the basis of integrating the model-process output error. The simplicity of this approach endows it with a significant advantage over the comparatively cumbersome scheme designed for the d.c. servo-system.

The two adaptive control algorithms for the electro-hydraulic servomechanism were observed to perform extremely well. In spite of differences in the hardware employed, the levels of performance observed with the two schemes were markedly similar. Model following, although not perfect, was maintained consistently. Such a level of performance was observed even when the dynamics of the controlled process were perturbed. Input command signals of varying forms were also used to test the control scheme. An excellent level of control system performance was observed when a band-limited, pseudo-random command signal was used; this was considered to be highly representative of the type of demand signal likely to be encountered in many real applications.

The material presented in this thesis has emphasised the relative ease of applying the adaptive controller design procedure and the exceptional levels of performance obtained with different applications. In addition to these observations, a number of secondary issues were also highlighted. It was shown, for example, that the need to implement adaptive control schemes on real systems calls for important modifications to the basic algorithm. Often, these alterations are related to device specific characteristics. Nevertheless, they represent an important aspect of the

controller design procedure which is frequently overlooked in studies that attempt to validate control schemes solely through simulations. Attention was also drawn to the issue concerning the behavioural patterns of the parameter adaptive algorithm. During the course of experimentation, it became clear that parameter adaptation was a complex phenomenon dependent upon a range of different factors. Some of these include the quality, or 'richness', of the input command signal and the characteristics of the variable dead-band function used in this thesis. The observations made from these tests were advantageously used to enhance the performance of the d.c. servomotor, integral-action control scheme. This was achieved by employing input command signals containing an offset signal.

The realisation of the adaptive control schemes presented in this thesis owes much to the use of a micro-processor system. Its greatest contribution was in making it possible to contemplate computationally intensive control schemes. In addition, it also facilitated the implementation of non-linear functions. These offered a simple means of overcoming undesirable performance characteristics associated with some of the hardware used in the test rigs. The appearance of computer-based, advanced control systems will accelerate at a much greater rate once positive attributes such as these become more widely recognised.

10.2 RECOMMENDATIONS FOR FUTURE WORK

There are three principal areas where further research is required. The first concerns the basic process control loop. In the work reported here, the control scheme was developed on the basis of an approximate model of the controlled process and the use of a pole-placement form of control law. One avenue for further research concerns the δ-operator modelling approach mentioned in chapter 2. Should this result in an improved representation of the controlled process then the adaptive scheme could be extended to handle more complex, higher order processes. The pole placement control law used in this study involved specifying a desired level of system performance in terms of a reference model transfer function. The possibilities for further studies in this field concern the development of a set procedure for initialising the reference model transfer function especially where prior information can be readily obtained about the controlled process.

The second area offering further scope for research concerns the parameter adaptive part of the control scheme. It has already been argued that this can be viewed as a second tier feedback loop added to the basic controlled process loop. Potential areas for research in this field involve the use of other forms of parameter updating algorithm in contrast to the integral form employed in this thesis. It would also be of interest to expand on the studies which examined the association between the behaviour of the parameter adaptive algorithm and the spectral content of the command input signal. A similar comment can be applied to the action of the error filter in the adaptation mechanism. Guidelines for initialising the error filter coefficients were devised in chapter 7. The development of a simpler procedure to supersede them would represent a significant improvement to the overall design process.

The final area suggested for further research involves the addition of a third tier control loop to the adaptive control scheme. With regard to the adaptive schemes presented here, the performance monitoring routines are a related aspect of this field. However, the advent of expert system and artificial intelligence techniques offer much greater potential for building upon these features. Their use would represent a significant advance in enhancing the properties of current 'classical' adaptive control schemes.

REFERENCES

[1] Marsh P.
Green Light For Lego Schoolrooms
Financial Times, July 28 1987, p 26

[2] Auslander D.M, Takahashi Y, Tomizuka M.
Direct Digital Process Control: Practice And Algorithms For Microprocessor Application
Proceedings Of The IEEE, Vol. 66, No. 2, February 1978, pp 199-208

[3] Monopoli R.V.
Model Following Control Of Gas Turbine Engines
Transactions Of The ASME, Journal Of Dynamic Systems, Measurement And Control, Vol. 103, September 1981, pp 285-289

[4] Astrom K.J.
Theory And Applications Of Adaptive Control - A Survey
Automatica, Vol. 19, No. 5, 1981, pp 471-486

[5] Vukobratovic M, Kircanski N.
An Approach To Adaptive Control Of Robotic Manipulators
Automatica, Vol. 21, No. 6, 1985, pp 639-647

[6] Cegrell T, Hedqvist T.
Successful Adaptive Control Of Paper Machines
Automatica, Vol. 11, 1975, pp 53-59

[7] Courtoil B, Landau I.D.
High Speed Adaptation System For Controlled Electrical Drives
Automatica, Vol. 11, 1975, pp 119-127

[8] Irving E, Barret J.P, Charcossey C, Monville J.P.
Improving Power Network Stability And Unit Stress With Adaptive Generator Control
Automatica, Vol. 15, 1979, pp 31-46

[9] Van Amerongen J.
Adaptive Steering Of Ships - A Model Reference Approach
Automatica, Vol. 20, No. 1, 1984, pp. 3-14

[10] Vaughan N.D, Whiting I.M.
Microprocessor Control Applied To A Non-Linear Electrohydraulic Position Servo System
7th International Fluid Power Symposium, Bath University, September 1986

[11] Finney J.M, de Pennington A, Bloor M.S, Gill G.S.
A Pole-Assignment Controller For An Electrohydraulic Cylinder Drive
Transactions Of The ASME, Journal Of Dynamic Systems, Measurement And Control, Vol. 107, June 1985, pp 145-150

[12] Hughes F.M.
Self-tuning And Adaptive Control - A Review Of Some Basic Techniques
Transactions Of The Institute Of Measurement And Control, Vol. 8, No. 2, April-June 1986, pp 100-110

[13] Whiting I.M.
Closed Loop Digital Control Of Electrohydraulic Systems Ph.D Thesis, University Of Bath, 1986

[14] Clarke D.W.
Introduction To Self-Tuning Controllers
SELF TUNING AND ADAPTIVE CONTROL - Theory And Applications
Eds. C.J.Harris, S.A.Billings
IEE Control Engineering Series 15, 1981, pp 36-71

[15] Young P.C.
Applying Parameter Estimation To Dynamic Systems: Part 1
Control Engineering, October 1969, pp 119-125

[16] Young P.C.
Applying Parameter Estimation To Dynamic Systems: Part 2
Control Engineering, November 1969, pp 118-124

[17] Isermann R.
Parameter Adaptive Control Algorithms - A Tutorial
Digital Computer Applications To Process Control
Eds. R.Isermann, H.Kaltenecker
IFAC 1980, pp 139-154

[18] Astrom K.J.
LQG Self-Tuners
IFAC Adaptive Systems In Control And Signal Processing, San Francisco, USA 1983, pp 137-146

[19] Astrom K.J, Eykhoff P.
System Identification - A Survey
Automatica, Vol. 7, 1971, pp 123-162

[20] Daley S.
A Study Of A Fast Self-Tuning Control Algorithm
Proceedings Of The Institution Of Mechanical Engineers, Vol. 200, No. 6, C6, 1986

[21] Clarke D.W.
Implementation Of Self-Tuning Controllers
SELF TUNING AND ADAPTIVE CONTROL - Theory And Applications
Eds. C.J.Harris, S.A.Billings
IEE Control Engineering Series 15, 1981, pp 144-165

[22] Andersson P.
Adaptive Forgetting In Recursive Identification Through Multiple Models
International Journal Of Control, Vol. 42, No. 5, 1985, pp 1175-1193

[23] Clarke D.W, Gawthrop P.J.
Implementation And Application Of Microprocessor-Based Self-Tuners
Automatica, Vol. 17, No. 1, 1981, pp 233-244

[24] Landau Y.D.
Adaptive Control: The Model Reference Approach
Marcel Dekker Inc. 1979

[25] Hang C, Parks P.C.
Comparative Studies Of Model Reference Adaptive Control Systems
IEEE Transactions On Automatic Control, Vol. AC-18, No. 5, October 1973, pp419-428

[26] Parks P.C.
Liapunov Redesign Of Model Reference Adaptive Control Systems
IEEE Transactions On Automatic Control, Vol. AC-11, No. 3, July 1966, pp 362-367

[27] Phillipson P.H.
Design Methods For Model Reference Adaptive Systems
Proceedings Of The Institution Of Mechanical Engineers, Automatic Control Group, Vol. 183, Pt. 1, No. 35, 1968-69, pp 695-706

[28] Porter B, Tatnall M.L.
Performance Characteristics Of Multi-Variable Model-Reference Adaptive Systems Synthesised By Liapunov's Direct Method
International Journal Of Control, Vol. 10, No. 3, 1969, pp 241-257

[29] Landau I.D.
A Survey Of Model Reference Adaptive Techniques - Theory And Applications
Automatica, Vol. 10, 1974, pp 353-379

[30] Gawthrop P.J.
Self-Tuning PID Controllers: Algorithms And Implementation
IEEE Transactions On Automatic Control, Vol. AC-31, No. 3, March 1986, pp 201-209

[31] Ortega R, Kelly R.
PID Self-Tuners: Some Theoretical And Practical Aspects
IEEE Transactions On Industrial Electronics, Vol. IE-31, No. 4, November 1984, pp 332-338

[32] Astrom K.J, Wittenmark B.
On Self Tuning Regulators
Automatica, Vol. 9, 1973, pp 185-199

[33] Edge K.A, Figueredo K.R.A.
An Adaptively Controlled Electro-Hydraulic Servomechanism
Part 1: Adaptive Controller Design
Proceedings Of The Institution Of Mechanical Engineers, Vol. 201, No. B3, pp 178-180

[34] Edge K.A, Figueredo K.R.A.
An Adaptively Controlled Electro-Hydraulic Servomechanism
Part 2: Implementation
Proceedings Of The Institution Of Mechanical Engineers, Vol. 201, No. B3, pp 181-190

[35] Bai E.W, Sastry S.S.
Persistency Of Excitation, Sufficient Richness And Parameter Convergence In Discrete Time Adaptive Control
Systems And Control Letters 6, August 1985, pp 153-163

[36] Boyd S, Sastry S.S.
Necessary And Sufficient Conditions For Parameter Convergence In Adaptive Control
Automatica, Vol. 22, No. 6, 1986, pp 629-639

[37] Jacobs O.L.R.
When Is Adaptive Control Useful?
3rd IMA Conference On Control Theory
Academic Press, 1981, pp 295-311

[38] Anex Jr. R.P, Hubbard M.
Modelling And Adaptive Control Of A Mechanical Manipulator
Tranasactions Of The ASME, Journal Of Dynamic Systems, Measurement And Control, Vol. 106, September 1984, pp 211-217

[39] Narendra K.S, Valvani L.S.
Direct And Indirect Model Reference Adaptive Control
Automatica, Vol. 15, 1979, pp 653-664

[40] Neuman C.P, Morris R.L.
Design And Microcomputer Implementation Of Adaptive Controllers
Proceedings Of The 1st International Micro And Mini Computer Conference, Houston, Texas, November 14-16 1979

[41] Van Den Bosch P.P.J, Tjahjadi P.I.
Model Updating Improves MRAC Performance
IEEE Transactions On Automatic Control, Vol. AC-29, No. 12, December 1984, pp. 1106-1108

[42] Franklin G.F, Powell J.D.
Digital Control Of Dynamic Systems
Addison-Wesley Publishing Company, Massachusetts, U.S.A. 1980

[43] Astrom K.J, Hagander P, Sternby J.
Zeros Of Sampled Systems
Automatica, Vol. 20, No. 1, 1984, pp. 31-38

[44] Goodwin G.C, Lozano Leal R, Maynes D.Q, Middleton R.H.
Rapprochement Between Continuous And Discrete Model Reference Adaptive Control
Automatica, Vol. 22, No. 2, 1986, pp. 199-207

[45] Neuman C.P, Baradello C.S.
Digital Transfer Functions For Microcomputer Control
IEEE Transactions On Systems, Man, And Cybernetics, Vol. SMC-9, No. 12
Dec. 1979

[46] Astrom K.J, Wittenmark B.
Computer Controlled Systems. Theory And Design
Prentice Hall Information & System Science Series, 1984
Ed. T. Kailath

[47] Jiashi C, Keller R.B.
The Adaptive Control Of Hydraulic Systems Using Filtered Input And Output Signals
ASME 1983 Winter Annual Meeting, 1983

[48] Keller R.B, Jiashi C.
A High Performance Adaptive Controller For Non-Linear Hydraulic Servo-Systems
ASME 1983 Winter Annual Meeting, 1983

[49] Dasgupta S, Johnson Jr. C.R.
Some Comments On The Behaviour Of Sign-Sign Adaptive Identifiers
Systems & Control Letters 7, 1986, pp 75-82

[50] Johnson Jr. C.R, Anderson B.D.O, Bitmead R.R.
A Robust, Locally Optimal Model Reference Adaptive Controller
Proceedings Of The 23rd IEEE Conference On Decision And Control, Las Vegas, NV, December 1984, pp 993-997

[51] Ioannou P.
Robust Direct Control
Proceedings Of The 23rd Conference On Decision And Control
Las Vegas, NV. December 1984, pp 1015-1020

[52] Isermann I, Lachmann K.-H.
Parameter-adaptive Control With Configuration Aids And Supervision Functions
Automatica, Vol. 21, No. 6, 1985, pp 625-638

[53] Rohrs C.E, Valvani L, Athans M, Stein G.
Robustness Of Adaptive Control Algorithms In The Presence Of Unmodelled Dynamics
Proceedings Of The 21st IEEE Conference On Decision And Control, 1982, pp 3-11

[54] Chen Z.J, Cook P.A.
Robustness Of Model-Reference Adaptive Control Systems With Unmodelled Dynamics
International Journal Of Control, Vol. 39, No. 1, 1984, pp 201-214

[55] Kidd P.T.
Robustness Of Model Reference Adaptive Systems In The Presence Of Unmodelled Dynamics And Output Disturbances
International Journal Of Control, Vol. 42, No. 5, 1985, pp 1213-1225

[56] Rohrs C.E.
How The Paper 'Robustness Of Model-Reference Adaptive Control Systems With Unmodelled Dynamics' Misrepresents The Results Of Rohrs And His Coworkers
International Journal Of Control, Vol. 41, No. 2, 1985, pp 575-580

[57] Rohrs C.E, Valvani L, Athans M, Stein G.
Robustness Of Continuous-Time Adaptive Control Algorithms In The Presence Of Unmodelled Dynamics
IEEE Transactions On Automatic Control, Vol. AC-30, No. 9, September 1985, pp 881-889

[58] Astrom K.J.
A Commentary On The C.E. Rohrs et al. Paper 'Robustness Of Continuous-Time Adaptive Control Algorithms In The Presence Of Unmodelled Dynamics'
IEEE Transactions On Automatic Control, Vol. AC-30, No. 9, September 1985, p 889

[59] Rohrs C.E.
Stability Mechanisms And Adaptive Control
Proceedings Of The 23rd IEEE Conference On Decision And Control, Las Vegas, NV, Decemmber 1984, pp 989-992

[60] Astrom K.J.
Analysis Of Rohrs' Counterexamples To Adaptive Control
Proceedings Of The 22nd IEEE Conference On Decision And Control, San Antonio, Texas, December 1983, pp 982-987

[61] Rohrs C.E, Athans M, Valvani L, Stein G.
Some Design Guidelines For Discrete-Time Adaptive Controllers
Automatica, Vol. 20, No. 5, 1984, pp 653-660

[62] Kreisselmeier G, Anderson B.D.O.
Robust Model Reference Adaptive Control
IEEE Transactions On Automatic Control, Vol. AC-31, No. 2, February 1986, pp 127-133

[63] Ortega R, Praly L, Landau I.D.
Robustness Of Discrete-Time Direct Adaptive Controllers
IEEE Transactions On Automatic Control, Vol. AC-30, No. 12, December 1985, pp 1179-1187

[64] Praly L.
Robustness Of Model Reference Adaptive Control
Proceedings Of The 3rd Yale Workshop, New Haven, CT, June 1983, pp 224-226

[65] Goodwin G.C, Sin K.S.
Adaptive Filtering Prediction And Control
Prentice Hall Information And System Science Series
Ed. Kailath T. 1984

[66] Spiegel M.R.
Mathematical Handbook Of Formulas And Tables
Schaum's Outline Series - Theory And Problems Of
McGraw Hill Book Company

[67] Phillips C.L, Troy Nagle Jr. H.
Digital Control System Analysis And Design, pp 198-201
Prentice Hall Inc. 1984

[68] Rohrs C.E, Valvani L, Athans M, Stein G.
Analytical Verification Of Undesirable Propertied Of Direct Model Reference Adaptive Control Algorithms
Proceedings Of The 20th IEEE Conference On Decision And Control, 1981, pp 1272-1284

[69] Yang D.R, Lee W. -K.
Effects Of Model Structure, Nonzero D.C.-Value And Measureable Disturbance On Adaptive Control
IFAC Adaptive Systems In Control And Signal Processing, San Fransisco, U.S.A. 1983, pp 253-259

[70] Hertzanu B, Tabak D.
Microprocessor-Based Control Of Industrial Sewing Machines
Automatica, Vol. 22, No. 1, 1986, pp 21-31

[71] Peterson B.B, Narendra K.S.
Bounded Error Adaptive Control
IEEE Transactions On Automatic Control, Vol. AC-27, No. 6, December 1982, pp 1161-1168

[72] Ambrosiano G, Celentano G, Garofalo F.
Adaptive Model Following Control Of Plants With Nonlinearities Of Known Form
IEE Proceedings, Vol. 132, Pt. D, No. 1, January 1985, pp 11-13

[73] King T.
TRIPOS User Guide
School Of Mathematics, University Of Bath, March 1983

[74] Richards R, Whitby-Strevens C.
BCPL The Language And Its Compiler
Cambridge University Press, 1980

[75] Higgins C.J.
MC68000 (POLESTAR/DARKSTAR) And Z-80 (POLESTAR/CLENLO) Comparative Benchmark Tests
University Of Bath, School Of Engineering Report No. 767, 1985

[76] Lindorff D.P, Carroll R.L.
Survey Of Adaptive Control Using Liapunov Design
International Journal Of Control, Vol. 18, No. 5, 1973, pp 897-914

[77] Figueredo K.R.A.
Application Of Micro-Processor Based Model Reference Adaptive Control To Servo-Systems - Program Documentation
University Of Bath, School Of Engineering Report No. 882, 1987

[78] Barnett S.
Introduction To Mathematical Control Theory
Clarendon Press, Oxford, 1975

[79] MACSYMA Reference Manual, Vols. 1 & 2
The Mathlab Group Laboratory For Computer Science
Massachusetts Institute For Technology
December 1983

APPENDIX 1

STABILITY CONCEPTS AND DEFINITIONS

The concept of stability can be explained in a number of different ways [78]. However, the following statements offer one interpretation that is adequately relevant to the subject under discussion.

Consider the case of a vector state, x. An equilibrium state x=0 is said to be:

1) stable if for any positive scalar, ϵ, there exists a positive scalar, δ, such that $||x(t_0)|| < \delta$ implies $||x(t)|| << \epsilon$, $t \geqslant t_0$.

2) asymptotically stable if 1) applies and if, in addition, $x(t) \rightarrow 0$ as $t \rightarrow \infty$.

3) unstable if 1) does not apply; that is, there exists an $\epsilon > 0$ such that for every $\delta > 0$, there exists an $x(t_0)$ with $||x(t_0)|| < \delta$, $||x(t_1)|| \geqslant \epsilon$ for some $t_1 > t_0$. If this holds for every $x(t_0)$ in $||x(t_0)|| < \delta$ the 'equilibrium' state, x=0, is unstable.

A two-dimensional geometrical perspective of these definitions is shown in figure A1:1. The origin of this figure is represented by the point O. If it corresponds to a stable point then, given the outer circle C, with radius ϵ, there exists an inner circle, C_1, with radius δ_1, such that trajectories starting within C_1 never leave C. If O is asymptotically stable then there is some circle C_2, with radius δ_2, having the same property as C_1 but in addition trajectories starting inside C_2 tend to O as t $\rightarrow \infty$.

In engineering applications, asymptotic stability is more desireable than stability. This is because it ensures eventual return to equilibrium, whereas stability allows continuing deviations within a 'small' tolerance band of the equilibrium state.

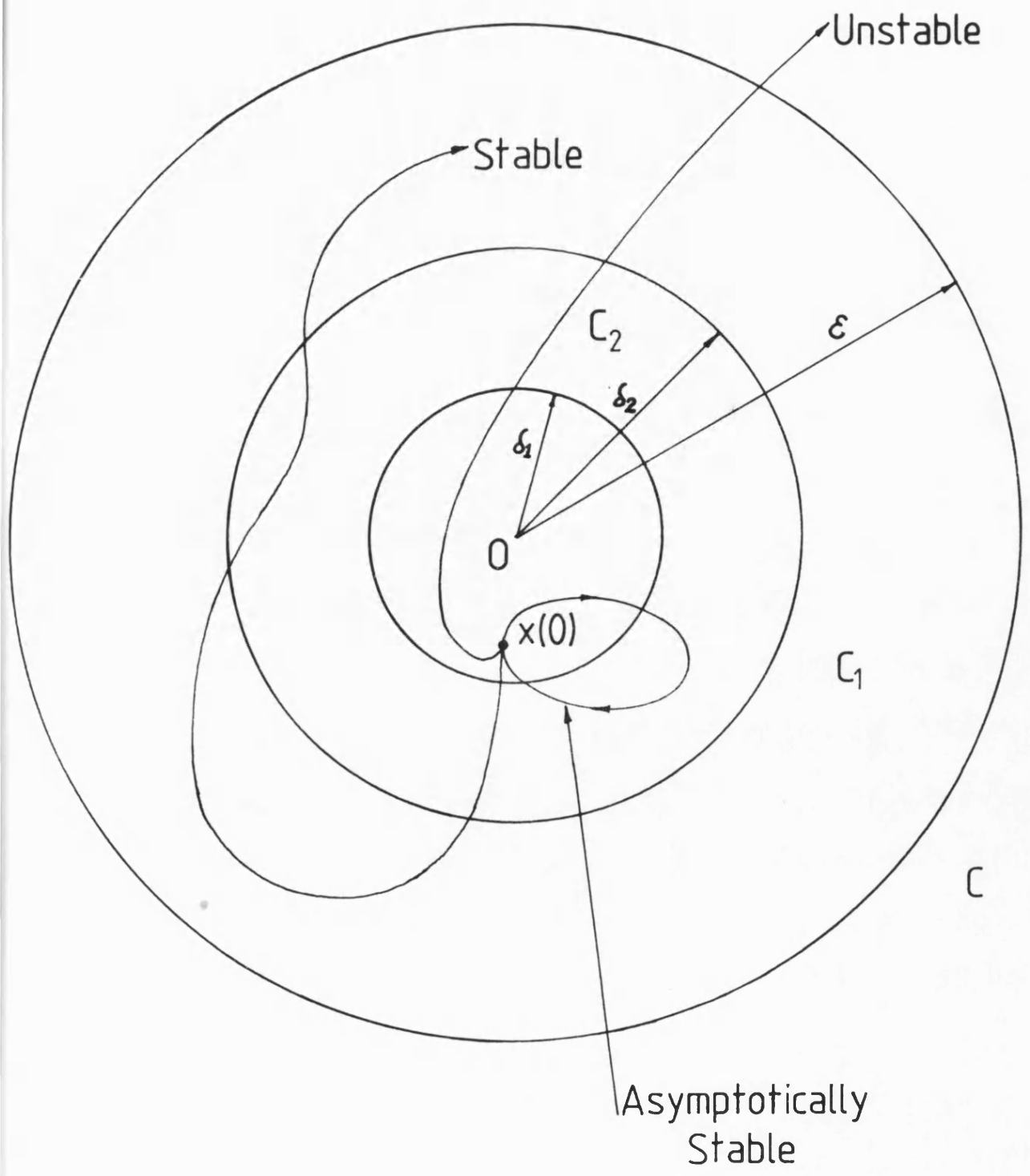

FIGURE A1:1 Diagrammatic Interpretation Of Stability Definitions

APPENDIX 2

HYPERSTABILITY ANALYSIS OF

ERROR SYSTEM FEEDBACK BLOCK

A2.1 PART A: 'a posteriori' SYSTEM CONFIGURATION

The detailed development of adaptive laws suitable for the parameter updating algorithm is considered in this appendix. Analysis is carried out in conjunction with standard results from hyperstability theory. To assist in the clarity of presentation, the problem is studied within the framework of a control system described by the following set of equations.

Process Model - Open Loop Transfer Function

$$\frac{y(z^{-1})}{u(z^{-1})} = \frac{b_0 z^{-2}(1+z^{-1})}{1+a_1 z^{-1}+a_2 z^{-2}}$$

$$= \frac{b_0 z^{-2} B(z^{-1})}{A(z^{-1})} \qquad \text{(A2.1)}$$

The process model can be interpreted as a second order system, with a unit sampling period delay.

Reference Model - Closed Loop Transfer Function

$$\frac{x(z^{-1})}{w(z^{-1})} = \frac{b_m z^{-2}(1+z^{-1})}{1+a_{m,1} z^{-1}+a_{m,2} z^{-2}+a_{m,3} z^{-3}}$$

$$= \frac{b_m z^{-2} B(z^{-1})}{A_m(z^{-1})} \qquad \text{(A2.2)}$$

Compensator Transfer Functions

$$F(z^{-1}) = f_0 + f_1 z^{-1} + f_2 z^{-2} \tag{A2.3}$$

$$G(z^{-1}) = g_0 + g_1 z^{-1} \tag{A2.4}$$

Pole-Placement Control Law

$$\frac{1}{b_m} A_m(z^{-1}) = \frac{1}{b_0} A(z^{-1}) F(z^{-1}) + z^{-2} B(z^{-1}) G(z^{-1}) \tag{A2.5}$$

Model-Process Output Error Signals

'a priori' output error,

$$e^{\circ}(k) = x(k) - y^{\circ}(k) \tag{A2.6}$$

'a posteriori' output error,

$$e(k) = x(k) - y(k) \tag{A2.7}$$

The origin of the 'a priori' and 'a posteriori' error signals can be traced back to the way in which the process control signal, u(k) is evaluated. If the control signal, for a given sampling period, k, is calculated in terms of the compensator coefficients generated during the previous sampling period, then it is termed the 'a priori' control signal. Conversely, the 'a posteriori' control signal is evaluated from compensator coefficients generated during the k^{th} sampling period. The latter situation is clearly artificial since it ignores the computational period required to evaluate the control signal. Nevertheless, it is introduced because it facilitates a convenient approach to the stability analysis problem.

Filtered 'a priori' and 'a posteriori' output error signals are defined in a similar fashion to the output error signals thus.

'a priori' filtered error signal,

$$\nu^o(k) = C(z^{-1})e^o(k) \tag{A2.8}$$

'a posteriori' filtered error signal,

$$\nu(k) = C(z^{-1})e(k) \tag{A2.9}$$

By following the procedure outlined in chapter 5, the following error system equation is derived. For ease of presentation the simplified notation, $A_m \equiv A_m(z^{-1})$ is used henceforth.

$$A_m e(k) = b_m z^{-2} B[\,(\hat{f}_0(k) - f_0)u(k) + (\hat{f}_1(k) - f_1)u(k-1) +$$

$$(\hat{f}_2(k) - f_2)u(k-2) + (\hat{g}_0(k) - g_0)y(k) +$$

$$(\hat{g}_1(k) - g_1)y(k-1)\,] \tag{A2.10}$$

$$= b_m z^{-2} B\left[\,\underline{\hat{\mathbf{d}}}^T(k) - \underline{\mathbf{d}}^T\,\right]\underline{\Phi}(k) = -b_m w_1(k) \tag{A2.11}$$

with, an adjustable parameter vector,

$$\underline{\hat{\mathbf{d}}}^T(k) = \left[\,\hat{f}_0(k)\;\; \hat{f}_1(k)\;\; \hat{f}_2(k)\;\; \hat{g}_0(k)\;\; \hat{g}_1(k)\,\right] \tag{A2.12}$$

a fixed parameter vector of coefficients which satisfy the pole-placement control law of equation (A2.5).

$$\underline{\mathbf{d}}^T = \begin{bmatrix} f_0 & f_1 & f_2 & g_0 & g_1 \end{bmatrix} \tag{A2.13}$$

an observation vector given by,

$$\underline{\Phi}(k) = \begin{bmatrix} u(k) & u(k-1) & u(k-2) & y(k) & y(k-1) \end{bmatrix}^T \tag{A2.14}$$

and,

$$w_1(k) = z^{-2}B\left[\underline{\mathbf{d}}^T - \underline{\hat{\mathbf{d}}}^T\right]\underline{\Phi}(k) \tag{A2.15}$$

The error system is now of a form suitable for analysis as a two component feedback system, as shown in figure A2:1. At this stage, the error system is expressed in terms of the 'a posteriori' filter coefficients. A suitable correction to reflect the true nature of the control system, will be demonstrated in part B of this appendix.

The forward path of this system is modified by the introduction of the error filter, $C(z^{-1})$. Now, the equation describing the non-linear feedback part of the system becomes,

$$\nu(k) = b_m z^{-2}B\left[\hat{\underline{\mathbf{d}}}^T(k) - \underline{\mathbf{d}}^T\right]\underline{\Phi}(k) \tag{A2.16}$$

The reference model gain, b_m has a fixed value; to simplify subsequent analysis, it is moved to the left hand side of equation (A2.14), the linear time-invariant part. Equation (A2.14) can thus be written as,

$$\frac{1}{b_m}\nu(k) = \left[\hat{\underline{\mathbf{d}}}^T(k) - \underline{\mathbf{d}}^T\right]\tilde{\underline{\Phi}}(k-2) \tag{A2.17}$$

where, $\underline{\tilde{\Phi}}(k-2)$ is a filtered version of the observation vector, $\underline{\Phi}(k)$. To develop suitable adaptive laws, it is necessary to study the input-output relationship of the feedback block of this system using stability concepts based on hyperstability theory. Stability of the feedback system is assured if its input-output relationship can be shown to satisfy the following condition.

$$\eta(0,k_1) = \sum_{k=0}^{k_1} w_1(k)v(k) \geq -\lambda_0^2 \quad \text{for all } k_1 \geq 0 \tag{A2.18}$$

This condition is also known as Popov's Integral Inequality.

The only adjustable parameters in this system are the compensator coefficients in the $\underline{\hat{d}}$ parameter vector; the remainder of the system consists of measureable signals, derived from the reference model and process responses, and the desired set of compensator coefficients which satisy the pole-placement control law given by equation (A2.5). The stability inequality is expressed in terms of these variables. Referring to equation (A2.11) and figure A2:1, the input to the summing junction is $b_m w_1(k)$. Since b_m is fixed and can be moved to the forward path of the feedback system, the output from the non-linear feedback block effectively becomes $w_1(k)$. Consequently, when equation(A2.15) is substituted for $w_1(k)$ in inequality (A2.18), the following result is obtained.

$$\eta(0,k_1) = \sum_{k=0}^{k_1} \left[\underline{d}^T - \underline{\hat{d}}^T(k) \right] \underline{\tilde{\Phi}}(k-2)v(k) \geq -\lambda_0^2 \quad \text{for all } k_1 \geq 0 \tag{A2.19}$$

For demonstration purposes, the five elements of the adjustable parameter vector, $\hat{d}_i$,$(i=0,4)$, are defined in the following manner,

$$\hat{d}_i(k) = \hat{d}_i(k-1) + \theta_{i,0}(v(k)) \quad i=0,4 \tag{A2.20}$$

$$= \sum_{l=0}^{k} \theta_{i,1}(v(k),k,l) + \hat{d}_i(-1) + \theta_{i,2}(v(k),k) \tag{A2.21}$$

where $\hat{d}_i(-1)$ is the initial estimate for the $\hat{d}_i$ coefficient. The first two parts of of the right hand side of equation (A2.21) constitute an integral form of parameter updating. As shown later, the third part allows for an added degree of sophistication to be built into the adaptation law. The generalised expression given above, is of a more complex form than is actually required. However, it serves as a demonstration for the potentially wide class of adaptation laws that can be derived.

Application of the Popov integral inequality to the new system representation results in the following expression,

$$\eta(0,k_1) = \sum_{i=0}^{4}\left[\sum_{k=0}^{k_1}\left[\sum_{l=0}^{k}\left[d_i - \theta_{i,1}(\nu(k),k,l) - \theta_{i,2}(\nu(k),k) - \hat{d}_i(-1)\right]\right]\tilde{\phi}_i(k-2)\nu(k)\right] \geq -\lambda_0^2$$

$$\text{for } all \;\; k_1 \geq 0 \qquad \text{(A2.22)}$$

The analysis of this inequality can be considerably simplified by noting that it is satisfied if each of the five adaptive parameters indiviudually satisfies an inequality of the same form. Thus, it is sufficient to only consider the case of one coefficient and translate the results obtained to the remaining four. Therfore, consider the case of the parameter $f_0 = \hat{d}_0$. The stability condition to be satisfied is,

$$\eta(0,k_1) = \sum_{k=0}^{k_1}\left[\sum_{l=0}^{k}\left[d_0 - \theta_{0,1}(\nu(k),k,l) - \hat{d}_0(-1) - \theta_{0,2}(\nu(k),k)\right]\right]\tilde{\phi}_0(k-2)\nu(k) \geq -\lambda_0^2$$

$$\text{for } all \;\; k_1 \geq 0 \qquad \text{(A2.23)}$$

This inequality can be advantageously reduced to the following form,

$$\eta(0,k_1) = I_1 + I_2 \geq -\lambda_0^2 \quad \text{for } all \;\; k_1 \geq 0 \qquad \text{(A2.24)}$$

where,

$$I_1 = \sum_{k=0}^{k_1} \left[\sum_{l=0}^{k} \left[d_0 - \theta_{0,1}(\nu(k),k,l) - \hat{d}_0(-1) \right] \right] \vec{\phi}_0(k-2)\nu(k) \geq -\lambda_1^2 \qquad \text{(A2.25)}$$

for *all* $k_1 \geq 0$

and,

$$I_2 = \sum_{k=0}^{k_1} -\theta_{0,2}(\nu(k),k)\vec{\phi}_0(k-2)\nu(k) \geq -\lambda_2^2 \qquad \text{(A2.26)}$$

for *all* $k_1 \geq 0$

By configuring the problem in this manner, it now becomes possible to analyse it as two simplified sub-problems. The two can be interpreted as a pair of parallel block functions. According to [24], hyperstability of the parallel block system is assured if the individual blocks are themselves hyperstable.

SUB-PROBLEM 1

Consider the application of the following relationship to sub-problem I_1.

$$\sum_{k=0}^{k_1} x(k) \left[\sum_{l=0}^{k} x(l) + c \right] = \frac{1}{2} \left[\sum_{k=0}^{k_1} x(k) + c \right]^2 + \frac{1}{2} \sum_{k=0}^{k_1} x^2(k) - \frac{c^2}{2} \geq -\frac{c^2}{2} \qquad \text{(A2.27)}$$

Intuitively, specify x(k) to be analogous to the product $\vec{\phi}_0(k-2)\nu(k)$ in equation (A2.25). Consequently, the application of Popov's integral inequality to I_1 will be satisfied if ,

$$-\theta_{0,1}(\nu(k),k,l) = \gamma_0 \vec{\phi}_0(k-2)\nu(k) \quad \gamma_0 > 0 \qquad \text{(A2.28)}$$

where, γ_0 is an adaptive gain.

SUB-PROBLEM 2

A wide class of solutions can be developed in applying Popov's integral inequality to sub-problem I_2. The explicit expression for this inequality is given by,

$$I_2 = \sum_{k=0}^{k_1} -\theta_{0,2}(\nu(k),k)\phi_0(k-2)\nu(k) \geq -\lambda_2^2 \quad \text{for all } k_1 \geq 0 \tag{A2.29}$$

The following range of solutions will satisfy this inequality:

Proportional Adaptation

$$-\theta_{0,2}(\nu(k),k) = \gamma_{PA}\phi_0(k-2)\nu(k) \quad \gamma_{PA} \geq 0 \tag{A2.30}$$

γ_{PA} is an adaptive gain.

Relay Adaptation

Three similar solutions are possible in this case. They are as follows,

$$-\theta_{0,2}(\nu(k),k) = \gamma_{RA}U(k) \quad \gamma_{RA} \geq 0 \tag{A2.31}$$

where, γ_{RA} is an adaptive gain and, U(k) can be any of the following,

$$1)\ U(k) = \phi_0(k-2)\left|\nu(k)\right| \tag{A2.32}$$

$$2)\ U(k) = \nu(k)\left|\phi_0(k-2)\right| \tag{A2.33}$$

$$3)\ U(k) = \left|\phi_0(k-2)\nu(k)\right| \tag{A2.34}$$

A combination of the solutions from sub-problem I_2 with that of sub-problem I_1 clearly offers a wide range of adaptation laws. In general, solutions to I_1 are always used because they are of an integral form; this means that they display memory-like qualities. As a consequence, they are able to maintain a fixed parameter value in spite of the model-process output error reducing to zero. The most basic version of the parameter updating algorithm of equation (A2.20) is thus given by,

$$\hat{d}_i(k) = \hat{d}_i(k-1) - \gamma_0 \tilde{\phi}(k-2)\nu(k) \qquad i=0,4 \tag{A2.35}$$

A2.2 PART B: 'a priori' SYSTEM CONFIGURATION

Thus far, a number options have been made available for constructing the parameter updating algorithm. Before full implementation can be made possible, it is first necessary to express the algorithm in a form which is dependent on the 'a priori' compensator coefficients; this is necessary if the true control system realisation is to be accounted for in the adaptation algorithm.

The 'a priori' and 'a posteriori' filtered error system equations can be written thus,

$$\nu^o(k) = b_m \left[\underline{\hat{d}}^T(k-1) - \underline{d}^T \right] \underline{\tilde{\Phi}}(k-2) \tag{A2.36}$$

$$\nu(k) = b_m \left[\underline{\hat{d}}^T(k) - \underline{d}^T \right] \underline{\tilde{\Phi}}(k-2) \tag{A2.37}$$

Subtracting equation (A2.36) from (A2.37) results in,

$$\nu(k) - \nu^o(k) = b_m (\underline{\hat{d}}^T(k) - \underline{\hat{d}}^T(k-1)) \underline{\tilde{\Phi}}(k-2) \tag{A2.38}$$

However, for the simplest case of an integral form of updating algorithm, as given

in equation (A2.35), equation (A2.38) can be reduced to the following form,

$$\nu(k)-\nu^o(k) = -b_m \sum_{i=0}^{4} (\gamma_i \tilde{\phi}_i(k-2))\tilde{\phi}_i(k-2)\nu(k)$$

$$= -\underline{\tilde{\Phi}}^T(k-2)\Gamma\underline{\tilde{\Phi}}(k-2)\nu(k) \qquad \text{(A2.39)}$$

where, Γ, in this particular case, is a 5×5 diagonal matrix of adaptive gains. The elements of this matrix include a scaling factor which arises from taking the fixed gain, b_m , into account. Rearranging equation (A2.39) results in an expression for $\nu(k)$ in terms of $\nu^o(k)$. Hence,

$$\nu(k) = \frac{\nu^o(k)}{1+\underline{\tilde{\Phi}}^T(k-2)\Gamma\underline{\tilde{\Phi}}(k-2)} \qquad \text{(A2.40)}$$

This result means that no drastic modification is required to the form of the adaptation algorithm. All that happens is that it can now be completely expressed in terms of measureable quantities, by replacing $\nu(k)$ with the expression derived above. A particularly simple form for the complete parameter updating algorithm can thus be expressed as,

$$\underline{\hat{d}}(k) = \underline{\hat{d}}(k-1) - \frac{\Gamma\underline{\tilde{\Phi}}^T(k-2)\nu^o(k)}{1+\underline{\tilde{\Phi}}^T(k-2)\Gamma\underline{\tilde{\Phi}}(k-2)} \qquad \text{(A2.41)}$$

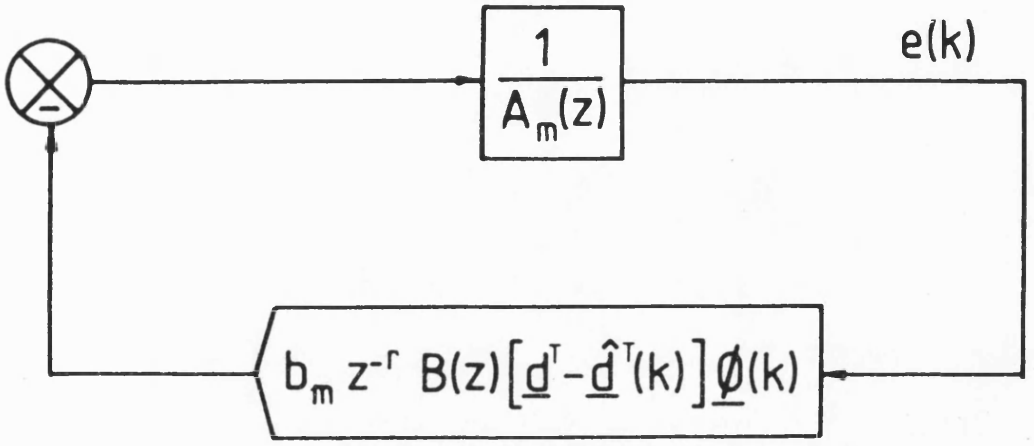

FIGURE A2:1 Feedback Representation Of Error Equation

APPENDIX 3

ERROR FILTER DESIGN USING 'MACSYMA'

A3.1 INTRODUCTION

MACSYMA is a program that was designed for the purpose of manipulating algebraic expressions. It was written at the M.I.T. laboratory for computer science and is currently available for general use on the Multics computer system at the University Of Bath [79].

The MACSYMA program is capable of a diverse range of operations. These include such functions as, differentiation, integration, solution of systems of linear or polynomial equations, curve plotting and matrix manipulation, to name but a few. The set of instructions employed in the subsequent presentation exercise but a small fraction of its capabilities.

The use of MACSYMA will be demonstrated with its application to the problem of formulating conditions on the 'c' coefficients of an error filter, $C(z^{-1})$, such that the transfer function, $C(z^{-1})/A_m(z^{-1})$, is strictly positive real. However, prior to a full consideration of this S.P.R. problem, an introductory session to demonstrate the usage of MACSYMA will be presented.

A3.2 INTRODUCTORY EXAMPLE OF A 'MACSYMA' USER SESSION

A MACSYMA user session is initiated with the Multics command, '>axl>macsyma'. Upon entering the MACSYMA system environment, a greeting message is sent to the user. This is then followed with the command line prompt:

(c1)

At this point, any mathematical expression, assignment or MACSYMA command may be input. As an example, consider the following,

(c1) (x+3)^5;

The MACSYMA command line may be typed on more than one line of the terminal. It must be terminated with a recognised character. In the example above, a semicolon has been used although it is also possible to use a dollar sign. If a semicolon is used, the command line is evaluated. The result is stored for future use and also output in a mathematical format, preceded by a label such as (d1). Hence, the output from the example above would be,

(d1) $(x + 3)^5$

If, however, the input command line is terminated with a dollar sign, it is evaluated and stored for future use, but is not displayed.

All command lines are prompted by '(cN)' and all result lines are preceded by '(dN)', where 'N' is incremented throughout the MACSYMA session. Any result from a command line may be referred to as 'dN', where 'N' is the number output on the command line prompt. An additional facility that is available allows the user to refer to the last result calculated with the symbol '%'. Thus, consider the following example,

(c2) x^2+2*x;

(d2) x^2+2x

(c5) y^2$

(c6) d2=%;

(d6) $x^2+2x=y^2$

The whole command line, even if it is more than one line long, may be cancelled by typing '??' before the terminating semicolon or dollar. If MACSYMA cannot perform an operation, it returns the expression given. This is most likely to occur when using the integration set of functions. The solution is to rewrite the expression in a simpler form though this is not guaranteed to work with very complex problems. When a MACSYMA session has been completed, the instruction 'quit();' has to be issued to return the Multics operating environment. As with all command line inputs, it too has to be terminated with one of the two forms of acceptable control characters.

A3.3 S.P.R. PROBLEM SPECIFICATION

The particular S.P.R. problem that is to be examined with the assistance of MACSYMA concerns the transfer function given below.

$$\frac{C(z^{-1})}{A_m(z^{-1})} = \frac{1+c_1z^{-1}+c_2z^{-2}}{1-1.6z^{-1}+0.62z^{-2}+0.02z^{-3}}$$

$$= \frac{z^3+c_1z^2+c_2z}{z^3-1.6z^2+0.62z+0.02} \qquad \text{(A3.1)}$$

The following sequence of operations outlines an ordered approach to the derivation of conditions, on the error filter coefficients, which satisfy the S.P.R. requirement.

1) Transform the $C(z)/A_m(z)$ transfer function into a pseudo-frequency, ω_w, domain.

2) Obtain the real part of this ω_w transfer function. The following example transfer function is used to specify the series of operations involved.

$$\frac{a+jb}{c+jd} = \frac{a+jb}{c+jd} \times \frac{c-jd}{c-jd}$$

$$= \frac{(ac+bd)+j(bc-ad)}{c^2+d^2} \qquad \text{(A3.2)}$$

Clearly, the real part of this transfer function is given by,

$$\frac{ac+bd}{c^2+d^2} \qquad \text{(A3.3)}$$

Since the precise magnitude of this term is not required, it is sufficient to determine the term, $ac+bd$.

3) Determine conditions on the error filter coefficients such that the real part of the ω_w transfer function is positive and non-zero.

A3.4 S.P.R. PROBLEM SOLUTION USING MACSYMA

The diversity of MACSYMA operating instructions mean that several approaches can be followed in examining the S.P.R. problem outlined above. The following listing provides just one such solution. Explanatory comments on the analytical procedure are interspersed within the the MACSYMA user session. They are differentiated from the main body of the MACSYMA text by being written in bold font.

```
>axl>mac

This is Macsyma 303
(c) 1976,1983, Massachussets Institute Of Technology.
All Rights Reserved.
Enhancements (c) 1983, Symbolics, Inc. All Rights Reserved.
Type trade_secret(); to see Trade Secret notice.

(c1) z:(1+%i*w)/(1-%i*w);
```

$$(d1) \qquad \frac{\%i\ w + 1}{1 - \%i\ w}$$

Command line (c1) is used to define the z to ω_w mapping. The simplified notation 'w' is used to represent ω_w while %i stands for the imaginary operator 'j'.

```
(c2) (z^3+cf1*z^2+cf2*z)/(z^3-1.6*z^2+0.62*z+0.02);
```

$$(d2) \qquad \frac{(\%i\ w+1)^3}{(1-\%i\ w)^3}+cf1\frac{(\%i\ w+1)^2}{(1-\%i\ w)^2}+cf2\frac{(\%i\ w+1)}{(1-\%i\ w)}$$

$$\frac{(\%i\ w+1)^3}{(1-\%i\ w)^3}-1.6\frac{(\%i\ w+1)^2}{1-\%i\ w)^2}+0.62\frac{(\%i\ w+1)}{(1-\%i\ w)}+0.02$$

The S.P.R. transfer function to be studied is entered in as command line (c2). It should be noted that the 'cf1' and 'cf2' are used to represent the error filter coefficients. The reason for not using 'c1' and 'c2' is to avoid any ambiguity with references to command line inputs, 'cN' as this will lead to confusion within the MACSYMA program.

```
(c3) ratsimp(%);

RAT replaced 0.02 by 1/50 = 0.02

RAT replaced 0.62 by 31/50 = 0.62

RAT replaced -1.6 by -8/5 = -1.6

(d3) (( -25 %i cf2 + 25 %i cf1 - 25 %i) w^3  + ( 25 cf2 + 25 cf1 -75) w^2

+ ( -25 %i cf2 + 25 %i cf1 + 75 %i) w + 25 cf2 + 25 cf1 + 25 )

/ ( - 80 %i w^3  - 101 w^2  + 18 %i w + 1 )
```

The MACSYMA operation, 'ratsimp(exp)', "rationally" simplifies the

expression 'exp' and all of its subexpressions including the arguments to non-rational functions. The result is returned as the quotient of two polynomials. Since MACSYMA defaults to integer arithmetic operation, real numbers in the S.P.R. transfer function are first converted into integer values. This explains the 'RAT replaced' messages that are output.

(c4) denom(d3);

(d4) $-80\ \%i\ w^3 - 101\ w^2 + 18\ \%i\ w + 1$

(c5) subst(-%i,%i,d4);

(d5) $80\ \%i\ w^3 - 101\ w^2 - 18\ \%i\ w + 1$

The first step in evaluating the real part of the (d3) expression requires the complex conjugate of its denominator. The denominator is first obtained with the command of line (c4). In line (c5) the complex conjugate is formed by replacing %i, (j), with -%i, (-j).

(c6) num(d3)*d5;

(d6) $(80\ \%i\ w^3 - 101\ w^2 - 18\ \%i\ w + 1)\ ((\ -25\ \%i\ cf2 + 25\ \%i\ cf1 - 25\ \%i)\ w^3$

$+ (\ 25\ cf2 + 25\ cf1 - 75)\ w^2 + (\ -25\ \%i\ cf2 + 25\ \%i\ cf1 + 75\ \%i\ )\ w$

$+ 25\ cf2 + 25\ cf1 + 25$

The command line (c6) takes the numerator of the 'w' transfer function and multiplies it with the complex conjugate of the denominator polynomial. The result obtained corresponds to the '(ac + bd)' term of equation A3.3. The (c^2+d^2) term is ignored as it is positive valued and does not depend on the error filter coefficients. Hence, it has no bearing on the sign properties of the real part of the 'w' transfer function.

(c7) ratsimp(d6);

(d7) $(2000\ cf2 - 2000\ cf1 + 2000)w^6 + (4252\ \%i\ cf2 - 525\ \%i\ cf1 - 3475\ \%i)w^5$

$+ (-975\ cf2 - 4075\ cf1 - 1125)w^4 + (-4050\ \%i\ cf2 - 950\ \%i\ cf1 - 4250\ \%i)w^3$

$+ (-2950\ cf2 - 2050\ cf1 - 1250)w^2 + (-475\ \%i\ cf2 - 425\ \%i\ cf1 - 375\ \%i)w$

$+ 25\ cf2 + 25\ cf1 + 25$

The expression evaluated by the previous command, (c6), is analogous to the numerator of the expression in equation A3.3. Command line (c7) simplifies this result into an 'w' polynomial. The real part of this polynomial is obtained via the command of line (c8) below. The resulting expression is devoid of odd-powered 'w' terms. Hence, it is guaranteed to be positive if the 'w' coefficients are themselves positive. Command lines (c9) to (c12) evaluate the coefficients of the respective even-powered 'w' terms.

```
(c8) realpart(d7);

(d8) (2000 cf2 - 2000 cf1 + 2000)w^6 + (-975 cf2 - 4075 cf1 + 1125)w^4

+ (-2950 cf2 - 2050 cf1 - 1250)w^2 + 25 cf2 + 25 cf1 + 25

(c9) coeff(d8,w,0);

(d9)              25 cf2 + 25 cf1 + 25

(c10) coeff(d8,w,2);

(d10)         -2950 cf2 - 2050 cf1 - 1250

(c11) coeff(d8,w,4);

(d11)         -975 cf2 - 4075 cf1 + 1125

(c12) coeff(d8,w,8);

(d12)          2000 cf2 - 2000 cf1 + 2000
```

(c13) quit();

The expressions of the output lines (d9) to (d12) can be rewritten as the following set of inequalities, after some algebraic manipulation.

$$cf2 > -cf1-1$$

$$cf2 > \frac{-2050cf1-1250}{2950}$$

$$cf2 > \frac{-4075cf1+1125}{975}$$

$$cf2 > cf1-1$$

Allowable values for the error filter coefficients can readily be established following a graphical representation of the aforementioned inequalities.

In addition to its use in deriving S.P.R. conditions on the error filter coefficients, it is also possible to employ a subset of MACSYMA commands to represent these constraints graphically. Before this can be done, the inequalities have to be rewritten in a suitable form. Consider, as an example, the first inequality, $cf2 + cf1 + 1 > 0$. The region satisfying this condition is bounded by the line, $cf2 = -cf1 - 1$. Consequently, the first step in a graphical representation of the S.P.R. inequalities, in the cf1-cf2, i.e. the c_1–c_2, parameter space, consists of plotting the boundaries of the allowable region.

For the example transfer function studied above, the procedure to be followed is outlined here. Before MACSYMA is entered, it is necessary to inform the Multics operating system that a graphics file is to be generated. This is done with the command,

sg -of filename

The command results in the creation of a graphics file, named 'filename.graphics'. Following this instruction, MACSYMA can be entered as before. The subsequent log

demonstrates its use as a graph plotting facility. Once again, explanatory comments are included within the MACSYMA user session, in bold text.

```
>axl>mac

This is Macsyma 303
(c) 1976,1983, Massachussets Institute Of Technology.
All Rights Reserved.
Enhancements (c) 1983, Symbolics, Inc. All Rights Reserved.
Type trade_secret(); to see Trade Secret notice.

(c1) multgraph:true;
(d1)                    true
```

The first instruction that is employed informs MACSYMA that if any graphical data is generated during the course of the user session then it is to be written to a file. This file should already have been created, prior to the commencement of the MACSYMA session. The 'multgraph' command can be cancelled by setting it as 'false'.

```
(c2) -cf1-1;
(d2)                          - cf1 - 1

(c3) (-2050*cf1-1250)/2950;
                    -2050cf 1-1250
(d3)                ---------------
                         2950

(c4) (-4075*cf1+1125)/975;
                    1125-4075cf 1
(d4)                --------------
                         975

(c5) cf1-1;
(d5)                    cf1 - 1
```

The four input lines, (c2), (c3), (c4) and (c5), are used to specify the S.P.R. space boundary conditions, in terms of the 'cf1' parameter.

```
(c6) plot([d2,d3,d4,d5],cf1,-2.,2.);
(d6)                    [d2,d3,d4,d5]

(c7) quit();
```

Commannd line (c6) uses an expanded form of the 'plot' instruction to obtain a graph of the cf1-cf2 parameter space. Use of this command requires a number of arguments to be specified. The first of these is a list, delimited by the square brackets,[...]. This technique of grouping together a number of 'equations' when they are passed to the 'plot' command ensures that they will all be drawn on a single set of axes: the usual form of the 'plot' command contains only a single expression to be drawn. The second argument passed to 'plot' indicates the manipulated variable, in this case , cf1. The final two arguments specify minimum and maximum, in that order, limits for the manipulated variable. Hence, it is possible to read command line (c6) as; plot the list of expressions [d2,d3,d4,d5] for values of cf1 ranging from -2.0 to 2.0. An important point to note is that the cf1 limit values, in conjunction with the first expression in the list to be plotted, define maximum and minimum values for the cf2 axis. For this reason, some care is called for when selecting the order of expressions in the list to be plotted: the cf1 and cf2 limits generated by the first expression might not be sufficiently well spread out for some of the lines, associated with subsequent expressions in the list, to appear on the graph.

A hard copy of the graph generated is shown in figure A3.1. By examining the equations that delimit the S.P.R. space it is possible to shade in the relevant region.

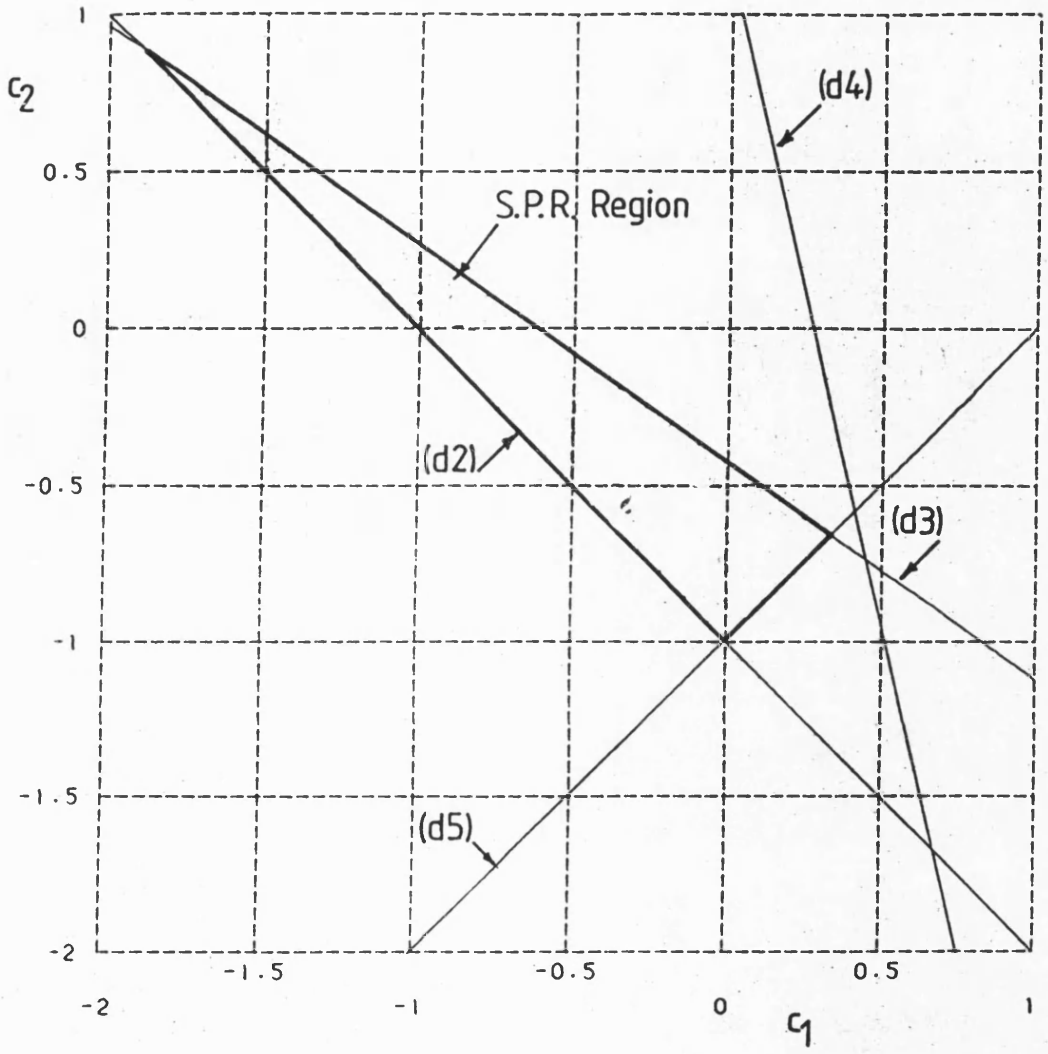

FIGURE A3:1 c_1—c_2 Parameter Graph Generated By MACSYMA

APPENDIX 4

SMALL PERTURBATION ANALYSIS OF AN ELECTRO-HYDRAULIC SERVOMECHANISM

A4.1 NOTATION

Symbol		Units
A_1	Area Of Actuator Jack - Piston Side	m^2
A_2	Area Of Actuator Jack - Annulus Side	m^2
B	Hydraulic Fluid Bulk Modulus	Pa
c	Coefficient Of Viscous Friction	N s/m
c_D	Coefficient Of Discharge	-
c_{D_1}	Spool Displacement Dependent Flow Gain - Piston Side	m^2/s
c_{D_2}	Spool Displacement Dependent Flow Gain - Annulus Side	m^2/s
c_{P_1}	Pressure Dependent Flow Gain - Piston Side	m^3/Pa s
c_{P_2}	Pressure Dependent Flow Gain - Annulus Side	m^3/Pa s
D , d	Spool Displacement	m
M	Mass Of Driven Load	Kg
P_S	Supply Pressure	Pa

Symbol		Units
P_T	Tank (Return Line) Pressure	Pa
P_1	Actuator Cylinder Pressure - Piston Side	Pa
P_2	Actuator Cylinder Pressure - Annulus Side	Pa
Q	Flow Of Hydraulic Fluid	m^3/s
ρ	Hydraulic Fluid Density	Kg/m^3
U	Underlap Of Servo-valve Spool	m
V_1	Volume In Piston Side Of Actuator Chamber	m^3
V_2	Volume In Annulus Side Of Actuator Chamber	m^3
Y, y	Displacement Of Inertial Load	m

A4.2 SYSTEM ANALYSIS

Figure A4:1 is a schematic representation of the system under consideration. Two important features to note in this figure are the use of an underlapped spool in the servo-valve and an asymmetric actuator.

A systematic examination of the servo-system, in figure A4:1, results in the following set of describing equations.

Side 1 (Piston) - Flow Equations

Consider the flow in the region of the orifices created by the spool opening.

$$Q_i = Q_1 - Q_2 \qquad \text{(A4.1)}$$

On the assumption of a regular shaped orifice opening, dependent upon the spool displacement, D, the flow Q_1 can be expressed as,

$$Q_1 = k_1 c_D \left(\frac{P_S - P_1}{\rho} \right)^{1/2} (U + D) \qquad \text{(A4.2)}$$

The term, $k_1(U+D)$, in equation (A4.2) quantifies the orifice opening area. Grouping together the parameters which are considered to remain constant, this expression can be simplified to the following,

$$Q_1 = k \sqrt{P_S - P_1}(U + D) \qquad \text{(A4.3)}$$

Using a similar line of argument, the flow Q_2 in equation (A4.1) can be defined as,

$$Q_2 = k \sqrt{P_1 - P_T}(U - D) \qquad \text{(A4.4)}$$

Since P_T, the return line pressure is taken to be atmospheric, this equation simplifies to the following,

$$Q_2 = k \sqrt{P_1}(U - D) \qquad \text{(A4.5)}$$

A second flow equation can be written to describe the flow action downstream of the spool. This condition arises as a consequence of the compressibility effects associated with the relatively large volume of hydraulic fluid present. The following equation describes the phenomenon that occurs.

$$Q_i - Q_{A_1} = Q_{c_1} \qquad \text{(A4.6)}$$

Here, Q_{c_1} represents the flow arising from the compressibility effect. Q_{A_1} and Q_{c_1} can be expressed in terms of the system parameters, as indicated below. Under steady state operating conditions, flow entering the actuator chamber imparts a given velocity to the piston, hence,

$$Q_{A_1} = A_1 sY \tag{A4.7}$$

where, 's' is the Laplace operator.

The flow term associated with compressibility effects is expressed as,

$$Q_c = \frac{V}{B}\frac{dP}{dt} \tag{A4.8}$$

The system equation for side 1 can now be written in terms of system related parameters. From equations (A4.1) and (A4.5),

$$Q_1 - Q_2 = Q_{c_1} + Q_{A_1} \tag{A4.9}$$

Substituting equations (A4.3), (A4.5), (A4.7) and (A4.8) for the terms in equation (A4.9) leads to the following expression,

$$k\sqrt{P_S - P_1}(U + D) - k\sqrt{P_1}(U - D) = A_1 sY + \frac{V_1}{B} sP_1 \tag{A4.10}$$

Side 2 (Annulus) - Flow Equation

A similar procedure as above is used in deriving the system describing equation for side 2. The relevant equations, with reference to figure A4:1, are,

$$Q_o + Q_3 = Q_4 \tag{A4.11}$$

$$Q_{A_2} = Q_o + Q_{c_2} \tag{A4.12}$$

Adopting the same procedure used in deriving equation (A4.10), equations (A4.11)

and (A4.12) can be combined to produce the following.

$$Q_{A_2} - Q_{c_2} = Q_4 - Q_3 \qquad \text{(A4.13)}$$

When this equation is expressed in terms of system parameters, the following result is obtained.

$$A_2 sY - \frac{V_2}{B} = k\sqrt{P_2}(U+D) - k\sqrt{P_S - P_2}(U-D) \qquad \text{(A4.14)}$$

Force Equation

With no external forces acting on the load and neglecting load damping, then, for a steady piston velocity, the force balance on the load can be written as.

$$(P_1 A_1 - P_2 A_2) = (Ms^2 + cs)Y \qquad \text{(A4.15)}$$

where c is the coefficient of viscous friction.

A4.3 SMALL PERTURBATION ANALYSIS

The valve flow equations, (A4.10) and (A4.14), are non-linear with respect to pressure. A small perturbation analysis is used, in the subsequent study, to generate a set of linearised system equations about localised operating conditions.

The expression given below is used to specify the relationship between valve flow, Q, and pressure, P, and spool displacement,D.

$$Q = F(P, D)$$

The following technique is used to express small changes in the valve flow. Lower case letters are used to represent perturbed parameters.

$$q = (\frac{\partial Q}{\partial D})d + (\frac{\partial Q}{\partial P})p$$

Application of this procedure to equations (A4.10), (A4.14) and (A4.15) yields the following set of linearised system equations.

Equation A10

$$k\sqrt{P_S - P_1}d - \frac{k(U+D)}{2\sqrt{P_S - P_1}}p_1 + k\sqrt{P_1}d - \frac{k(U-D)}{2\sqrt{P_1}}p_1 = A_1 sy + \frac{V_1}{B}sp_1 \qquad \text{(A4.16)}$$

which, when rearranged, gives,

$$c_{D_1}d = A_1 sy + \left(\frac{V_1}{B}s + c_{P_1}\right)p_1 \qquad \text{(A4.17)}$$

where,

$$c_{D_1} = k\sqrt{P_S - P_1} + k\sqrt{P_1} \qquad \text{(A4.18)}$$

and,

$$c_{P_1} = \frac{k(U+D)}{2\sqrt{P_S - P_1}} + \frac{k(U-D)}{2\sqrt{P_1}} \qquad \text{(A4.19)}$$

Equation A14

$$A_2 sy - \frac{V_2}{B}sp_2 = k\sqrt{P_S - P_2}d + \frac{k(U-D)}{2\sqrt{P_S - P_2}}p_2 + k\sqrt{P_2}d + \frac{k(U+D)}{2\sqrt{P_2}}p_2 \qquad \text{(A4.20)}$$

which can be rewritten as,

$$A_2 sy = \left(\frac{V_2}{B} s + c_{P_2} \right) p_2 + c_{D_2} d \qquad \text{(A4.21)}$$

where,

$$c_{D_2} = k\sqrt{P_2} + k\sqrt{P_S - P_2} \qquad \text{(A4.22)}$$

and,

$$c_{P_2} = \frac{k(U-D)}{2\sqrt{P_S - P_2}} + \frac{k(U+D)}{2\sqrt{P_2}} \qquad \text{(A4.23)}$$

Equation A15

$$A_1 p_1 - A_2 p_2 = (Ms^2 + cs)y \qquad \text{(A4.24)}$$

A4.4 TRANSFER FUNCTION DERIVATION

Figure A4:2 provides a block diagram representation of these linearised system equations, (A4.17), (A4.21) and (A4.24). The transfer function, relating y to d, yields the following result.

$$\frac{y}{d} = \frac{n_1 s + n_0}{d_4 s^4 + d_3 s^3 + d_2 s^2 + d_1 s^1} \qquad \text{(A4.25)}$$

where,

$$n_1 = A_1 B V_2 c_{D_1} + A_2 B V_1 c_{D_2} \qquad \text{(A4.26)}$$

$$n_0 = A_1 B^2 c_{D_1} c_{P_2} + A_2 B^2 c_{D_2} c_{P_1} \qquad \text{(A4.27)}$$

$$d_4 = M V_1 V_2 \qquad \text{(A4.28)}$$

$$d_3 = V_1 V_2 c + MBV_2 c_{P_1} + MBV_1 c_{P_2} \qquad \text{(A4.29)}$$

$$d_2 = (Bcc_{P_1} + BA_1^2) V_2 + (Bcc_{P_2} + BA_2^2) V_1 + MB^2 c_{P_1} c_{P_2} \qquad \text{(A4.30)}$$

$$d_1 = B^2 c c_{P_1} c_{P_2} + A_1^2 B^2 c_{P_2} + A_2^2 B^2 c_{P_1} \qquad \text{(A4.31)}$$

Equation (A4.25) is a fourth order, type 1 transfer function with one real zero.

A4.5 SYMMETRIC ACTUATOR - MID-STROKE OPERATING POINT

The transfer function of an asymmetric actuator system, with the actuator in its mid-stroke position, can be obtained from the transfer function derived above. The following alterations have to be made to the system describing equations. Since the actuator is a symmetrical one, $A_1 = A_2 = A$. In addition, $V_1 = V_2 = V$, when the actuator lies in its central position. For a fixed spool displacement, which results in the actuator travelling with a constant velocity, the flow into and out of the actuator cylinder is equal. Hence, $Q_i = Q_o$ and, $P_1 = P_2$ because the inertial load is not being accelerated. Moreover, since the flows entering and leaving the actuator are identical the following condition can be deduced.

$$P_S - P_1 = P_2 \qquad \text{(A4.32)}$$

As a consequence, the following identity is derived.

$$P_1 = P_2 = \frac{P_S}{2} \tag{A4.33}$$

A comparison of equations (A4.18),(A4.22),(A4.19) and (A4.23) therefore means that it is possible to write,

$$c_{D_1} = c_{D_2} \tag{A4.34}$$

$$c_{P_1} = -c_{P_2} = -c_P \tag{A4.35}$$

In view of these simplifications, the new linearised system equations become,

$$c_{D_1} d - c_P p_1 = Asy + \frac{V}{B} s p_1 \tag{A4.36}$$

$$c_{D_1} d + c_P p_2 = Asy - \frac{V}{B} s p_2 \tag{A4.37}$$

$$(Ms^2 + cs)\frac{y}{A} = p_1 - p_2 \tag{A4.38}$$

The system transfer function derived from this set of simultaneous equations is,

$$\frac{y}{d} = \frac{2ABc_{D_1}}{MVs^3 + (BMc_P + cV)s^2 + Bcc_P s} \tag{A4.39}$$

This form of transfer function represents a third order, type 1 system. It is considerably simpler than the transfer function of equation (A4.25).

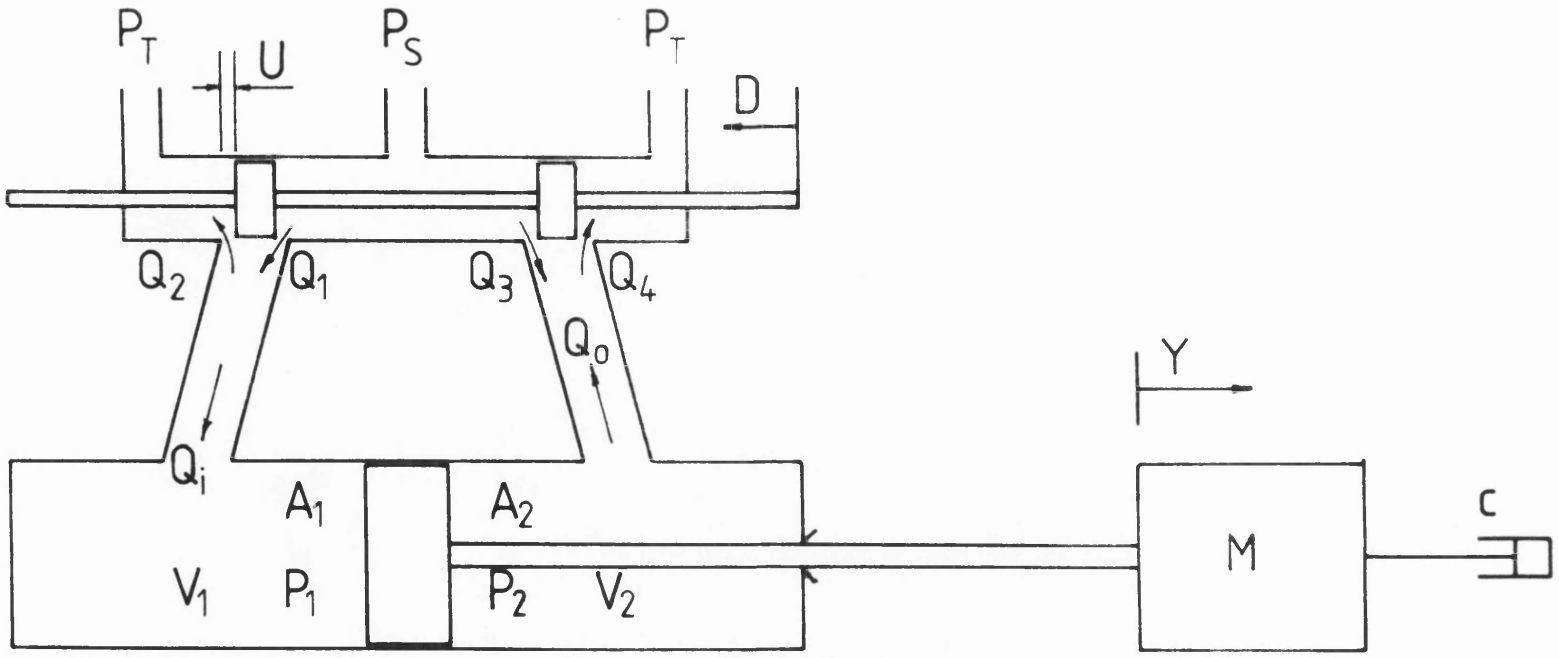

FIGURE A4:1 Schematic Representation Of Electro-Hydraulic Servomechanism

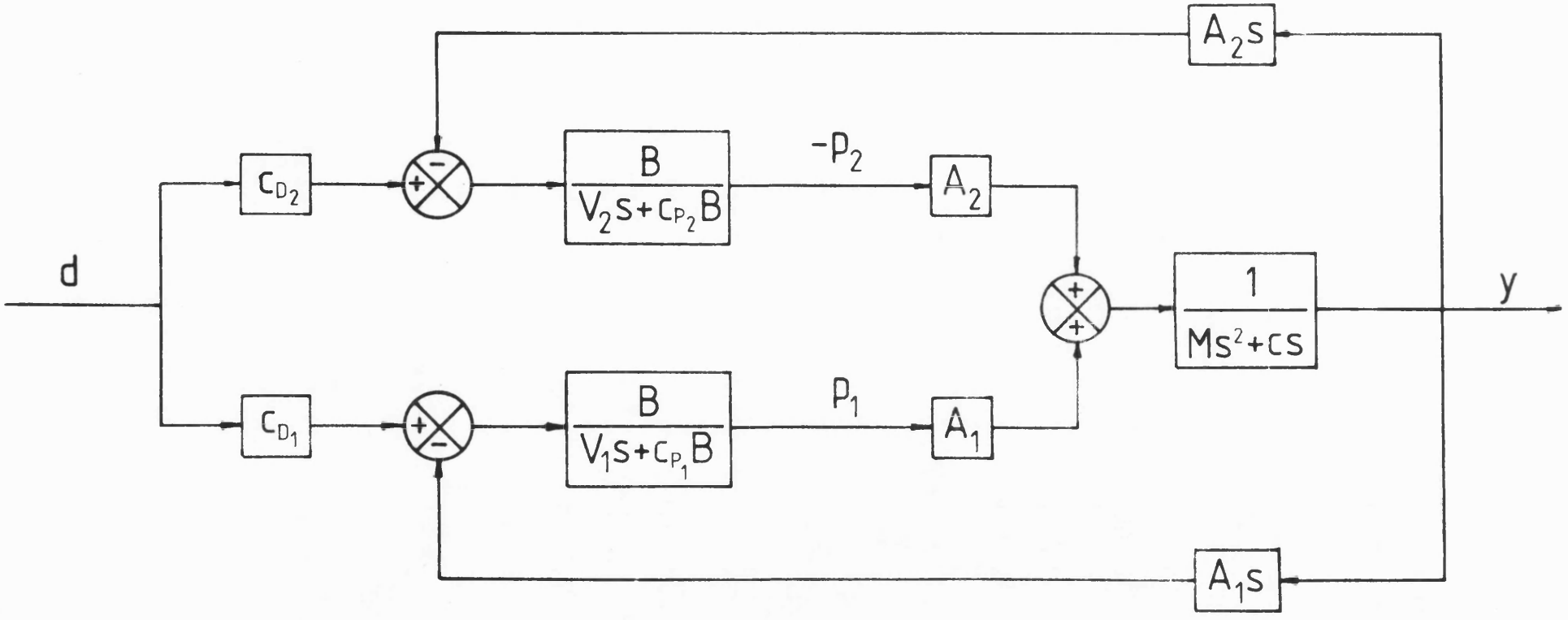

FIGURE A4:2 Block Diagram Representation Of Linearised Electro-Hydraulic Servomechanism Equations

APPENDIX 5

ASYMMETRIC ACTUATOR GAIN

A5.1 NOTATION

Symbol		Units
A_1	Exposed Area Of Actuator Jack - Piston Side	m^2
A_2	Exposed Area Of Actuator Jack - Annulus Side	m^2
e	Magnitude Of Servo-Valve Spool Opening	m
M	Load Inertia	Kg
P_1	Pressure In Actuator Chamber Downstream Of Supply Line	Pa
P_2	Pressure In Actuator Chamber Upstream Of Return Line	Pa
P_S	System Supply Pressure	Pa
Q_1	Flow Entering Actuator Chamber	m^3/s
Q_2	Flow Exiting Actuator Chamber	m^3/s
$\dot{y}$	Actuator Jack Velocity	m/s

A5.2 SYSTEM ANALYSIS

The use of an asymmetric actuator implies a level of system performance which is dependent upon the direction of actuator travel. The analysis carried out in this appendix attempts to quantify the influence of this phenomenon in terms of the velocity of the actuator jack. The system to be studied is shown in figure A5:1.

The servo-valve in this analysis is assumed to have a zero-lapped spool. The following study is still considered to be applicable to systems containing underlapped servo-valves. The reason for this is that the operating conditions examined here relate to substantial magnitudes of spool displacement. The flow passages thus created are considered to be the same for both underlapped and zero-lapped servo-valves.

In the following presentation, equations are derived for the steady state piston velocities corresponding to the two directions of actuator travel. These are obtained by considering the response of the servosystem, in the two directions, for a given magnitude of spool opening, e.

Case 1 - Supply Pressure Vented To Piston Side Of Actuator

The actuator velocity in this case is denoted as $\dot{y}_P$. Under steady state operating conditions, the flow entering the actuator cylinder is given by the orifice equation as,

$$Q_1 = k\sqrt{P_S - P_1}e = A_1\dot{y}_P \qquad \text{(A5.1)}$$

The parameter, k, represents a flow gain; it is a linear function of the flow port geometry and a flow discharge coefficient.

Consideration of the flow leaving the cylinder leads to the following set of expressions,

$$Q_2 = k\sqrt{P_2}e = A_2\dot{y}_P \qquad \text{(A5.2)}$$

The load mass, M, is considered to be displaced at a constant velocity. Viscous friction within the system is assumed to be negligible. Hence, the force balance on the actuator jack yields the following condition,

$$P_1A_1 = P_2A_2 \qquad \text{(A5.3)}$$

This equation can be rearranged to the following expression,

$$P_2 = P_1 \frac{A_1}{A_2} \tag{A5.4}$$

Upon manipulation of the two expressions for the actuator velocity, A5.1 and A5.2, the following equation is obtained,

$$\frac{P_S - P_1}{A_1^2} = \frac{P_2}{A_2^2} \tag{A5.5}$$

However, substituting for P_2 from equation A5.4 , means that equation A5.5 can be rewritten as,

$$P_S - P_1 = \left(\frac{A_1}{A_2} \right)^3 P_1 \tag{A5.6}$$

Thus,

$$P_1 = \frac{A_2^3}{A_1^3 + A_2^3} P_S \tag{A5.7}$$

and,

$$P_2 = \frac{A_1 A_2^2}{A_1^3 + A_2^3} P_S \tag{A5.8}$$

Using equation A5.2, the actuator velocity, for a given spool displacement, e, can now be expressed in terms of the system supply pressure, thus,

$$\dot{y}_P = \frac{k}{A_2}\left(\frac{A_1 A_2^2 P_S}{A_1^3 + A_2^3}\right)^{1/2} e \qquad \text{(A5.9)}$$

Case 2 - Supply Pressure Vented To Annulus Side Of Actuator

The situation corresponding to this mode of operation involves venting the supply pressure to the annulus side of the actuator. This corresponds to a spool opening of -e units and an actuator velocity denoted as $\dot{y}_A$. The notation of figure A5:1 has to be altered to reflect the new situation. The pressure in the piston side of the actuator chamber is now referred to as P_1, while that in the annulus side becomes P_2. As in the previous case, consideration of the flow entering and leaving the actuator cylinder results in the following set of equations.

$$-A_2\dot{y}_A = -k\sqrt{P_S - P_1}\,e \qquad \text{(A5.10)}$$

$$-A_1\dot{y}_A = -k\sqrt{P_2}\,e \qquad \text{(A5.11)}$$

Under steady operating conditions, the force balance on the actuator jack leads to the following expression,

$$P_1 A_2 = P_2 A_1 \qquad \text{(A5.12)}$$

By combining and rearranging these equations, as earlier, the actuator chamber pressures can be obtained. Hence,

$$P_1 = \frac{A_1^3}{A_1^3 + A_2^3} P_S \qquad \text{(A5.13)}$$

$$P_2 = \frac{A_1^2 A_2}{A_1^3 + A_2^3} P_S \qquad \text{(A5.14)}$$

Substituting back into equation A5.11, the magnitude of the new, actuator velocity becomes,

$$\dot{y}_A = \frac{k}{A_1}\left(\frac{A_1^2 A_2 P_S}{A_1^3 + A_2^3}\right)^{1/2} e \qquad \text{(A5.15)}$$

The ratio of the actuator velocities in the two directions, for the same valve opening, is given as,

$$\frac{\dot{y}_P}{\dot{y}_A} = \frac{ke}{A_2}\left(\frac{A_1 A_2^2 P_S}{A_1^3 + A_2^3}\right)^{1/2} \frac{A_1}{ke}\left(\frac{A_1^3 + A_2^3}{A_1^2 A_2 P_S}\right)^{1/2} \qquad \text{(A5.16)}$$

$$= \left(\frac{A_1}{A_2}\right)^{1/2} \qquad \text{(A5.17)}$$

According to this analysis, the velocity ratio is simply an area dependent function.

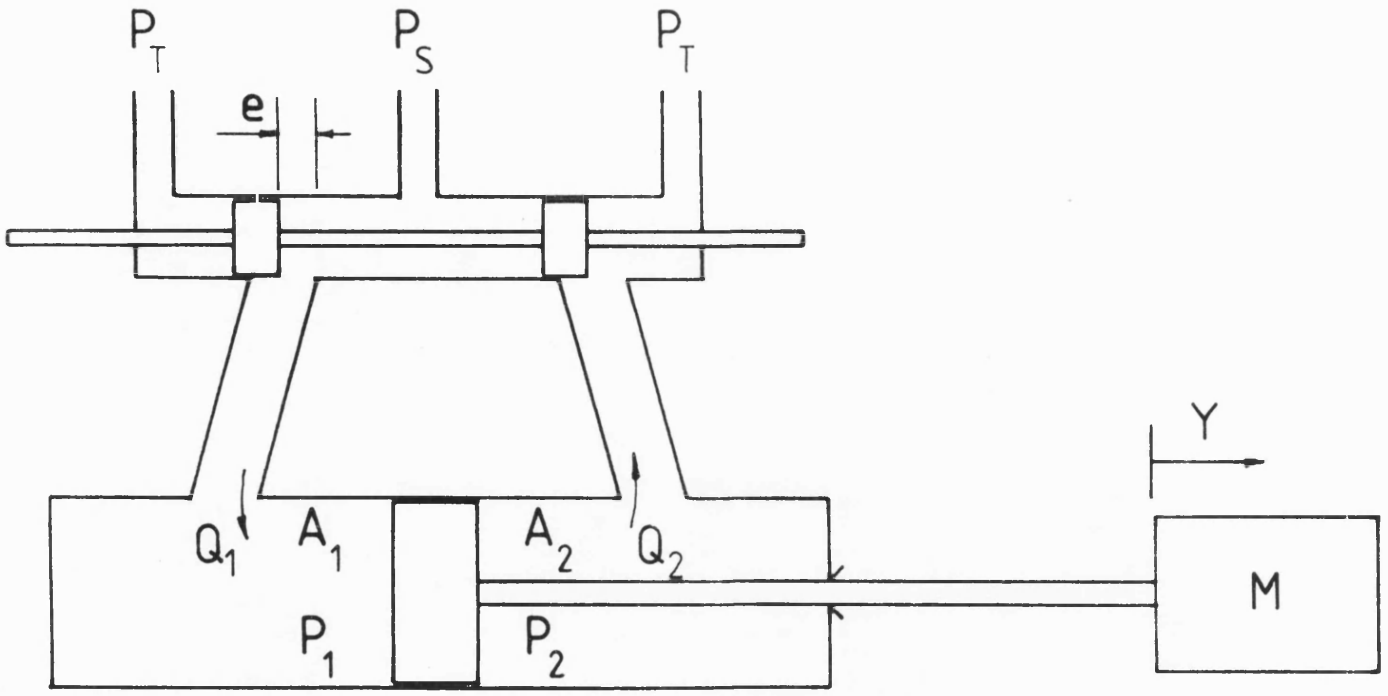

FIGURE A5:1 Schematic Representation Of Electro-Hydraulic Servomechanism
(Notation Corresponds To Case 1)